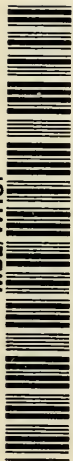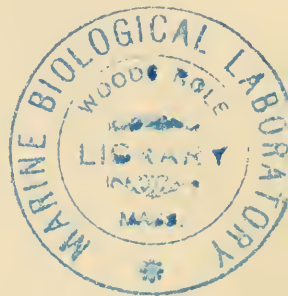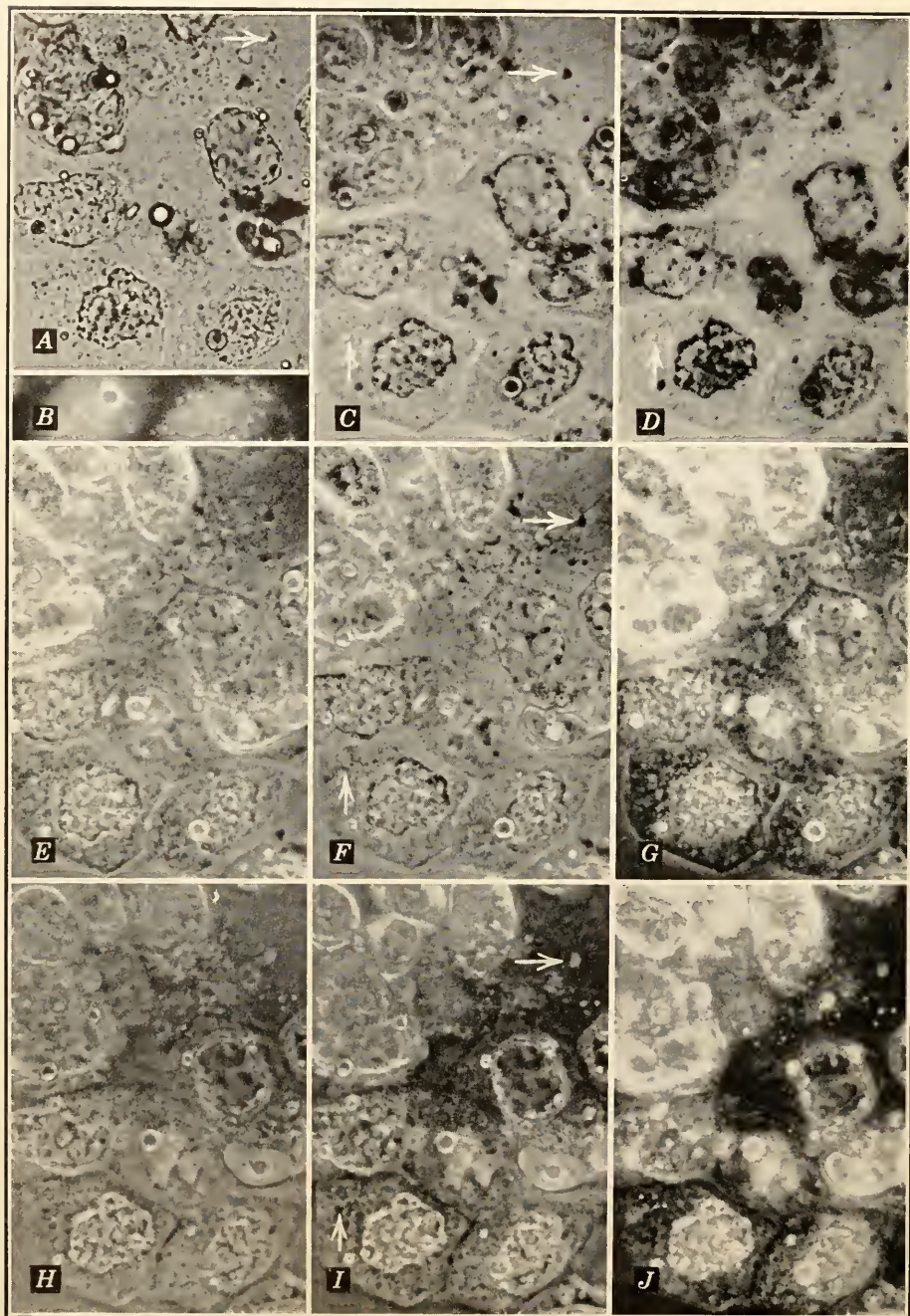# PHASE MICROSCOPY

Frontispiece

Epithelial cells from the dorsum of an Axolotl tadpole, showing range of contrast control for unstained tissue with Spencer phase microscope. 500×. *A*, brightfield; *B*, darkfield. *C–D*, low and medium B − dark-contrast phase. *E–G*, low, medium, and high A − dark-contrast phase. *H–J*, low, medium, and high A + bright-contrast phase. Note details at arrows.

PHASE MICROSCOPY
Principles and Applications

ALVA H. BENNETT   HAROLD OSTERBERG

HELEN JUPNIK   OSCAR W. RICHARDS

RESEARCH LABORATORY
AMERICAN OPTICAL COMPANY
STAMFORD, CONNECTICUT
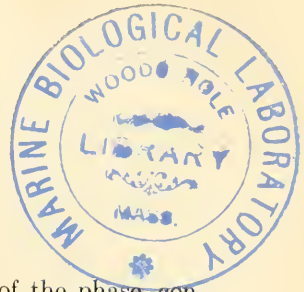
PREFACE

The announcement of the microscopic application of the phase con-
trast method by Professor F. Zernike in 1935 marked the beginning of
new and outstanding progress in the field of microscopy. The phase
contrast procedure has made possible the microscopy of an important
class of materials that could not be satisfactorily examined with previ-
ously existing microscopic methods. In the early stages of the wide-
spread, international development of the phase technic the authors of
this book began their investigations which resulted in significant con-
tributions to the theory, instrumentation, and application of this highly
effective procedure. Concurrently and independently, scientific workers
in several countries were also making important advances in the technic
of phase microscopy.

The aim of this book is to present the results of these investigations
to the numerous microscopists engaged in scientific and technical work
so that they can advantageously apply phase microscopy to their wide
variety of problems. The possibilities of the phase method have been
found to be so extensive that we believe that practically every micros-
copist will find some suggestions in this book which will be of value.

In presenting this material the authors have individually written the
various chapters. In each of these chapters the subject matter relates
to the specific type of investigation in which the author concerned has
been engaged. It is hoped that any resulting non-uniformity in style
of presentation will be amply offset by a corresponding gain in authentic-
ity. The writer, however, being concerned with the more general aspects
and correlations of the problems of this subject, contributed Chapter I,
wherein is indicated the place of the phase method in the general scope
of microscopy. Another purpose of Chapter I is to give the reader a
simplified but basic insight into the optical principles involved in the
attainment of the results unique to phase microscopy.

The section of this book relating to theory was prepared by Dr.
Harold Osterberg. The theoretical considerations given in Chapter II
provide the reader with a statement of the elementary theory of phase
microscopy. This material has been simplified so as not to be beyond
the ability of the reader of moderate mathematical attainment, yet it is
intended to be sufficiently precise to be of use to the microscopist who
wishes to gain a theoretical understanding of the principles involved in

vii

the application of the phase microscope. In addition, Chapter II will guide the microscopist in selecting those instrumental conditions which provide the most efficient results under a wide variety of conditions of the microscopic specimen.

In the Appendix (Chapter VII) Dr. Osterberg presents a detailed mathematical treatment of the diffraction theory of image formation in the phase microscope when used in conjunction with the commonly used Köhler method of illumination. This diffraction theory is treated in its entirety in the Appendix because it is a subject in which the specialist in physical optics rather than the microscopist will probably be chiefly interested.

The instrumentation necessary for the application of phase microscopy is described by Dr. Helen Jupnik in Chapter III. The functions and properties of the various elements of the phase microscope are described. An important part of this chapter from the point of view of the microscopist is the description of the necessary alignment and adjustment of the microscope so that the most satisfactory and meaningful images can be obtained. The comparison of the salient features of the phase microscope equipment supplied by different manufacturers indicates the substantial progress which has been made by these manufacturers in their efforts to provide the microscopist with suitable, adequate, and available instrumentation. The most recent technics, marking the borderline between commercially available and non-available equipment, are described in the latter part of Chapter III. This material is intended to give the reader an idea of the present frontier of developments.

Chapters IV, V, and VI were written by Dr. Oscar W. Richards, who has made an extensive investigation of the applications of phase microscopy in the fields of biology, medicine, and industry. These chapters deal comprehensively with the practice of phase microscopy, and illustrate by numerous and typical examples the wide extent of successful applications of the phase procedure. For these examples the older microscopic methods are found to be insufficient.

The great quantity of research work relating to the subject of phase microscopy since its comparatively recent inception is shown by the extensive bibliography.

During the course of their phase microscope investigations, extending over a period of nine years, the authors have fortunately received suggestions and active encouragement from so many people that it is impossible to express here our deep gratitude to all of them individually. In particular, we wish to acknowledge with thanks the kind cooperation of Dr. George O. Gey, of the Johns Hopkins School of Medicine, who

greatly encouraged us at an early stage of our work with his favorable observations of living cancer cells by means of our initial phase microscopic equipment. We wish to express our indebtedness to Mr. Bryant Glenny, Jr., General Manager of the Instrument Division, American Optical Company, Buffalo, New York, for his encouragement throughout our investigations. This work would have been incomplete without the cooperation of many of the world's outstanding makers of microscopes and allied equipment. These manufacturers have kindly supplied the illustrations of commercially available phase microscopes. Accordingly, the authors wish to express their thanks and deep obligations to the American Optical Company, Bausch and Lomb Optical Company, Cooke, Troughton and Simms, Ltd., Henry Wild Surveying Instruments Supply Company, Ltd., Winkel-Zeiss, Officine Galileo, Koristka, and C. Reichert Optical Works for their permission to use the illustrations of the equipment.

<div style="text-align: right">

Alva H. Bennett
Director of Research
Research Laboratory
American Optical Company
Stamford, Connecticut

</div>

August, 1951

CONTENTS

INTRODUCTION TO
PHASE MICROSCOPY

1. SEEING MICROSCOPIC PARTICLES

The microscope is commonly described as an instrument used for seeing small objects. This definition leaves more unsaid than said. What do we mean by seeing small objects? The human eye sees because of two properties of the light entering the eye from the objects seen. The eye recognizes only differences in brightness and differences in color. Visual images are based on these two properties and no other. Differences in brightness of different objects or their component parts give rise to brightness contrast; differences in color cause color contrast. Almost all our knowledge of observed scientific phenomena is based on our ability to see. No matter how simple or how complicated is the physical apparatus used in making our observations, the final presentation of results must be in a form that can be seen. These results may be scale readings, graphs in one or more colors, or direct images as in the microscope. But they all appear to the human eye as brightness or color contrast in the objects viewed. Brightness is a function of the amplitude of the vibrations of light waves proceeding from the objects viewed. Hence, brightness contrast might be called amplitude contrast. Color depends on the wavelength of the light entering the eye. Physically, then, the eye is responsive only to the amplitudes and wavelengths of light. As will be brought out later we, as microscopists, might be tempted under certain conditions to wish that the eye were sensitive to some of the other physical properties of light.

The microscope, more broadly, can be considered an instrument that utilizes the action of a specimen on the probing illumination supplied to it for the purpose of our gaining knowledge of the specimen through visual impressions. We are interested in several properties of the specimen, such as, for example, size, shape, and density of its details. If the only properties in which we were interested were light absorption or selective absorption, giving rise to brightness and color contrasts, the microscopical problem would remain simple. But we are interested in other properties, and we must by some instrumental means cause these

other properties to reveal themselves as brightness or color contrasts.

The improvement of microscopes since their invention about 350 years ago has proceeded along two general lines, both of which have been necessary. First, there has been improvement of the instrument itself in order to make it a better and more convenient image-forming apparatus. Thus more effective forms of illumination have been developed, such as lamps and condensers. The microscope objectives and eyepieces have been improved by optical designers to provide sharper images and improved resolving power. Microscope designers of the past and present have been notably successful in these aims, and they are still attempting to make the microscope a more nearly perfect optical instrument for gaining the nearest possible approach to "point-for-point" imagery, that is, to obtain the image that most nearly reproduces the brightness and color differentiations of the object specimen with greatest fidelity. We have microscopes which, at least over the central portion of the field of view, achieve the full resolving power considered attainable from theory based on the wavelength of light.

The above-mentioned line of progress does not depend on the specimen and its peculiar optical properties. The second approach in the improvement of the microscope is to consider the specimen as an essential part of the optical system and, as it were, to build the microscope around the specimen. To be sure, this results not in simplification of the microscope as an instrument but rather in greater diversification.

Let us consider what optical properties of the specimen are to be "seen" in order that profitable information regarding its details may be acquired. The ordinary, conventional microscope is without rival for observing areas of light absorption and color differences in specimens. The darkfield microscope is designed to reveal particles by virtue of their property of scattering light. Details that polarize the light or have birefringence are revealed with the polarization microscope. If a specimen fluoresces under the action of radiation a fluorescence microscope is used. But a common property of all these microscopes is the formation of an image in terms of brightness or color contrasts which the eye is capable of observing or which can be converted into an observable image.

Until the invention of the phase microscope no very useful means were available for observing differences in optical path in a specimen. Optical path is the linear path of light through a transmitting medium multiplied by the index of refraction of the medium. Refractive index in a microscopic specimen depends upon the specimen's physical and chemical properties. Optical path differences may arise from differences in either refractive index or thickness or a combination of both. The

details of many biological and industrial specimens are characterized by differences in refractive index rather than by differences in light absorption. Under an ordinary microscope such details are invisible, unless the aperture of the condenser or objective is made so small that the resolving power suffers a serious deterioration with resultant loss in the observer's ability to interpret what he sees.

Light can be considered a form of wave motion consisting of sinusoidal waves. When a light wave traverses a medium of different optical path the phase of the light wave is altered. This alteration may be visualized as simply a displacement of the wave in its direction of propagation. If a microscopic specimen contains details that differ from each other in optical path, the phase of that portion of the illuminating wave front passing through the detail is changed. If a microscope can delineate change of phase as a change in brightness or color, the eye, photographic plate, or photocell will be able to detect the microscopic areas causing the phase changes. The phase microscope does this, and it makes available another type of microscope specifically designed to utilize a particular optical property of the specimen.

2. HISTORICAL BACKGROUND

The formation of images in the microscope is an effect of the diffraction of light. In this connection the classical experiments of Abbe are brought to mind. In these experiments are found the first reported facts on the effect of introducing phase changes on light waves within the optical system of the microscope. Abbe, according to Bratuscheck (1892), introduced glass wedges into the rear focal plane of the microscope objective and thereby changed the phase relationships existing between the diffraction spectra produced by a grating, having opaque lines, which was used as the microscopic specimen. He found that the contrast between the lines and their spaces could be reversed when he introduced a phase difference of 180° between the light waves composing the zero- and first-order diffraction spectra. Later Bratuscheck introduced absorbing strips of soot at the back focal plane of the microscope objective to weaken the brightness of the zero-order spectrum. As an object specimen he used alternate clear and slightly absorbing strips of soot. The strips of soot were so lightly coated that they were almost transparent and, hence, difficult to see with the ordinary microscope. By means of the above-mentioned absorbing plate in the rear focal plane of the objective, the visibility of the strips was greatly enhanced. Thus, he proved that by weakening the zero order of the diffraction spectra of this nearly transparent specimen the contrast in the image could be increased. Not only was Bratuscheck able to in-

crease the contrast of the specimen; he also actually reversed it, causing
the light strips to appear darker than the coated ones.   This was done
by replacing the specimen strips of soot with thin strips of platinum.
Bratuscheck pointed out that by substituting platinum for soot he
slightly changed the phase of the light which had passed through the
platinum lines with respect to the phase of the light passing through the
open spaces between.   These observations were made before 1892 at the
time when Abbe was much concerned with establishing the diffraction
theory of image formation in the microscope, and they were aimed to
substantiate such knowledge.   It is certain that they did not find their
way into practical applications of the microscope.

In outlining the earlier experiments and theoretical considerations
which form a background for the subject of phase microscopy the work
of A. E. Conrady and J. Rheinberg should be included.   In 1905
Conrady published experimental results showing that a phase reversal
exists in different orders of diffraction spectra produced by the light
diffracted by specimens in the form of gratings.   As will be shown later,
this is an important fact in phase microscopy.   Rheinberg (1905) used
a grating in which the slits were twice as wide as the bars.   He screened
off all the spectral orders except the first- and second-order spectra on
one side and showed a complete reversal of contrast, providing an
example of contrast control in the image by gaining control of phase in
the diffraction spectra through proper selection of these spectra.

It is to Professor F. Zernike, of the University of Groningen, that we
are indebted for the first application of phase contrast principles to the
microscope and for an explanation of these principles.   Zernike's first
published work (1934) on this subject showed the advantage of the phase
contrast method over the familiar knife-edge method in testing the
quality of optical systems.   In the same year, C. R. Burch (1934)
published his results on the experimental application of the then-new
Zernike method to the evaluation of defects in concave reflecting mirrors.
This original application and its later important incorporation in micro-
scopes appear as a logical step when we consider that errors in optical
systems and concave mirrors are detrimental, because they impress
unwanted differences in the paths of various portions of the transmitted
or reflected light wave, and that in the testing of such systems it is es-
sential to observe and evaluate these path differences.   In a somewhat
similar manner, in phase microscopy the structures within the specimen
impress path and, consequently, phase differences that we wish to detect
visually and localize within the specimen.

In 1935 Zernike discussed the application of the phase contrast method
to microscopy, although patent rights granted to the firm of Carl Zeiss

indicate that Zernike realized the importance of the phase contrast method in microscopy as early or earlier than 1932. However, it was not until 1941 that Köhler and Loos, of the firm of Carl Zeiss, published a paper showing the results of their extensive and convincing experiments with the Zernike method. The publication of this paper stimulated much interest in the method, especially among those concerned with the design of microscopes. Burch and Stock (1942) described their experiments with a slit-shaped light source and an accelerating Zernike strip in the back focal plane of the microscope objective. This system had the merit of ease of construction, but manufacturers have adopted the ring form of substage annulus and Zernike strip because, as pointed out by Köhler and Loos, this form of phase plate with its complete axial symmetry introduces practically no undesirable lack of symmetry into the image.

Although the possibility is mentioned by Köhler and Loos, it is interesting to note that the earlier experiments with phase contrast microscopy show no indications of the use of absorbing material in the Zernike strip until Zernike (1942) published photomicrographs, at least one of which was taken with a strongly absorbing phase strip.

The image produced by a microscope cannot duplicate the object specimen completely. This inability arises largely from the finite wavelength of light (or other electromagnetic radiation) and the limited numerical aperture of the optical system. Hence, the microscopist may encounter optical images that may, unless properly interpreted, give incorrect information regarding the size, shape, and uniformity of microscopical specimens. When a new method of microscopy is under trial, the question of interpretation of the image becomes important. Phase microscopy offered no exception to the requirement of interpretation (Anon., 1934). The phase method reached its present wide acceptance only after careful theoretical and experimental studies of the correct interpretation had been made. The theoretical considerations and experimental results presented in subsequent chapters indicate that images produced by phase microscopy are not more difficult to interpret than those produced by other methods of microscopy. In practice, by means of a series of phase microscope objectives, different views of the specimen can be obtained, each adding to the composite information obtainable regarding the specimen.

3. OPTICAL FUNDAMENTALS

This chapter will not present in detail the theory on which phase microscopy is based. In later chapters and in the Appendix may be found a detailed mathematical presentation of this subject. However,

for those who wish, a readily understandable explanation will be given
here.

Phase microscopy is based on the effect of the combining of light waves.
The properties of these waves on which phase microscopy depends are
amplitude and phase. Let us consider a small, transparent specimen
located on the optical axis of the microscope optical system. We will
assume that this specimen is an ideal one for phase microscopy. Hence,
we will embed this specimen in a medium having almost the same index
of refraction as the specimen. As the specimen is transparent it will
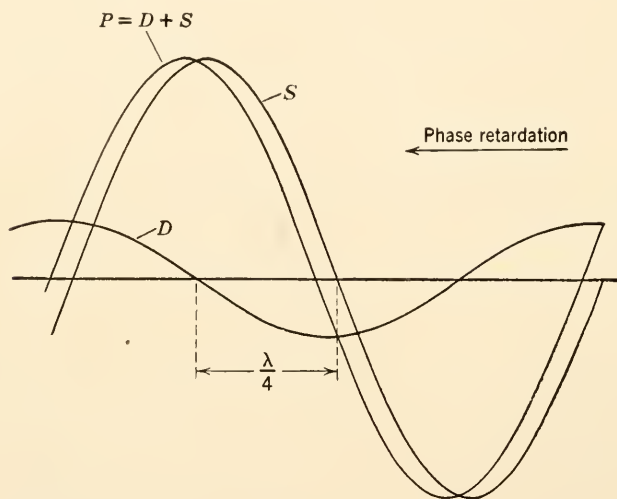
FIG. I.1. Retardation of a light wave by a particle (*P*) of greater index of refraction
than its surround (*S*).

differ from the surrounding medium in only one particular, i.e., in re-
fractive index, and this difference gives rise to a slight difference in
optical path between the specimen and its surroundings. Let us think
of a single light wave incident on the specimen and its surrounding
medium. In Fig. I.1 the sine curve, *S*, represents the light transmitted
by the surround; *P* is the wave transmitted by the particle. If the
particle has a slightly higher index of refraction than that of the sur-
round, the wave after transmission through the particle is retarded, or,
in other words, a small phase difference is introduced between the waves
S and *P*. This phase difference is represented as a slight displacement
of the two sine curves along the horizontal axis in the appropriate
direction. We may now determine just how the curve *P* differs from
the curve *S* by subtracting *S* from *P*. It is found that the difference is

the sine curve D, which is almost exactly $\frac{1}{4}$ wavelength out of phase with the curve S, provided that the retardation of P is small. D represents the light deviated by diffraction at the specimen. The light represented by S acts as if no specimen were present; i.e., it is undeviated. S and D represent the two waves entering the microscope objective. If we were to obstruct S by blocking it off in the objective lens system, we would have simply darkfield illumination; if we were to obstruct D and let S through, we would have no detailed imagery
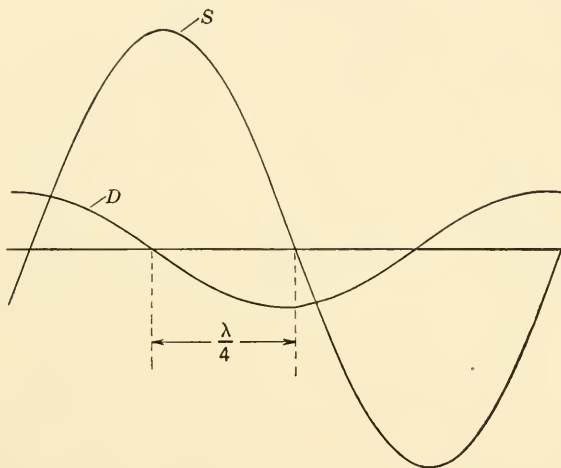
FIG. I.2. Deviated ray retarded by $\frac{1}{4}$ wavelength.

of the specimen. Microscopic images in general are obtained by allowing both the undeviated wave, S, and the deviated (by diffraction) wave, D (Fig. I.2), to pass through the microscope objective and interfere in the neighborhood of the geometrical image of the particle formed by the objective. Here the waves D and S recombine and form the wave P. The image of the surround is formed by the wave S. Since the amplitudes of S and P are equal, because the specimen is transparent, there is no contrast between the image of the particle and its background, and the particle is invisible. This situation is characteristic of the ordinary microscope.

Now, if we can change the phase of D with respect to S so that S and D are either in exactly the same phase or $\frac{1}{2}$ wavelength out of phase, we can obtain striking contrast between the specimen and its background. That this shift in phase can be accomplished by artificial means will be shown presently. Figure I.3 represents the combination of the waves D and S when the phase of D has been advanced (or that of S retarded)

by $\frac{1}{4}$ wavelength.   Here it can be seen that the amplitude of $D + S$, representing the light in the image of the particle, is considerably greater than that of S, the background light, and the particle will appear lighter than its background.   But suppose that we now retard the deviated wave, D, by $\frac{1}{4}$ wavelength (or advance S by this amount).   The condition shown in Fig. I.4 is the result.   The light in the image of the particle is now $S - D$, and, as in the previous example, the background
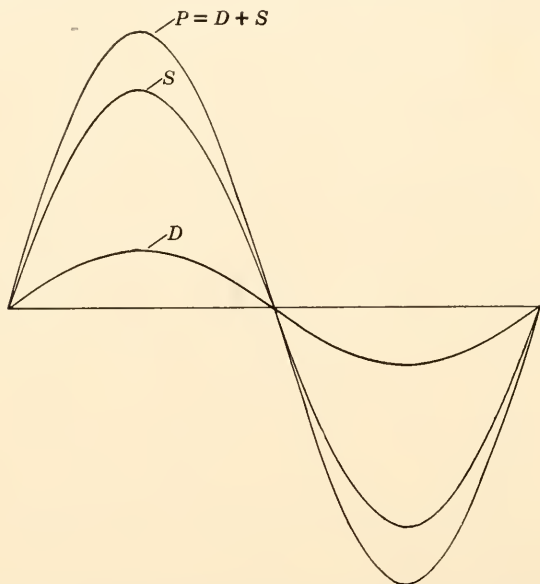
Fig. I.3.   Increased brightness from additive summation of direct and deviated light.

remains of amplitude S.   Now the particle appears darker than the remainder of the field of view.

Thus, if the phase of the deviated light can be changed with respect to the direct (undeviated) light from a single point in the original source of illumination, we have a means for changing the invisible phase differences arising in the specimen into amplitude differences in its image, which is thereby rendered visible.   Figure I.5 illustrates how this change is accomplished in a simple example.   Starting at the bottom of the drawing, let us consider a beam of light proceeding upward from a single point in the *condenser diaphragm*.   This point is on the axis of the optical system and is located at or near the lower focal plane of the *condenser*, from which the beam emerges as a bundle of parallel or nearly

parallel rays. The *specimen* is an important part of the optical system because of its action on the light-wave surface perpendicular to the rays. The specimen diffracts the light, provided that it is inhomogeneous with respect to the refractive index and/or absorption of light. The deviated light is represented by the rays diverging from the specimen and originating there. The parallel rays continue their course, without deviation, into the microscope *objective* system and are brought to a focus at its *back focal plane*, whereas the bundle of deviated rays is focused at
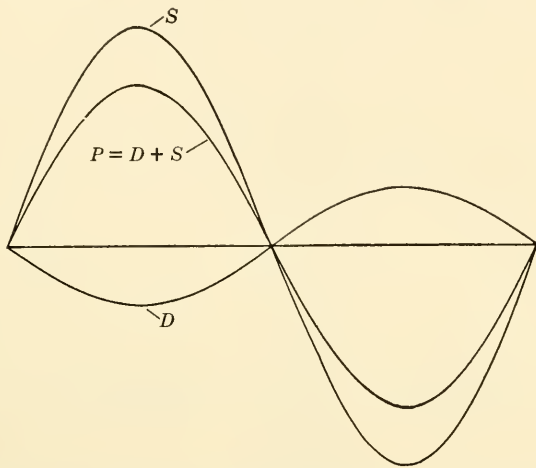
Fɪɢ. I.4. Decreased brightness from subtractive summation of direct and deviated light.

the *focal plane of the eyepiece* by the objective lenses. At the *diffraction plate** the direct and deviated bundles are definitely segregated with only very little overlapping. The phase of either the direct or the deviated light can therefore be changed by introducing a layer of dielectric material, such as magnesium fluoride, on that portion of the diffraction plate covered by these rays. In Fig. I.5 the direct light is retarded by the layer of dielectric material introduced at the small central portion of the diffraction plate to increase the optical path. For most systems the phase retardation introduced here should be $\frac{1}{4}$ wavelength, as shown in Figs. I.3 and I.4, in order to produce maximum contrast in the image.

* The term "diffraction plate" was originated by the authors and is used in preference to "phase plate," which, although emphasizing that this plate changes the *phase* between the deviated and the direct light from the specimen, does not indicate that it is of equal importance that this plate should *absorb* a part of the energy of one set of rays. The designation "diffraction plate" refers to the entire action of this plate on the diffraction spectra produced by the specimen.

At the focal plane of the eyepiece the direct light has spread over the field of view, and the deviated light, now converged, interferes with the
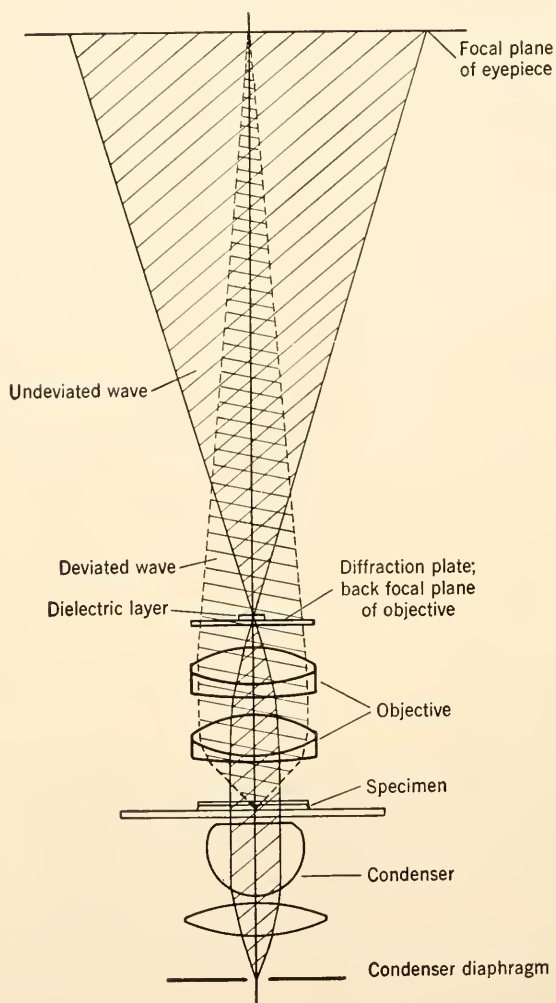
FIG. I.5.   Diagram of light path through a phase microscope.

direct light to form a light or dark image of the corresponding point in the specimen.

Referring again to Figs. I.3 and I.4, in order to obtain a maximum difference between the light in the image of the particle P and that in its background S, we should make the amplitudes of the waves S and D

equal. Generally, the deviated light, D, is much weaker than the direct light, S, and since we cannot increase the intensity of S without also increasing D proportionately we have available only the alternative of decreasing the intensity of the direct light, S. This decrease is accomplished by placing some absorbing material on the diffraction plate in the path of the light S. In many specimens suitable visibility of the desired details requires control of the contrast in the image in order to avoid too strong or too weak a contrast. This requirement has led to the use of a series of diffraction plates having different absorption and retardation characteristics or to the changing of either the absorption or retardation or both in the diffraction plate by methods discussed in Chapters II and III.

Although the foremost function of the microscope is to make small particles visible, the phase microscope, particularly one in which the absorption and retardation of the diffraction plate can be varied, is a useful instrument for measuring properties of the specimen (Osterberg and Pride, 1950).

Since the specimen diffracts light by virtue of its light-absorbing and/or light-retarding properties, phase microscopy is of value in the examination of specimens which, in addition to introducing small optical path differences, also weakly absorb the light. Such specimens have a combination of density and phase contrasts, designated in Chapter IV as *densiphase* contrast.

In the literature of Zernike and Köhler and Loos, the term "phasenkontrast" denotes the kind of microscopy discussed in this book. This term, translated as "phase contrast," is much used. Since the above authors refer to phase contrast, as distinguished from amplitude contrast, in the specimen, it seems likely that the designation "phase contrast microscopy" really means "the microscopy of specimens possessing phase contrast." In England the earlier writers on this subject refer to it as "phase difference microscopy," presumably because phase differences exist in the light traversing various portions of the specimen. In the United States the authors at the outset of their work applied the simpler term "phase microscopy." They preferred to base the name on the unique properties of the apparatus rather than on one of the optical properties which a specimen may or may not possess. The microscopic equipment introduces phase changes in the light passing through the microscope, and preferably the observer should have some choice in selecting these phase changes in order to present the greatest variety of aspects of the many kinds of specimens (see Frontispiece). But, regardless of whether the emphasis should be placed on the phase contrast of the specimen or on the phase changes introduced by the

diffraction plate of the present form of apparatus, or whether an entirely new system for favorably altering the phase of the light passing through the microscope to obtain better visibility of the specimens is developed, the term "phase microscopy" appears both sufficiently inclusive and sufficiently descriptive.

AN ELEMENTARY THEORY
OF PHASE MICROSCOPY

1. INTRODUCTORY REMARKS

Image formation in the phase microscope depends so intimately upon the phenomena of diffraction that even a qualitative explanation of phase microscopy must involve some of the principles of diffraction. The main purpose of the elementary theory is to provide insight into the physical action of a phase microscope without resorting to the more complicated and rigorous theory based upon Kirchhoff's or Luneberg's diffraction formula. A second purpose of the elementary theory is to obtain a set of quantitative relations which have proved of assistance in the application of phase microscopy. Whereas these relations are admittedly but the first approximation to the truth, they may be used in a surprisingly large number of cases to predict the character of the contrast which will be produced in the image of a given particle by a proposed diffraction plate. Conversely, these relations often enable the observer to deduce significant information about the relative optical properties of the particle and its surround from the properties of the diffraction plate which is required for producing darkest contrast in the image of the particle.

The minimum essentials of a qualitative explanation of phase microscopy have been included in Section 3, Chapter I. The qualitative explanation of phase microscopy will be presented in greater detail in Sections 2 and 3 of this chapter. The remaining sections deal with the quantitative aspects of the elementary theory. These quantitative relations will be derived with the aid of complex numbers rather than in terms of the equivalent but cumbersome pseudo-vectors. In this way the laws of phase microscopy can be presented with greater simplicity and clarity. Only the simplest rules of operation with complex numbers are required, and these will be described as they are needed. The final laws of phase microscopy do not involve complex numbers. These laws are stated in sufficient detail so that the microscopist will be able to apply them without referring to the methods of derivation.

The reader who is interested in the fundamentals of the more general

theory of phase microscopy with Köhler illumination may consult the Appendix, which is included as Chapter VII.

2. LIGHT WAVES AND THEIR INTERFERENCE

Light waves are regarded in classical physics as electromagnetic waves whose electric and magnetic vibrations are at right angles to the direction of propagation of the wave. Only the electric vibration is of direct importance to the phenomenon of light. Consequently, a light wave is usually represented as a transverse electric wave whose magnetic vibra-
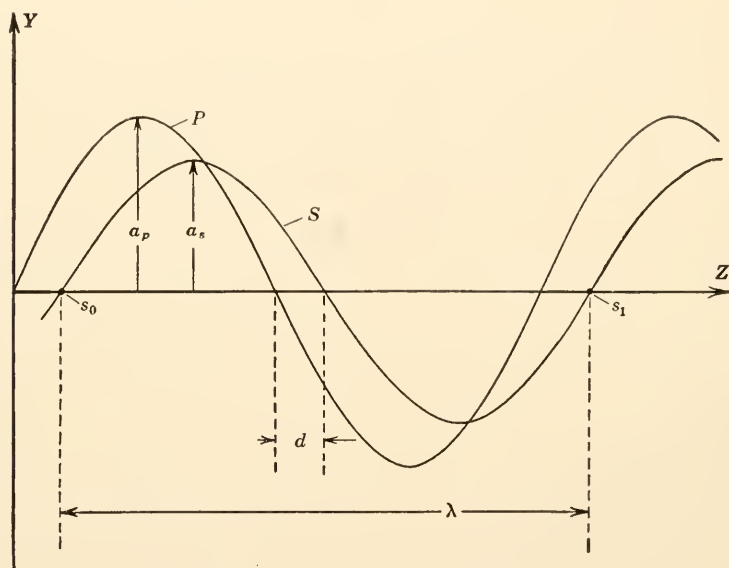
Fig. II.1. Representation of two light waves P and S of equal wavelength, λ. The P and S waves vibrate in the same plane, YZ, and are propagated along Z. The amplitudes of the P and S waves are a_p and a_s, respectively. The P wave is shown retarded with respect to the S wave by the amount d/λ wavelengths.

tion is ignored. The height of the wave is chosen to represent the instantaneous value of the electric vector.

Two related light waves are illustrated in Fig. II.1. These waves are traveling in the Z direction. Their electric vibrations are parallel to each other and to the Y direction. The maximum height, a_s, of the S wave is by definition the *amplitude* of the S wave. The P and S waves are illustrated as having different amplitudes, a_p and a_s, respectively. The wavelengths, λ, of the two waves are illustrated as alike and are equal to the distance s_0s_1. The entire P wave lags behind the S wave by

the actual distance d or by d/λ wavelengths. We say, accordingly, that the two waves differ in *phase* by d/λ wavelengths. We may also say that the P wave has been *retarded* with respect to the S wave by d/λ
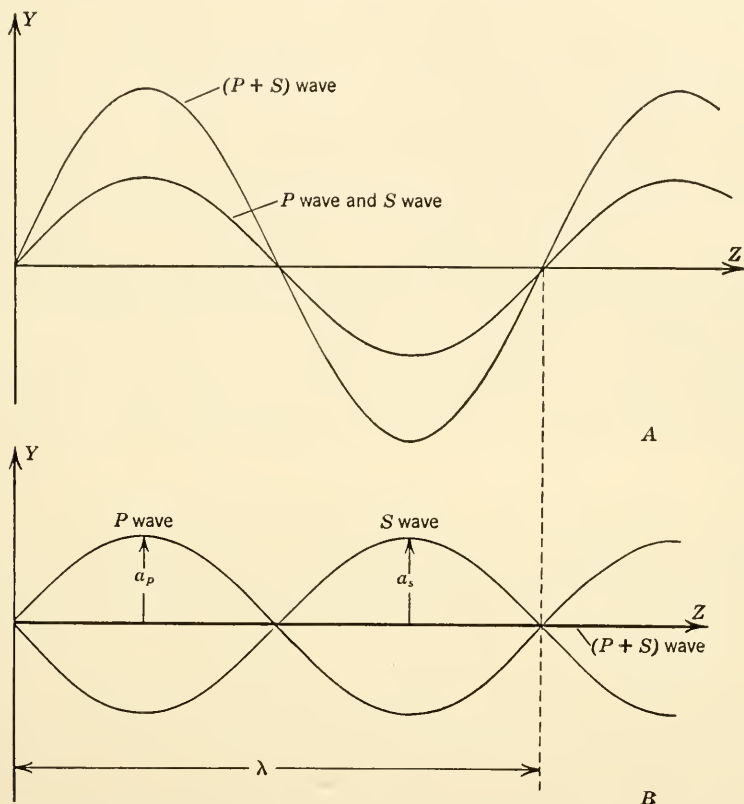
FIG. II.2. The resultant wave $(P + S)$ formed by the constructive and destructive interference of P and S waves of equal amplitude. Constructive and destructive interference occurs in A and B, respectively.

wavelengths or that the S wave has been *advanced* with respect to the P wave by d/λ wavelengths.

If the ordinates y of the P and S waves are added, the wave $(P + S)$ so obtained produces the same physical effects as the combined waves P and S. The wave $(P + S)$ is called the *resultant* wave. The physical process by means of which the P and S waves combine to form the resultant wave $(P + S)$ is called *interference*. In other words, two waves interfere to form the resultant wave.

The sum of two waves, i.e., the new wave that results from the inter-

ference of the two waves, depends on the amplitudes a_p and a_s of the two waves and on the phase difference d/λ between the two waves. Suppose that the P and S waves have the same amplitude and zero phase difference. They then coincide as in Fig. II.2A. The amplitude of the resultant wave $(P + S)$ is twice as great as the amplitude of the P or S wave. Evidently the two waves add or interfere with maximum effect when their phase difference is zero. Waves are said, accordingly, to interfere *constructively* when their phase difference is zero. Suppose, on the other hand, that the P and S waves have the same amplitude but differ in phase by $\frac{1}{2}$ wavelength. A crest of one wave is then displaced over a trough of the second wave, as in Fig. II.2B. The amplitude of the resultant wave $(P + S)$ is zero, and so the two waves destroy one another. Evidently the two waves add or interfere with minimum effect when their phase difference is $\frac{1}{2}$ wavelength. Waves are said to interfere *destructively* when their phase difference is $\frac{1}{2}$ wavelength.

As we shall see, constructive and destructive interference of light waves of equal amplitude form the physical means for obtaining brightest or darkest contrast in the image of the object particle in phase microscopy.

The brightness of an area that is illuminated by a light wave is proportional to the square of the amplitude of the wave. If the area is illuminated by two waves that belong to the same wave train emitted by an elementary particle in the source of light, the brightness of the area is proportional to the square of the amplitude of the resultant wave formed by the interference of the two waves.

3. A QUALITATIVE EXPLANATION OF PHASE MICROSCOPY

We shall suppose that the object specimen consists of a single particle which is surrounded by a homogeneous medium. The primary purpose of the microscope illuminator and substage condenser is to illuminate the object specimen in a controlled manner. If the source of light is focused upon the iris diaphragm of the substage condenser, as it is when the system has been adjusted for Köhler illumination, the opening in the condenser diaphragm may be regarded as the source of illumination. Light waves radiate from each point in the condenser diaphragm. These light waves are incident upon the object specimen, are diffracted by the specimen, and are subsequently refocused by the objective to form the complete image of the specimen. In discussing the properties of the complete image, we shall avoid a great amount of difficulty by considering only the image formed by a light wave that is radiated from a single point in the condenser diaphragm. We may suppose that, except for certain refinements which fall outside the scope of a rudimentary

discussion, the main effect of including the light from the remaining points in the condenser diaphragm is simply to produce a brighter image of the specimen.

The optical path of a given thickness of a uniform medium is equal to the product of the thickness and the refractive index of the medium.

The most important application of the phase microscope is to improve the visibility of particles that differ from their surrounding medium only by a small amount in optical path. We shall suppose throughout this section that neither the particle nor its surround absorbs light and that the optical path difference between the particle and the surround is a small fraction of a wavelength, for example $\lambda/20$. In order to distinguish more clearly between the behavior of an ordinary microscope and a phase microscope, this section will be subdivided into five parts. The first part, 3.1, will explain why the contrast in the image is poor in the ordinary microscope when the particle differs from the surround only in refractive index. The second part, 3.2, will show how the contrast in the image of such particles can be improved by a suitable choice of diffraction plate in the phase microscope.

3.1. Phenomena of all microscopes

The following diffraction phenomena occur in all microscopes and, on the basis of the simplified theory, lead to the conclusion that particles differing from their surround only in optical path should not be visible in the ordinary microscope.

If the condenser diaphragm is placed near the first focal plane of the substage condenser, the light wave radiated from a point C in the opening of the iris emerges from the substage condenser as a substantially plane wave so that the rays from C are parallel upon passing through the object specimen as in Fig. II.3. The object particle forms an obstacle in the path of the incident wave. Consequently, the incident wave does not pass without interruption through the object plane but is diffracted. A portion of the diffracted incident wave continues on its original course undeviated, but the remaining portion of the diffracted wave is deviated away from the direction of propagation at incidence. We may therefore regard the incident wave as broken into two related waves by diffraction at the object. The undeviated portion of the incident wave is called the *undeviated wave,* whereas the deviated portion is called the *deviated wave.*

The rays belonging to the undeviated wave are drawn as solid lines in Fig. II.3. These rays pass through a small neighborhood about the point C' in the second focal plane of the objective. The point C in the condenser diaphragm is imaged about the point C'. After passing

through C', the undeviated rays diverge and spread with a high degree of uniformity over the image plane. The rays belonging to the deviated wave are drawn as broken lines in Fig. II.3. The deviated rays diverge from the neighborhood of the particle. Subsequently they spread out over the second focal plane of the objective. The deviated rays are focused by the objective upon the neighborhood of the geometrical
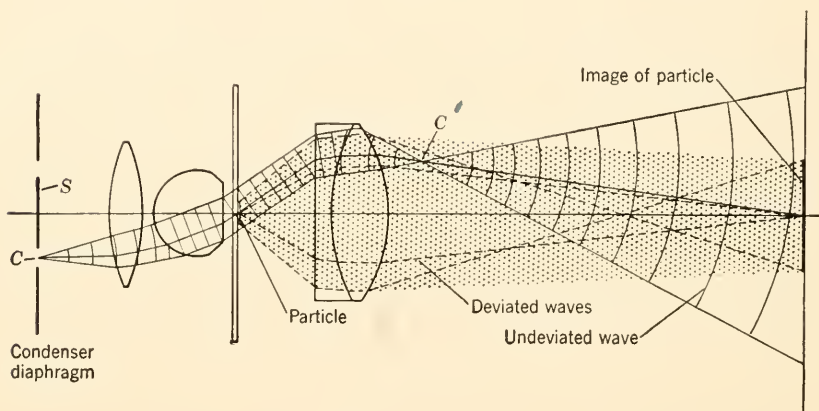
Fig. II.3. Spatial distribution of the undeviated and deviated waves that arise by diffraction at the object particle. Coherent light radiated from a point C in the opening of the condenser diaphragm is incident as a substantially plane wave upon the object particle and its surround. The stop S may assume different forms or may be absent. The undeviated rays are drawn as continuous lines, and the undeviated wave is distinguished by the expanding or contracting arcs. The undeviated rays obey the laws of geometrical optics and so form an image C' of C in the second focal plane of the objective. The deviated rays are drawn as broken lines, and the spatial distribution of the deviated waves is indicated by the shaded area. The deviated rays arise in the neighborhood of the particle and are converged by the objective into the neighborhood of the geometrical image of the particle.

image of the particle. A remarkable and important difference between the undeviated and deviated waves consists in the fact that the undeviated wave is concentrated in the second focal plane of the objective upon the neighborhood of the geometrical image of the source of light and is subsequently spread out over the image plane, whereas the deviated wave is spread out over the second focal plane of the objective and is subsequently concentrated upon the neighborhood of the geometrical image of the particle.

Curiously enough, the quantitative relations between the amplitudes and phases of the deviated and undeviated waves can be deduced from the following simple considerations: Returning again to the wave that

is incident upon the object specimen, we note that one portion of the incident wave is intercepted by the surround and that the remainder of the incident wave is intercepted by the particle. We denote the portion of the incident wave that is intercepted by the surround as the S wave and the portion that is intercepted by the particle as the P wave. Because we have supposed that neither the particle nor the surround
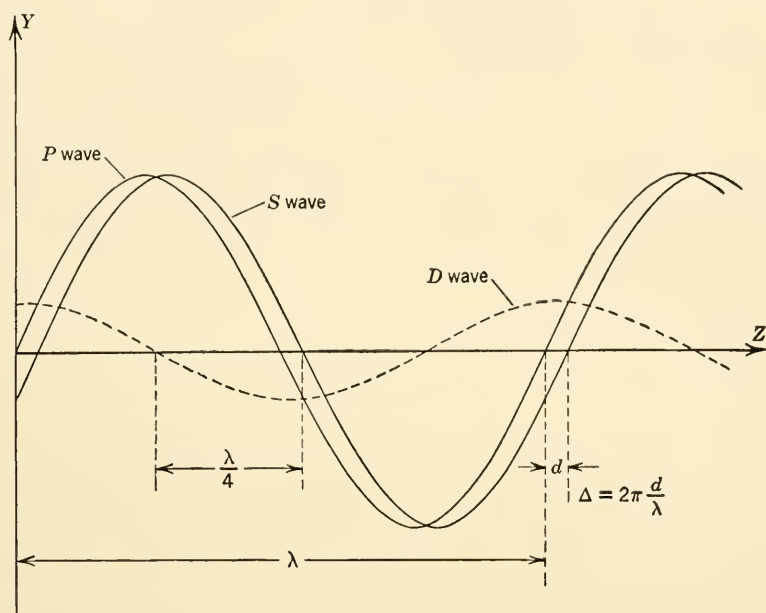
FIG. II.4.   Graphical relations among the P, S, and D waves such that $D + S = P$. The P wave is shown as retarded with respect to the S wave by a small phase angle, Δ, in radians.   The constructed D wave is retarded with respect to the S wave by approximately $\lambda/4$ wavelength or $\pi/2$ radians.

absorb light, the amplitudes of the P and S waves should be equal to each other and to the amplitude of the incident wave. Suppose that the optical path difference Δ between the particle and surround is a small fraction of a wavelength and that the optical path of the particle exceeds that of the surround. The P wave will then lag behind the S wave by the amount Δ, as in Fig. II.4. Now, it is possible to construct after the manner indicated in Fig. II.4 a wave D that, when added to the S wave, produces a resultant wave identical to the P wave. In other words, it is possible to find a D wave such that $D + S = P$. The only graphical requirement is that the ordinates y of the D and S waves shall add up to equal the ordinates y of the P wave. The pair of waves

D and S is not only equal to the P wave mathematically but is also indistinguishable from the P wave physically. We may suspect already that the D wave is the deviated wave. Since the portion of the incident wave that is intercepted by the surround is the S wave, and since the portion of the incident wave that is intercepted by the particle can be split into a D wave and another wave identical to the S wave, *the incident wave can be regarded as broken by diffraction into the S wave, which extends over the entire object plane, and into the D wave, which extends over the neighborhood of the particle.* The S and D waves may be identified with the undeviated and deviated waves from the following observations: We note from the construction of Fig. II.4 that when $\Delta = 0$, so that the particle vanishes, the D wave disappears whereas the S wave remains unchanged. This means that the S wave can only be the undeviated wave, for it is the wave that is present in the absence of an object particle. Since we know that there are but two waves produced by diffraction at the object specimen, namely the undeviated wave and the deviated wave, it follows by elimination that the D wave must be the deviated wave. The observation that the D wave vanishes when the particle vanishes is consistent with the conclusion that the D wave is the deviated wave.

The construction of Fig. II.4 gives the relative amplitudes of the S and D waves, together with the phase difference between these two waves, which are, respectively, the undeviated and deviated waves. It will be noted from Fig. II.4 that the D wave lags $\frac{1}{4}$ wavelength behind the S wave when the optical path of the particle exceeds that of the surround by a small amount Δ. On the other hand, if the optical path of the particle were less than that of the surround by a small amount Δ, the S wave in Fig. II.4 would have been drawn so as to lag behind the P wave by the amount Δ. The D wave would then be found* to have

---

* The laborious method of the graphical construction can be avoided by the following simple analytical considerations: Let s denote the amplitude of the S wave, and let the phase constant, ϕ_s, of the S wave be chosen as reference with $\phi_s = 0$. Then for the S wave the displacements y_s are

$$y_s = s \sin (z + \phi_s) = s \sin z. \tag{1}$$

Since the amplitudes of the S and P waves are equal, we have correspondingly for the P wave

$$y_p = s \sin (z + \Delta), \tag{2}$$

in which Δ is the amount by which the P wave is retarded with respect to the S wave. Let d denote the required amplitude of the D wave, and let ϕ denote the required phase retardation of the D wave. Then

$$y_d = d \sin (z + \phi). \tag{3}$$

the same amplitude as in Fig. II.4, provided that the numerical value of Δ remains unchanged, but would be found to lead the S wave by ¼ wavelength.   These conclusions about the phase difference between the undeviated and deviated waves are so important to phase microscopy that they are worth stating as the following theorem (Theorem 1):

When the light transmissions of the particle and the surround are equal and when the optical path of the particle differs from the optical path of the surround by a small fraction of a wavelength, the deviated wave is retarded or advanced in phase by ¼ wavelength with respect to the undeviated wave according as the optical path of the particle exceeds or is less than the optical path of an equal thickness of the surround.

Since the deviated wave is focused upon the neighborhood of the geometrical image of the particle and since the undeviated wave is

---

The statement that the sum of the D and S waves shall be equal to the P wave is now equivalent to writing

$$y_p = y_s + y_d$$

or

$$s \sin (z + \Delta) = s \sin z + d \sin (z + \phi). \tag{4}$$

If Δ is so small that $\sin \Delta \to \Delta$, Eq. 4 reduces to the equation

$$s\Delta \cos z = d \cos \phi \sin z + d \sin \phi \cos z. \tag{5}$$

If the waves $D + S$ are to be equal to the P wave for all values of z, Eq. 5 must be true for all values of z.   But this situation holds if and only if

$$d \cos \phi \sin z = 0;$$

$$s\Delta \cos z = d \sin \phi \cos z. \tag{6}$$

Hence $\cos \phi = 0$ so that

$$\phi = \pm \frac{\pi}{2} \tag{7}$$

with

$$s\Delta = d \sin \phi. \tag{8}$$

When $\Delta > 0$ so that the optical path of the particle exceeds that of the surround, we must choose the alternative $\phi = +\pi/2$, since neither s nor d can be negative. When $\Delta < 0$ so that the optical path of the particle is less than that of the surround, we must choose the alternative $\phi = -\pi/2$.   For either alternative the amplitude d of the deviated wave is given from Eq. 8 by

$$d = s|\Delta|, \tag{9}$$

in which $|\Delta|$ denotes the absolute value of Δ.   We see, therefore, that the amplitude of the deviated wave is proportional to both s and $|\Delta|$ when Δ is small and that the deviated wave is retarded by $\pm$¼ wavelength with respect to the undeviated wave according as Δ is greater than or less than zero, i.e., according as the optical path of the particle is greater than or less than the optical path of an equal thickness of the surround.

spread over the entire image plane, the image of the surround is illuminated by the undeviated wave whereas the image of the particle is illuminated by both the undeviated and the deviated wave. The phase and amplitude distribution of the light that illuminates the image of the surround is therefore that of the undeviated wave, i.e., of the S wave of Fig. II.4. Because the undeviated and deviated waves overlap upon the geometrical image of the particle, these two waves interfere to produce the resultant wave $(D + S)$ over the image of the particle. From the construction of Fig. II.4, $D + S = P$. The deviated and undeviated waves thus combine over the image of the particle to reproduce the P wave. The phase and amplitude distribution of the light that illuminates the image of the particle is therefore that of the P wave. In conclusion, the amplitude and phase distributions over the image of the surround and over the image of particle are, respectively, those of the S wave and those of the P wave. This conclusion is true irrespective of the value of Δ, the optical path difference between the particle and surround. It is also true irrespective of any differences in absorption which may be present between the particle and the surround.

It has been seen how the P and S waves originate in the object plane as the portions of the incident wave that are intercepted by the object particle and its surround, respectively. The amplitude and phase of the light that leaves the particle is therefore that of the P wave, whereas the amplitude and phase of the light that leaves the surround is that of the S wave. The conclusion of the previous paragraph is that the amplitude and phase of the light that enters the image of the particle is likewise the amplitude and phase of the P wave, whereas the amplitude and phase of the light that enters the image of the surround is that of the S wave. We conclude, therefore, that the phase and amplitude distributions over the object and image plane will be similar and that, consequently, the image will be similar to the object. This conclusion can be stated as a theorem which is usually attributed to Lummer (Theorem 2):

When the entire deviated and undeviated bundles of light which originate by diffraction at the object are admitted and transmitted by an aberration-free objective, the amplitude and phase distributions over the object plane and over the sharply focused image plane are similar and the image is similar in all details to the object.

As applied to real objectives, this theorem is an idealization, for no real objective is capable of transmitting the entire deviated bundle. The agreement between the theorem and experimental facts becomes closer as the numerical aperture of the objective and the size of the object details are increased.

It follows directly from Lummer's theorem that the image of a particle should show no contrast, irrespective of the optical path difference between the particle and the surround, when the light transmissions of the particle and the surround are alike. If the light transmissions of the particle and the surround are alike, the amplitude distribution over the object plane will be uniform. According to Lummer's theorem, the amplitude distribution over the image plane will then be uniform. Since the eye or photographic plate is sensitive only to the amplitude or to the energy density that is proportional to the square of the amplitude, the image plane will appear to be uniformly illuminated even though the phase distribution over the image plane is non-uniform. Consequently, the particle should be invisible when its light transmission does not differ from that of the surround.

One of the weaknesses or oversimplifications of the simplified theory of microscopy appears in the prediction that the particle should be invisible in the microscope whenever the light transmissions of the particle and the surround are alike no matter what optical path differences exist between the particle and the surround. It is a well-known experimental fact that when the optical path differences between the particle and its surround are greater than $\frac{1}{8}$ wavelength the particle is visible whether or not the iris in the substage condenser is stopped down. Furthermore, when the optical path difference is less than $\frac{1}{8}$ wavelength the visibility of the particle can be increased by stopping down the iris diaphragm in the substage condenser and by readjusting the state of focus of the image. Depending on the spherical aberration of the objective, the particle may be rendered visible when the optical path difference between the particle and its surround is only 0.04 wavelength. With these small optical path differences the visibility or contrast is poor, however, and the image becomes unduly distorted by the necessity of observing an out-of-focus image surrounded by an increased amount of adverse diffraction effects. The visibility of such particles in the ordinary microscope is due largely to the fortunate circumstance arising from the failure of real objectives to fulfill the conditions postulated in Lummer's theorem. When the optical path differences between the particle and the surround become small enough, the degree of visibility of the particle approaches zero, the value predicted by Lummer's theorem if the light transmissions of the particle and of the surround are equal.

3.2. Phenomena of phase microscopes

In phase microscopy a diffraction plate is introduced for the purpose of obtaining additional controlled violations of the conditions of Lum-

mer's theorem. These additional violations consist in altering the relative amplitude and phase of the deviated and undeviated waves originating by diffraction at the object specimen. This alteration is accomplished by taking advantage of the facts that the undeviated wave passes through the conjugate area of the diffraction plate and that most of the deviated wave passes through the complementary area of the diffraction plate. Because the characteristics of the image are determined by the interference phenomena that take place between the undeviated and deviated waves as they reach the plane of the image, and because the amplitude and phase of the resultant wave formed by the interference of the undeviated and the deviated waves depend on the relative amplitude and phase of the undeviated and deviated waves, it is possible to choose a diffraction plate that produces optimum contrast in the sharply focused image plane. The manner in which optimum contrast can be obtained in the sharply focused image plane will now be discussed in detail for the particle differing from its surround only by a small amount in optical path.

If the opening in the condenser diaphragm is chosen in the usual manner as a narrow annulus, as in Fig. II.5, the conjugate area of the diffraction plate formed by the image of the opening in the condenser diaphragm will also be a relatively narrow annulus. The complementary area is then the remaining area of the diffraction plate within the clear aperture of the second focal plane of the objective.

As we have seen in Section 3.1, the light radiated from a point C in the condenser diaphragm is incident as a substantially plane wave upon the object plane. The incident wave is split by diffraction at the object specimen into an undeviated S wave, which emerges from all elements of area in the object plane, and into a deviated D wave, which emerges from elements of area that are confined almost entirely to the particle. The undeviated wave passes through the conjugate area and is subsequently spread over the entire image plane, whereas the deviated wave is spread mainly over the complementary area of the diffraction plate and is then reconcentrated upon the neighborhood of the geometrical image of the particle. These phenomena are illustrated in Fig. II.5. The amplitude and phase distribution over the image of the surround is determined by the undeviated wave alone, whereas the amplitude and phase distribution of the light over the geometrical image of the particle is determined by the resultant wave produced by the interference of the undeviated and deviated waves as they pass through the geometrical image of the particle.

The ordinary microscope is one whose diffraction plate is uncoated so that the amplitude and phase transmissions of the conjugate and

complementary areas are equal.   We have seen that in the ordinary
microscope the deviated D wave, Fig. II.4, is retarded by practically
¼ wavelength with respect to the undeviated S wave when the optical
path of the particle exceeds the optical path of the surround by a small
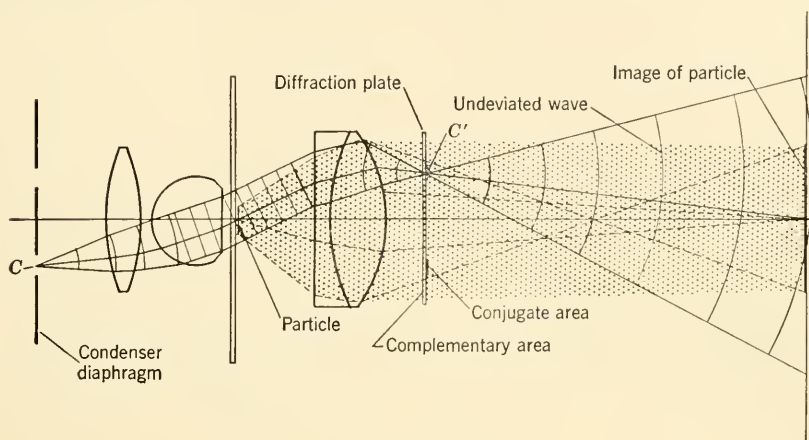
FIG. II.5.   Passage of the light radiated from a point C in the opening of the con-
denser diaphragm through the optical system of a phase microscope.   The undeviated
portion of the light wave diverging from any point C in the opening of the condenser
diaphragm is converged upon the conjugate area of the diffraction plate located near
the plane of the image of the condenser diaphragm and near the second focal plane
of the objective.   The *conjugate area* coincides with the image of the opening of the
condenser diaphragm.   All the undeviated rays from points C pass through the
conjugate area in a properly designed and adjusted system.   The deviated rays are
distinguished by the broken lines.   They arise by diffraction at the particle and may
occupy the entire shaded cross section and the entire area of the diffraction plate.
If the conjugate area is small compared with the total area of the diffraction plate,
most of the deviated rays pass through the *complementary area*, i.e., through that
area of the diffraction plate which is unoccupied by the image of the opening of the
condenser diaphragm.

amount, Δ, for a particle whose amplitude transmission is substantially
the same as that of the surround.   When Δ is very small, the amplitude
of the D wave is less than that of the S wave and becomes vanishingly
small as Δ approaches zero.

Suppose that the undeviated S wave is artificially retarded by ¼
wavelength.   This artificial retardation can be brought about by apply-
ing a coating of refracting material, such as magnesium fluoride, to the
conjugate area of the diffraction plate.   If the thickness of the magnesium
fluoride is such as to increase the optical path of the conjugate area by
¼ wavelength with respect to the uncoated complementary area, only

the undeviated wave will be retarded by ¼ wavelength. This selective retardation follows directly from the fact that the undeviated wave passes through the conjugate area whereas the deviated wave passes through the complementary area. The effect of retarding the undeviated S wave by ¼ wavelength is to slide the entire S wave of Fig. II.4
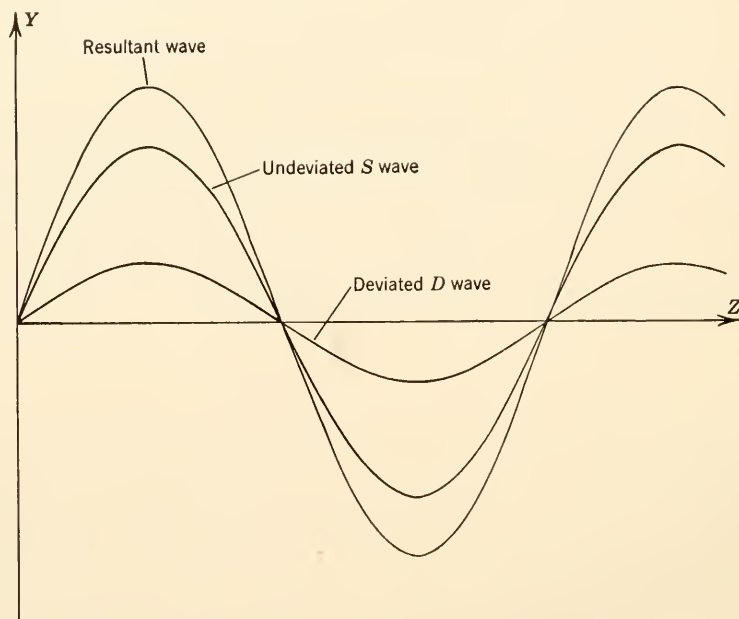
FIG. II.6. Constructive interference between the undeviated S wave and the deviated D wave as they overlap the image of an object particle whose optical path difference Δ with respect to its surround is small and positive. In the phase microscope, the undeviated and deviated waves have been made to agree in phase by introducing a phase retardation of ¼ wavelength into the undeviated wave with respect to the deviated wave, whose relative phase retardation is nominally ¼ wavelength with respect to the S wave. The resultant wave is stronger than the undeviated S wave. Consequently the particle will appear brighter than its surround in the plane of sharpest focus.

to the left by ¼ wavelength. The relation between the deviated and undeviated waves becomes that illustrated in Fig. II.6. It can be seen that the undeviated and deviated waves interfere constructively to produce the indicated resultant wave of greater amplitude than that of the S wave. Since the geometrical image of the particle is illuminated by this resultant wave whereas the image of the surround is illuminated by the S wave alone, the particle appears brighter than its surround.

Suppose that, on the other hand, the deviated D wave of Fig. II.4 is retarded by an additional amount of $\frac{1}{4}$ wavelength with respect to the undeviated S wave by placing the refracting coating upon the complementary area of the diffraction plate. The total retardation of the deviated wave with respect to the undeviated wave is then $\frac{1}{2}$ wave-
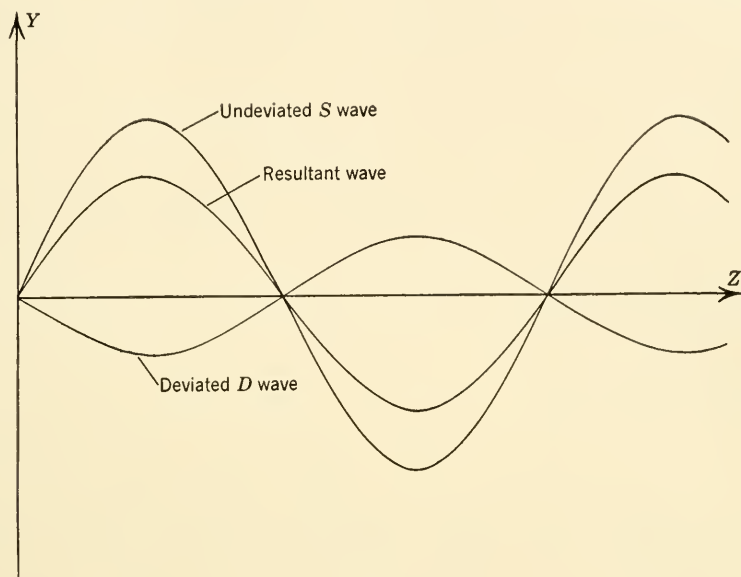
Fɪɢ. II.7. Destructive interference between the undeviated S wave and the deviated D wave as they overlap the image of an object particle whose optical path difference Δ with respect to its surround is small and positive. The deviated wave has been rendered $\frac{1}{2}$ wavelength out of phase with respect to the S wave by the introduction of an additional quarter-wave phase retardation into the D wave beyond its nominal quarter-wave phase retardation with respect to the undeviated S wave. The resultant wave is now weaker than the S wave. The particle will therefore appear darker than its surround. Destructive interference is not complete, because the amplitude of the undeviated wave still exceeds the amplitude of the deviated wave.

length. Consequently, the undeviated and deviated waves interfere destructively over the geometrical image of the particle, as indicated in Fig. II.7, to produce a resultant wave of smaller amplitude than that of the undeviated wave. The particle therefore appears darker than its surround. In summary of the last two paragraphs, a particle whose optical path exceeds that of the surround by a small amount will appear brighter or darker than its surround according as the optical path of the conjugate area of the diffraction plate is increased or decreased by $\frac{1}{4}$

wavelength with respect to the optical path of the complementary area of the diffraction plate.

The early phase microscopes were constructed with diffraction plates whose conjugate area consisted of a suitably shaped groove etched to a sufficient depth in a glass plate to reduce the optical path of the groove by $\frac{1}{4}$ wavelength with respect to the unetched portion of the plate. By etching the groove more deeply and by filling it with a clear cement of higher index than that of the glass plate, the optical path of the groove could be increased by $\frac{1}{4}$ wavelength with respect to the unetched portion of the plate.   In accordance with the conclusions stated above, a particle whose optical path was slightly greater than that of the surround appeared brighter or darker than the surround according as the etched groove was filled or unfilled.   Although it is possible to find particles that appear in excellent bright or dark contrast when the conjugate and complementary areas of the diffraction plate are treated by etching or by deposition of refracting materials so that they differ in optical path by $\frac{1}{4}$ wavelength, it was soon discovered that the contrast in the image of most particles can be improved greatly by adding an absorbing material to the conjugate area.

The reason for the above-mentioned improvement in contrast can be understood from Figs. II.6 and II.7.   It has been noted that the deviated D wave vanishes with the optical path difference Δ and has an amplitude that is small compared with the amplitude of the undeviated S wave when the optical path difference Δ between the particle and surround is small and when the particle and surround are equally transparent. Under these circumstances the wave that is deviated from its course by diffraction at the object is much weaker, as is to be suspected, than the wave that is undeviated by diffraction at the object.   With reference first to Fig. II.7, suppose that the amplitude of the undeviated wave is reduced by passage through an absorbing material placed upon the conjugate area to the amplitude of the deviated wave.   The amplitudes of the D and S waves of Fig. II.7 are now to be drawn alike, as in Fig. II.8.   These two waves are, therefore, equal and opposed and so annihilate one another by destructive interference; thus their resultant is zero.   Because the particle is illuminated by the vanishing resultant wave whereas the surround is illuminated by the S wave of reduced amplitude, the particle should appear black against a surround of reduced brightness.   Provided that the original source of illumination is strong enough, the particle should appear in greatly improved dark contrast.   This phenomenon, which is predictable from the simplified theory, is in qualitative agreement with experiment.

With reference to Fig. II.6, suppose again that the amplitude of the

undeviated wave has been reduced to the amplitude of the deviated wave by passage through an absorbing material placed on the conjugate area of the diffraction plate. The undeviated and deviated waves now coincide and produce by constructive interference a resultant wave whose amplitude is twice as large as the amplitude of the undeviated wave. Because brightness is proportional to the square of the amplitude and because the image of the particle is illuminated by the resultant wave whereas the image of the surround is illuminated by the undeviated
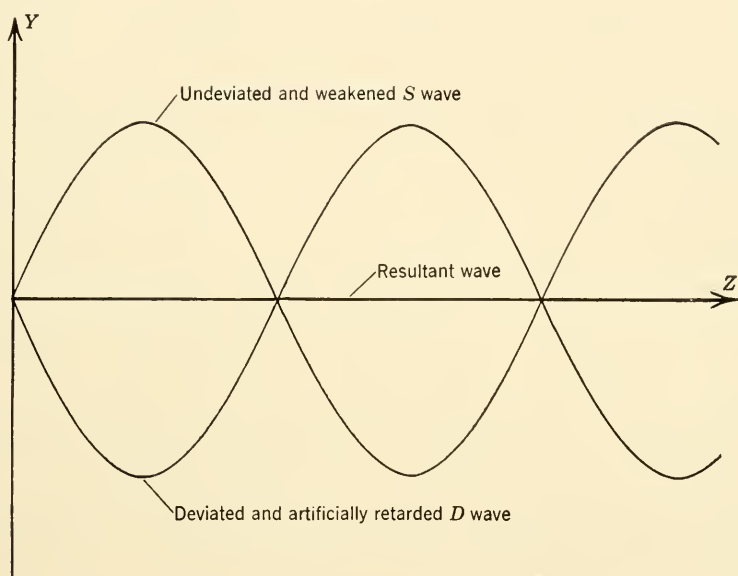
Fig. II.8. Complete destructive interference between the undeviated S wave and the deviated D wave as they overlap the sharply focused image of the particle after passing through a diffraction plate that equalizes the amplitudes of the undeviated and deviated waves and that renders these two waves different in phase by $\frac{1}{2}$ wavelength. The particle will appear black against a background of reduced brightness.

wave, the image of the particle is four times as bright as the image of the surround. The effect of adding the absorbing material to the conjugate area is, therefore, to reduce the brightness of the surround more rapidly than the brightness of the particle until the particle appears distinctly brighter than the surround. In principle, the relative brightness of the particle can be increased in this manner until the conjugate area is opaque and the surround is black as in the well-known Schlieren method.

Although the particle appears with maximum bright contrast in the

Schlieren method, the image is not advantageous for the usual purposes of microscopy on account of the ensuing loss of definition in the image. Deterioration in the definition results from the fact that the image is formed by the deviated wave alone when the undeviated wave has been blocked at the conjugate area. At least some of the undeviated wave should be transmitted in order to obtain a reasonably good image.

As a compromise between the degree of bright contrast and definition, a fairly reliable rule of thumb is to add no more absorbing material to the conjugate area than is required to reduce the amplitude of the undeviated wave to the amplitude of the deviated wave. Optimum useful contrast in the image is therefore obtained when the conjugate and complementary areas of the diffraction plate are coated with absorbing materials to equalize the amplitudes of the undeviated and deviated waves and with refracting materials to cause the undeviated and deviated waves to interfere constructively or destructively according as the particle appears in bright or dark contrast. We have seen that, when the particle differs from its surround only in optical path and when the optical path of the particle exceeds that of the surround by a small amount, the particle appears bright or dark according as the optical path of the conjugate or complementary area is increased by $\frac{1}{4}$ wavelength. Such particles are common in biological research.

Particles whose optical path is slightly smaller than that of the surround are encountered less frequently. With such particles the S wave of Fig. II.4 lags behind the particle P wave by a small amount Δ. If the D wave is constructed so that $D + S = P$, the required D wave leads the S wave by almost $\frac{1}{4}$ wavelength. Since the undeviated wave is now retarded by $\frac{1}{4}$ wavelength with respect to the deviated wave, the two waves can be made to interfere constructively for obtaining a bright particle by increasing the optical path of the complementary area of the diffraction plate by $\frac{1}{4}$ wavelength with respect to the optical path of the conjugate area, or the two waves can be made to interfere destructively for obtaining a dark particle by increasing the optical path of the conjugate area by $\frac{1}{4}$ wavelength with respect to the complementary area. Contrast in the image can be expected again to be optimum when enough absorbing material is added to the conjugate area to equalize the amplitudes of the undeviated and deviated waves. Also these conclusions drawn from the simplified theory for particles of lower refractive index than their surround are in qualitative agreement with experiment.

The above considerations relative to the phase microscopy of particles that differ from their surround only by a small amount in optical path

are worth summarizing as the following important and practical theorem (Theorem 3):

If the optical path of the particle exceeds the optical path of its surround by a small amount, the particle will appear bright or dark according as the optical path of the conjugate area of the diffraction plate is increased or decreased by $\frac{1}{4}$ wavelength with respect to the optical path of the complementary area. If, on the other hand, the optical path of the surround exceeds the optical path of the particle by a small amount, the particle will appear bright or dark according as the optical path of the conjugate area is decreased or increased by $\frac{1}{4}$ wavelength with respect to the optical path of the complementary area. Furthermore, the contrast in the image is near optimum when enough absorbing material is added to the conjugate area to equalize the amplitudes of the undeviated and deviated waves which arise by diffraction at the object specimen.

The practical importance of this theorem is enhanced by the fact that also its converse is true (Theorem 4):

If the particle appears bright or dark according as the optical path of the conjugate area is increased or decreased by $\frac{1}{4}$ wavelength with respect to the complementary area, then the optical path of the particle exceeds the optical path of an equal thickness of its surround. If, on the other hand, the particle appears bright or dark according as the optical path of the conjugate area is decreased or increased by $\frac{1}{4}$ wavelength with respect to the optical path of the complementary area, the optical path of the particle is less than the optical path of an equal thickness of the surround. The conjugate area of the diffraction plate coincides with the image of the opening in the diaphragm of the substage condenser. This image is projected by the substage condenser and the intervening lenses of the objective upon the diffraction plate and is clearly visible as the brightly illuminated area when the objective is viewed down through the body tube in the absence of the eyepiece. Whether or not the quarter-wave coating has been applied to the conjugate area or to the adjacent complementary area can be ascertained from the catalogue data of the phase objective. From this important information it is possible to determine from the above theorem whether the refractive index of the particle is higher or lower than the refractive index of its surround, provided that the optical paths of the particle and the surround differ only slightly, for example by $\frac{1}{20}$ wavelength or less.

We have seen that, as the optical path difference Δ between the particle and the surround approaches zero, the amplitude of the deviated wave approaches zero also. This means that in order to obtain optimum contrast it is necessary to add increasing amounts of absorption to the

conjugate area as Δ approaches zero. Finally, both the undeviated and deviated waves become so weak with diminishing Δ that the entire image appears dark and the particle becomes invisible. The value of Δ at which the particle is invisible will depend on the intensity of the available sources of light and on the amount of scattering of the optical system. With present-day phase microscopes the particle can be rendered visible when the optical path difference Δ is well below $\frac{1}{100}$ wavelength. It is advantageous to use light of short wavelength as the optical path differences become small.

It will be apparent from the previous paragraph that, even with the restricted class of particles that differ from their surround only by small amounts in optical path, more than one diffraction plate is required in order to obtain optimum contrast with particles of different optical path. The series of diffraction plates will have conjugate and complementary areas differing by the fixed amount of $\frac{1}{4}$ wavelength in optical path. However, the plates will vary appreciably as regards the amount of absorbing material added to the conjugate area. Fortunately, a single diffraction plate serves moderately well for the entire practical range of small optical path differences Δ, provided that sufficient absorption has been added to its conjugate area. It is to be expected that with particles whose optical path difference with respect to the surround is not small or with particles that absorb selectively with respect to their surround the relation between the undeviated and deviated waves that arise by diffraction at the object specimen will vary greatly from one particle to another. Correspondingly, the conjugate and complementary areas of the diffraction plate must be coated differently for use with the various particles in order to obtain optimum contrast in the image. In fact, particles exist for which the deviated wave is stronger than the undeviated wave so that the absorbing material has to be applied to the complementary area of the diffraction plate in order to equalize the amplitudes of the undeviated and deviated waves for optimum contrast in the image. The need for a series of diffraction plates can therefore be seen even from this simplified discussion of phase microscopy.

3.3. Extension of the elementary theory to object fields containing more than one particle

The elementary theory of phase microscopy is easily extended to include object fields consisting of more than one particle. Each particle gives rise to a deviated wave that, after passage through the objective, is reconcentrated upon the neighborhood of the image of the particle from which it originated. The undeviated S wave remains substantially the same as when the field contains but a single particle. If the particles

are far enough apart with relation to the resolving power of the objective, a negligible amount of overlapping will take place in the image plane of the deviated waves that belong to different particles. Under these circumstances, the images of the various particles will be formed independently of one another. The above-described principles which apply to the image formation of a single particle apply, therefore, to the imagery of each particle in a field consisting of several well-separated particles. When the separation of two or more particles becomes so small that the overlapping of their diffraction images is no longer negligible, more general considerations are required in order to understand the resulting image formation.

3.4. Extension of the elementary theory to object specimens having periodic structure

If a simple diffraction grating is employed as the object specimen, the troughs of the grating can be regarded as a complex particle and the elevations of the grating can be regarded as the surround, or vice versa. Provided that the light transmission of the troughs and elevations are alike, and provided that the optical path difference between the elevations and troughs is a small fraction of a wavelength, the state of contrast between the geometrical images of the troughs and of the elevations can be predicted from the very same rules that have been explained in the above subsections for an object field consisting of a single particle in a uniform surround. Suppose, for example, that the optical path through the elevations of the grating exceeds the optical path through the troughs. Let us regard the elevations as the "particle." The particle, and hence the elevations, should appear brighter or darker than the troughs according as the optical path of the conjugate area is increased or decreased with respect to the optical path of the complementary area by $\frac{1}{4}$ wavelength. Contrast in the image should be optimum when the amplitudes of the undeviated and deviated waves have been equalized by placing the absorbing material upon the conjugate area of the diffraction plate. These predictions are in good qualitative agreement with experiment so long as the optical path difference between the elevations and troughs is small.

The crossed or double periodic structure of many object specimens is due to a lattice arrangement of particles. If the optical path of these particles exceeds that of their surround by a small amount, the conclusions of the elementary theory may be applied to predict that the particles will appear brighter or darker than the surround according as the optical path through the conjugate area of the selected diffraction plate has been increased or decreased by approximately $\frac{1}{4}$ wavelength

with respect to the optical path through the complementary area. Furthermore, contrast in the image will be reversed as the refractive index of the surround is increased from a value below that of the particle to a value slightly higher than the refractive index of the particles. Theorems 3 and 4 may, therefore, be applied to a variety of object specimens.
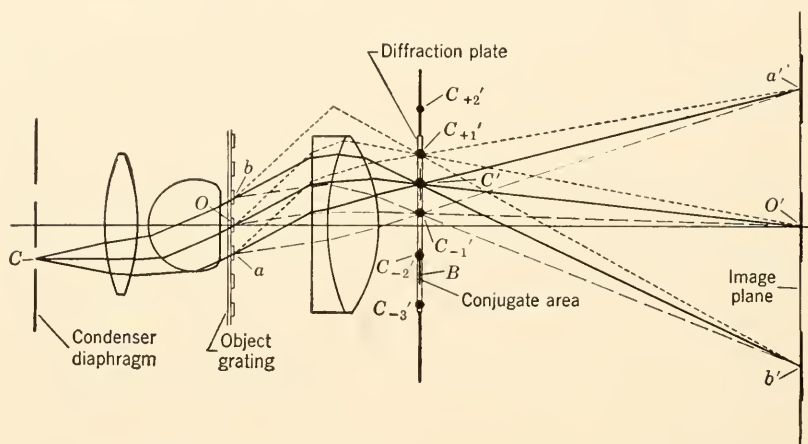
FIG. II.9. Passage of the spectral orders from an object grating through the phase microscope. Only selected rays of the zero and first orders are shown, in order to avoid confusion. In reality the grating spacing is much smaller than illustrated. The rays of the zero and first order are drawn as full and broken lines, respectively. The lines with short dashes illustrate that portion of the first order which has been deviated upward at the object grating. The lines with long dashes illustrate that portion of the first order which has been deviated downward at the object grating. C' is the image of C as formed by the light in the zero order. C_{+n}' is the image of C as formed by the higher orders $n = 1, 2, 3$, etc. Note how the undeviated and deviated rays from, for example, point a in the object grating are focused by the objective to form the image a' of a.

3.5. Passage of the undeviated and deviated waves from a simply periodic object grating through a phase microscope

It is highly instructive to examine, if only briefly, the paths followed by the undeviated and deviated waves that arise by diffraction at a simple diffraction grating employed as the object specimen and which then pass through the phase microscope. Light rays from a point C in the condenser diaphragm emerge from the substage condenser as a substantially parallel bundle of rays, as in Fig. II.9. One portion of this bundle of rays is undeviated by the grating and continues through the

optical system in the manner indicated by the unbroken rays.   These rays of the zero spectral order converge upon the point C' to form an image of point C within the conjugate area of the diffraction plate. Thereafter the undeviated rays diverge and spread with a high degree of uniformity over the plane of the image.   A second portion of the bundle of rays which is incident upon the grating becomes deviated by diffraction as a set of rays which belong to the first spectral order.   One of the families of rays which belong to the first order is deviated downward with respect to the undeviated rays of the zero order; the second of the two families is deviated upward.   The upward family of rays is focused about the point C_{+1}'; the downward family is focused about the point C_{-1}'.   Points C_{+1}' and C_{-1}' fall in the plane of the diffraction plate and constitute secondary images of the point C as formed by the set of rays belonging to the first spectral order.   In a similar manner the rays belonging to any higher spectral order n form secondary images of C at points $C_{\pm n}'$.   Only a limited number of the secondary images $C_{\pm n}'$ fall within the clear aperture of the diffraction plate.   For example, C_{+2}' is illustrated as blocked by a limiting diaphragm which restricts the clear aperture of the objective.   Whenever a secondary image produced by any spectral order does not fall within the clear aperture of the objective, the corresponding portion of this order is blocked and cannot participate in the image formation of the object specimen.

In the illustration of Fig. II.9 only the secondary images C_{+1}', C_{-1}', C_{-2}', and C_{-3}' can participate with the primary image C' to determine by interference the image formed in the plane of the image.   In Fig. II.9 not even the secondary image C_{+1}' is complete, for the first-order ray emanating from point b cannot reach point C_{+1}'.   The primary and secondary images can be observed in a microscope by placing at the plane of the condenser diaphragm an opaque disk which contains a small opening at point C and by looking down the body tube of the microscope whose eyepiece has been removed.   If desired, the plane of the diffraction plate may be examined with the auxiliary telescope which is ordinarily furnished for the purpose of aligning the optical system of the phase microscope.   If the system has been aligned properly, the bright primary image C' of the zero order will fall well within the conjugate area.   When white light is used, the secondary images will be spread into a spectrum because rays of longer wavelength suffer the greater deviation at the object grating.   Now the light carried by the first and higher spectral orders belongs to the deviated wave.   Hence we see from the above considerations and experiments that in general

only a portion of the deviated wave succeeds in reaching the plane of the image. One assumption made in the elementary theory of phase microscopy is that the entire deviated bundle reaches the plane of the image.

The separations $C_{\pm n}'$, C' increase with decreasing spacing of the lines of the object grating, and conversely. If, therefore, the lines of the grating are suitably spaced, points C_{+1}' and C_{-1}' will fall in the complementary area. But with relatively coarse gratings it is possible that one or both of points C_{+1}' and C_{-1}' may fall within the conjugate area. With an unfortunately spaced fine grating it is possible that point C_{-1}' may escape the portion of the conjugate area which is adjacent to C', only to fall into another portion of the conjugate area near point B. In such special cases another diffraction plate whose conjugate area is located elsewhere must be selected in order to meet the physical requirements for obtaining phase microscopy. In Fig. II.9 the secondary spectral image C_{-2}' is illustrated as falling within the conjugate area. Although such an occurrence can be expected to impair contrast in the image, its effect is not likely to be serious. If the conjugate area is made very narrow, the likelihood that any point $C_{\pm n}'$ will fall within the conjugate area becomes so small that the first or higher spectral orders may be said to pass through the complementary area. A second assumption of the elementary theory is then fulfilled. In fact, the method of phase microscopy hinges upon the physical possibility of complete or partial separation of the undeviated and deviated spectral orders at the conjugate and complementary areas of the diffraction plate, whether these orders are determined by diffraction at an object grating or at some other object specimen.

It will be noted that the undeviated and deviated rays which leave a particular point in the object grating, for example point a, are refocused about the corresponding image point a'. It is seen how the undeviated rays pass through the conjugate area, how the deviated rays spread over the complementary area, and how these rays (and hence the undeviated and deviated waves) overlap in the plane of the image to form the image a' of a.

If the object grating is removed, there will be no deviated rays. Consequently, the light incident upon the object plane obeys the laws of geometrical optics and passes only through the conjugate area. For this reason, it is preferable to remove the object specimen in aligning the phase microscope. If the object specimen is allowed to remain on the stage, specimens such as gratings, diatoms, and paramecia are likely to deviate so much light into the complementary area that accurate alignment of the instrument becomes difficult or impossible.

4. REPRESENTATION OF THE AMPLITUDE AND PHASE BY COMPLEX NUMBERS

The laws expressed verbally and graphically in the preceding section can be formulated more elegantly and comprehensively by stating the interference phenomena which take place between the undeviated and deviated waves either in terms of the trigonometric functions, as in a recent paper by Keck and Brice (1949), or in terms of the equivalent complex numbers. Complex numbers are preferred because they are more readily multiplied or added than the trigonometric functions.

The undeviated and deviated waves are vectors whose complete specifications include direction, phase, and amplitude of vibration. The direction of vibration may be ignored because all portions of a wave train which is emitted by the source of light continue to vibrate in the same direction as the wave train traverses the object specimen and the optical system of a phase microscope. Within the scope of an elementary treatment of phase microscopy the direction of vibration of the wave train has no influence upon the character of the image. It is, however, necessary to bear in mind that the undeviated and deviated waves both originate and recombine as two simple harmonic motions oscillating in the same straight line.

A number z of the form

$$z = x + iy, \tag{4.1}$$

in which x and y are real numbers and $i \equiv (-1)^{\frac{1}{2}}$, is called a complex number. x and y are called the real and imaginary parts of the complex number z. The absolute value of z is denoted by $|z|$ and is defined as

$$|z| = (x^2 + y^2)^{\frac{1}{2}}. \tag{4.2}$$

The square of the absolute value of a complex number is equal to the sum of the squares of its real and imaginary parts. The complex number z can be represented geometrically as the vector OP drawn from O to P in the rectangular coordinate system XY of Fig. II.10. The direction of the vector OP is specified by means of its angular rotation θ. It will be noted that $(x^2 + y^2)^{\frac{1}{2}} \equiv |z|$ is equal to the length or amplitude a of the vector OP. The absolute value of a complex number is therefore equal to the amplitude of the complex number.

As indicated in Fig. II.10, $x = a \cos \theta$ and $y = a \sin \theta$. If these values of x and y are substituted into Eq. 4.1, the complex number z assumes the polar form

$$z = a(\cos \theta + i \sin \theta). \tag{4.3}$$

By definition

$$e^{i\theta} = \cos\theta + i\sin\theta; \tag{4.4}$$

$$e^{-i\theta} = \cos\theta - i\sin\theta. \tag{4.5}$$

Hence any complex number can be written in the form

$$z = a(\cos\theta + i\sin\theta) = ae^{i\theta} \tag{4.6}$$

in which a is the amplitude and θ is the argument or phase of the complex number. Equation 4.6 states the two forms of complex numbers as we
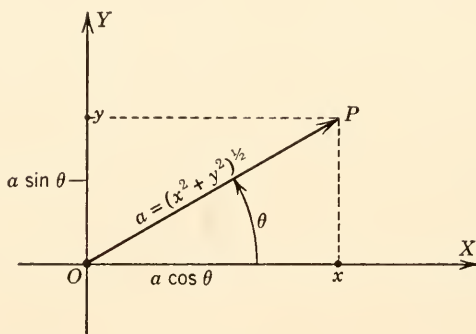
FIG. II.10.   Representation of a complex number
$z = x + iy = a(\cos\theta + i\sin\theta)$ as a vector OP in the XY plane.

shall use them in the theory of phase microscopy.   It is worth noting that

$$z = a \text{ when } \theta = 0;$$

$$z = -a \text{ when } \theta = \pi; \tag{4.7}$$

$$z = \pm ia \text{ according as } \theta = \pm\pi/2.$$

Suppose that we are given two complex numbers z in the form

$$z_1 = a_1(\cos\theta_1 + i\sin\theta_1);$$

$$z_2 = a_2(\cos\theta_2 + i\sin\theta_2).$$

The rule of addition is

$$z_1 + z_2 = (a_1\cos\theta_1 + a_2\cos\theta_2) + i(a_1\sin\theta_1 + a_2\sin\theta_2). \tag{4.8}$$

To add two complex numbers, add their real parts and their imaginary parts.

In order to multiply two complex numbers, it is more convenient and

significant to write them in their exponential forms:

$$z_1 = a_1 e^{i\theta_1};$$

$$z_2 = a_2 e^{i\theta_2}.$$

Then, just as

$$h_1 e^{m\theta_1} \cdot h_2 e^{m\theta_2} = h_1 h_2 e^{m(\theta_1 + \theta_2)},$$

so also

$$z_1 z_2 = a_1 a_2 e^{i(\theta_1 + \theta_2)}. \tag{4.9}$$

To multiply two complex numbers, multiply their amplitudes and add their phases.

Furthermore,

$$\frac{z_1}{z_2} = \frac{a_1}{a_2} e^{i(\theta_1 - \theta_2)}. \tag{4.10}$$

To divide two complex numbers, divide their amplitudes and subtract their phases.

The above elementary properties of complex numbers suffice for the purposes of an elementary theory of phase microscopy. The reader to whom complex numbers are new should not attempt to attach any significance to a complex number beyond the definition of a complex number, together with its amplitude and phase, and beyond the rules of addition and multiplication of two complex numbers. It is natural to use complex numbers in treating the interference between two waves or the passage of a wave through a diffraction plate for the following reasons:

1. The amplitude and phase of a wave are exactly analogous to the amplitude and phase of a complex number.

2. The interference between two waves of different amplitude and phase is exactly analogous to the addition of two complex numbers.

3. The alteration of the amplitude and phase of a wave upon passing through a medium, for example the diffraction plate, is exactly analogous to the multiplication of two complex numbers one of which represents the amplitude and phase of the incident wave and the other of which represents the amplitude and phase transmission of the medium.

The first analogy is self-evident. With respect to the second analogy, let the amplitude and phase of the two interfering waves be denoted by the complex numbers $z_1 = a_1 e^{i\theta_1}$ and $z_2 = a_2 e^{i\theta_2}$ and let the vectors representing z_1 and z_2 be drawn upon the XY plane as in Fig. II.11. The parallelogram construction for finding the amplitude a and the phase angle θ of the complex number z which is equal to the sum of the complex numbers z_1 and z_2 will be recognized as identical with the

parallelogram method for finding the resultant of two different simple harmonic motions oscillating in the same straight line.   If, therefore, the amplitudes and phases of two interfering waves are represented by two complex numbers z_1 and z_2, the amplitude and phase of the resultant wave is given by the complex number which is equal to the sum of the complex numbers z_1 and z_2.   With respect to the third analogy, let the amplitude and phase of the wave which is incident upon a medium be represented by the complex number $z_1 = a_1 e^{i\theta_1}$, and let the amplitude
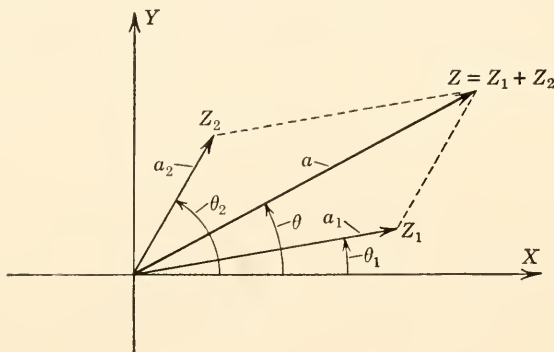
FIG. II.11.   Geometrical representation of the sum $ze^{i\theta}$ of two complex numbers $z_1 = a_1 e^{i\theta_1}$ and $z_2 = a_2 e^{i\theta_2}$.

and phase transmission of the medium be represented by the complex number $z_2 = a_2 e^{i\theta_2}$. θ_2 is then the optical path of the medium expressed in radians instead of wavelengths.   Now it is a well-known experimental fact that, when an incident wave of amplitude a_1 and phase θ_1 has passed through a medium of amplitude transmission a_2 and phase transmission θ_2, the amplitude of the emergent wave is $a_1 a_2$ and the phase of the emergent wave is $\theta_1 + \theta_2$. If we now represent the emergent wave by the complex number $z = ae^{i\theta}$, experiment requires that

$$z = ae^{i\theta} = a_1 a_2 e^{i(\theta_1 + \theta_2)} = a_1 e^{i\theta_1} \cdot a_2 e^{i\theta_2}. \qquad (4.11)$$

The complex number describing the amplitude and phase of the emergent wave is therefore given by the product of the complex numbers representing the amplitude and phase of the incident wave and the amplitude and phase transmission of the medium.

5. VISUAL EFFECT PRODUCED BY A COMPLEX WAVE

Light waves vibrate so rapidly that the eye is not able to follow the instantaneous values of the electric vector but can detect only the time

average of the energy density associated with the wave. The instantaneous state of vibration of a wave can also be represented by a complex number z which includes the time t and the period T of a complete vibration in accordance with the relation

$$z = ac^{-i\left(\frac{2\pi t}{T}-\phi\right)}. \tag{5.1}$$

Alternately,

$$z = ae^{\frac{-2\pi it}{T}}e^{i\phi}. \tag{5.2}$$

In these equations a is the amplitude of the wave and ϕ is the phase angle or *phase retardation*. It follows from Eq. 4.6 that the time factor $e^{-2\pi it/T}$ assumes the same value each time t is increased by the period T. The vibration described by Eq. 5.1 or 5.2 is therefore periodic.

It will be noted that the phase retardation ϕ appears with the positive sign in the phase factor $e^{+i\phi}$ of Eq. 5.2. We see from Eq. 5.1 that, if the phase retardation ϕ or optical path is increased, t will have to be increased in order to leave the state of vibration represented by z unaffected. This means physically that, if we increase the optical path of a medium, it will take the wave a longer time to present to the observer a preassigned state of vibration. In other words, a given portion of the wave train arrives at a later moment. Accordingly, the phase retardation ϕ will be considered henceforth as positive when it corresponds to an increase in the optical path, and the phase retardation will be preceded by $+i$ in the phase factor $e^{+i\phi}$.

The time average of the energy density produced by the wave is proportional to $|z|^2$. It is often convenient in manipulating complex numbers z from equations of the type of Eq. 5.2 to write $|z|$ in its expanded form:

$$|z| = a|e^{-2\pi it/T}| \ |e^{i\phi}|. \tag{5.3}$$

Since

$$|e^{i\theta}|^2 = |\cos\theta + i\sin\theta|^2 = \cos^2\theta + \sin^2\theta = 1,$$

where θ is equal to ϕ or $-2\pi t/T$,

$$|z|^2 = a^2. \tag{5.4}$$

The average energy density is therefore proportional to the square of the amplitude a. With rapid vibrations the eye can detect only the average energy density as given by Eq. 5.4. Since brightness is proportional to the average energy density, we conclude that the brightness is proportional to the square of the amplitude of the complex number which represents the amplitude and phase of the image-producing light wave.

6. REPRESENTATION OF THE UNDEVIATED AND DEVIATED WAVES

It will be noted from Fig. II.5 that the light radiated from a point C in the condenser diaphragm passes through the object specimen obliquely. With extended sources of light most of the light is necessarily incident obliquely upon the object plane. This obliquity is usually ignored in the elementary discussions of phase microscopy, but even a simplified explanation should take into account the large phase varia-
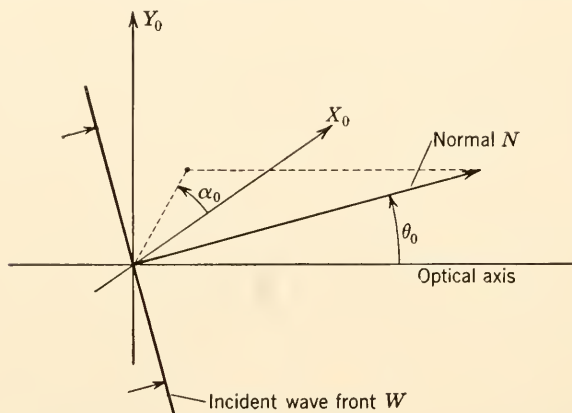
FIG. II.12. The incidence of an arbitrarily inclined wave front W upon the object plane X_0Y_0. The polar angle θ_0 and the azimuthal angle α_0 of the normal N to the wave front are arbitrary.

tions introduced by the inclination of the wave fronts which illuminate the object specimen. The incidence of an inclined wave front upon the object plane X_0Y_0 is illustrated in Fig. II.12. It is sufficient to select a wave front that intersects the object plane along the X_0 axis and to consider the simpler orientation of Fig. II.13.

The amplitude of the incident wave front will be taken as unity and its phase retardation ϕ as zero, so that the number unity represents the amplitude and phase along the incident wave front. Because the wave front is inclined at an angle θ_0 with respect to Y_0, the inclined wave front induces a variable phase distribution along the Y_0 direction in the object plane. The wave front that intersects a point y_0 will be a wave front which is parallel to W but which belongs to a slightly earlier portion of the incident wave train. The phase of the wave disturbance at $y_0 = y_0$ is therefore advanced with respect to the wave disturbance present at $y_0 = 0$. Since $d = y_0 \sin \theta_0$, the optical path difference d is $n_0 y_0 \sin \theta_0 / \lambda$ wavelengths or $2\pi n_0 y_0 \sin \theta_0 / \lambda$ radians. Let all

distances be measured in wavelengths and let

$$\sin \theta_0 \equiv \rho_0. \tag{6.1}$$

The optical path difference along d is then $2\pi n_0 y_0 \rho_0$ radians, where n_0 is the refractive index of the object space. The wave disturbance incident at $y_0 = y_0$ is therefore *advanced* by $2\pi n_0 y_0 \rho_0$ radians with respect to the wave disturbance incident at $y_0 = 0$. In accordance with the
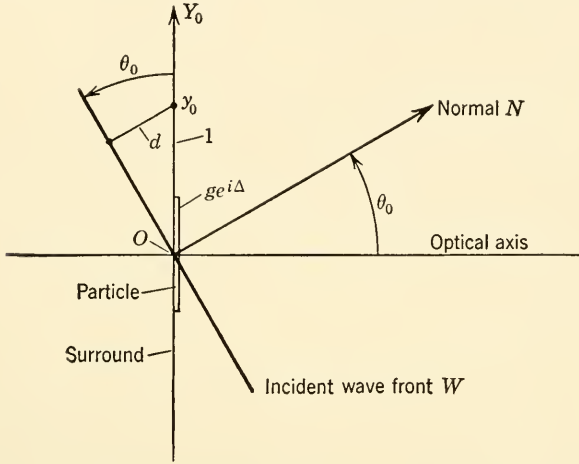
FIG. II.13. Reorientation of the X_0 direction so that the incident wave front W intersects the X_0 axis. The azimuthal angle α_0 is then zero. $ge^{i\Delta}$ is a complex number which specifies the amplitude and phase transmission of the particle relative to the surround.

convention adopted with respect to the phase factor $e^{+i\phi}$ in Eq. 5.2, ϕ is negative when it represents an advance in phase. Hence

$$\phi = -2\pi n_0 y_0 \rho_0. \tag{6.2}$$

If we now let w denote the amplitude and phase of the incident wave disturbance which is in actual contact with the object plane,

$$w = 1 \cdot e^{i\phi} = e^{-2\pi i n_0 y_0 \rho_0}. \tag{6.3}$$

We shall refer henceforth to w as the incident wave. It is to be distinguished from the inclined wave front W which we shall henceforth ignore.

Several advantages are gained without any essential loss of generality by representing the amplitude and phase transmission of the medium surrounding the particle by the number unity, provided that the sur-

rounding medium is uniform optically. The particle will be assumed to be optically uniform also. As indicated in Fig. II.13, the relative amplitude and phase transmission of the particle may now be represented by the complex number $ge^{i\Delta}$. *g is physically the ratio of the amplitude transmission of the particle to the amplitude transmission of an equal thickness of the surround, and Δ is the difference between the optical path of the particle and the optical path of an equal thickness of the surround, with Δ expressed in radians and considered positive when the optical path of the particle exceeds that of the surround.*

In describing the undeviated and deviated waves which arise by diffraction at the object specimen, we have only to retrace in a more quantitative manner the steps already taken in Section 3. A portion of the incident wave w, with amplitude and phase described by Eq. 6.3, passes through the surround and is designated as the S wave. The second portion of the wave w passes through the particle and is designated as the P wave. The P wave is then broken into two waves, one of which is identical with the S wave and the other of which is designated as the D wave. The incident w wave may therefore be regarded as broken by diffraction into an S wave which extends over the whole object plane and into a D wave which extends over the neighborhood of the particle. The extended S wave was shown to have the properties of the undeviated wave, and the D wave was shown to have the properties of the deviated wave. Since the amplitude and phase transmission of the surround is represented by the complex number unity, the incident w wave emerges from the surround with amplitude phase which we describe by the complex number S and which obeys the relation

$$S = 1 \cdot w = w = e^{-2\pi i n_0 y_0 \rho_0}. \tag{6.4}$$

Since the amplitude and phase transmission of the particle is represented by the complex number $ge^{i\Delta}$, the incident w wave emerges from the particle with the amplitude and phase which we represent by the complex number P and which obeys the relation

$$P = wge^{i\Delta} = ge^{i\Delta}e^{-2\pi i n_0 y_0 \rho_0}. \tag{6.5}$$

Breaking the P wave into an S wave and a D wave is equivalent to the statement that $P = S + D$ or that

$$D = P - S = ge^{i\Delta}e^{-2\pi i n_0 y_0 \rho_0} - e^{-2\pi i n_0 y_0 \rho_0},$$

whence

$$D = e^{-2\pi i n_0 y_0 \rho_0}(ge^{i\Delta} - 1). \tag{6.6}$$

In summary, the relative amplitude and phase of the undeviated and deviated waves as they emerge from the object specimen are given re-

spectively by the equations

$$U = e^{-2\pi i n_0 y_0 \rho_0};$$ (6.7)

$$D = e^{-2\pi i n_0 y_0 \rho_0}(ge^{i\Delta} - 1);$$ (6.8)

in which U and D are complex numbers which will be used henceforth in referring to the undeviated and deviated waves, respectively. It will be noted that the phase factor $e^{-2\pi i n_0 y_0 \rho_0}$ which arises from the inclination of the incident wave front is common to both the undeviated and the deviated wave.

7. REPRESENTATION OF THE MODIFIED UNDEVIATED AND DEVIATED WAVES

The relative amplitude and phase of the undeviated and deviated waves is given by Eqs. 6.7 and 6.8 as these waves emerge from the object plane. In a standard, highly corrected microscope these waves are transported to the conjugate image plane without further relative modification other than a loss of the more steeply inclined portion of the deviated bundle of rays. Let the plate which supports the coating material of the diffraction plate be regarded as a component part of a fully corrected microscope objective, and let the optical path from the object to the image plane be V radians. In the absence of any coating material on the diffraction plate, the undeviated and deviated waves then arrive at the image plane with relative amplitude and phase given by

$$U = e^{iV}e^{-2\pi i n_0 y_0 \rho_0};$$ (7.1)

$$D = e^{iV}e^{-2\pi i n_0 y_0 \rho_0}(ge^{i\Delta} - 1).$$ (7.2)

It has been seen in Section 3 that the undeviated and deviated waves pass through the conjugate and complementary areas of the diffraction plate, respectively. Let the amplitude and phase transmission of the conjugate area and of the complementary area be represented by the complex numbers $h_0 e^{i\delta_0}$ and $h_1 e^{i\delta_1}$, respectively. In the presence of coating materials on the diffraction plate the undeviated and deviated waves will now arrive at the image plane with amplitude and phase determined by the equations

$$U = e^{iV}e^{-2\pi i n_0 y_0 \rho_0}h_0 e^{i\delta_0};$$ (7.3)

$$D = e^{iV}e^{-2\pi i n_0 y_0 \rho_0}(ge^{i\Delta} - 1)h_1 e^{i\delta_1}.$$ (7.4)

These equations are obtained by multiplying the right-hand members of Eqs. 7.1 and 7.2 by $h_0 e^{i\delta_0}$ and $h_1 e^{i\delta_1}$, respectively. When $h_0 = h_1 = 1$ and $\delta_0 = \delta_1 = 0$, the conjugate and complementary areas of the dif-

fraction plate are uncoated and Eqs. 7.3 and 7.4 reduce to Eqs. 7.1 and 7.2 which apply to the standard microscope.

To find the resulting amplitude and phase over the image of the surround and over the image of the particle, we recall that the undeviated wave is spread over the entire plane of the image and that the undeviated and deviated waves overlap on the neighborhood of the geometrical image of the particle. Let S' and P' be complex numbers representing the amplitude and phase of the resultant wave over the geometrical image of the surround and the particle, respectively. Then

$$S' = U = e^{iV}e^{-2\pi in_0y_0\rho_0}h_0e^{i\delta_0} \tag{7.5}$$

because the geometrical image of the surround is illuminated by the undeviated wave only; and

$$P' = U + D = e^{iV}e^{-2\pi in_0y_0\rho_0}[h_0e^{i\delta_0} + (ge^{i\Delta} - 1)h_1e^{i\delta_1}] \tag{7.6}$$

because the undeviated and deviated waves interfere as $U + D$ over the geometrical image of the particle. By factoring out $h_1e^{i\delta_1}$ from the right-hand members of Eqs. 7.5 and 7.6 and by defining

$$he^{i\delta} \equiv \frac{h_0}{h_1}\frac{e^{i\delta_0}}{e^{i\delta_1}} = \frac{h_0}{h_1}e^{i(\delta_0-\delta_1)}, \tag{7.7}$$

we find that

$$S' = (e^{iV}e^{-2\pi in_0y_0\rho_0}h_1e^{i\delta_1})he^{i\delta}; \tag{7.8}$$

$$P' = (e^{iV}e^{-2\pi in_0y_0\rho_0}h_1e^{i\delta_1})(he^{i\delta} + ge^{i\Delta} - 1). \tag{7.9}$$

In summary, Eqs. 7.8 and 7.9 describe the amplitude and phase distribution produced over the image plane of a phase microscope by the incidence upon the object plane of a single, inclined wave front whose orientation is that of Fig. II.13 with $\rho_0 \equiv \sin\theta_0$. g is the ratio of the amplitude transmission of the particle to the amplitude transmission of its surround. Δ is the optical path difference in radians between particle and surround. V is the optical path in radians from the object plane to the image plane. h_1 and δ_1 are, respectively, the amplitude and phase transmission of the complementary area of the diffraction plate. It follows from the definition of Eq. 7.7 that *h is physically the ratio of the amplitude transmission of the conjugate area to the amplitude transmission of the complementary area and that δ is physically the optical path difference between the conjugate and complementary areas. δ is measured in radians and is considered positive when the optical path of the conjugate area exceeds that of the complementary area.*

The manner in which $he^{i\delta}$ enters into Eqs. 7.8 and 7.9 shows that the amplitude ratio h and the phase difference δ are the essential properties of the diffraction plate. This follows because the complex number in

parentheses in Eqs. 7.8 and 7.9 is common to S' and P' and so does not alter the relative amplitude and phase of the wave S' which reaches the image of the surround and the resultant wave P' which reaches the image of the particle.

Let M denote the magnification of the objective in focusing the $X_0 Y_0$ plane into the image plane XY. Then $y = My_0$ so that

$$e^{-2\pi i n_0 y_0 \rho_0} = e^{-2\pi i n_0 \rho_0 (y/M)}. \tag{7.10}$$

The appearance of the phase factor of Eq. 7.10 in Eqs. 6.7 and 6.8 and in Eqs. 7.8 and 7.9 is consistent with Lummer's theorem for, according to this theorem, phase variations produced over the object plane are reproduced over the image plane. A closer comparison of Eqs. 6.7 and 6.8 and Eqs. 7.8 and 7.9 shows that not all amplitude and phase variations produced over the object plane are reproduced over the image plane except in the trivial case $h = 1$ and $\delta = 0$ in which the phase microscope degenerates into the ordinary idealized microscope. Depending, therefore, on the choice of the properties h and δ of the diffraction plate relative to the properties g and Δ of the object particle, contrast in the image can be made to depart considerably from the contrast predicted from Lummer's theorem. We are now in a position to discuss quantitatively within the scope of the elementary theory the contrast variations which are possible in a phase microscope for a variety of object specimens.

8. DISTRIBUTION OF ENERGY DENSITY OVER THE IMAGE PLANE

The energy density produced over the image of the surround by the light in the incident wave front of Fig. II.13 is proportional to $|S'|^2$ with S' given by Eq. 7.8. Since S' can be written in the form

$$S' = h_1 h e^{i(V + \delta_1 + \delta - 2\pi n_0 y_0 \rho_0)},$$

and since the absolute value of the exponential is unity,

$$|S'|^2 = h_1{}^2 h^2. \tag{8.1}$$

Similarly the energy density over the image of the particle is proportional to $|P'|^2$ with

$$P' = e^{i(V + \delta_1 - 2\pi i n_0 y_0 \rho_0)} h_1 (h e^{i\delta} + g e^{i\Delta} - 1).$$

Therefore

$$|P'|^2 = \left| e^{i(V + \delta_1 - 2\pi i n_0 y_0 \rho_0)} \right|^2 h_1{}^2 \left| h e^{i\delta} + g e^{i\Delta} - 1 \right|^2$$

or

$$|P'|^2 = h_1{}^2 \left| h e^{i\delta} + g e^{i\Delta} - 1 \right|^2. \tag{8.2}$$

We see at once that the average energy density produced over the image plane by the incidence of a single inclined wave front which originates from a point in the opening of the condenser diaphragm is independent of the inclination of the wave front, of the optical path V between the object and image planes, and of the phase transmission δ_1. *Since the distribution of the energy density does not depend on the inclination of the incident wave front, the light radiated from all points in the opening of the condenser diaphragm serves only to increase the total energy density in the image.* Hence the brightness of the image of the surround and particle will be proportional to $|S'|^2$ and $|P'|^2$, respectively, with $|S'|^2$ and $|P'|^2$ determined from Eqs. 8.1 and 8.2.

In order to avoid confusion, let us henceforth denote the total energy density in the image plane by G and let G_s and G_p refer to the total energy density over the image of the surround and of the particle, respectively. Then

$$G_s = h_1{}^2 h^2; \tag{8.3}$$

$$G_p = h_1{}^2 |he^{i\delta} + ge^{i\Delta} - 1|^2. \tag{8.4}$$

If desired, G_s and G_p can be interpreted as the brightness of the image of the surround and particle, respectively. Now

$$he^{i\delta} + ge^{i\Delta} - 1 = (h \cos \delta + g \cos \Delta - 1) + i(h \sin \delta + g \sin \Delta). \tag{8.5}$$

Since the square of the absolute value of a complex number is equal to the sum of the squares of its real and imaginary parts,

$$|he^{i\delta} + ge^{i\Delta} - 1|^2 = (h \cos \delta + g \cos \Delta - 1)^2 \\ + (h \sin \delta + g \sin \Delta)^2. \tag{8.6}$$

In summary, from Eqs. 8.3, 8.4, and 8.6

$$G_s = h_1{}^2 h^2; \tag{8.7}$$

$$G_p = h_1{}^2[(h \cos \delta + g \cos \Delta - 1)^2 + (h \sin \delta + g \sin \Delta)^2]; \tag{8.8}$$

in which G_s and G_p are proportional to the total energy density or brightness of the image of the surround and of the particle, respectively. g is the ratio of the amplitude transmission of the particle to the amplitude transmission of its surround. Δ is the optical path difference between the particle and the surround, measured in radians and considered positive when the optical path of the particle exceeds that of the surround. h is the ratio of the amplitude transmission of the conjugate area of the diffraction plate to the amplitude transmission of the complementary area of the diffraction plate. δ is the optical path difference between the conjugate and complementary areas. δ is measured in

radians and is considered positive when the optical path of the conjugate area exceeds that of the complementary area. h_1 is the amplitude transmission of the complementary area of the diffraction plate. The numerical value of h_1 does not affect the relative value of G_s and G_p, and hence the contrast in the image. In fact one may usually set $h_1 = 1$ without any essential loss of generality.

Equations 8.7 and 8.8 are the most general equations of phase microscopy within the scope of the simplified theory of phase microscopy. These equations contain the logical consequences which follow from the assumptions involved in Zernike's vector model for phase microscopy. These equations may be used to calculate G_s/h_1^2 and G_p/h_1^2 when the properties g and Δ of the particle and the properties h and δ of the diffraction plate are assigned particular values. When G_s and G_p have been computed, the contrast ratios G_p/G_s or $(G_s - G_p)/G_s$ may be computed also. Explicit formulas for these contrast ratios will not be given.

9. CONDITION FOR DARKEST CONTRAST OF THE PARTICLE

The particle is said to appear in dark or bright contrast according as the particle appears darker or brighter than its surround. At darkest possible contrast the particle appears to be black and $G_p = 0$ in Eq. 8.8. We suppose that the relative amplitude transmission g and the optical path difference Δ are assigned and that it is desired to find the values h and δ which the diffraction plate must have in order that $G_p = 0$. It is supposed that $h_1 = 1$. Since the two squared terms in the right-hand member of Eq. 8.8 are never negative, the condition for $G_p = 0$ is that

$$h \cos \delta + g \cos \Delta - 1 = 0;$$

$$h \sin \delta + g \sin \Delta = 0. \tag{9.1}$$

These form a pair of simultaneous equations for determining h and δ from g and Δ, or vice versa. The solution for h and δ is

$$h = (1 - 2g \cos \Delta + g^2)^{\frac{1}{2}} ; \tag{9.2}$$

$$\sin \delta = \frac{-g \sin \Delta}{(1 - 2g \cos \Delta + g^2)^{\frac{1}{2}}} ; \tag{9.3}$$

$$\cos \delta = \frac{1 - g \cos \Delta}{(1 - 2g \cos \Delta + g^2)^{\frac{1}{2}}} . \tag{9.4}$$

Equations 9.2–9.4 are the conditions for darkest contrast in the image of the particle. h is the ratio of the amplitude transmission of the conjugate area to the amplitude transmission of the complementary area. δ is the optical path difference in radians or in degrees between these two

areas of the diffraction plate and is considered positive when the optical
path through the conjugate area exceeds that through the comple-
mentary area. g is the ratio of the amplitude transmission of the particle
to the amplitude transmission of the surround. Δ is the optical path
difference in radians or degrees between the particle and its surround
and is considered positive when the optical path through the particle
exceeds that through an equal thickness of the surround.   It is impor-
tant to note from Eqs. 9.2–9.4 that it is always possible to find a diffraction
plate for which a microscopic particle appears black or at least darkest
in the event that scattering of light cannot be neglected.

10. DARKEST CONTRAST WITH PARTICLES WHOSE AMPLITUDE TRANSMISSION IS EQUAL TO THAT OF THE SURROUND

In a broad class of particles which includes unstained biological
particles the amplitude transmission of the particle and surround are so
nearly alike that we may set

$$g = 1. \tag{10.1}$$

By introducing $g = 1$ into Eqs. 9.2–9.4, we find that after slight simpli-
fication

$$h = 2 \left| \sin \frac{\Delta}{2} \right| ; \tag{10.2}$$

$$\sin \delta = \frac{-\sin \Delta/2 \cos \Delta/2}{|\sin \Delta/2|} = -sgn \left(\sin \frac{\Delta}{2} \right) \cos \frac{\Delta}{2} ; \tag{10.3}$$

$$\cos \delta = \frac{\sin^2 \Delta/2}{|\sin \Delta/2|} = \left| \sin \frac{\Delta}{2} \right| ; \tag{10.4}$$

in which $|\sin \Delta/2|$ denotes the absolute value of $\sin \Delta/2$ and in which
$sgn(x)$ denotes $x/|x|$.   Equations 10.3 and 10.4 are equivalent to the fol-
lowing simple relation between δ and Δ.

$$\delta = \frac{\Delta}{2} - \frac{\pi}{2} ; \qquad 0 < \Delta \leqq \pi;$$

$$\delta = \frac{\Delta}{2} + \frac{\pi}{2} ; \quad -\pi < \Delta < 0. \tag{10.5}$$

In summary, the values that h and δ must have in order that the
particle shall appear in optimum dark contrast when $g = 1$ are given by
the equations

$$h = 2 \left| \sin \frac{\Delta}{2} \right| ; \tag{10.6}$$

$$\delta = \frac{\Delta}{2} - \frac{\pi}{2} ; \qquad 0 < \Delta \leqq \pi; \tag{10.7}$$

$$\delta = \frac{\Delta}{2} + \frac{\pi}{2} ; \quad -\pi \leqq \Delta < 0. \tag{10.8}$$

It will be noted that the required phase difference δ of the diffraction plate is discontinuous at $\Delta = 0$.

With particles whose optical path Δ is so small that we can replace $\sin \Delta/2$ by $\Delta/2$,

$$h = |\Delta| \tag{10.9}$$

and

$$\delta \rightarrow \mp \frac{\pi}{2} \tag{10.10}$$

according as $\Delta > 0$ or as $\Delta < 0$.

Equations 10.7 and 10.8 state that the optical path of the conjugate area of the diffraction plate must be less than the optical path of the complementary area by $(\pi/2 - \Delta/2)$ radians or by $(\frac{1}{4} - \Delta/4\pi)$ wavelengths in order to make the particle appear darkest when its optical path exceeds that of the surround by a small amount, but that the optical path of the conjugate area must exceed the optical path of the complementary area by $(\pi/2 + \Delta/2)$ radians or by $(\frac{1}{4} + \Delta/4\pi)$ wavelengths in order to make the particle appear darkest when its optical path is less than that of the surround by a small amount, Δ radians. These conclusions are consistent with those established in Section 3 but indicate definitely the direction and amount by which δ should depart from $\mp \pi/2$. According to Eq. 10.9, the optimum amplitude ratio h of the diffraction plate decreases with $|\Delta|$ when Δ is so small that we can with negligible error replace $\sin \Delta/2$ by $\Delta/2$.

Suppose that the optical path difference between the particle and the surround falls in the neighborhood of $\Delta = \pm \pi/2$, that is, in the neighborhood of $\pm \frac{1}{4}$ wavelength. Then

$$h \rightarrow 2 \left| \sin \frac{\pi}{4} \right| = \sqrt{2};$$

$$\delta \rightarrow -\frac{\pi}{4} \text{ radians} = -\tfrac{1}{8} \text{ wavelength when } \Delta = \frac{\pi}{2} ;$$

$$\delta \rightarrow \frac{\pi}{4} \text{ radians} = +\tfrac{1}{8} \text{ wavelength when } \Delta = -\frac{\pi}{2}.$$

This means that, when the optical path differences between the particle and the surround are $\pm \lambda/4$, δ must be chosen as $-\lambda/8$ or as $+\lambda/8$ and

the h value must be chosen as $\sqrt{2}$ in order to obtain optimum darkest contrast in the image of the particle.   In order to obtain h values exceeding unity, the absorbing material must be placed upon the complementary area so as to weaken the deviated wave rather than upon the conjugate area of the diffraction plate.

Suppose that $\Delta = \pm\lambda/6$.   Then

$$h = 1;$$

$$\delta = \frac{\lambda}{12} - \frac{\lambda}{4} = \frac{-\lambda}{6} \text{ when } \Delta = \frac{\lambda}{6} ;$$

$$\delta = \frac{-\lambda}{12} + \frac{\lambda}{4} = \frac{+\lambda}{6} \text{ when } \Delta = \frac{-\lambda}{6}.$$

The case $\Delta = \pm\lambda/6$ when $g = 1$ is the point of demarcation between diffraction plates for which $h \gtrless 1$.   When $h = 1$, no absorbing material is required on either the conjugate or complementary area.   It will be noted that the required δ for darkest contrast is $\lambda/6$ when $\Delta = -\lambda/6$. Diffraction plates for which $\delta = \lambda/6$ and $h = 1$ are radically different from diffraction plates for which $\delta = \pm\lambda/4$ and $h \rightarrow |\Delta|$ with Δ small. The theoretical necessity for a series of diffraction plates in order to secure *optimum* contrast with different particles therefore becomes apparent.

We learn from Eq. 10.6 that $h = 2$ is the largest useful h value.   Correspondingly, the energy transmission ratio between the conjugate and complementary areas is $h^2 = 4$.   The value $h = 2$ is required when $\Delta = \pm\pi$ radians.   From Eq. 10.7 or 10.8 the required δ value is then $\delta = 0$.   This example shows that particles whose amplitude transmission is equal to that of the surround and whose optical path difference with respect to the surround approaches $\frac{1}{2}$ wavelength will appear in darkest contrast in the sharply focused image plane of an aberration-free objective when a diffraction plate is selected whose h value approaches $h = 2$ and whose δ value approaches $\delta = 0$.   It follows from Eqs. 8.7 and 8.8 that G_s, the energy density over the image of the surround, approaches 4 when $h_1 = 1$, and that G_p, the energy density over the image of the particle, approaches zero.   The relative value of G_s and G_p as produced by the ordinary microscope in the sharply focused image plane in the case of the class of particles of this example is obtained by substituting $h_1 = h = g = 1$, $\delta = 0$, and $\Delta = \pm\pi$ into Eqs. 8.7 and 8.8. The result is $G_s = G_p = 1$.   This equality of G_s and G_p is another illustration of the fact that the contrast produced in the image of an unstained particle by an ordinary microscope is due to the failure of the

microscope to satisfy the conditions of Lummer's theorem or to an out-of-focus image or to both. Since an out-of-focus image is necessarily distorted, we see that the phase microscope is in principle capable of producing images of better contrast and definition than should be expected from the ordinary microscope even when the optical path difference between the particle and its surround becomes large.

11. DARKEST CONTRAST WITH PARTICLES DIFFERING FROM THEIR SURROUND ONLY IN ABSORPTION

Suppose that $\Delta = 0$ but that $g \neq 1$. In this case Eqs. 9.2–9.4 reduce to the set

$$h = |1 - g|; \tag{11.1}$$

$$\sin \delta = 0; \tag{11.2}$$

$$\cos \delta = \frac{1 - g}{|1 - g|} = sgn(1 - g). \tag{11.3}$$

Equations 11.2 and 11.3 are equivalent to the statements

$$\delta = 0 \quad \text{when } g < 1; \tag{11.4}$$

$$\delta = \pi \quad \text{when } g > 1. \tag{11.5}$$

This means that the particle should appear darkest by choosing h in accordance with Eq. 11.1 and by choosing $\delta = 0$ or π according as the particle transmits less or more light than its surround. Since G_p, the energy density over the geometrical image of the particle, is theoretically zero when h and δ are chosen in accordance with Eqs. 11.1, 11.4, and 11.5, it is theoretically possible to bring about a great improvement in the contrast in the image of particles that differ from their surround by a slight amount in absorption. As the amplitude transmission of the particle approaches that of the surround, g approaches unity and the required h value approaches zero so that an increasing amount of absorbing material has to be added to the conjugate area of the diffraction plate as the particle approaches the surround in amplitude transmission. If the particle is viewed in a polanret microscope (Osterberg, 1947a), a polanret δ setting of $\delta = 0$ or π at optimum darkest contrast constitutes experimental evidence that Δ is negligibly small and enables the observer to decide whether $g \gtrless 1$.

In summary, we can expect that, when the particle differs from its surround only by a slight amount in absorption, contrast in the image of the particle can be improved by selecting a diffraction plate from a series of diffraction plates whose conjugate and complementary areas differ in optical path by either zero or $\frac{1}{2}$ wavelength and whose amplitude transmission ratios h are small.

If the optical path difference Δ is not negligible, the required h and δ values can be ascertained from the more general Eqs. 9.2–9.4. In such cases δ must be expected to depart significantly from $\delta = 0$ or π. We see, therefore, that the simplified theory is capable of predicting that the phase microscope can improve contrast in the image of slightly stained biological specimens. Also, this prediction is in accord with experiment.

12. EQUALITY OF THE AMPLITUDES OF THE UNDEVIATED AND DEVIATED WAVES AT THE CONDITIONS FOR DARKEST CONTRAST

By factoring out $h_1 e^{i\delta_1}$ from the right-hand members of Eqs. 7.3 and 7.4, we find that

$$U = e^{iV} e^{-2\pi i n_0 y_0 \rho_0} e^{i\delta_1} h_1 h e^{i\delta}; \tag{12.1}$$

$$D = e^{iV} e^{-2\pi i n_0 y_0 \rho_0} e^{i\delta_1} h_1 (g e^{i\Delta} - 1). \tag{12.2}$$

The complex numbers U and D determine the amplitude and phase of the undeviated and deviated waves, respectively, as they arrive at the plane of the image. Since the absolute values of the exponentials are unity, it follows at once that

$$|U| = h_1 h; \tag{12.3}$$

$$|D| = h_1 |g e^{i\Delta} - 1|. \tag{12.4}$$

Since

$$g e^{i\Delta} - 1 = (g \cos \Delta - 1) + i(g \sin \Delta);$$

$$|g e^{i\Delta} - 1| = [(g \cos \Delta - 1)^2 + (g \sin \Delta)^2]^{\frac{1}{2}}$$

$$= (1 - 2g \cos \Delta + g^2)^{\frac{1}{2}}. \tag{12.5}$$

From Eqs. 12.4 and 12.5,

$$|D| = h_1 (1 - 2g \cos \Delta + g^2)^{\frac{1}{2}}. \tag{12.6}$$

From Eq. 9.2 the condition on h for darkest contrast is that $h = (1 - 2g \cos \Delta + g^2)^{\frac{1}{2}}$. Therefore, when h is chosen so as to satisfy the condition for darkest contrast,

$$|U| = |D| = h_1 h. \tag{12.7}$$

Since $|U|$ and $|D|$ are the amplitudes of the undeviated and deviated waves, respectively, this means physically that the amplitudes of the undeviated and deviated waves are equal when the diffraction plate has been chosen to satisfy the conditions for darkest contrast.

13. CONDITIONS FOR OPTIMUM BRIGHT CONTRAST

Thus far, our attention has been limited to the conditions which h and δ must satisfy in order to cause the particle to appear in darkest contrast. Whereas definite, unique conditions can be discovered for darkest contrast, the same is not true with respect to the conditions for optimum bright contrast.

Returning to Eqs. 8.3 and 8.4, we see that

$$G_s = 0; \tag{13.1}$$

$$G_p = h_1{}^2 |ge^{i\Delta} - 1|^2$$
$$= h_1{}^2 (1 - 2g \cos \Delta + g^2); \tag{13.2}$$

when $h = 0$. Since $(1 - 2g \cos \Delta + g^2)$ is not equal to zero unless $\Delta = 0$ and $g = 1$ so that the particle is indistinguishable from its surround in white light, $G_p \neq 0$ when $G_s = 0$. The Schlieren case, $h = 0$, produces the greatest bright contrast, therefore, for the particle appears bright against a theoretically black background. In the Schlieren case, however, the quality of the image is deteriorated because the image is formed by the deviated wave alone. We can expect that a more favorable compromise between contrast and definition will be obtained when the h value is chosen no smaller than the value required to equalize the amplitudes of the undeviated and deviated waves. It has been shown in Section 12 that this is precisely the value of h that is required for obtaining darkest contrast in the image of the particle. We shall accordingly define *optimum bright contrast* as the brightest contrast that can be obtained by varying δ with h fixed at its value for darkest contrast. The problem of discovering the maximizing value of δ reduces therefore to the task of finding the value of δ for which $\partial G_p / \partial \delta = 0$, where G_p is the total energy density over the geometrical image of the particle as given by Eq. 8.8.

$$\frac{\partial G_p}{\partial \delta} = 2h_1{}^2 h[-(h \cos \delta + g \cos \Delta - 1) \sin \delta + (h \sin \delta + g \sin \Delta) \cos \delta];$$

$$= 2h_1{}^2 h[(1 - g \cos \Delta) \sin \delta + g \sin \Delta \cos \delta].$$

Thus, $\partial G_p / \partial \delta = 0$, provided that

$$\tan \delta = \frac{-g \sin \Delta}{1 - g \cos \Delta}. \tag{13.3}$$

Now Eq. 13.3 can also be obtained through division of Eqs. 9.3 and 9.4. If δ_d denotes the value of δ computed from Eqs. 9.3 and 9.4, it follows that δ_d is a solution of Eq. 13.3 where δ_d is the optical path difference between the conjugate and complementary areas of the

diffraction plate when the particle appears in darkest contrast. On account of the trigonometric identity

$$\tan x = \tan (x + \pi),$$

$\delta = \delta_d + \pi$ is a second solution of Eq. 13.3. The remaining solutions of Eq. 13.3 differ from δ_d and $(\delta_d + \pi)$ by integral multiples of 2π. δ_d is the first solution for which G_p is minimum, whereas $\delta_d + \pi$ is the first solution for which G_p is maximum. This result is summarized as the important theorem (Theorem 5):

If the particle appears in darkest contrast when h and δ are set at the values h_d and δ_d, then the particle will appear in optimum bright contrast when the phase difference δ_d between the conjugate and complementary areas of the diffraction plate is altered by $\frac{1}{2}$ wavelength.

The conditions for optimum bright contrast may therefore be found in a simple manner from the conditions for darkest contrast. If, for example, the particle appears darkest with a diffraction plate for which $h = 0.4$ and $\delta = +\lambda/8$, the particle will appear in optimum bright contrast with another diffraction plate for which $h = 0.4$ and $\delta = 5\lambda/8$, or, equivalently, $-3\lambda/8$.

We will now show that $G_p = 4G_s$ when the particle appears in optimum bright contrast. The conditions of Eqs. 9.2–9.4 for dark contrast show that

$$h_d \sin \delta_d = -g \sin \Delta;$$

$$h_d \cos \delta_d = 1 - g \cos \Delta. \tag{13.4}$$

If we let δ_b denote the δ value for optimum bright contrast, then

$$\delta_b = \delta_d + \pi. \tag{13.5}$$

Therefore

$$h_d \sin \delta_b = -h_d \sin \delta_d = g \sin \Delta;$$

$$h_d \cos \delta_b = -h_d \cos \delta_d = g \cos \Delta - 1. \tag{13.6}$$

When $g \sin \Delta = h_d \sin \delta_b$ and $g \cos \Delta - 1 = h_d \cos \delta_b$ are substituted into Eq. 8.8, it is found almost directly that

$$G_s = h_1{}^2 h_d{}^2, \quad G_p = 4h_1{}^2 h_d{}^2;$$

whence

$$G_p = 4G_s \tag{13.7}$$

at optimum bright contrast. Brighter contrasts than that indicated by Eq. 13.7 are possible at the expense of reducing the amplitude of the undeviated wave below the amplitude of the deviated wave.

14. CHOICE OF DIFFRACTION PLATE WITH PARTICLES HAVING SMALL OPTICAL PATH DIFFERENCES AND THE AMPLITUDE RATIO $g = 1$.

Darkest or optimum bright contrast in the image will not be obtained except with suitably chosen object particles when the phase microscope is provided with a single diffraction plate. As the number of different diffraction plates is increased, the range of choice of object particle increases. We shall see that the choice of diffraction plate is not at all critical. Contrast in the image falls off slowly from its darkest or optimum bright value as the amplitude ratio h and the phase difference δ of the diffraction plate depart from the values required for darkest or optimum bright contrast. The variation in the contrast with h and δ will now be described for the case in which $\Delta = +\lambda/18$ and $g = 1$. This case applies, for example, to unstained biological specimens whose optical path difference Δ is so small that contrast in the ordinary microscope is poor.

The energy densities G_s and G_p have been computed as functions of δ at several fixed values of h and are plotted for comparison in Fig. II.14 in which δ is represented in degrees. The corresponding values of δ in wavelengths can be obtained by dividing by 360. It will be noted that the energy density G_p in the image of the particle is maximum in all cases when $\delta = 100°$ and minimum when $\delta = -80°$. Beginning with the curves drawn for $h = 0.1225$, we see that $G_p > G_s$ for all values of δ. If we define the contrast K by the equation

$$K \equiv \frac{G_p - G_s}{G_s}, \qquad (14.1)$$

K is a maximum of 13.7 at $\delta = 100°$. The maximum value of K decreases steadily with increasing h and is equal to 3 when $h = 0.3473$, the value of h at which the amplitudes of the undeviated and deviated waves are alike and at which the contrast is defined as optimum bright contrast. Since $G_p = 4G_s$ at optimum bright contrast, K is always equal to 3 at optimum bright contrast. When $h = 0.1738$, the curve G_p touches the curve G_s at $\delta = -80°$. For larger values of h the curve G_p dips below the curve for G_s in the neighborhood of $\delta = -80°$. Contrast in the image may now be reversed by changing, for example, δ from $100°$ to $-80°$. With $h = 0.3473$, $G_p = 0$ and $K = -1$ at $\delta = -80°$, the point of darkest possible contrast. As h is increased from 0.3473 to 0.50, the contrast value K at $\delta = -80°$ increases slowly from $K = -1$ to $K = -0.9$ at $h = 0.5$. Both the dark and bright contrasts deteriorate steadily with h when $h > 0.3473$. Since $h^2 = 0.12$ when $h = 0.3473$, the energy transmission ratio between the conjugate and
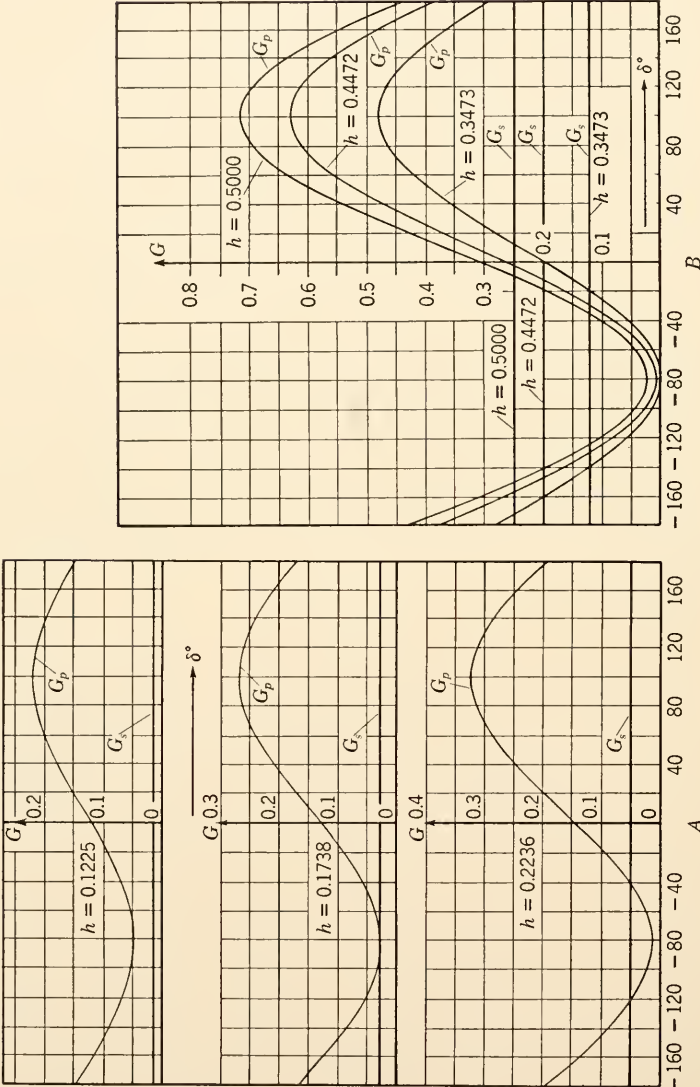
Fig. II.14. The energy densities G_p and G_s of the particle and the surround, respectively, as functions of δ at the indicated fixed values of the amplitude ratio h. $g = 1$ and $\Delta = +\lambda/18$.

complementary areas is 12%. The h^2 values predicted by the simplified theory are usually smaller than those employed in the phase microscope. Thus, h^2 values in the range 15% to 25% have been preferred experimentally for particles whose Δ value varies through a considerable range about the point $|\Delta| = \lambda/18$.

The most pertinent properties of the curves of Fig. II.14 for the thesis of the present section are:

1. The energy densities G_p and the contrast K change only slightly as δ varies by $\pm 10°$ about the points $\delta = -80°$ and $100°$ for dark and bright contrast, respectively. In fact, a range of $\pm 20°$ in δ can be tolerated for many purposes. Since the tolerable range of variation in δ amounts to almost $\frac{1}{8}$ wavelength, it is to be expected that the phase differences between the conjugate and complementary areas in a series of diffraction plates need be spaced no nearer than $\frac{1}{8}$ wavelength apart.

2. Since the values $\delta = \pm 90° = \pm \lambda/4$ fall only $10°$ from the best values of $-80°$ and $100°$ for the case $\Delta = \lambda/18$, the particle discussed in this section should appear in good to excellent contrast when viewed with the aid of diffraction plates whose phase difference δ is $\pm\lambda/4$ as recommended by Zernike.

3. Since the K value at dark contrast varies only from -0.7 to -1 to -0.95 and since the K value at bright contrast varies only from 5.5 to 2.2 as h is varied from 0.2236 to 0.4472, a wide tolerance also on the h value is admissible.

It can therefore be expected on the one hand that in constructing a diffraction plate for obtaining good contrast with a given object specimen the required values of h and δ are not critical and that on the other hand a diffraction plate with a given pair of h and δ values can be used with excellent to moderate success for object specimens having a range of optical path differences Δ. In order to illustrate more explicitly how a single diffraction plate performs over a range of Δ values, the contrast values K have been plotted as a function of Δ in Fig. II.15 for the indicated values of δ and with h fixed at the value of 0.3473. The curve of A applies to a diffraction plate selected for dark contrast; the curve of B applies to a diffraction plate selected for bright contrast. A shows that the indicated diffraction plate can be expected to produce good to excellent contrast for Δ values in the range $8° < \Delta < 32°$. For Δ values outside this range, for example with $\Delta = 3.6° = \lambda/100$, another diffraction plate should be selected. B shows that the indicated diffraction plate can be expected to produce good to excellent bright contrast for Δ values in the range $8°$ to $40°$ but that another diffraction plate should be selected when Δ falls in or below the neighborhood of $3.6° = \lambda/100$.
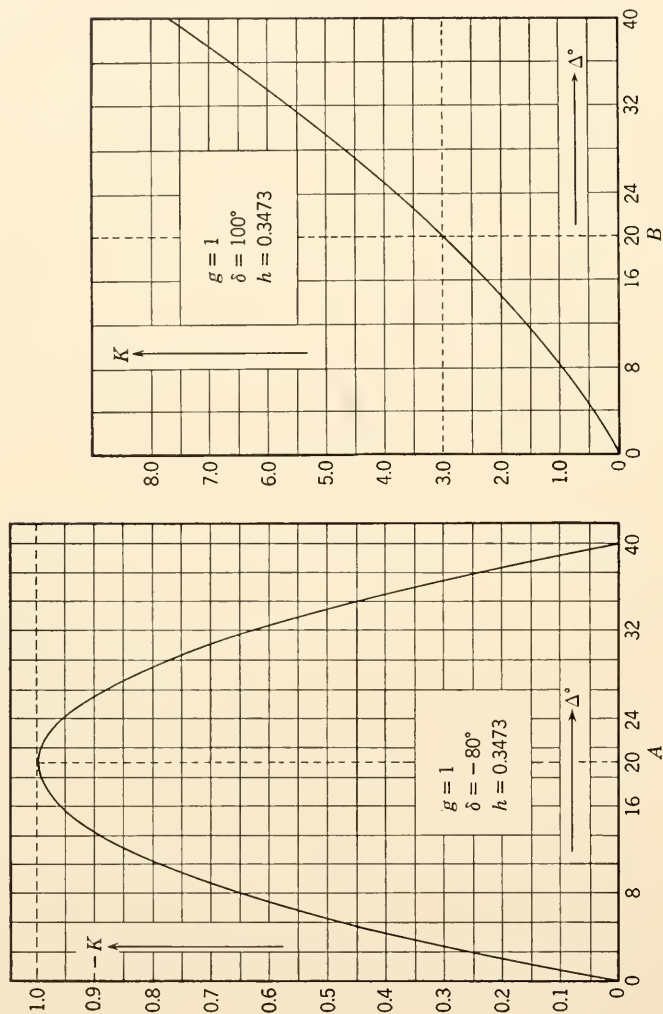
Fig. II.15.   The contrast values K as functions of the optical path difference Δ between particle and surround at the indicated values of h and δ.
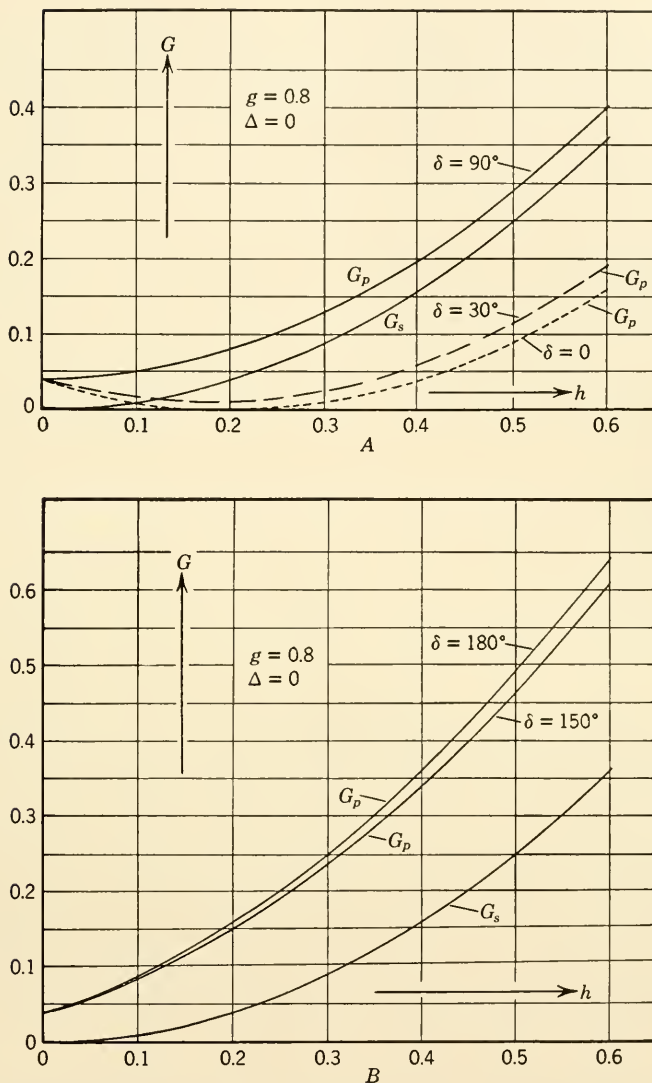
FIG. II.16.   The energy densities G_s and G_p as functions of h for a particle whose g and Δ values are 0.8 and zero, respectively.   The phase differences δ between the conjugate and complementary areas are fixed at the indicated values.

15. CHOICE OF DIFFRACTION PLATE WITH STAINED PARTICLES WHOSE REFRACTIVE INDEX EQUALS THAT OF THE SURROUND

Consider first a particle whose refractive index is the same as that of the surround but whose amplitude transmission is 0.8 that of the sur-

round.   Such a particle transmits $0.8^2 = 0.64$ times as much light as its surround and will be visible in the standard microscope.   According to Eqs. 11.1 and 11.4 this particle should appear black against an illuminated background in the phase microscope with the use of a
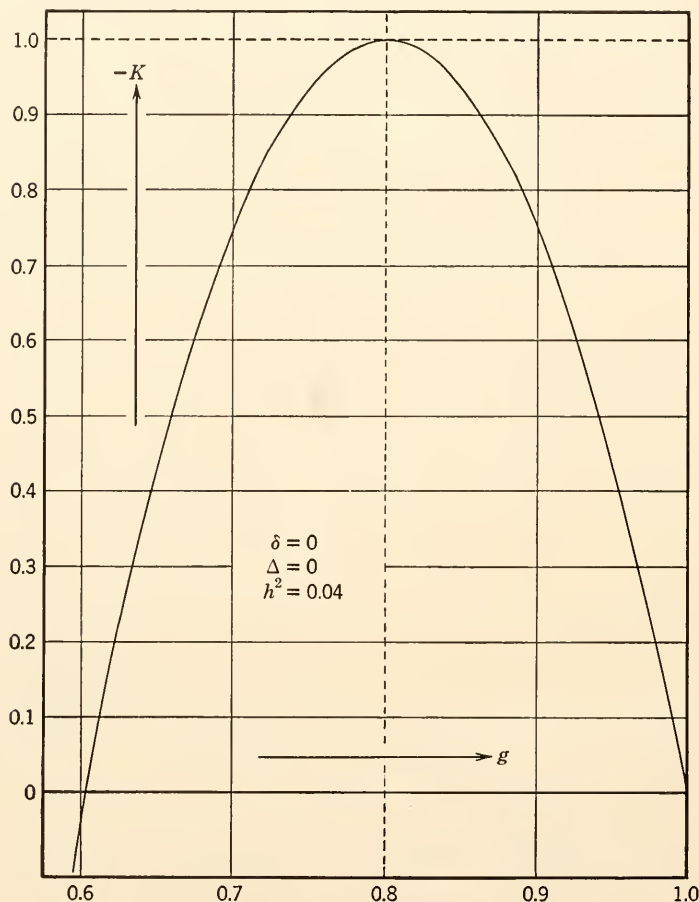
FIG. II.17.   The contrast values K as a function of g with a diffraction plate whose h and δ values are 0.2 and zero, respectively.   The optical path difference Δ between particle and surround is zero.

diffraction plate for which $h = 0.2$ and $\delta = 0$.   According to Section 13 the particle should appear four times as bright as its surround when another diffraction plate is selected for which $h = 0.2$ and $\delta = \lambda/2$.

   The energy densities G_s and G_p have been computed for the above particle as functions of h at several fixed values of δ and are plotted for

comparison in Fig. II.16. In A, G_p vanishes and the contrast $K = -1$ at the point $h = 0.2$ for the curve $\delta = 0$. For the curve $\delta = 30°$, $K = -0.7$ at $h = 0.2$. Provided that the h value is set at 0.2, variations of $20°$ in δ from its preferred value $\delta = 0$ will not alter the contrast seriously. Provided that $\delta = 0$, h may be permitted to vary by the amount ± 0.04 about the point $h = 0.2$. Although the choice of h and δ is not critical, it must be made with care. The curve with $\delta = 90°$ has been included in order to illustrate that quarter-wave diffraction plates are not useful with particles in this category. It is interesting to observe from the curves drawn for $\delta = 0$ and $30°$ that it is theoretically possible to reverse contrast in the image by reducing the h value below $h = 0.1$. This behavior is to be expected, for the particle must appear in bright contrast in the ultimate Schlieren case, $h = 0$. An inspection of B shows that conditions for bright contrast are more flexible than those for dark contrast. Thus, at $h = 0.2$, K is reduced only from $K = 3.0$ to 2.7 as δ is reduced by $30°$ with respect to its best value of $180°$. The contrast $K = \infty$ at $h = 0$ and decreases with increasing h.

The contrast K has been plotted in Fig. II.17 as a function of g for a diffraction plate for which $h = 0.2$ and $\delta = 0$. The contrast values $-K$ obtained with this diffraction plate are seen to exceed 0.8 for particles having g values in the range $0.712 < g < 0.887$.

16. CHOICE OF DIFFRACTION PLATE WITH STAINED PARTICLES WHOSE OPTICAL PATH DIFFERENCE IS $+\lambda/4$

The energy densities G_s and G_p are plotted in Fig. II.18 as functions of h at the indicated fixed values of δ for the case $\Delta = +\lambda/4$ and $g = 0.9$. Since $g^2 = 0.81$, the particle transmits 0.81 times as much light as its surround. Such particles are weakly stained and will show fair contrast in the standard microscope. On the other hand, such particles should appear to be black in the phase microscope with the choice of a diffraction plate for which $h = 1.345$ and $\delta = -42°$. The curves G_p with $\delta = -27°$ and $-57°$ practically coincide. Variations of $\pm 15°$ in δ from the best value $\delta = -42°$ do not produce serious deteriorations in the contrast.

Furthermore, h may be varied from 1.0 to 1.7 without seriously disturbing the contrast. Contrast in the image of the particle will be dark so long as $h > 0.7$, but the h values must exceed unity in order to produce excellent contrast with a particle for which $\Delta = +\lambda/4$ and $g = 0.9$. Diffraction plates for which $h > 1$ are called* the B type and differ from the A type in that the absorbing material is placed upon the complementary area instead of upon the conjugate area. The useful-

---

* See Section 2.5, Chapter III.

ness of the B-type diffraction plate in observing stained and other biological or industrial particles was appreciated after the utility of the A-type diffraction plate had been well established.   Since $h^2 = 1.81$
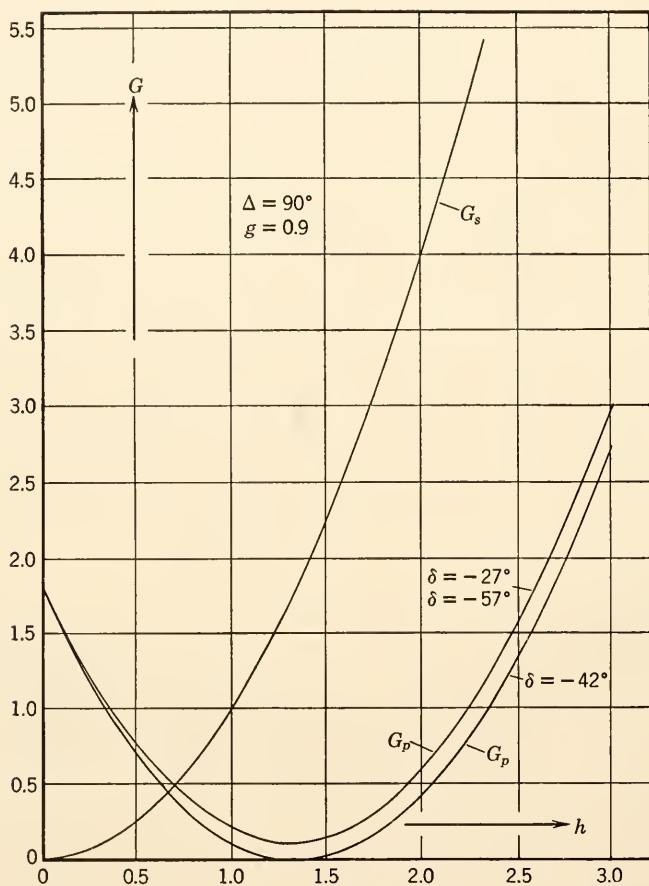
FIG. II.18.   The energy densities G_s and G_p as functions of h at the indicated fixed values of δ with a particle for which $\Delta = +\lambda/4$ and $g = 0.9$.

and since $-42° = -0.1166\ \lambda$, the best B-type diffraction plate for use with a particle for which $\Delta = +\lambda/4$ and $g = 0.9$ will be the $1.8B-0.117\lambda$ diffraction plate.

The curve of Fig. II.19 for the contrast value K has been plotted as a function of g for a diffraction plate whose h and δ values are fixed at $h^2 = 1.81$ and $\delta = -42°$.   The optical path difference of the particle is fixed at $\Delta = +\lambda/4$, but the g value extends over the entire range from

opaque to unstained particles.   Since $-K$ does not fall below 0.55, the single diffraction plate $1.8B-0.117\lambda$ serves moderately well over the entire range of stained particles whose optical path is $+\lambda/4$ and serves particularly well for particles whose g values fall in the range $0.6 < g < 1$.
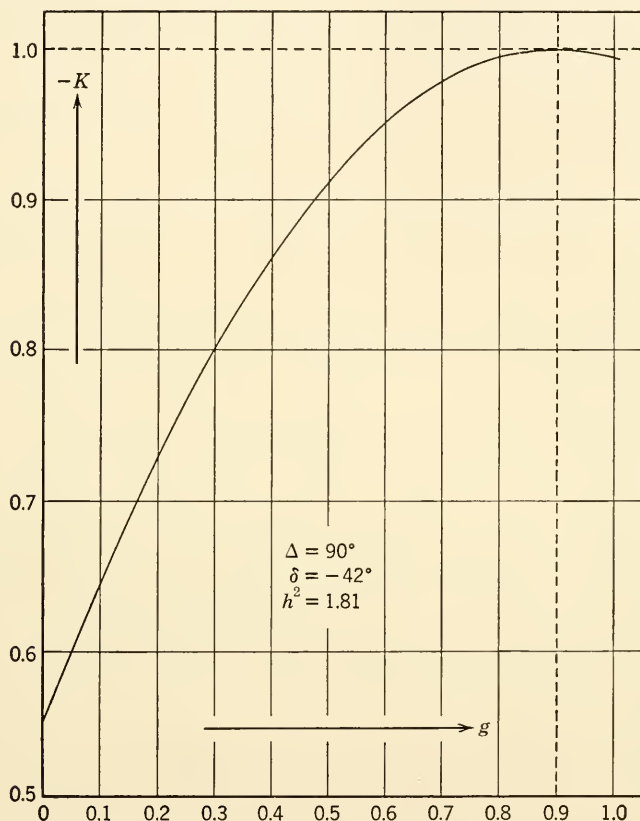
Fig. II.19.   The contrast K as a function of g at $\Delta = +\lambda/4$, $\delta = -42°$, and $h^2 = 1.81$.

It should not be concluded, however, that the B-type diffraction plate is superior to the A type for all stained particles.   Thus when the optical path difference of the particle is zero, as in Section 15, the optimum h values are less than unity and lead to A-type diffraction plates.

17.   GENERALIZATION OF THE THEORY TO MORE THAN ONE OBJECT PARTICLE

If the object slide contains more than one particle, as it does, of course, in actual practice, the S wave is again constructed as for a single particle.

There will now be a different P wave and hence a different D wave for each particle, but the undeviated wave remains the same as for the single particle. The undeviated wave passes through the conjugate area and is subsequently spread over the entire plane of the image. The undeviated waves diverge from the particles at which they originate, are spread over the complementary area, and are reconcentrated upon the geometrical images of the respective particles from which they originate. The amplitude and phase distribution over the image of the surround is again determined by the undeviated wave alone, whereas the amplitude and phase distribution over the geometrical images of the various particles is determined by the resultant wave produced by the interference of the undeviated wave with the deviated waves over the geometrical image of each of the particles. Within the scope of the elementary theory, the deviated waves from the various particles act independently in the sense that they do not disturb one another. Consequently the amplitude and phase distribution may be computed for each particle from the laws already described for the single particle. It is to be expected, as can be verified from the more complete theory, that the amplitude and phase distributions computed from the elementary theory will depart further from the truth as the particles are crowded together.

If the object specimen is a grating, the elevations of the grating may be regarded as the surround and the troughs may be regarded as constituting the various particles or, indeed, a single particle. The generalization of the quantitative elementary theory to complex object specimens is therefore similar to the generalization of the more qualitative theory as described in Sections 3.3 and 3.4.

The following theorems follow from the statements of this section and are valid within the scope of the elementary theory.

Theorem 6: *Those particles which appear with similar contrast, no matter which diffraction plate is selected, have similar amplitude transmissions and optical paths.*

Theorem 7: *Those particles which appear with dissimilar contrast have dissimilar amplitude transmissions and optical paths.*

These theorems are of practical value in making comparisons among the object particles and can be expected to hold with at least fair degree of reliability when the particles are separated by distances greater than four times the limit of resolution of the objective. On the basis of the general theory also, the size, shape, and separations of the particles are found to influence contrast in the images of the particles. Consequently, Theorems 6 and 7 cannot be applied without reservation.

18. EFFECT OF THE DIFFRACTION PLATE ON RESOLVING POWER

The question of whether or not the resolving power of the microscope is impaired by the diffraction plate is a proper concern of the critical microscopist.   Whereas it is true that the zonal spherical aberrations of the microscope objective are purposely increased in order to achieve phase microscopy, both theory and experiment have shown that phase microscopy is not necessarily obtained at the expense of resolving power. The phase microscope was intended originally to improve contrast in the image of unstained particles whose optical path differs so little from that of the surround that the particle is practically invisible in the ordinary microscope.   In resolving two such particles a properly constructed phase microscope possesses greater resolving power than is inherent in the ordinary microscope.   This unpublished conclusion is derivable from the more general theory of phase microscopy and is based on more fundamental considerations than the obvious criterion that two particles must be seen before they can be resolved.

Unfortunately, a presentation of the more advanced theories of resolution is beyond the scope of this book.   These theories have shown that both the ordinary and the phase microscopes are capable of greater resolution than is indicated by the Airy limit of resolution, that the resolution of two particles depends to a marked extent on their absolute and relative dimensions and on their amplitude and phase transmissions, and that the less general classical theory of resolution is at best qualitative.   The following qualitative considerations based on the usual classical concepts indicate that the resolving power of a phase microscope need not differ appreciably from the resolving power of the ordinary microscope.

One effect of introducing a diffraction plate is to modify the diffraction image which the objective forms of an object consisting of a pinhole in a silvered slide.   The plot of the energy density in this diffraction image as a function of the radial distance from the center of the image will be called the primary diffraction curve of the objective.   The center of the diffraction image will be called the diffraction head.   An Airy-type objective is defined as one whose diffraction curve obeys the usual law

$$\frac{G(r)}{\pi^2 \rho_m{}^4} = 4 \left[\frac{J_1(2\pi\rho_m r)}{2\pi\rho_m r} \right]^2 \tag{18.1}$$

in which $G(r)$ is the energy density in the diffraction image as a function of the radial distance r in wavelengths from the diffraction head, J_1 is a Bessel function of the first kind and first order, and

$$\rho_m \equiv \sin\theta_m, \tag{18.2}$$

where θ_m is the maximum angular aperture of the objective in its image space as illustrated in Fig. II.20. ρ_m is related to

$$\rho_{0m} \equiv \sin \theta_{0m}, \qquad (18.3)$$

with θ_{0m} defined in Fig. II.20, in accordance with the Abbe sine condition, as

$$|M|\rho_m = n_0\rho_{0m} = n_0 \sin \theta_{0m} \equiv \text{N.A.}, \qquad (18.4)$$

where n_0 is the refractive index of the object space and N.A. is the usual numerical aperture of the objective.
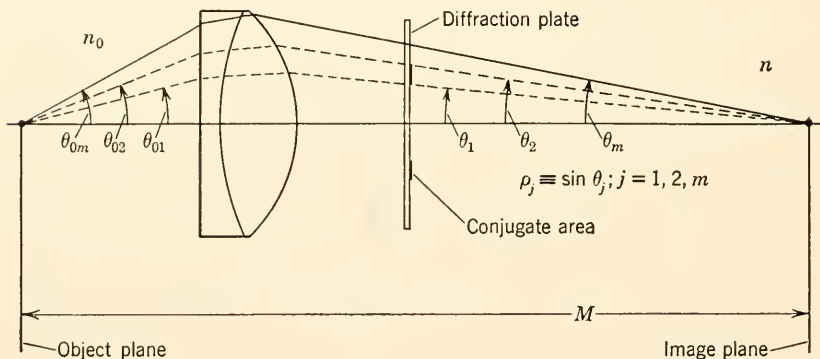
FIG. II.20. The zonal apertures of the objective and its diffraction plate whose conjugate area is annular in shape.

It will be noted from Eq. 18.1 that $G(r) = 0$ when $J_1(2\pi\rho_m r) = 0$. The first value of $r > 0$ for which $J_1(2\pi\rho_m r) = 0$ is denoted by r_a and is called the Airy limit with respect to the image space. Since $J_1(z) = 0$ when $z = 3.8317$,

$$r_a = \frac{3.8317}{2\pi\rho_m} = \frac{0.6098}{\rho_m} \text{ wavelengths.} \qquad (18.5)$$

r_a is physically the distance from the diffraction head to the first zero in the energy density. If $r_a{}^o$ denotes the Airy limit as measured in the object plane with an objective of magnification ratio M,

$$r_a{}^o = \frac{r_a}{|M|} = \frac{0.6098}{|M|\rho_m} = \frac{0.6098}{\text{N.A.}} \text{ wavelengths.} \qquad (18.6)$$

Equation 18.6 is the usual expression for the Airy limit.

Since

$$2\pi\rho_m r = 3.8317 \frac{r}{r_a}, \qquad (18.7)$$

it is advantageous to write Eq. 18.1 in the universal form

$$\frac{G(r)}{\pi^2 \rho_m{}^4} = 4 \left[\frac{J_1(3.8317 r/r_a)}{3.8317 r/r_a} \right]^2 \tag{18.8}$$

in which r/r_a is physically the distance from the diffraction head measured in Airy units r_a. The distance from the diffraction head to the first zero in the energy density is therefore given by $r/r_a = 1$.

The energy densities $G(r)/\pi^2 \rho_m{}^4$ computed from Eq. 18.8 are plotted in Fig. II.21A as a function of r/r_a. The primary diffraction curve of Fig. II.21A is universal in the sense that it applies to Airy-type objectives of any numerical aperture. Aberration-free objectives of low numerical aperture approximate the Airy-type objective closely.

It has been shown by Luneberg (1944, p. 391) that the Airy-type objective has the highest possible energy density at the diffraction head. The effect of introducing spherical aberration or diffraction plates is necessarily to lower the energy density at the diffraction head. When the energy density at the diffraction head is lowered, the energy content of the diffraction rings is invariably increased. A pronounced increase in the relative energy content of the diffraction rings may lead to a loss of resolving power or to reduced contrast in the image or to both.

The primary diffraction curves have been computed for aberration-free objectives for five different diffraction plates and are plotted in Figs. II.21B to II.23B so as to permit comparison with one another and with the Airy-type diffraction curve of Fig. II.21A. The type of diffraction plate is indicated together with the h^2 and δ values. The ratios $\rho_1/\rho_m = \sin \theta_1 / \sin \theta_m$ and $\rho_2/\rho_m = \sin \theta_2 / \sin \theta_m$ of the zonal numerical apertures of the conjugate area are indicated also. It is emphasized that, on account of the universal nature of the curves, these curves apply to all objectives having the zonal ratios ρ_1/ρ_m and ρ_2/ρ_m and the given h^2 and δ values, irrespective of the actual N.A. $= |M|\rho_m$ of the objective. The labeled ordinates to which the energy densities $G(r)/\pi^2 \rho_m{}^4$ are plotted are alike. As a consequence, the fact that $G(0)/\pi^2 \rho_m{}^4 = 0.5$ in Fig. II.21B whereas $G(0)/\pi^2 \rho_m{}^4 = 1.0$ in Fig. II.21A means that the energy density at the diffraction head with the objective of Fig. II.21B is 0.5 of the value of the energy density at the diffraction head of the corresponding Airy-type objective. It will be noted that the primary diffraction curves are identical for all δ values of opposite sign. For example, the primary diffraction curve of Fig. II.21B applies to $\delta = \pm \lambda/4$.

An examination of the five primary diffraction curves drawn for the indicated diffraction plates shows that the first minimum in the energy density occurs in all cases near $r/r_a = 1$, that is, near the Airy limit.
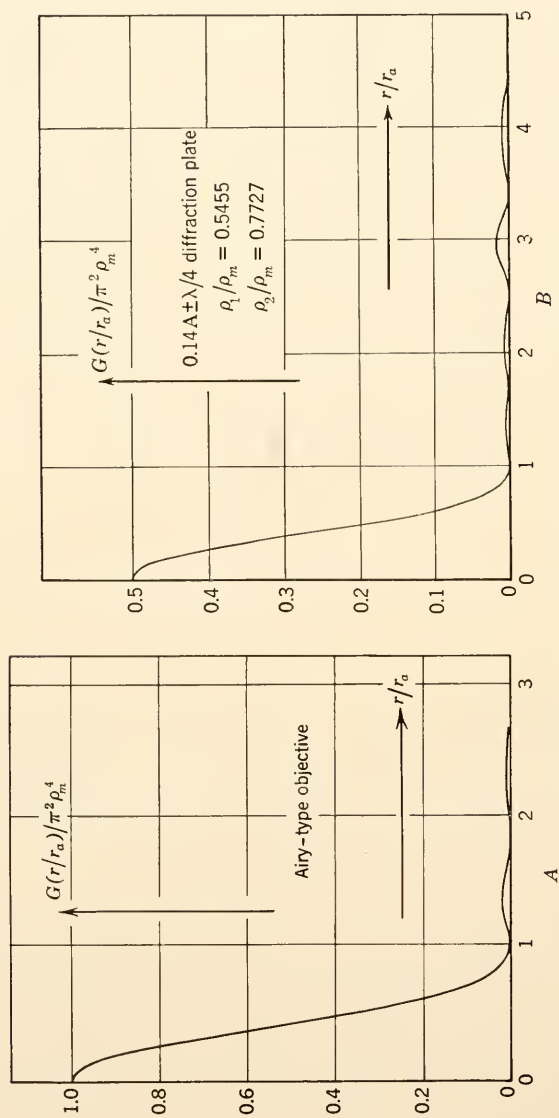
FIG. II.21.   Comparison of the primary diffraction images produced by the classical Airy-type objective and by an objective containing a 0.14A ±λ/4 diffraction plate. $h^2 = 0.14$ in B.

This does not prove that the position of the first minimum is unaffected by the choice of diffraction plate but demonstrates that it is possible to choose the zonal aperture ratios ρ_1/ρ_m and ρ_2/ρ_m and the h and δ values of the diffraction plate in such a manner that the first minimum of the primary diffraction curve falls practically at the Airy limit. In some cases the constants of the diffraction plate can be chosen so that the first minimum in the energy density occurs at a position slightly inside the Airy limit, as in Fig. II.21B. On the basis of Airy's criterion for resolution, the resolving power of an objective for two particles is determined by the distance r from the diffraction head to the first minimum in the energy density of the primary diffraction curve. Since it is possible to choose diffraction plates so that the first minimum in the energy density falls practically at the Airy limit, no significant gain or loss in resolution is to be expected on this account from a well-chosen diffraction plate.

The diffraction plates of Fig. II.22A and B differ only in ring width. Thus $\rho_2 - \rho_1$ is greater in B than in A. It will be noted that the first minimum in the energy density occurs at a greater distance from the diffraction head with the diffraction plate which has the narrower ring width. One can expect that with the h^2 and δ values of Fig. II.22 the diffraction plate having the wider ring width should give the better resolution. In general, higher contrasts can be produced by diffraction plates having the narrower annuli. This can be expected from the fact that the undeviated and deviated waves are separated more completely at diffraction plates with the smaller conjugate area. In practice, the difficulties of designing a diffraction plate so as to attain the most favorable compromise between contrast and definition are augmented by the spherical aberration which is always present in objectives of high numerical aperture and by the curvature of field in the image of the opening in the condenser diaphragm.

It will be seen that the energy densities at the diffraction head are decidedly lower for all illustrated diffraction plates than with the Airy-type objective. A particularly marked loss of energy density at the diffraction head occurs with the $2.50B \pm \lambda/4$ diffraction plate. A portion of the lost energy is due to absorption at the conjugate or complementary area. Since the complementary area bears the absorbing material in a B-type diffraction plate and since the complementary area is large compared to the conjugate area, most of the reduction in the energy density at the diffraction head with the $2.50B \pm \lambda/4$ diffraction plate can be attributed to absorption at the diffraction plate. Losses due to such widespread absorption at the diffraction plate serve mainly to lower the energy content of the entire diffraction image and
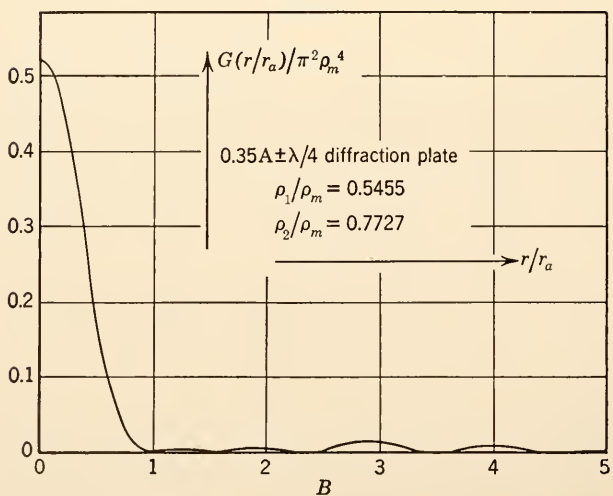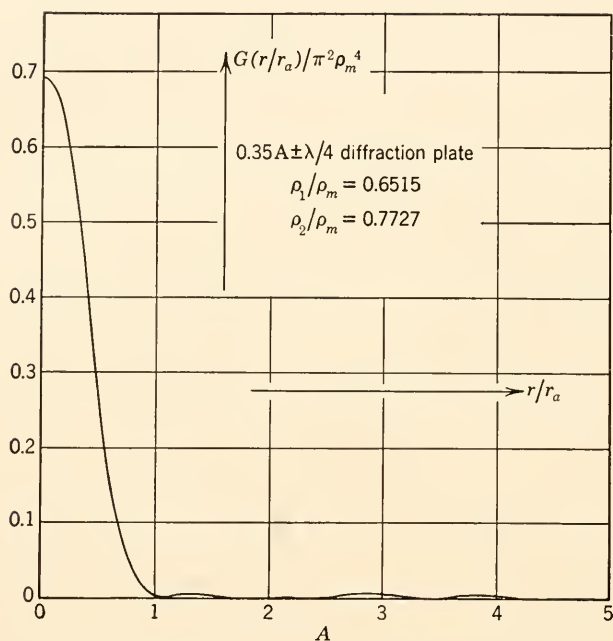
FIG. II.22. The effect of the choice of width of the annular conjugate area of a $0.35A\pm\lambda/4$ diffraction plate upon the primary diffraction image. The location of the first minimum is displaced towards larger values of r/r_a as the width of the conjugate area is reduced. $h^2 = 0.35$ in A and B.
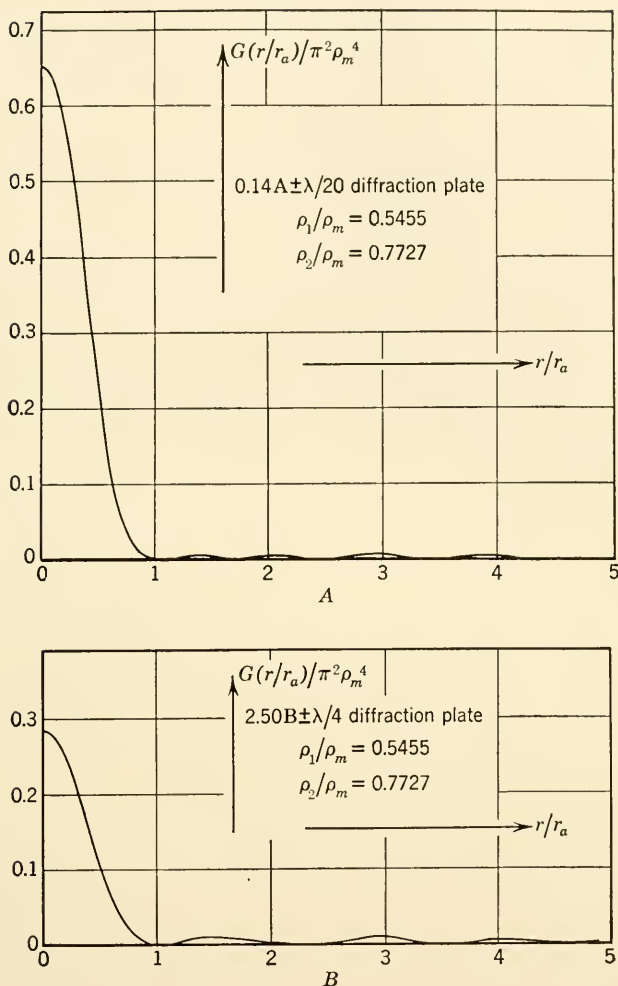
FIG. II.23. Comparison of the primary diffraction images produced by a 0.14A $\pm \lambda/20$ and by a 2.50B$\pm\lambda/4$ diffraction plate. Whereas the first minimum occurs near $r/r_a = 1$, that is, near the Airy limit of resolution, the B-type diffraction plate produces a lower central maximum in the energy density, $G(0)$, and a greater relative amount of energy density in the diffraction rings. $h^2 = 0.14$ in A; $h^2 = 2.50$ in B.

play only a secondary role in modifying the shape of the primary diffraction curve and hence in modifying the contrast or resolution in the image.

The relative energy content in the diffraction rings is less with the Airy-type objective than with any of the illustrated objectives, but the

increase in the relative energy content is not important except with the B-type objective.   It can be shown that the main effect of the increased relative energy content in the diffraction rings is to offset the degree of contrast obtained in the phase microscope.

The above considerations indicate that no marked loss of resolution is to be expected with the use of a phase microscope provided that the diffraction plate has been chosen so as to obtain the most favorable compromise between contrast and resolution.   In general, this conclusion is in accord with experiment.   It is well to bear in mind, however, that the resolution of two particles depends on the dimensions and optical properties of the particles as well as on the properties of the diffraction plate.   Consequently, sweeping generalizations about the relative resolutions possible with two different diffraction plates or between a phase microscope and an ordinary microscope should be regarded with skepticism.

INSTRUMENTATION

1. GENERAL CONSIDERATIONS OF DESIGN

The preceding chapters have shown that the ordinary microscope can be converted to a phase microscope by the addition of two essential elements, namely, the diffraction (or phase) plate and a specialized condenser diaphragm. Thus the schematic diagram of Fig. II.5 contains a condenser diaphragm with an annular opening as aperture located at the first focal plane of the substage condenser and a diffraction plate located at the second focal plane of the objective. The condenser diaphragm and the diffraction plate perform definite functions in the phase microscope. The performance of these functions is modified by both the specimen and the optical design of various components of the microscope. The spherical aberration of the objective and curvature of field in the image of the condenser diaphragm, for example, may introduce limitations. The minimization of the adverse effects produced by these modifications leads to some of the most difficult problems of designing and making a phase microscope.

It has also been shown in the previous chapters that the main function of the restricted opening in the condenser diaphragm is to provide an optical means for separating the light that is deviated by diffraction at the object specimen from the light that remains undeviated by diffraction at the object specimen. This separation occurs at the diffraction plate. The undeviated rays obey the laws of geometrical optics and pass through that area of the diffraction plate which is occupied by the geometrical image of the opening in the condenser diaphragm. This area is called the conjugate area. The remaining area of the diffraction plate intercepts most of the deviated rays and is called the complementary area. The chief function of the diffraction plate is to alter the amplitude ratio between the undeviated and deviated waves and to change the phase difference between these two waves. To accomplish this the amplitude transmission and the optical path of the conjugate area are deliberately made different from the amplitude transmission and the optical path of the complementary area by any one of several methods.

The essential requirement governing the relative location of the condenser diaphragm and of the diffraction plate is that the condenser

diaphragm shall be focused upon the diffraction plate by the lenses which lie between the condenser diaphragm and the diffraction plate. The choice of the first focal plane of the substage condenser as the location of the condenser diaphragm makes the most practicable use of the diffraction phenomena. However, it is not essential that the condenser diaphragm be placed at the first focal plane of the condenser. If the condenser diaphragm is put at the first focal plane of a well-corrected substage condenser and if an image of the light source is formed on the condenser diaphragm, then the object specimen is illuminated by substantially parallel light. With an Abbe-type substage condenser, the spherical aberration necessarily present in this type of condenser destroys to some degree the parallelism of the rays which are incident on the object specimen. However, an Abbe-type condenser is a satisfactory substage condenser for the phase microscope, provided that the condenser has the numerical aperture required by the design of the diffraction plate. It can be shown theoretically that the departure from parallelism of the illuminating rays plays only a secondary part in modifying the contrast produced by the phase microscope. Experiment also shows that very little effect is produced on contrast in the image when the rays illuminating the specimen are not parallel. The presence of spherical aberration in the substage condenser can affect the distance between the last surface of the condenser and the specimen slide when the phase microscope is lined up and adjusted for use. This may modify the numerical aperture at which the full aperture of the condenser can function if the diaphragm is removed and the position of the condenser is not changed. In the presence of aberrations the magnification ratio between the condenser diaphragm and the conjugate area of the diffraction plate depends on the distance between the last surface of the substage condenser and the first surface of the objective.

In order to minimize any effects which may be due only to the orientation of some specimens with respect to the conjugate area of the diffraction plate, the opening in the condenser diaphragm should be circular or annular and should be centered on the optical axis. Burch and Stock (1942) described an experimental arrangement in which the aperture in the diaphragm and the conjugate area of the diffraction plate were slit-shaped. They reported that the image of long, striated muscle fibers, for example, vanished completely when the fibers were oriented exactly perpendicular to the conjugate area.

Under conditions necessary for good performance the undeviated light and only a very small part of the deviated light will pass through the conjugate area of the diffraction plate, and the greatest fraction of the deviated light will pass through the complementary area. Since in

practice an extended opening in the condenser diaphragm and hence an extended source of light is used to illuminate the specimen, it is not possible with most object specimens to separate completely the deviated from the undeviated light. The use of a white light source rather than a monochromatic source will increase the amount of overlap of the deviated and undeviated light at the conjugate area. As the range of numerical aperture included in the opening of the condenser diaphragm becomes smaller (i.e., as the opening becomes narrower) the conjugate area of the diffraction plate becomes narrower and there is less overlap of the deviated and undeviated light at the conjugate area. This is the most important reason for making the conjugate area narrow.

It is known that loss of resolution occurs when the numerical aperture of the condenser is reduced in value below that of the objective. The resolving power of a phase microscope is discussed to some extent in Section 18 of Chapter II. If the specimen is illuminated by a hollow cone of light, as when the condenser diaphragm contains an annular aperture, theory shows that resolution can be expected to increase as the outer diameter of the illuminating cone is increased (greater ρ_2, Fig. II.20). If the numerical aperture corresponding to the outer diameter of the illuminating cone is sufficiently great, then some further advantage may be gained by also increasing the inner diameter of the illuminating cone (smaller $[\rho_2 - \rho_1]$, Fig. II.20). The relative transmission of the conjugate and complementary areas and the optical path difference between these areas will have some additional effect on resolution. However, this effect will be of secondary importance, at least when the optical path difference between the particle and its surround is small. Therefore, in order to gain the improvement in contrast which can result from the choice of relatively narrow conjugate areas and in order to maintain as high resolution as possible, an annular opening in the condenser diaphragm is generally preferred to a circular aperture centered on the optical axis.

It is also a fact that an extremely narrow opening in the condenser diaphragm and the correspondingly very narrow conjugate area superimpose undesirable diffraction effects on the image of some specimens. For some purposes, notably when photomicrographic records that require short exposure times are to be made, a very small condenser opening may cause too great a loss in illumination. A useful rule of thumb is to make the width of the conjugate area (the zone included between θ_1 and θ_2, Fig. II.20) approximately equal to one-fifteenth of the clear aperture of the objective in the plane of the diffraction plate (Zernike, 1942).

When existing condenser and objective systems are used in the design

of a phase microscope, it may be impossible to avoid the occurrence of parallax between the image of the opening in the condenser diaphragm and the diffraction plate. Epstein (1950) has treated theoretically the problem of the edge effect in phase contrast when the image of a point source of light is projected on the edge of the conjugate area of the diffraction plate but is defocused with respect to it. Excessive parallax produces deterioration of contrast in the image of the object specimen. It is evident that there is more overlap of the deviated and the un-deviated light at the diffraction plate as the parallax increases. Curvature of field of the group of lenses forming the image of the condenser diaphragm may cause the parallax to become sufficiently greater as the mean diameter of the opening in the condenser diaphragm increases that it becomes necessary to limit the mean diameter of the opening in the condenser diaphragm.

The spherical aberration of the objective often restricts the outer radius of the conjugate area. Spherical aberration produces non-uniform phase changes in the wave front as it passes through the objective. Such relative changes in phase are equivalent to changes in optical path and will be different for different wavelengths of light. Curves of chromatic lateral spherical aberration for most of the higher power achromatic and apochromatic refracting objectives show a rapid but smooth change near the outer edge of the aperture. Any change in phase due to spherical aberration is superimposed on the change in phase deliberately introduced by means of a diffraction plate. Elementary theory shows that, to obtain optimum contrast with objectives which are free from spherical aberration, the amplitude transmission and the optical path across the diffraction plate should be described by a step function; i.e., an abrupt discontinuity in optical path or in amplitude transmission or in both should take place at the boundary between the conjugate and complementary areas, but within each area the optical path and the amplitude transmission should be constant, as in Zernike's arrangement. When the conjugate area of a step-type diffraction plate lies too far out in the aperture of an objective with spherical aberration, the spherical aberration so modifies the region of the conjugate area that changes in optical path can no longer take the shape of a step. Instead of an optical path step at the conjugate area, a region of rapidly changing optical path exists which is different in magnitude, shape, and extent from what is required for good phase contrast. A second rule of thumb is to select a value of the mean diameter of the conjugate area in the range ½ to ⅔ the diameter of the aperture of the objective in the plane of the diffraction plate.

It is a familiar fact that the spherical aberration of an objective is

altered by a change in the thickness of the cover glass. Since spherical aberration affects the performance of the phase objective, it is often important to select cover glasses having a thickness deviating by not more than 0.02 or 0.03 mm from the thickness for which the phase objective has been adjusted.

The angular spread of the light deviated by diffraction at the object specimen depends on the dimensions and shape of the specimen and on the optical properties of the specimen relative to those of its surround. Some specimens deviate the light in such a manner that the amount of deviated light which passes through the conjugate area is negligible. With other specimens this will not be true if the size and location of the conjugate area remain the same. When optimum contrast is demanded in the image, a change in the optical properties of the specimen relative to those of the surround requires a change in the relative amplitude transmission and in the optical path difference between the conjugate and complementary areas of the diffraction plate, even when the deviated light is completely separated from the undeviated light. The changes in the amplitude transmission and optical path of the diffraction plate are quantitatively different when the overlap of the deviated and undeviated light at the conjugate area becomes sufficiently great. The favored amount of contrast depends largely on the specific application of the phase microscope. It is not necessary to produce greatest possible contrast in order to study the detail in a specimen; in fact, gradations in contrast may offer additional information. The amount of contrast preferred even for a given specimen may be different according as visual observations or photographic records are made.

There exists a large group of object specimens which differ from their surround by a small amount in optical path but which do not differ appreciably from their surround in absorption. The optical path difference is said to be small when it is less than $\frac{1}{8}$ wavelength. Because the useful range of contrast is wide, it is possible to design a diffraction plate that is satisfactory for observing this entire group of specimens. The size and location of the conjugate area of such a diffraction plate can be determined by the two rules of thumb mentioned previously in this section. The energy transmission of the conjugate area is chosen to fall between 25% and 40% of the energy transmission of the complementary area. The magnitude of the optical path difference between the conjugate and complementary areas is made equal to $\frac{1}{4}$ wavelength at 5461 A. Suppose that the optical path through the conjugate area exceeds the optical path through the complementary area by $\frac{1}{4}$ wavelength. Then a particle will appear in bright or dark contrast according as its optical path is greater than or less than that of

the surrounding material. If the optical path through the conjugate area is $\frac{1}{4}$ wavelength less than the optical path through the complementary area, then the contrast of the image of the above particle will be reversed.

Let us discuss the phenomena of phase contrast in terms of the properties g and Δ of the specimen and in terms of the essential physical constants h and δ of the diffraction plate. The symbols g, Δ, h, and δ are defined in Chapter II following Eq. 8.8. The general-purpose diffraction plates suggested in the preceding paragraph have the design specifications $0.25 \leqq h^2 \leqq 0.40$ and $\delta = \pm\lambda/4 = \pm90°$. Such diffraction plates do produce satisfactory contrast in the image of object specimens for which $g = 1$ and for which $0 < |\Delta| < \lambda/8 = 45°$. The following paragraphs will show that this empirical conclusion is at least consistent with the simple theory presented in Chapter II.

Figure II.14B refers to a particle for which $g = 1$ and for which $\Delta = +\lambda/18$ and describes the changes that occur in the light intensity in the image of the particle and in the image of its surround as h and δ are varied. No serious deterioration in either dark or bright contrast is predicted as δ varies between $-70°$ and $-110°$ or between $70°$ and $110°$. The variation in the light intensity in the image of the particle is not symmetrical about the points $\delta = \pm90°$ since optimum contrast does not occur at $|\delta| = 90°$. The h value for the general-purpose diffraction plate lies between $h = 0.5$ and $h = 0.632$. Only the greatest value for h in Fig. II.14B belongs to this range. Nevertheless, the tolerance on the value of δ suggested by these curves is at least in qualitative agreement with observations. Figure II.14B has another point of interest. The figure indicates that, if the diffraction plate is fabricated of materials that have indices of refraction which remain constant throughout the visible region and if $\delta = \pm90°$ at $\lambda = 5461$ A, then satisfactory contrast in the image may still be expected if white light rather than a narrow band of wavelengths in the neighborhood $\lambda = 5461$ A is used to illuminate the object specimen. A variation of $\pm20°$ in δ from $\delta = 90°$ at $\lambda = 5500$ A is equivalent to the phase variation associated with wavelengths in the range 4500 A to 7000 A.

Equations II.10.2 and II.10.5 describe the conditions for darkest possible contrast when $g = 1$. They state that as the optical path difference between the particle and its surround approaches zero the amplitude transmission of the conjugate area should also approach zero. Further, as the optical path difference between the particle and its surround increases, the necessary optical path difference between the conjugate and complementary areas becomes less than $90°$ in absolute value. Theorem 5 in Section 13 of Chapter II requires that the step in

optical path across the diffraction plate be greater than 90° as the optical path difference between the particle and its surround increases when the particle is to be viewed in optimum bright contrast. It is also of great interest to investigate the range of Δ for which good contrast is obtained in the image of a transparent particle (the case $g = 1$) when δ is fixed at $-90°$ and h is assigned different values which may depart considerably from the particular h values required for darkest possible contrast or for optimum bright contrast. Let the fixed values $\delta = -90°$, $g = 1$, and $h_1 = 1$ be substituted into Eqs. II.8.7 and II.8.8. It follows from Eq. II.8.8 that the value of $\Delta \equiv \Delta_{\min}$ for which the light intensity in the image of the particle is a minimum is related to the assigned h value by the equation

$$\tan \Delta_{\min} = h. \tag{1.1}$$

Also

$$(G_p)_{\min} = h^2 + 2[1 - (1 + h^2)^{\frac{1}{2}}], \tag{1.2}$$

in which G_p is proportional to the amount of light energy in the image of the particle. G_s is similarly proportional to the amount of light energy in the image of the surround and is given by

$$G_s = h^2. \tag{1.3}$$

The data of Table III.1 have been calculated from Eqs. 1.1–1.3. This table shows that, if the relative amplitude transmission h of the conju-

Table III.1

The minimum energy densities $(G_p)_{\min}$ and the contrast values K as functions of $\Delta_{\min}$ and h when $0 \leqq h \leqq 0.7$ in the case $g = 1$ and $\delta = -90°$

h	$\Delta°_{\min}$	$(G_p)_{\min}$	G_s	$K \equiv (G_p - G_s)/G_s$
0	0	0	0	. . . . .
0.1	5.72	0.0000248	0.01	−0.998
0.2	11.32	0.000392	0.04	−0.990
0.3	16.70	0.00194	0.09	−0.978
0.4	21.80	0.00593	0.16	−0.963
0.5	26.57	0.0139	0.25	−0.944
0.6	30.97	0.0276	0.36	−0.923
0.7	35.00	0.0487	0.49	−0.901

gate area is adjusted so that $G_p = (G_p)_{\min}$, then the contrast values K depart only slightly from the limiting value $K = -1$ corresponding to darkest possible contrast. The range in Δ includes the optical path differences normally encountered in phase microscopy. It still holds that, as Δ becomes very small, h must also become very small in order to obtain good contrast. The energy densities G_s and G_p associated

with the fixed values $\delta = -90°$, $g = 1$, and $h_1 = 1$ also follow from
Eqs. II.8.7 and II.8.8 and are given by the relations

$$G_s = h^2; \tag{1.4}$$

$$G_p = h^2 + 2 - 2\cos\Delta - 2h\sin\Delta. \tag{1.5}$$

Consequently when Δ approaches zero, G_p approaches G_s, so that finally
the particle cannot be distinguished from its surround. When $\Delta = 0$,
$G_p = G_s = h^2$. The curves of Fig. III.1 have been computed from
Eqs. 1.4 and 1.5 for the special case, $h = 0.5$. They show G_s and G_p as
functions of the optical path difference Δ. As Δ increases from zero,
the light intensity in the image of the particle first decreases until
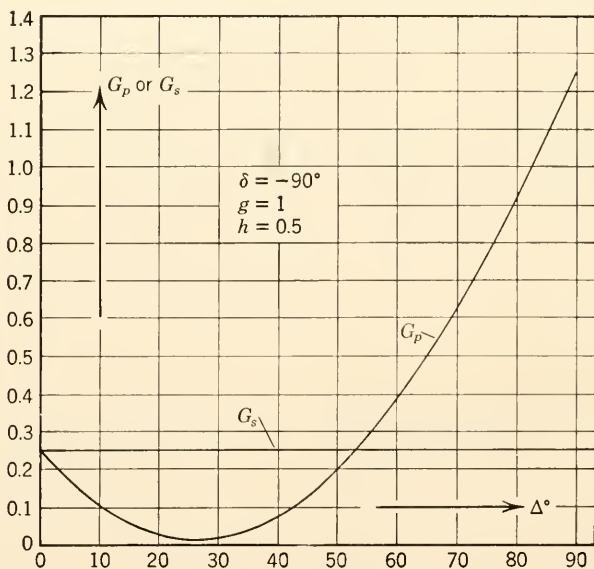
FIG. III.1. The energy densities G_s and G_p as a function of the value of Δ for par-
ticles for which $g = 1$ and which are observed with a phase objective described by
$\delta = -90°$ and $h = 0.5$.

$(G_p)_{\min}$ is reached, and then increases. For values of Δ greater than
$53.13°$ the image of the particle becomes brighter than the image of
the surround. A reversal of contrast may therefore be expected at the
point $\Delta = 53.13°$ when $\delta = -90°$ and $h = 0.5$. If, as a criterion of
good dark contrast, the value of K is taken between the limits
$-1 \leqq K \leqq -\frac{2}{3}$, i.e., if the light intensity in the image of the particle
shall not exceed $\frac{1}{3}$ the intensity in the image of the surround, there will
exist for every value of h a pair of values Δ_1 and Δ_2 such that the diffrac-

tion plate can be expected to produce good contrast for all values of Δ in the interval $\Delta_1 \leqq \Delta \leqq \Delta_2$. Such pairs of Δ_1 and Δ_2 have been computed from Eqs. 1.4 and 1.5 and are listed in Table III.2 as functions of h. The simple theory predicts therefore that the general-purpose diffraction plate ($0.5 \leqq h \leqq 0.632$; $\delta = -90° = -\lambda/4$) will result in good dark contrast for values of Δ lying between 12° and 47° and that the particle will be visible against its surround for an even greater range of values of Δ.

Table III.2

The interval $\Delta_1 \leqq \Delta \leqq \Delta_2$ for which the contrast K lies between the limits $-1 \leqq K \leqq -\frac{2}{3}$ as a function of h when $0.1 \leqq h \leqq 0.7$ in the case $g = 1$ and $\delta = -90°$

h	$\Delta_1°$	$\Delta_2°$
0.1	2.42	9.00
0.2	4.85	17.77
0.3	7.32	26.10
0.4	9.77	33.83
0.5	12.25	40.67
0.6	14.78	47.13
0.7	17.37	52.62

The specifications for a general-purpose diffraction plate for obtaining bright contrast with transparent particles whose optical path exceeds that of the surround are again $0.5 \leqq h \leqq 0.632$, but $\delta = +90°$ instead of $-90°$. Let the fixed values $\delta = +90°$, $g = 1$, and $h_1 = 1$ be substituted into Eqs. II.8.7 and II.8.8. Then

$$G_s = h^2;$$

$$G_p = h^2 + 2 - 2\cos\Delta + 2h\sin\Delta. \tag{1.6}$$

The contrast values $K = (G_p - G_s)/G_s$ of Table III.3 have been computed with the aid of Eqs. 1.6 for values of Δ in the first quadrant (i.e., for the interval $0 \leqq \Delta \leqq 90°$) and for values of h in the range $0 \leqq h \leqq 0.7$. Table III.3 shows that, when h is fixed at any value, K is an increasing function of Δ throughout the first quadrant. The behavior of the bright-contrast values $K > 0$ for particles with Δ values which lie in the first quadrant differs in two notable respects from the behavior of the dark-contrast values $K < 0$ which result from setting $\delta = -90°$ instead of $+90°$. First, at fixed values of h the bright-contrast values K do not reach either a maximum or a minimum for any point Δ which falls within the first quadrant. Second, since the contrast values of Table III.3 are all positive, reversal of contrast does not occur at any value of h or Δ listed in the table. Table III.3 shows also that optimum

Table III.3

The contrast values K as functions of h and Δ when
$0 \leqq \Delta \leqq 90°$ in the case $g = 1$ and $\delta = +90°$

$\Delta°$ \ h	0	0.1	0.2	0.3	0.4	0.5	0.6	0.7
0	..	0	0	0	0	0	0	0
5	∞	2.51	1.06	0.67	0.48	0.38	0.31	0.26
10	∞	6.51	2.50	1.50	1.06	0.82	0.66	0.56
20	∞	18.9	6.44	3.62	2.46	1.85	1.48	1.22
30	∞	36.8	11.7	6.31	4.17	3.07	2.41	1.98
40	∞	59.6	18.1	9.48	6.14	4.44	3.44	2.79
50	∞	86.8	25.5	13.0	8.30	5.92	4.54	3.65
60	∞	117	33.7	16.9	10.6	7.46	5.66	4.52
70	∞	150	42.3	20.9	12.9	9.02	6.79	5.37
80	∞	185	51.2	24.9	15.3	10.6	7.87	6.19
90	∞	220	60.0	28.9	17.5	12.0	8.89	6.94

bright contrast, $K = 3$, has already been exceeded when $\Delta = 45° = \lambda/8$ for all listed values of h. Optimum contrast is not reached, however, for h values in the range $0.5 \leqq h \leqq 0.632$ when Δ is less than $30°$. If as a criterion of good bright contrast it is required that $K \geqq 2$, i.e., it is required that the light intensity in the image of the particle shall be at least three times the light intensity in the image of the surround, there will exist for every value of $h > 0$ a value of $\Delta \equiv \Delta_3$ such that the diffraction plate can be expected to produce good bright contrast for all values of Δ in the interval $\Delta_3 \leqq \Delta \leqq 90°$. These values of Δ_3 have been determined from Eqs. 1.6 and are listed as a function of h in Table III.4. Tables III.3 and III.4 indicate that good bright contrast may be expected with a $0.25A+\lambda/4$ diffraction plate (see Fig. III.3a) in observing particles for which Δ falls in the range $21° < \Delta \leqq 90°$. For smaller values of Δ the simple theory indicates that h must be less than 0.5 in order to obtain sufficiently good bright contrast. It is possible that the phase microscopist will prefer a general-purpose bright-contrast plate with a more highly absorbing conjugate area than would be selected for a general-purpose dark-contrast plate.

Object specimens which are absorbing and which have a refractive index equal to the refractive index of the surround ($g \neq 1$, $\Delta = 0$) present a different set of requirements for a useful diffraction plate. If the values $\Delta = 0$ and $h_1 = 1$ are substituted into Eq. II.8.8, then when either $\delta = +90°$ or $\delta = -90°$ is also substituted into Eq. II.8.8 the expression for G_p becomes

$$G_p = (g - 1)^2 + h^2. \tag{1.7}$$

Sections II.11 and II.15 have shown that the diffraction plate for which $\delta = \pm 180°$ or for which $\delta = 0$ can be expected to be more useful in producing bright or dark contrast, respectively, than the diffraction plate

Table III.4

The values Δ_3 as a function of h

h	$\Delta_3°$
0.0	0.0
0.1	4.2
0.2	8.4
0.3	12.6
0.4	16.9
0.5	21.3
0.6	25.7
0.7	30.3

for which $\delta = \pm 90°$. When $\Delta = 0$ and $\delta = \pm 180°$, Eq. II.8.8 becomes

$$G_p = [h + (1 - g)]^2. \tag{1.8}$$

When $\Delta = 0$ and $\delta = 0$, Eq. II.8.8 becomes

$$G_p = [h - (1 - g)]^2. \tag{1.9}$$

In each case

$$G_s = h^2.$$

Table III.5 permits comparison of the contrast values $K = (G_p - G_s)/G_s$ which are computed with the help of Eqs. 1.7, 1.8, and 1.9 for values of h in the range $0.02 \leq h \leq 1.0$ and for a particle for which $\Delta = 0$ and $g = 0.9$. Such a particle transmits $0.9^2 = 0.81$ times as much light as its surround. The diffraction plates for which $\delta = \pm 90°$ produce only bright contrast, but as bright-contrast plates they do not compare favorably with the diffraction plates for which $\delta = \pm 180°$. The dark contrast produced by the diffraction plate for which $\delta = 0$ and for which $0.1 \leq h \leq 1.0$ does not deteriorate so rapidly with increasing value of h as does the bright contrast produced by the diffraction plate for which $\delta = \pm 180°$. Table III.5 shows that a value less than 0.5 must be assigned to h if good contrast, either bright or dark, is to be obtained. The ordinary objective ($h = 1$, $\delta = 0$) produces dark contrast $K = -0.19$. Even when the value of h is as high as 0.5 on a diffraction plate for which $\delta = 0$, the resulting dark contrast $K = -0.36$ certainly shows an improvement over the contrast produced by an ordinary objective.

Although the simple theory states that the diffraction plates characterized by $\delta = \pm 90°$ are not generally useful when the object specimen is slightly absorbing and has an optical path equal to that of the sur-

Table III.5

The contrast values K as a function of h and δ in the case $g = 0.9$ and $\Delta = 0$

δ \ h	0.02	0.05	0.1	0.2	0.3	0.4	0.5	0.6	0.7	0.8	0.9	1.0
$\pm 90°$	25.00	4.00	1.00	0.25	0.11	0.06	0.04	0.03	0.02	0.016	0.012	0.01
$\pm 180°$	35.00	8.00	3.00	1.25	0.78	0.56	0.44	0.36	0.31	0.27	0.23	0.21
$0°$	15.00	0.00	−1.00	−0.75	−0.56	−0.44	−0.36	−0.31	−0.27	−0.23	−0.21	−0.19

round, this prediction no longer holds when the optical path of a slightly absorbing particle is not negligible with respect to the optical path of the surround. The comparative usefulness of the general-purpose plate can be estimated from Eq. II.8.8 by substituting into this equation the pertinent values of g, Δ, h, and δ. For example, Table III.1 states that $K = -0.944$ when $g = 1$, $\Delta = \Delta_{\min} = 26.57°$, $h = 0.5$, and $\delta = -90°$. If Eq. II.8.8 is solved with $h = 0.5$ and $\delta = -90°$ when $g = 0.9$ and Δ is again $26.57°$ and if K is computed as before, then $K = -0.81$. This is still good dark contrast. An example that concerns itself with bright contrast may be obtained by substituting $g = 0.9$, $\Delta = 30°$, $h = 0.5$, and $\delta = 90°$ into Eq. II.8.8 and then computing the value of K. K is then 2.80. This is good bright contrast. From Table III.3 it is seen that, if $\delta = 90°$, $h = 0.5$, $g = 1$, and $\Delta = 30°$, then $K = 3.07$. No comprehensive consideration, even from the point of view of the simple theory, can be included here for the class of particles $\Delta \gtrless 0$, $g \neq 1$.

It is implicit in the simple theory that Lummer's theorem holds and that there is no overlap of the deviated and undeviated light in the conjugate area. No dependence on the shape and dimensions of the object specimen is included. However, it is not to be expected that the more general theory of phase microscopy will nullify the qualitative aspects of the simple theory. Sections 14 and 15 of Chapter VII show that there can exist within the geometrical image of the particle an extended area, called the A region, for which the laws predicted by the general theory reduce to the laws of the simple theory. In practice the preferred value of h depends strongly on the size of the conjugate area. Users of the phase microscope have found a very wide field of applicability for bright- and dark-contrast diffraction plates for which δ, the optical path difference between the conjugate and complementary areas, is either $+90°$ or $-90°$ but for which h, the amplitude transmission ratio of these areas, may be less than or greater than unity. The range $0.3 < h < 0.7$ is the most useful. It is obvious that the manufacturer of phase microscopes must depend on observations of many microscopists in order to determine what compromise results in the best

diffraction plate or series of diffraction plates to be incorporated into a given objective. At times it may be necessary to provide a diffraction plate that does not belong to the category of general-purpose diffraction plates in order to help solve a special problem.

2. THE DIFFRACTION PLATE

The first part of this section will describe briefly methods for producing a diffraction plate in which the value of the optical path difference between the conjugate and the complementary area is established for a given wavelength and remains fixed, and in which the value of the energy transmission of the conjugate area relative to that of the complementary area is also fixed. Apparatus that permits a gradual variation of either
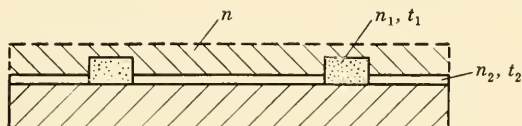
Fig. III.2. Schematic drawing for the design of a non-absorbing diffraction plate.

the optical path difference or the relative energy transmission or both by making use of the properties of polarized light will be discussed in Section 9.

Suppose that a diffraction plate is to be made with an optical path difference equal to some fraction d of a wavelength between the conjugate and the complementary area, and suppose that there is to be no absorption in either area. It is simplest to delineate the case in which materials are to be deposited on a support such as a flat, parallel, homogeneous glass plate in order to produce the conjugate and complementary areas. A design for a non-absorbing diffraction plate is shown schematically in Fig. III.2. A thickness t_1 of material with a refractive index n_1 forms the conjugate area. Over the complementary area is a thickness t_2 of a second dielectric material which has a refractive index n_2. The coatings on both areas are surrounded by a medium which has a refractive index n. The optical path difference between the conjugate and complementary areas is

$$(n_1 - n)t_1 - (n_2 - n)t_2 = d\lambda. \tag{2.1}$$

It is usually most practicable to choose materials that will allow the condition $t_1 = t_2 = t$ to be satisfied when the required optical path difference is introduced. Here it is convenient to take the point of view either that the embedding material with refractive index n becomes the material that forms the complementary area and $n_2 = n$, or that, if a

substance with refractive index n_1 is selected for the conjugate area, the use of a material with refractive index n_2 for the complementary area eliminates any contribution of the embedding material to $d\lambda$. With this choice of coating materials Eq. 2.1 becomes

$$(n_1 - n_2)t = d\lambda. \tag{2.2}$$

If an absorbing material is also deposited upon or incorporated into either the conjugate or the complementary area, then the amount $n_3 t_3$ must be added to the optical path of that area. Here $n_3 \equiv$ refractive index of the absorbing material and $t_3 \equiv$ thickness of the absorbing material. If the absorbing substance is applied on the conjugate area of the plate represented by Fig. III.2 and if the optical path difference between the conjugate and complementary areas remains $d\lambda$, then

$$(n_1 - n)t_1 + (n_3 - n)t_3 - (n_2 - n)t_2 = d\lambda. \tag{2.3}$$

If, on the other hand, the absorbing material is applied on the complementary area of such a diffraction plate and if the optical path difference between the conjugate and complementary areas is again $d\lambda$, then

$$(n_1 - n)t_1 - (n_3 - n)t_3 - (n_2 - n)t_2 = d\lambda. \tag{2.4}$$

As before, it is convenient to choose $n = n_2$. Equations 2.3 and 2.4 become

$$(n_1 - n_2)t_1 + (n_3 - n_2)t_3 = d\lambda; \tag{2.5}$$

$$(n_1 - n_2)t_1 - (n_3 - n_2)t_3 = d\lambda. \tag{2.6}$$

It will be seen (Sections 2.3 and 2.4) that the design specifications for either an achromatic or a color diffraction plate can be satisfied if the refractive indices of the materials constituting the coating on the diffraction plate are given functions of the wavelength. If the dispersion is important, then the Eqs. 2.1–2.6 can be written to include the dependence on wavelength explicitly. It may also become advantageous when such specialized diffraction plates are required to consider only the more general Eq. 2.1 and work with three materials having refractive indices $n_1(\lambda)$, $n_2(\lambda)$, and $n(\lambda)$.

Procedures and materials are available which will allow the contribution $(n_3 - n_2)t_3$ to be neglected because the required amount of absorption is obtained when t_3 is still very small compared with t_1. For purposes of the discussion it will be sufficient to consider that the optical path difference between the conjugate and complementary areas is given by

$$(n_1 - n_2)t_1 = d\lambda \tag{2.7}$$

and that $(n_3 - n_2)t_3$ either is negligible or is applied later as a small correction. A series of equations with the form of Eq. 2.7 formulate the problem if the dependence of the refractive index on wavelength is relevant, and any such considerations must be superimposed upon the general discussion included in Section 2.1. The phase accessories now supplied as standard equipment by various manufacturers produce a neutral, i.e., a black, gray, and white image of most transparent specimens when white light is incident on the specimen. If the conjugate area of the diffraction plate is colored, the image of the material surrounding a specimen (the field of view) will appear similarly colored. The color of the image of a particle will be affected by color in either the conjugate or the complementary area. Wavelengths transmitted by the complementary area but not by the conjugate area will superimpose a colored image like that produced by darkfield illumination with these wavelengths. The introduction of color in either the conjugate or the complementary area or in both is not a satisfactory method for producing color phase contrast. Color phase contrast is a means of causing the detail in a specimen to appear colored whereas the background in the image remains more or less neutral. To convert an ordinary objective to a phase objective, one or more of the existing lens surfaces may be altered to produce the conjugate and the complementary areas, or an additional unit may be mounted in the objective. For example, the additional unit may consist of one or more plane parallel glass plates which have been coated or otherwise treated to form the diffraction plate. The existing optical design of an objective system may not always permit the insertion of an additional glass plate at a suitable plane in the objective.

2.1. Making a diffraction plate

It is mentioned in Section 3.2 of Chapter II that an etching process was used to make some of the first diffraction plates. These plates did not include an additional absorbing layer on either the conjugate or the complementary area. A possible procedure is to etch a glass surface in order to form a trough having the shape of the conjugate area and then to cement a second glass surface over the etched surface. This second glass surface should introduce no additional change in optical path across the diffraction plate. The cement which fills the trough forms the conjugate area. The complementary area consists of a layer of glass equal in thickness to the depth of the trough. If the index of refraction of the cement is greater than that of the etched glass element, then the optical path through the conjugate area is greater than the optical path through the complementary area. If the index of refraction of the cement is

less than that of the etched glass element, then the optical path through the conjugate area is less than the optical path through the complementary area.   If a lens surface is etched, its refractive index has been predetermined by the optical design, and either the depth of the etch or the refractive index of the cement is varied to produce the specified optical path difference.   Obviously, it is possible to begin by etching the trough in the shape of the complementary area and again to achieve the required optical path difference by using a cement with a suitable index of refraction.   It would also be possible to add an absorbing coating over the specified area of the etched surface or over the second glass surface.   If the absorbing film of the correct size and shape is applied over the second glass surface, this second element must be centered with respect to the etched surface so that the discontinuity in amplitude transmission occurs at the same place as the discontinuity in optical path.   At present other methods of forming the optical path step are preferred.

The technics developed for evaporating thin films in a high vacuum offer a very useful method for making diffraction plates.   Optical path differences may be produced by evaporating a dielectric material to the required thickness, and absorption may be introduced by evaporating a metallic film.   However, the absorbing film need not be a metallic one. In general, a neutral conjugate area is preferred.   For example, magnesium fluoride and Inconel form a suitable combination of materials. It is possible to proceed by evaporating soft films which are then partly rubbed off to leave a coating having the required shape and area, or it is possible to use masks during the evaporation so that durable films of only the required pattern are deposited.   A second surface may or may not be cemented over the coated surface.   For the purposes of this discussion it will be assumed that the optical path is produced by a transparent dielectric film and that the absorption is produced by a film so thin that the optical path through it is negligible compared with the final optical path difference required.   Many metallic films, if properly formed, have a thickness equivalent to an optical path of less than $\lambda/20$ even at energy transmissions of only a few per cent.

If soft dielectric and absorbing films are successively deposited on the same surface and if a single ruling procedure is used to remove the coating from the complementary area, then the coating that remains on the conjugate area forms an absorbing step which has a greater optical path than the adjacent air path through the complementary area.   This by itself would make a bright-contrast plate for particles having an optical path greater than that of the surround.   If a second element is cemented over the coated surface, then a cement with a higher or lower index of

refraction than that of the dielectric film will cause the conjugate area to have, respectively, a smaller or greater optical path than the complementary area. To produce a given optical path difference, the thickness to which the coating must be deposited depends on the refractive index of both the dielectric and the cement, according to Eq. 2.7. A single ruling process can also be followed if it is required that the complementary area absorb part of the deviated light. In this case the coating is cleaned off the conjugate area, and again cements with the correct index of refraction will produce the necessary optical path step. Another variation is to deposit the absorbing film on one surface and the dielectric on the other of two surfaces to be ruled and cemented together. This procedure may be useful if it is preferred that the absorbing and dielectric films be on adjacent areas of the diffraction plate. For example, the dielectric material is removed from the conjugate area and the absorbing material is removed from the complementary area. Then a cement of higher index of refraction than the dielectric forms a conjugate area which has a greater optical path than the complementary area. Such a procedure requires more steps and makes the additional demand that the two parts be centered with respect to each other. The final diffraction plate should always be centered on the optical axis of the objective.

A very satisfactory way to shield part of the surface during the evaporation is to hold rings or disks punched out of very thin iron or steel sheet in contact with the surface being coated by means of a pair of small, unlike magnetic pole pieces placed behind the second surface of the plate or lens. If the films so formed are embedded in cement, the considerations concerning optical path differences are the same as when part of the coating is ruled off. If air rather than cement is adjacent to the coating, then the dielectric film must be deposited on the conjugate area if a particle having a greater optical path than its surround is to appear in bright contrast; but if this same particle is to appear in dark contrast, the dielectric must be placed on the complementary area. With thin steel masks it is possible to shield one area while coating the adjacent region, and then to remove the first mask, cover the coated part of the surface with a second mask, and deposit a film over the area that had been protected during the first evaporation. When an annular conjugate area is being produced, a non-magnetic cap fitting over the outer portion of the surface being coated or a holder with the required aperture is used in conjunction with the steel disk in order to shield both parts of the complementary area.

Several facts should be kept in mind if evaporated metal and dielectric films are used. Equation 2.7 states that the greater the difference

between the refractive index of the dielectric forming the conjugate area and the refractive index of the dielectric forming the complementary area, the smaller the thickness of the coating need be. With the technics generally used, some dielectric films which are evaporated on glass tend to scatter and peel if the optical path through the film exceeds 1 μ. If materials are so chosen that a very thin evaporated layer of dielectric substance produces an optical path difference of, say, $\frac{1}{4}$ wavelength, the thickness of the deposition during the evaporation must be more carefully controlled than if a greater thickness of material produces the same optical path difference. Whenever a thin film is deposited on a support that has a refractive index different from that of the film, or if several films with different refractive indices are superimposed on a support, then multiple reflections of light take place at all interfaces at which there is a change in index of refraction. These multiple reflections are accompanied by interference phenomena which cause the transmitted light to be colored. The color and its intensity will depend on the thickness of the films, the refractive indices, and the order of succession of the films if there are more than one. The superposition of metal and dielectric films on the diffraction plate can result, therefore, in a broad-band interference filter. For a given choice of materials, such color effects can be minimized by properly arranging the order of deposition of the films. If, for example, magnesium fluoride and Inconel are to be superimposed and deposited on glass and if air is the other dielectric medium adjacent to the coating, then least color is introduced if the magnesium fluoride is evaporated directly on the glass and the Inconel is deposited on top of the magnesium fluoride. Introducing color by forming an interference filter on the diffraction plate is generally not considered favorable.

Plastic films are a versatile medium for making diffraction plates. Thin films (e.g., about 6 μ thick) can be produced by using a doctor blade to spread a layer of the plastic in solution uniformly over a smooth, flat surface such as a glass plate and allowing it to dry. Obviously, different thicknesses of the layer of the solution and different concentrations of the solution will dry as films of different thicknesses. A punch and die or a cutting blade can be used to form a section of the film in the shape of either the complementary or the conjugate area. The plastic sections are then cemented between two supporting surfaces such as flat glass plates or lens components. The thickness of the plastic film, the index of refraction of the plastic, and the index of refraction of the cement can be changed according to Eq. 2.7 in order to introduce the necessary optical path difference between the conjugate and complementary areas. Dyes can be incorporated into the plastic solution

so that films of both the required thickness and the required transmission are spread.

Plastic films are particularly of interest when some control of the dispersion of the materials constituting the diffraction plates is necessary. It will be seen later in this section that the problem of finding substances with a given dispersion occurs when either achromatic or color diffraction plates are made. Glasses and those substances which can be evaporated to produce a usable film do not offer so much variety and flexibility as do plastics and cements in changing the relative dispersions of the materials which form the conjugate and complementary areas. For example, if cellulose nitrate, cellulose acetate, or cellulose butyrate in solution, or a mixture of these, is spread on glass to produce the plastic film, plasticizers are available which can be added to the solution in order to control the dispersion of the final film. Also, as an example, the addition of chlorinated or brominated aromatic hydrocarbons such as bromonaphthalene is a means of changing the dispersion of the common cement, Canada balsam.

It is known that a phase objective which contains a diffraction plate made with magnesium fluoride and Inconel adjacent to air as the second dielectric material produces an image with good contrast, either bright or dark, when white light is used to illuminate the specimen, although the optical path step has been made equal to $\frac{1}{4}$ wavelength at $\lambda =$ 5461 A. Such a diffraction plate is not achromatic; i.e., the optical path is not equal to $\frac{1}{4}$ wavelength for all wavelengths of visible light. The dispersion of the common dielectric optical substances, including magnesium fluoride, is such that the index of refraction for the blue wavelengths of light is greater than that for the red wavelengths. Therefore, if one of these substances is used adjacent to air in order to produce an optical path step of $\lambda/4$ at $\lambda = 5461$ A, the dispersion is such as to increase a deviation from $\frac{1}{4}$ wavelength at both the blue and the red ends of the visible range. Some predictions made by the simple theory about the deterioration in contrast due to the use of white light rather than a monochromatic source were discussed in Section 1. If the optical paths through the two areas of the general-purpose diffraction plate are paths through magnesium fluoride, metal, and air, some improvement in image contrast occurs if a green filter, such as the Wratten B No. 58, is placed in front of a heterochromatic light source. At least in some instances this improvement may be due in part to the fact that some of the adverse effects due to the aberrations of the objective have been decreased when the filter is used. If the general-purpose plate produces good contrast with white light, it will, in general, still produce satisfactory contrast if any one of the Wratten M series of filters for

photomicrography is used in front of the light source, although the green filter is preferred.

2.2. Diffraction plate with $3\lambda/4$ optical path step

In Section 1 the diffraction plate recommended for producing dark contrast when the object specimen has an optical path greater than that of its surround is one in which the optical path through the complementary area exceeds the optical path through the conjugate area by $\frac{1}{4}$ wavelength. A diffraction plate in which the optical path through the conjugate area exceeds the optical path through the complementary area by $\frac{3}{4}$ wavelength will also produce dark contrast in the image of the same specimen. If the diffraction plate is made of materials which do not form an achromatic diffraction plate when the optical path step is $\lambda/4$ at some wavelength, then the departure from achromatism is even greater when the optical path step is $3\lambda/4$ at that same wavelength.

If a diffraction plate is incorporated into an objective and the condenser diaphragm is removed, the phase objective will function as an ordinary objective, but the definition may be impaired by a small amount. Just as the spherical aberration of the objective affects the performance of the diffraction plate, so the coating of the diffraction plate alters the spherical aberration of the objective as it was originally designed. A $3\lambda/4$ step in a diffraction plate would alter the spherical aberration of the ordinary objective more than would a $\lambda/4$ step. For very critical work with the ordinary objective, it is in general advisable not to use an objective containing a diffraction plate.

2.3. Principles of the achromatic diffraction plate

The advantages of an achromatic diffraction plate are seen best when the optical path difference between the object specimen and its surround is so small that the diffraction plate is producing low contrast, especially if photomicrographs of the low contrast image are taken with colored filters in front of the light source, and when some detail in a strongly colored object specimen can be made better visible by the phase microscope.

To simplify the considerations for the achromatic and the color diffraction plates in the remaining subsections, reference to a dark-contrast diffraction plate will imply that $\delta = -90°$, and reference to a bright-contrast diffraction plate will imply that $\delta = +90°$. Again, it will be assumed that any absorbing material incorporated into the diffraction plate produces only a negligible change in the optical path differences introduced by the dielectric materials. It is also to be as-

sumed that the object specimen is non-absorbing and has an optical
path greater than that of its surround, unless otherwise specified.

If a dark-contrast diffraction plate is to be achromatized for a wave-
length λ_1 at the blue end of the spectrum and for a wavelength λ_2 at the
red end of the spectrum, the following two equations must be satisfied:

$$n_1 - n_2 = -\frac{\lambda_1}{4t} ; \qquad (2.8)$$

$$n_3 - n_4 = -\frac{\lambda_2}{4t} . \qquad (2.9)$$

In Eqs. 2.8 and 2.9,

$n_1 \equiv$ refractive index of conjugate area for λ_1;
$n_3 \equiv$ refractive index of conjugate area for λ_2;
$n_2 \equiv$ refractive index of complementary area for λ_1;
$n_4 \equiv$ refractive index of complementary area for λ_2;
$t \equiv$ thickness of the conjugate and the complementary area.

The refractive index of dielectrics is greater for the shorter wavelengths
of the visible range than for the longer wavelengths. Therefore, let

$$n_3 = n_1 - d_1; \qquad (2.10)$$

$$n_4 = n_2 - d_2. \qquad (2.11)$$

If Eqs. 2.10 and 2.11 are substituted into Eqs. 2.8 and 2.9 and if $4t$ is
eliminated from these equations, then

$$(d_2 - d_1) = \frac{\lambda_2 - \lambda_1}{\lambda_1} (n_1 - n_2). \qquad (2.12)$$

Equation 2.12 also follows if a bright-contrast diffraction plate is achro-
matized at λ_1 and λ_2. However, to produce dark contrast it must be
true that $(n_1 - n_2) < 0$; therefore, according to Eq. 2.12 the dis-
persion of the material forming the conjugate area must be greater than
the dispersion of the material forming the complementary area. To
produce bright contrast it must be true that $(n_1 - n_2) > 0$, and in this
case Eq. 2.12 states that the dispersion of the material forming the com-
plementary area must be greater than the dispersion of the material
forming the conjugate area. The same two dielectric substances may be
used in making either an achromatic dark-contrast or an achromatic
bright-contrast diffraction plate provided that each one of these sub-
stances is applied over the correct area of the diffraction plate. The
material with the higher refractive index must have the lower dispersion.
When Eq. 2.12 is satisfied, the diffraction plate is achromatized at λ_1 and

λ_2, but it is not necessarily exactly achromatized for all wavelengths between λ_1 and λ_2. If the diffraction plate is to be exactly achromatized at N wavelengths, then a set of N simultaneous linear equations of the form of Eqs. 2.8 and 2.9 must be satisfied.

Dark contrast and achromatism are also obtained at wavelengths λ_1 and λ_2 if, instead of conditions 2.8 and 2.9, the equations $(n_1 - n_2)t = -(\lambda_1/4 + k\lambda_1)$, and $(n_3 - n_4)t = -(\lambda_2/4 + k\lambda_2)$, in which k is an integer, either positive or negative, are satisfied. Equations 2.8 and 2.9 are the special cases in which $k = 0$. Similarly the conditions for bright contrast and achromatism at wavelengths λ_1 and λ_2 are also satisfied if $(n_1 - n_2)t = (\lambda_1/4 + k\lambda_1)$ and $(n_3 - n_4)t = (\lambda_2/4 + k\lambda_2)$, in which k is again an integer, either positive or negative. However, Eq. 2.12 follows unchanged, regardless of how high a multiple of $\frac{1}{4}$ wavelength is chosen for the optical path difference between the conjugate and the complementary area. At any wavelength, the difference between the indices of refraction of the two substances forming the conjugate and complementary areas is proportional to that wavelength, provided that the conjugate and complementary areas are of equal physical thickness.

2.4. Principles of color phase contrast

Color phase contrast was first discussed by Zernike in 1948 (National Academy of Sciences, Spring Meeting, 1948, and Symposium on Electron and Light Microscopy, June 1948). However, the published abstracts and reports of these meetings contain no mention of color phase contrast. Since that time Saylor, Brice, and Zernike (1949 and 1950) have described additional investigations of the technics available for designing color phase plates by controlling or selecting the dispersions of the substances forming the conjugate and complementary areas. Zernike also considered the use of controlled dispersions to make achromatic diffraction plates. Some discussion of the achromatic diffraction plate is contained in the publication by Saylor et al. (1950). Grigg (1950) substituted colored filters for the ordinary diaphragm of the substage condenser in order to achieve color phase contrast with a phase objective which contained a neutral diffraction plate of standard design. Two filters of contrasting colors were so assembled that undeviated light of one color passed through that area of the diffraction plate which normally forms the conjugate area, and undeviated light of the second color passed through that area which has been designated as the complementary area of the standard diffraction plate.

The color phase microscope forms a colored image of a transparent specimen which differs in optical path from its surround. In the ideal

color phase contrast image the surround appears neutral. A phenomenon of phase microscopy is that the image of a particle is accompanied by a halo of the opposite sign. In other words, the dark phase contrast image of a particle is surrounded by a bright band or halo which is brighter than the image of the general background, and the bright phase contrast image is surrounded by a dark halo which is darker than the image of the general surround. The colored phase contrast image of a particle is surrounded by a halo of a different color. In order that a phase microscope produce a colored image of an object specimen when the microscope and illuminating system have been set up according to the procedure for Köhler illumination, the curve which describes as a function of wavelength the relative phase difference which the diffraction plate introduces between the undeviated and the deviated light must show that either of the following two conditions exists. In the one, a limited band of wavelengths forms either a bright-contrast or a dark-contrast image of the object specimen, and the remaining wavelengths of the spectrum contribute an ordinary, non-phase contrast image of the object specimen. In the second, the requirement for bright contrast is satisfied for one set of wavelengths, the requirement for dark contrast is satisfied for another set of wavelengths, and an ordinary image also may be superimposed by a third band of wavelengths, preferably very narrow, which lies between those producing the bright- and dark-contrast images of the object specimen. More complicated or less favorable designs which give rise to a color phase contrast image will not be discussed here. The wavelengths that interfere to form a dark-contrast image of a particle and those that produce an ordinary image of the particle and its surround contribute to the color of the halo. The color corresponding to the wavelengths that interfere constructively to form a bright-contrast image of the particle is absent in the halo. The halo is a phenomenon associated with the discontinuity in optical path due to the presence of the object specimen, and the halo is not being taken into account here when references are made to the image of the surround. Color phase microscopy not only produces striking images, but it also helps the microscopist to distinguish between those effects caused by small amounts of absorption in the object specimen and those caused by small differences in optical path.

To achieve color phase microscopy by the Zernike method, the dispersion of the substance forming the conjugate area is so chosen in relation to the dispersion of the substance forming the complementary area that phase contrast is not observed if the specimen is illuminated by some wavelengths in the visible range but that good phase contrast exists if the specimen is illuminated by other wavelengths. The two kinds of

color diffraction plates to be discussed in this section will be called the simple color phase or diffraction plate and the reversal color diffraction plate. The simple color diffraction plate does not change the phase difference between that part of the deviated and the undeviated light which includes the wavelengths near one end of the visible spectrum, but it does introduce a relative phase change of approximately 90° between that part of the deviated and the undeviated light which includes the wavelengths at the other end of the visible spectrum. If a reversal color diffraction plate is mounted in the objective, bright contrast is obtained if the illumination incident on the specimen is limited to wavelengths that lie near one end of the visible spectrum, dark contrast is observed if the wavelengths lie near the other end of the visible range, and no phase contrast occurs if the light incident on the specimen consists only of a band of wavelengths at some intermediate region of the visible spectrum.

For example, consider a simple color diffraction plate designed to produce dark contrast if the object specimen has an optical path greater than that of its surround and if it is illuminated with light containing the yellow, green, and blue wavelengths. With the same object specimen consider also a reversal color diffraction plate designed to produce bright contrast if red illumination is used, dark contrast if blue or green light only is incident on the specimen, and no phase contrast if yellow light illuminates the specimen. References to the color of the image of the specimen should be interpreted only as meaning that the color is predominantly or approximately that mentioned. If the source of light is white and if the phase objective contains a simple color diffraction coating, the image of a particle with an optical path greater than that of the surround is red. If a green filter is placed in front of the light source the image of the specimen is dark or black, but if a red filter is placed in front of the light source the image of the particle is hardly distinguishable from that of the surround. If the diffraction plate or coating in the objective is of the reversal color type, then the image of the same particle is again red if a white light source is used. If a red filter is in the light beam the image of the specimen appears brighter than the image of the surround, but if a green filter is used the image of the specimen is dark or black.

If, in this example, a particle has an optical path less than that of the surround, then all the color contrast phenomena are reversed and the following effects are observed. The combination of the phase objective with the simple color plate and a white light source produces a greenish image of the particle. The addition of a green filter at the light source causes the particle to appear brighter than the surround, but the particle

is hardly distinguishable from its surround if a red filter is inserted in front of the light source. If a reversal color diffraction plate is mounted in the objective, then with white light illumination the particle appears green. If a green filter is introduced the image of the particle is brighter than that of the surround, but if the filter is red the particle appears black or darker than the surround.

The reversal color diffraction plate is more efficient than the simple color diffraction plate. If white light illuminates the specimen the color of the image of a particle and of the halo may be considered to be complementary in the ideal case and the image of the background is gray. The publication by Saylor et al. (1950) is mainly concerned with what has here been called reversal color contrast.

Suppose that the design of a simple color diffraction plate is being considered and that the undeviated light of a green wavelength λ_1 is to be retarded by an amount $\lambda_1/4$ relative to the deviated light but that the undeviated and the deviated light of the red wavelength λ_2 undergo no relative phase change on passing through the diffraction plate. The conditions to be satisfied by the refractive indices of the materials constituting the diffraction plate are

$$(n_1 - n_2)t = \frac{\lambda_1}{4}, \tag{2.13}$$

$$(n_3 - n_4)t = 0, \tag{2.14}$$

in which $n_1 \equiv$ refractive index of conjugate area at λ_1;

$n_3 \equiv$ refractive index of conjugate area at λ_2;

$n_2 \equiv$ refractive index of complementary area at λ_1;

$n_4 \equiv$ refractive index of complementary area at λ_2;

$t \equiv$ thickness of the conjugate and the complementary area.

Since t cannot be equal to zero, then, from Eq. 2.14, $n_3 = n_4$. Again, let

$$n_3 = n_1 - d_1; \tag{2.15}$$

$$n_4 = n_2 - d_2. \tag{2.16}$$

If Eqs. 2.15 and 2.16 are substituted into Eq. 2.13, it follows that

$$(d_1 - d_2) = \frac{\lambda_1}{4t}. \tag{2.17}$$

Equation 2.17 is intuitively obvious. The refractive indices of the materials forming the conjugate and complementary areas must be equal at λ_2, and the dispersion of the material on the conjugate area is greater in such a way that the optical path step between the conjugate and complementary areas becomes $\lambda_1/4$ at λ_1. Similarly, if it is preferred that

the diffraction plate produce phase contrast at the wavelength λ_2 but
not at the wavelength λ_1, then

$$(n_1 - n_2) = 0, \tag{2.18}$$

and

$$(d_2 - d_1) = \frac{\lambda_2}{4t}. \tag{2.19}$$

No optical path difference exists between the conjugate and comple-
mentary area at λ_1, but at λ_2 the greater dispersion of the complementary
area introduces an optical path difference of $\lambda_2/4$.

The wavelengths at which no phase contrast occurs form images of
equal or nearly equal brightness of both the particle and the surround.
In the examples related to Eqs. 2.17 and 2.19 the refractive index of the
substance selected for the conjugate area is greater than or equal to the
refractive index of the material deposited over the complementary area.
Then, if the optical path of the particle exceeds that of the surround, the
wavelengths at which phase contrast is produced form a brighter image
of the particle than of the surround. The phase contrast and non-phase
contrast images are superimposed so that the image of the particle is
brighter than the image of the surround and is colored. However, if a
dielectric coating described by n_1 and d_1 is applied over the comple-
mentary area and the coating described by n_2 and d_2 is deposited over
the conjugate area, then the materials selected according to Eq. 2.17
produce dark contrast with the wavelength λ_1 and neighboring wave-
lengths. Therefore the color corresponding to these (green) wave-
lengths is subtracted from the ordinary white or gray image of the parti-
cle and the image has the color corresponding to the complementary
wavelengths. Similarly, materials can be selected according to Eq.
2.19 and deposited on the diffraction plate to produce dark contrast at
λ_2 and neighboring wavelengths so that the image of the particle is
composed only of the shorter wavelengths of the spectrum. In order
that a color diffraction plate of this type function most efficiently with
white light illumination, the conditions for achromatic phase contrast
should be satisfied for a band of wavelengths at a selected part of the
spectrum, and the transition to no phase contrast for a band of wave-
lengths in the other part of the spectrum should take place over a
relatively narrow band of wavelengths.

Several procedures for combining various dispersion characteristics of
materials in order to make a reversal color diffraction plate have been
suggested by Saylor et al. (1950). If the materials forming the conju-
gate and complementary areas have normal dispersion curves, then a
diffraction plate can function satisfactorily as a reversal color plate,

provided that no optical path difference exists between the conjugate and complementary areas for some wavelength λ_0 and the dispersions are such that the optical path difference is $-\lambda_1/4$ for some wavelength λ_1 and is $+\lambda_2/4$ for some other wavelength λ_2. λ_0, λ_1, and λ_2 are related either by the inequality $\lambda_1 < \lambda_0 < \lambda_2$ or by the inequality $\lambda_1 > \lambda_0 > \lambda_2$. The dispersion curves cross at λ_0. It is assumed that the conjugate and complementary areas are of equal thickness t, and it is convenient to consider the reversal color diffraction plate in terms of an example.

Suppose that $\lambda_1 < \lambda_0 < \lambda_2$ and that, if a particle has an optical path greater than that of the surround, λ_2 and neighboring wavelengths contribute a bright-contrast image of the particle whereas λ_1 and neighboring wavelengths form a dark-contrast image of the particle. The ideal color phase contrast image would be obtained if the requirements for achromatic dark contrast were satisfied for all wavelengths $\lambda_i \leqq \lambda_0 - \epsilon$, the requirements for achromatic bright contrast were satisfied for all wavelengths $\lambda_j \geqq \lambda_0 + \gamma$, and the transition from dark to bright contrast took place within a very narrow wavelength band $\epsilon + \gamma$. This would mean that the difference between the refractive indices of the substances constituting the conjugate and complementary areas is proportional to the wavelength in the regions $\lambda_i \leqq \lambda_0 - \epsilon$ and $\lambda_j \geqq \lambda_0 + \gamma$ and that the phase-accelerating or phase-retarding function of either area of the diffraction plate is reversed for each of these wavelength regions; i.e., the two dispersion curves are effectively interchanged on either side of the band of wavelengths included between $\lambda_0 - \epsilon$ and $\lambda_0 + \gamma$. Therefore, in order for the conditions for ideal reversal color phase contrast to be fulfilled, the dispersion curve for the material with the lower index of refraction in the region of shorter wavelengths must describe a refractive index that decreases with increasing wavelength in the region $\lambda_i \leqq \lambda_0 - \epsilon$, then increases rapidly by an amount approximately equal to $\lambda_0/4t$ with increasing wavelength from $\lambda_0 - \epsilon$ to $\lambda_0 + \gamma$ and again decreases with increasing wavelength (or remains constant) in the region $\lambda_j \geqq \lambda_0 + \gamma$. At present, no material with such dispersion characteristics is known, and it is impossible to realize the ideal reversal color phase plate.

If two substances with ordinary dispersion properties are selected for the reversal color diffraction plate, the material with the greater dispersion in the range $\lambda_2 - \lambda_1$ is deposited on the complementary area if the optical path difference between the conjugate and complementary areas is to change from $-\lambda_1/4$ for λ_1 to $\lambda_2/4$ for λ_2. Suppose that the band of wavelengths around λ_1 corresponds to a blue-green color and that the band of wavelengths around λ_2 corresponds to the color red.

Let λ_0 fall within the yellow region of the spectrum. It is known that if a phase microscope produces a dark-contrast image of a particle having an optical path exceeding that of the surround it also forms a bright-contrast image of a particle with an optical path less than that of the surround. Therefore the diffraction plate in this example is designed so that, in an approximate sense, the color of the image of a particle with an optical path greater than that of the surround is red and the color of the image of a particle is blue-green if the particle has an optical path less than that of the surround. The halo around the blue-green image is red, and the halo around the red image is blue-green. The color of the image of the particle and that of the halo is of course altered when there is any change in the composition of the bands of wavelengths which interfere to form bright- or dark-contrast images. If the two dielectric substances selected for a reversal color diffraction plate are interchanged as the materials from which the conjugate and complementary areas are made, then also the colors which designate whether the particle has an optical path greater or less than that of the surround are interchanged.

The conditions which the reversal color diffraction plate in the example must satisfy are

$$(n_1 - n_2)t = -\frac{\lambda_1}{4}; \tag{2.20}$$

$$(n_3 - n_4)t = \frac{\lambda_2}{4}; \tag{2.21}$$

$$(n_5 - n_6)t = 0. \tag{2.22}$$

In these last equations n_1, n_3, and n_5 are the refractive indices of the conjugate area for λ_1, λ_2, and λ_0, respectively, and n_2, n_4, and n_6 are the refractive indices of the complementary area for λ_1, λ_2, and λ_0, respectively. t is again the thickness of the complementary and conjugate areas, and $\lambda_1 < \lambda_0 < \lambda_2$. As before, let

$$n_1 - n_3 = d_1; \tag{2.23}$$

$$n_2 - n_4 = d_2. \tag{2.24}$$

If t is eliminated between Eqs. 2.20 and 2.21 then

$$d_1 - d_2 = \frac{\lambda_1 + \lambda_2}{\lambda_1}(n_1 - n_2) < 0. \tag{2.25}$$

The condition 2.22, which is related to the value of λ_0, has not been used in obtaining Eq. 2.25. Equation 2.25 does not fix the value of λ_0, the

point of intersection of the two dispersion curves which describe the change in n_1 and n_2 with wavelength.   A number of pairs of materials may satisfy Eqs. 2.20 and 2.21 and therefore Eq. 2.25, but each pair may satisfy Eq. 2.22 for a different wavelength λ_0.

The combination consisting of Eqs. 2.20 and 2.22 or the combination consisting of Eqs. 2.21 and 2.22 has a solution of the same form as Eq. 2.17 or 2.19.   Let

$$n_1 = n_5 + a_1; \tag{2.26}$$

$$n_2 = n_6 + a_2; \tag{2.27}$$

$$n_3 = n_5 - a_3; \tag{2.28}$$

$$n_4 = n_6 - a_4. \tag{2.29}$$

Then, if two materials are selected which have the same index of refraction for the wavelength λ_0 and if Eqs. 2.20 and 2.21 are also satisfied, it follows that

$$(a_2 - a_1) = \frac{\lambda_1}{4t}, \tag{2.30}$$

and

$$(a_4 - a_3) = \frac{\lambda_2}{4t}. \tag{2.31}$$

Equations 2.20, 2.21, and 2.22 together with Eqs. 2.26–2.29 also show that $(a_1 - a_2) = (n_1 - n_2) < 0$ and that $(a_3 - a_4) = (n_4 - n_3) < 0$ in this particular design for a reversal color diffraction plate.   In general, it is not possible to satisfy Eqs. 2.20, 2.21, and 2.22 simultaneously for any three arbitrary, preselected values of λ_1, λ_2, and λ_0 unless it is possible to introduce, also arbitrarily, second-order effects into the dispersion characteristics of at least one of the substances forming the diffraction plate.

The designs presented here for color phase microscopy represent the simplest and most direct approach to the problem if a result is to be obtained by making use of the different dispersions of materials.   Theory does not limit the choice of optical path difference between the conjugate and complementary areas to $\frac{1}{4}$ wavelength for λ_1 and λ_2, for example, and to no path difference for λ_0.   Schemes are also allowed in which the optical path difference for λ_1 and λ_2 are higher multiples of $\frac{1}{4}$ wavelength and in which the optical path difference for λ_0 is $\frac{1}{2}$ wavelength or a multiple of $\frac{1}{2}$ wavelength.   For best performance it is necessary that the amplitude of the deviated light and that of the undeviated light be balanced with a color diffraction plate as with the standard, neutral diffraction plate.   A neutral absorbing material may be in-

corporated in the proper area of the diffraction plate in order to obtain a favorable amplitude transmission ratio between the conjugate and complementary areas. Decreasing the width of the conjugate annulus decreases the amount of absorption ordinarily required in the conjugate area.

The modification described by Grigg (1950) will also serve as a method for obtaining reversal color contrast. In this scheme, the opaque area of the standard condenser diaphragm for phase microscopy is replaced by a color filter, and a filter of contrasting color is mounted over the normally transmitting area of the diaphragm. This bi-colored diaphragm is used together with the standard, neutral diffraction plate. Suppose that the area of the phase condenser diaphragm which normally transmits all the incident illumination and which is imaged on the conjugate area of the diffraction plate is now made to transmit light of color A. Suppose also that the normally opaque region of the phase condenser diaphragm is replaced by a filter which transmits light of color B. This area of color B is imaged on the complementary area of the diffraction plate. Assume that the diffraction plate is a general-purpose dark-contrast plate. Then, if a particle having an optical path exceeding that of the surround is moved into the field of the microscope, the diffraction plate again functions as a dark-contrast plate for the light of color A. Since for the light of color B the conjugate and complementary areas of the diffraction plate have in effect been interchanged, a bright-contrast image of the particle is formed with the light of color B. The image of color B is superimposed upon the black image, so that the particle appears color B. The halo appears color A, and the general surround appears some color intermediate between A and B. Similar reasoning will show that, if the particle has an optical path smaller than that of the surround, the color of the image of the particle is A, the color of the halo is B, and the color of the image of the surround is intermediate between A and B. Too much chromatic overlapping of the substage condenser filters should be avoided. With this method and the standard diffraction plate, the intensity of the light admitted by the normally opaque area of the substage condenser diaphragm must be less than that admitted by the normally transmitting area. Polaroids mounted over the proper regions allow control of this intensity.

2.5. Nomenclature for diffraction plates

As the variety of available diffraction plates increases, a generally accepted nomenclature for designating the diffraction plate with which a particular observation is made will become increasingly important. The essential characteristics of a diffraction plate are $h^2 \equiv T$, the ratio of the energy transmission of the conjugate area to the energy transmission

of the complementary area, and δ, the optical path difference between the conjugate and complementary areas of the diffraction plate. It is relevant to point out any dependence of the value of h on wavelength such that colored images analogous to those observed with darkfield illumination are introduced and to indicate the dependence of δ on wavelength if variations in dispersions produce color phase contrast. A complete description of a diffraction plate should also contain the values of the numerical aperture corresponding to the boundaries of the conjugate area ($\rho_2 - \rho_1$, Fig. II.20). In particular, a statement concerning the effect produced in an image by a given, definite change in the value of T is quantitatively meaningful only if the size and location of

$$
\begin{array}{cccc}
a & b & c & d \\
\end{array}
$$

$TA+\delta\lambda$	$TA+\delta\lambda$	$TB+\delta\lambda$	$TB+\delta\lambda$
$T = h^2 \leqq 1$	$T < 1$	$T \geqq 1$	$T > 1$
$\delta \geqq 0$	$\delta < 0$	$\delta \leqq 0$	$\delta > 0$

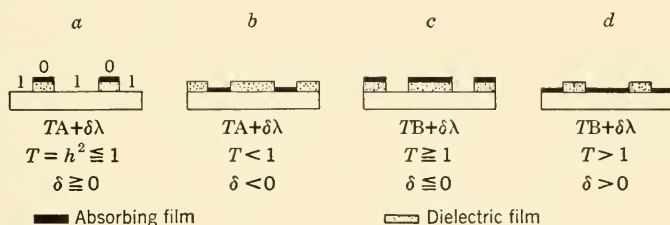■■ Absorbing film   ▭ Dielectric film

FIG. III.3.   Notation devised by Bennett et al. to describe neutral diffraction plates.

the conjugate area are also known. The notation adopted in this book to describe diffraction plates that form neutral images with white light was devised by Bennett et al. (1946). This nomenclature does not include a designation of ρ_1 and ρ_2, but it is useful in a general discussion of phase microscopy despite this limitation. This system of notation is explained as follows:

The letter A is used to identify all plates that reduce the ratio of the energy transmission of the conjugate area to the energy transmission of the complementary area, and the letter B identifies all plates that increase this ratio. The value of the energy transmission ratio is designated by T and precedes the letter A or B. T is less than or equal to 1 for A-type diffraction plates and greater than or equal to 1 for B-type plates. If the diffraction plate increases the optical path of the undeviated light relative to that of the deviated light, the letter A or B is followed by a $+$ sign. If the optical path of the undeviated light is decreased relative to that of the deviated light, the letter A or B is followed by a $-$ sign. The magnitude of the optical path difference, expressed in fractions δ of the wavelength λ of the Hg line for which $\lambda = 5461$ A, is written after the $+$ or $-$ sign. The application of this notation to diffraction plates with an annular conjugate area is illustrated in Fig. III.3. The four ambiguities which may arise are avoided by the inclusion of the inequalities contained in the more explicit

definitions a, b, c, and d. In terms of this notation, phase objectives of the type $TA - 0.25\lambda$ produce dark contrast in most biological applications, and phase objectives of the type $TA + 0.25\lambda$ generally produce bright contrast. The value of T required to produce a given amount of contrast depends strongly on the dimensions of the conjugate area. The omission of any designation of ρ_1 and ρ_2 is a shortcoming when a particular observation is being described, and a more inclusive nomenclature would be very useful.

3. ALIGNMENT OF THE PHASE MICROSCOPE

The most successful use of either the ordinary or the phase microscope demands correct alignment of the optical system and the source of light. The phase microscope needs only a few relatively simple adjustments in addition to those required for the correct alignment of the ordinary microscope. As in brightfield microscopy with central conical illumination, optimum performance is obtained when the light source is centered with respect to the substage mirror; when the center of the substage mirror, the optical axis of the substage condenser, the optical axis of the objective, and that of the ocular are in line; and when the required field and aperture of the objective are uniformly illuminated. Phase microscopy imposes the additional conditions that the plane of the image of the opening in the condenser diaphragm shall coincide with the plane of the conjugate area of the diffraction plate and that the image of this opening shall fall within the conjugate area. Definition and contrast in the image are sensitive to this alignment of the opening in the condenser diaphragm with respect to the conjugate area of the diffraction plate. Passage of part of the undeviated light through the complementary area generally causes a rapid loss of contrast in the image. It was pointed out in Section 1 that parallax between the image of the opening in the condenser diaphragm and the conjugate area of the diffraction plate also can cause loss of contrast. The diffraction plate should be centered on the optical axis of the objective by the maker.

No two manufacturers supply an identical set of phase accessories, just as no two manufacturers make identical microscope stands and identical sets of optics. However, as with the ordinary microscope, each maker's equipment performs similar functions, and a recommended procedure for aligning the phase microscope may be described in terms of the equivalence of the various parts. The diffraction plate may be separable from the objective or it may be fixed in the objective. There is a mount into which a condenser is fitted and which also carries the diaphragm to be used with a given phase objective. The substage

condenser mount may be a single-unit type such that a cell containing a diaphragm is screwed in or out of position or such that a plate provided with a diaphragm can be slid beneath the substage condenser and locked into the correct plane. Means are provided for centering the condenser diaphragm with respect to the conjugate area of the diffraction plate. (The diaphragm containing the opening required by the diffraction plate will be referred to as the condenser diaphragm, and the iris diaphragm which controls the numerical aperture of the condenser and which is usually found at or near the first focal plane of the substage condenser in the ordinary microscope will be designated as the iris diaphragm of the condenser.) Sometimes means are provided for centering the substage condenser with respect to the objective.

An auxiliary optical system is supplied in order to enable the user to view the plane of the diffraction plate at sufficient magnification to facilitate the centering of the condenser diaphragm with respect to the conjugate area of the diffraction plate. Often this is a separate unit which fits into the body tube of the microscope stand in place of an eyepiece. This unit, which is a microscope having a long working distance and which is generally called the centering telescope, is usually adjustable in length so that the working distance and magnification can be changed. Sometimes, as on the stand manufactured by the firm of Galileo, the eyepiece of the phase microscope remains in position and another lens element is moved into place below the eyepiece so that the combination forms the centering telescope. The objective lens of this centering telescope is removed from the path of light when the eyepiece is again to serve as the ocular of the phase microscope.

The elementary theory developed in Chapter II specified Köhler illumination. Section 16 of Chapter VII discusses the fact that under certain conditions of critical illumination the appearance of the image of the object specimen in the phase microscope is similar to the appearance of the image with Köhler illumination. The conditions necessary in order that critical illumination cause the energy density in the image to become similar to the energy density produced with Köhler illumination are that the source of illumination be broad and fairly uniform, that a large field of view be illuminated, and that the speed of both the lamp and the substage condenser be high. These conditions are usually satisfied in the normal use of the microscope with critical illumination. When the method of alignment recommended by a manufacturer follows the procedure for Köhler illumination, the user is assured that, if he so adjusts his equipment, not only is the field of view as uniformly illuminated as is feasible but also that the image of the opening in the condenser diaphragm is formed with the correct magnification and as

close to the plane of the conjugate area of the diffraction plate as is practicable.

It has been stressed that the size and location of the image of the opening in the condenser diaphragm with respect to the conjugate area of the diffraction plate is important. If a lamp with a coiled filament is used in Köhler illumination, a plate of diffusing glass may finally be put in front of the lamp without loss of contrast or definition. Emphasis is laid on the fact that the procedure recommended by the manufacturer should be followed in order to obtain the correct position of the substage condenser and the diaphragm relative to the objective and the diffraction plate. After such instructions have been carried out, the lamp filament can be imaged by means of the lamp condenser so that the proper conditions for either critical or Köhler illumination are satisfied.

The following enumerated steps are suggested as a useful procedure for the inexperienced but critical microscopist in setting up his phase microscope. However, the experienced microscopist may find it desirable to modify this procedure. Köhler illumination will be indicated to the extent that the iris diaphragm in front of the lamp will form the field stop and that the lamp filament will be imaged in the plane of the condenser diaphragm. A plate of diffusing glass may later be placed in front of the lamp. It will be assumed that a separate lamp together with a substage mirror directs the light through the substage condenser. The stands of some phase microscopes contain a built-in source of illumination which should be adjusted according to instructions given by the maker.

1. Mount the substage condenser together with the appropriate diaphragm, the phase objective, and the eyepiece on the microscope stand. Place the specimen slide on the stage. Set the lamp so that the iris diaphragm which controls its aperture is a suitable distance from the substage mirror. Some manufacturers specify the distance from the iris diaphragm of the lamp to their substage condenser. If the substage condenser is of the Abbe type, N.A. 1.25, then 5 to 8 inches is a nominal distance. Adjust both the lamp and the substage mirror so that light reaches the center of the mirror and is reflected approximately through the center of the substage condenser and of the objective. If the working distance of the substage condenser is known, it is helpful for the next step to rack the condenser upward to approximately this distance from the specimen slide. The user must learn from the manufacturer whether the substage condenser must be immersed (e.g., in oil) when it is used with an immersion phase objective. The method of phase microscopy requires that the lamp and substage condenser fill only the conjugate area of the diffraction plate with light. Therefore some manufacturers have designed the diaphragm for the immersion phase objective so that the substage condenser is used dry. Open the iris diaphragm of the substage condenser beyond the opening in the condenser diaphragm. Make certain that the tube length of the microscope is that required by the design of the objective.

2. Focus the microscope on the specimen. The image seen at first may be a poor one. If the optical properties of the specimen are such that its image is detected with difficulty with an ordinary microscope, it may become necessary approximately to center the opening in the condenser diaphragm with respect to the conjugate area of the diffraction plate in order to detect any part of the specimen. This is done by replacing the eyepiece with the centering telescope, focusing the telescope on the coating of the diffraction plate, and manipulating the centering adjustments of the condenser diaphragm until the image of the opening in the condenser diaphragm appears over the conjugate area of the diffraction plate. Replace the eyepiece and then focus the microscope on the specimen. If the substage condenser together with the diaphragm has been racked too far away from the specimen slide, the central opaque area of the diaphragm may block too much of the light from the lamp, and the center of the field of the microscope will appear dark. In fact, if the substage condenser together with the diaphragm is either too far from or too close to the specimen slide the center of the field of the microscope may appear dark or colored or both, particularly if the iris diaphragm of the lamp has been closed to a small aperture. Spherical aberration of the substage condenser may introduce additional vignetting of light from the lamp, and chromatic aberration of the substage condenser may introduce color in the field of the microscope. It is sometimes advantageous to use a low-power phase objective as a finder. In this connection, if a phase objective is used together with the condenser diaphragm for a higher power phase objective, the center stop of the condenser diaphragm may be large enough to simulate the conditions for darkfield illumination, and this can also be helpful in locating some specimens. Before going to step 3, make certain that the diaphragm in the substage condenser is the diaphragm supplied for the particular phase objective.

3. After the microscope has been focused on the specimen, close the iris diaphragm on the lamp housing to form a small aperture. Raise or lower the substage condenser until the image of the lamp diaphragm is focused on the specimen. If the substage condenser is of the Abbe type, the image of the edge of the lamp iris appears colored, and more strongly so when the condenser diaphragm with an annular opening is in position than when the condenser is used with a central clear aperture. The substage condenser is considered to be in good focus when the image of the edge of the lamp diaphragm is in the color range blue-green to purple-blue-purple. On account of the spherical aberration of an Abbe-type substage condenser, the position of the so-called good focus for this condenser will be different with annular than with central openings in the condenser diaphragm. It may also be advantageous to refocus this substage condenser when a phase objective which requires an opening of one mean diameter and width in the condenser diaphragm is replaced by a phase objective which requires an opening of another mean diameter and width. Adjust the substage mirror so that the image of the lamp diaphragm is at least approximately centered in the field of view.

4. Image the lamp filament on the condenser diaphragm or on the iris diaphragm of the substage condenser by focusing the lamp condenser. If a plate of diffusing glass has been placed in front of the lamp, it should be removed during this step, but it may be replaced after the lamp has been adjusted. Full use should be made of whatever means have been built into the lamp housing to adjust the lamp for optimum illumination. The image of the filament should extend at least over the annular opening in the condenser diaphragm. If the lamp envelope is frosted, the envelope is imaged on the condenser diaphragm.

5. Open the iris diaphragm of the lamp so that approximately the entire field of view of the microscope can be observed. The procedure that follows this depends on the type of substage condenser unit. If both the substage condenser and the condenser diaphragm are separately centerable with respect to the optical axis of the microscope, then the next step is to align the optical axis of the substage condenser with the optical axis of the objective and, following that, to adjust the condenser diaphragm so that the image of the annular opening is centered upon the conjugate area of the diffraction plate. If the substage condenser has been precentered, it is necessary only to center the condenser diaphragm. In order to make either or
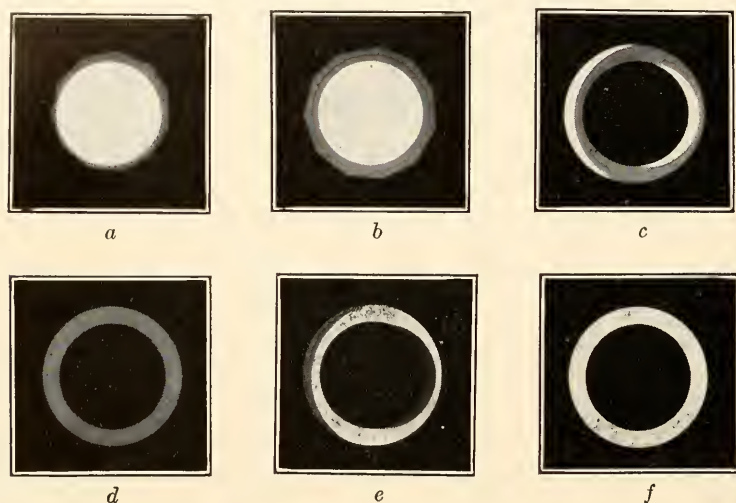
Fig. III.4. Centering the substage condenser and diaphragm for phase microscopy. (a) The substage condenser is decentered with respect to the optical axis of the microscope. (b) The substage condenser is centered with respect to the optical axis of the microscope. (c) The phase diaphragm is decentered with respect to a diffraction plate of the type $TA + \delta$. (d) The phase diaphragm is centered with respect to a diffraction plate of the type $TA + \delta$. (e) The phase diaphragm is decentered with respect to a diffraction plate of the type $TB + \delta$. (f) The phase diaphragm is centered with respect to a diffraction plate of the type $TB + \delta$.

both of these adjustments, replace the eyepiece of the microscope by the centering telescope and focus the telescope on the coating of the diffraction plate. If the substage condenser is to be centered, remove the diaphragm which has been inserted for use with the diffraction plate and close the iris diaphragm on the substage condenser mount until it appears in the field of the centering telescope. If the optical axis of the condenser is not in alignment, the image of the iris diaphragm appears decentered as in Fig. III.4a. Turn the proper centering screws until the iris diaphragm appears centered as in Fig. III.4b. For final use of the phase microscope, open the iris diaphragm until the entire conjugate area of the diffraction plate is visible. Replace the condenser diaphragm for the phase objective and manipulate the centering adjustments for the diaphragm until the image of the opening is centered upon the conjugate area. Figure III.4c shows the appearance of the image

in the field of the centering telescope when the conjugate area is absorbing and the condenser diaphragm is not centered. Figure III.4d shows the appearance of this image after the condenser diaphragm has been centered with respect to the conjugate area of the diffraction plate. If the object specimen is such that it deviates a considerable amount of light into the complementary area, the overlap between the edges of the conjugate area and the image of the edges defining the annular opening in the condenser diaphragm can easily be seen. Figure III.4e shows the condenser diaphragm decentered with respect to a diffraction plate in which an absorbing coating has been put on the complementary area of the diffraction plate, and Fig. III.4f shows the correct alignment in this case.

6. Remove the centering telescope and replace the eyepiece. Close the lamp diaphragm until its image is slightly smaller than the field of the microscope. If necessary, adjust the substage mirror until the image of the lamp iris is centered in the field of the microscope. With regard to the opening in the iris diaphragm of the lamp, the phase microscope differs in two ways from the ordinary microscope. The diffraction plate will cause a halo to appear around the image of the lamp diaphragm. For this reason the diaphragm in front of the lamp should not be closed so far that the halo about its image is superimposed on the image of the detail being observed. Further, if a high-power phase objective (e.g., an oil immersion objective) is used with an Abbe-type substage condenser set in the position for Köhler illumination, a check should be made to ascertain that when the lamp diaphragm is closed down as a field stop the back aperture of the phase objective is uniformly illuminated at least to the outer edge of the conjugate area. Spherical aberration may produce vignetting when an annular opening at high numerical aperture admits light through the condenser unless the source of light at the lamp is made broad. To check this, use the centering telescope to look at the conjugate area of the diffraction plate. It may be helpful to remove the condenser diaphragm temporarily in making this check. This check may indicate the necessity of increasing the opening in the iris diaphragm of the lamp beyond the minimum opening contemplated for the purposes of a field stop.

The number of refinements which the user of the phase microscope wishes to make depends on his problem and on the type of phase accessories. After the microscopist is familiar with his equipment, setting up the phase microscope to perform well takes very little more time than setting up the ordinary microscope to perform well. There will always be variations in procedure due to differences in the design of the many available microscope stands. Sometimes the instructions are, simply, instead of step 3, to insert the centering telescope and to move the condenser up or down until the image of the opening in the condenser diaphragm almost fills the conjugate area of the diffraction plate when the condenser diaphragm has been centered with respect to the diffraction plate. This procedure substitutes for steps 3 and 5.

A separate step to align the iris diaphragm of the lamp, the substage iris diaphragm, and the eyepiece is sometimes recommended. This procedure requires that the lamp be set at a suitable distance from the substage condenser mount and that the filament of the lamp be imaged

on the substage iris diaphragm before the phase objective, the ocular, the substage condenser, and the condenser diaphragm are mounted on the microscope stand. To continue this method of alignment, place a pinhole eyepiece in the body tube of the microscope and close both the substage iris diaphragm and the iris diaphragm of the lamp to their smallest apertures. Adjust the substage mirror so that the aperture of the lamp is seen through the pinhole eyepiece and the closed substage iris diaphragm. Then, without moving the substage mirror again, follow the remainder of the procedure suggested in steps 1, 2, 3, 5, and 6. However, if the condenser to be used is not in a centering mount, it may be necessary to readjust the mirror to center the image of the iris diaphragm of the lamp in the field of the microscope when step 6 is reached. It may also be impossible to insert the condenser in its mount without tilting the substage mirror. Therefore this additional check on alignment was not included in the suggested general procedure.

If the coating on the diffraction plate consists of only transparent dielectric materials, then it is difficult to distinguish the boundaries of the conjugate area by means of the centering telescope when the diffraction plate is illuminated by the entire cone of light admitted by the annular opening in the condenser diaphragm. This introduces a visibility problem in centering the condenser diaphragm. Usually the manufacturer of microscopes of good quality has taken sufficient care in centering the optical components of the objective, including the diffraction plate or coating, with respect to each other and with respect to the mount so that if one phase objective is replaced by another of the same power the opening in the condenser diaphragm may be only slightly decentered with respect to the conjugate area of the diffraction plate. Therefore one may center the opening in the condenser diaphragm with respect to the conjugate area of a phase objective which contains an absorbing material, replace this phase objective with the non-absorbing phase objective, insert the eyepiece of the microscope, and adjust the condenser diaphragm until best contrast is obtained in the image of the object specimen. However, it is possible to make the edges of the conjugate area of a transparent diffraction plate visible in the field of the centering telescope by cutting off part of the cone of light which illuminates the conjugate area in order to produce oblique illumination. This can be done either by tilting the substage mirror or by blocking out one side of the light beam which normally enters the substage condenser by sliding any convenient opaque obstacle into the light beam. When the condenser diaphragm has been centered, the mirror is readjusted or the obstacle is removed.

Some manufacturers supply a phase condenser with a long working

distance for use with specimens mounted on slides of greater than standard thickness or for use with specimens in cells or flasks. Curved surfaces on a specimen cell or flask can distort the image of the condenser diaphragm enough to make the diffraction plate useless. If the slide or cell has a sufficiently great wedge angle or if it has a wavy surface, it may be necessary to keep recentering the condenser diaphragm with respect to the conjugate area of the diffraction plate as the slide or cell is moved across the field of the microscope. If the mounted specimen acts as a lens and changes the magnification of the image of the condenser diaphragm, this can be compensated for by substituting a new condenser diaphragm or by introducing a substage condenser with variable power.

4. SOME FEATURES OF PHASE EQUIPMENT OF DIFFERENT MANUFACTURE

Brief descriptions of various makes of phase accessories available at present will illustrate some of the means adopted to satisfy the requirements of phase microscopy. The starting point for each has been the objectives, the condensers, and the stands designed previously for ordinary microscopy. Some manufacturers have released for publication photographs of their phase microscope stands, and reproductions of these photographs are included in Fig. III.5. Most of the photographs and much of the descriptive information were obtained during the summer of 1949. The notation (1949) either on the photograph or in the text indicates this fact. Reference will be made to achromatic or apochromatic objectives for phase microscopy. This describes the objective before the diffraction plate or coating was added and does not imply, for example, that the diffraction plate itself has been achromatized.

4.1. Phase objectives

Phase objectives have been made by adding diffraction plates or coatings to objectives of existing design. The standard phase accessories now being sold form neutral images, in general, if white light illuminates a thin, transparent specimen. Also, the standard phase objectives are supplied as units which contain a diffraction plate, or the equivalent, that is not separable from the objective. There is nothing in the external appearance of the phase objective to distinguish it from the ordinary objective except that the maker takes care to engrave identification marks on the mount. The diffraction plate or coating can be seen only by looking through the objective.

All manufacturers offer a series of phase objectives which produce dark contrast with a transparent object specimen that has an optical path

exceeding that of the surround by a small fraction of a wavelength.
This is the type of contrast observed in ordinary brightfield microscopy
with such a specimen, although the contrast is very much less.   The
phase objectives for dark contrast which are supplied by a given maker
include a series of focal lengths.   Achromatic objectives for dark
contrast with focal lengths of approximately 16 mm and 8 mm, initial
magnifications of approximately $10\times$ and $20\times$, and numerical apertures
of approximately 0.25 and 0.50, respectively, are made by the American
Optical Co., Bausch and Lomb Optical Co., R. and J. Beck, Ltd. (1949),
Cooke, Troughton and Simms, Ltd. (1949), C. Reichert Co. (1949),
Henry Wild Surveying Instruments Supply Co., Ltd. (1949), and Carl
Zeiss, Jena (1949).   A dark-contrast achromatic objective with a focal
length of approximately 4 mm, initial magnification of approximately
$43\times$, and a numerical aperture of about 0.65 is available from American
Optical Co., Bausch and Lomb Optical Co., Cooke, Troughton and
Simms, Ltd., Reichert Co., Wild Co., and Zeiss, Jena.   A dark-contrast
objective of 4-mm focal length but with N.A. 0.85 is offered by Beck,
Ltd.   R. Winkel G.M.B.H. (Zeiss-Winkel, 1949) lists two dry achro-
matic objectives for dark contrast: $10\times$, N.A. 0.25; and $42\times$, N.A. 0.85.
Officine Galileo (1949) offers for dark contrast three dry achromatic
objectives: $10.5\times$, N.A. 0.28; $25\times$, N.A. 0.65; and $52\times$, N.A. 0.88.
The series of dry, achromatic objectives for dark contrast available from
I. Koristka and Co. (1949) are described as $12\times$, N.A. 0.30; $26\times$, N.A.
0.65; $45\times$, N.A. 0.85; and $60\times$, N.A. 0.87.   Immersion phase objec-
tives which produce dark contrast are supplied by all manufacturers of
phase microscopes, and the manufacturers and phase objectives may be
summarily listed as follows: American Optical Co., 1.8 mm, $97\times$, oil,
N.A. 1.25, achromatic; Bausch and Lomb Optical Co., 1.8 mm, $97\times$,
oil, N.A. 1.25, achromatic; Beck, Ltd., 2 mm, oil, N.A. 1.30, achromatic;
Cooke, Troughton and Simms, Ltd., 1.8 mm, $95\times$, oil, N.A. 1.30,
achromatic; Officine Galileo, $\frac{1}{12}$ inch, $100\times$, oil, N.A. 1.30, achromatic;
I. Koristka and Co., $\frac{1}{7}$ inch, $55\times$, oil, N.A. 0.90, achromatic; Koristka,
$\frac{1}{12}$ inch, $100\times$, oil, N.A. 1.30, achromatic; Koristka, $\frac{1}{15}$ inch, $100\times$,
water, N.A. 1.20, achromatic; Koristka, $\frac{1}{15}$ inch, $100\times$, oil, N.A. 1.32,
semi-apochromatic; Reichert Co., $100\times$, oil, N.A. 1.25, achromatic;
Wild Co., 2.2 mm, $85\times$, oil, N.A. 1.25, achromatic; Zeiss-Winkel, $90\times$,
oil, N.A. 1.30, achromatic; and Zeiss, Jena, $90\times$, oil, N.A. 1.25, achro-
matic.   The series of achromatic phase objectives for dark contrast
made by the American Optical Co. includes both type $TA-0.25\lambda$ and
type $TB-0.25\lambda$, and an objective of a given focal length is supplied
with one of several values of T in either type.   The different values of T
produce different amounts of contrast with a given object specimen.

At present, fewer manufacturers supply phase objectives that form a bright-contrast image of a particle having an optical path greater than that of the surround by a small fraction of a wavelength.   I. Koristka and Co. offers as extensive a series of objectives for producing bright contrast as for producing dark contrast.   The firm of Galileo lists an achromatic oil immersion objective, $\frac{1}{12}$ inch, $100\times$, and N.A. 1.30, for producing bright contrast.   The American Optical Co. makes bright-contrast achromatic objectives as follows: 16 mm, $10\times$, N.A. 0.25; 8 mm, $20\times$, N.A. 0.50; 4 mm, $43\times$, N.A. 0.66; and 1.8 mm, $97\times$, oil immersion, N.A. 1.25; and several objectives of a given focal length can be obtained to produce different amounts of bright contrast. The American Optical Co. also supplies a phase objective in which the coating that forms the diffraction plate consists of only an absorbing film applied over the conjugate area $(T\lambda + \delta\lambda, 0 < \delta \leqq 0.05)$.

The phase objectives mentioned above have an annular conjugate area.   C. Baker, Ltd. (1950), has been making phase objectives in which the conjugate area is cruciform.   These phase objectives produce dark contrast and include the standard three dry achromatic objectives and an achromatic oil immersion objective.

4.2. Substage condensers and condenser mounts

The substage mount carries the condenser and the condenser diaphragm.   When each diaphragm is inserted separately beneath the condenser and must be removed from the substage unit before another diaphragm can be used, the condenser mount is designated as the single-unit type.   Such a single-unit mount is available from the American Optical Co. for use with an Abbe-type condenser, N.A. 1.25.   Each diaphragm is contained in a cell which is screwed into place below the condenser whenever the diaphragm is needed.   Figures III.5.1a and III.5.1b show, respectively, a cell containing a diaphragm and the substage condenser mount.   The condenser is shown in the mount, and it is centered by means of the back pair of screws.   The diaphragm cell is screwed into the bottom of the mount, and the front, lower pair of screws are used to center the diaphragm cell.   R. and J. Beck, Ltd. (1949), also provides a single-unit condenser mount.   The phase condenser may be obtained in either a fixed or centering mount.   Each condenser diaphragm is contained in a tray which is attached to the substage condenser mount by the quick-change method.   The diaphragm can be centered in its tray with respect to its corresponding phase objective.   If the diaphragm is centered and the tray is removed and reinserted, recentering of the diaphragm is not required if the same phase objective is used.   C. Baker, Ltd., supplies a single-unit substage
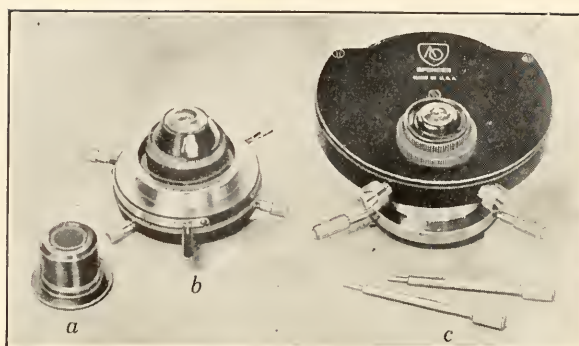
Fig. III.5.1.   (a) Cell and diaphragm for Spencer single-unit substage condenser
mount.   (b) Substage condenser in Spencer single-unit mount.   (c) Spencer con-
denser for phase microscopy with diaphragm turret mount.   (d) Spencer phase
microscope equipped with turret mount for diaphragms and condenser.   Courtesy
of American Optical Co. (1949, 1950).

condenser mount. The diaphragms possess a cross-shaped aperture and are mounted in a plate which is centerable after it has been fitted into the substage mount. I. Koristka and Co. also makes a single-unit condenser mount for its "simplified" phase microscope stand.

A design which has been very convenient includes a rotatable plate or turret mounted at or near the first focal plane of the substage condenser. As a rule, the rotatable plate carries four diaphragms and has at least one clear aperture. Any one of the diaphragms or the clear aperture can be rotated into position for use below the substage condenser. The combination of a rotatable turret and either a multiple, revolving nosepiece or a quick-change nosepiece permits rapid and convenient changes from one phase objective to another or from phase microscopy to ordinary microscopy. The clear aperture is also helpful during the procedure of aligning the phase microscope. Figure III.5.1c and Figs. III.5.2a and III.5.2b are illustrations of the general appearance of substage condenser mounts with a rotatable changer plate.

Most of the manufacturers offer a substage unit with a revolvable plate. The greatest point of difference between such substage condenser mounts lies in the centering action provided for the condenser diaphragms. Some manufacturers such as Wild Co. and the American Optical Co. have made each diaphragm in the changer individually centerable. If each of the diaphragms in the changer is initially centered with respect to its corresponding phase objective, then these phase objectives together with their corresponding diaphragms may be interchanged without the necessity of interrupting the observation in order to recenter a condenser diaphragm. For rapidity of procedure together with best performance, either the objectives should be centered to a common optical axis by the maker, or the objectives should be mounted in quick-change, centering nosepieces.

Figure III.5.1c shows the turret substage unit supplied by the American Optical Co. (1949). The wrenches are inserted into the upper guides to center the condenser diaphragms. Figure III.5.1d is a bottom view of a similar substage turret mount modified slightly to fit a later model of microscope stand. The condenser is of the Abbe type, N.A. 1.25, and is separately centerable. Figures III.5.2a and III.5.2b show, respectively, a top and bottom view of the condenser mount with a revolving changer plate for diaphragms as supplied by the Wild Co., Ltd. (1949). Figure III.5.2c is a photograph of the Wild stand listed as a research and routine microscope for medical purposes and fitted with the substage condenser mount shown in Fig. III.5.2a. Centering wrenches and the auxiliary centering telescope are also
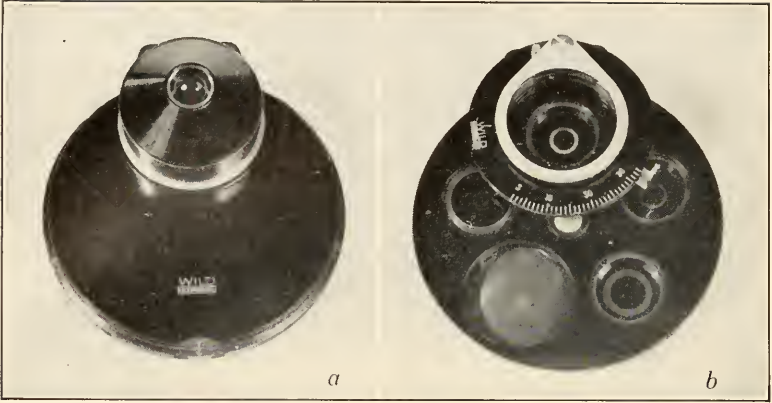
included. A special phase condenser, N.A. 0.9, is supplied in a non-centering mount.

In other makes of substage condenser mounts which have a revolvable changer plate for the condenser diaphragms, the entire plate is moved when any one of the diaphragms is centered. Rotating a second diaphragm into place below the condenser may require recentering of the changer disk. Several photographs were made available to illustrate this type of turret substage mount. Figure III.5.3 is a photograph of a Bausch and Lomb microscope stand fitted with phase objectives and with a substage condenser mount having a rotatable changer. The condenser is an Abbe type, N.A. 1.25, and fits into a non-centering mount. Figure III.5.4 shows the Cooke, Troughton and Simms phase microscope and the auxiliary centering telescope. A condenser with N.A. 1.0 is available for slides of standard thickness. I. Koristka and Co. (Fig. III.5.5) also supplies such a rotatable changer disk on the substage condenser mount of its phase contrast "universal" model microscope. The condenser may be obtained in either a centering or a non-centering mount. Koristka and Co. includes in this turret mount a means for passing gradually from phase contrast illumination to central conical illumination in each phase objective. (The method for accomplishing this has been described by Köhler and Loos, 1941. Three polarizing elements are used. One element contains an annular opening free of polarizing material. A second element has a central, clear aperture, the diameter of which is smaller than the inner diameter of the annular opening in the first element. These two elements of polarizing material are crossed and are mounted together in the rotatable disk. A third uniform polarizing element is mounted below the condenser and can be rotated through 90°. It is so oriented that at one extreme position light passes to the condenser only through the central aperture and such that at the other extreme position light is admitted only through the annular aperture.) Figure III.5.6 is a photograph of the Reichert phase microscope with a turret substage mount. The numerical aperture of the condenser is 0.95. The auxiliary centering telescope is also shown. Figure III.5.7 shows the substage condenser mount with changer disk for diaphragms on the Zeiss-Winkel phase

Fig. III.5.2.   (a) Top view of Wild substage condenser mount with rotatable changer plate for diaphragms.   (b) Bottom view of Wild substage condenser mount with rotatable changer plate for diaphragms.   (c) Wild phase contrast accessories on stand listed as a research and routine microscope for medical purposes.   Courtesy of Henry Wild Surveying Instruments Supply Co., Ltd. (1949).
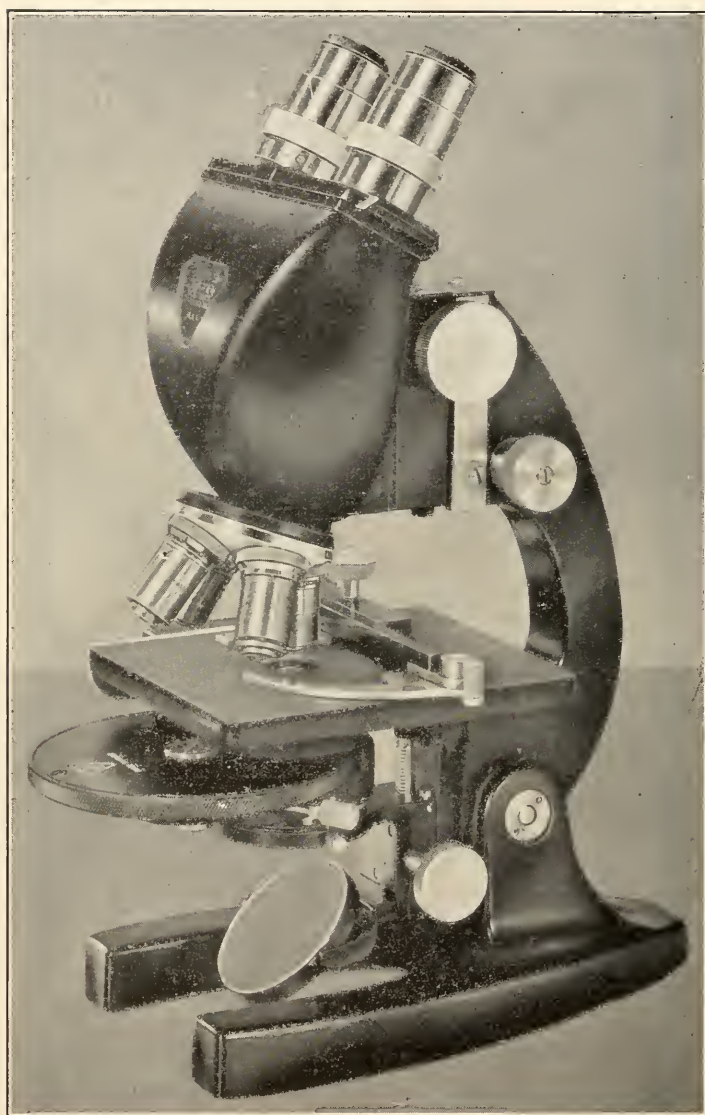
Fig. III.5.3.   Bausch and Lomb phase contrast microscope with rotatable changer
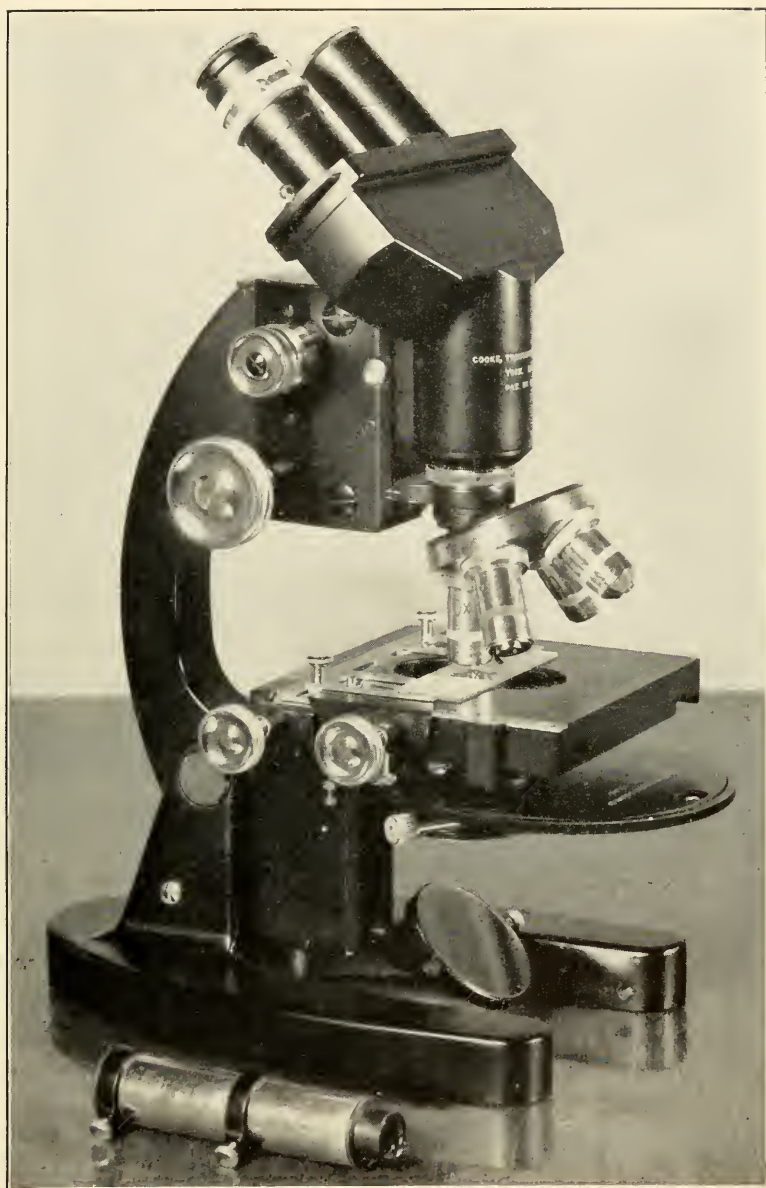plate for diaphragms.   Courtesy of Bausch and Lomb Optical Co. (1949).

Fig. III.5.4.   Phase microscope with rotatable changer plate for diaphragms supplied by Cooke, Troughton and Simms, Ltd.   Courtesy of Cooke, Troughton and Simms, Ltd. (1949).

microscope. The centering telescope is included. The firm of Zeiss, Jena (1949) also supplies a revolving turret substage mount of the type under discussion. The phase condenser, N.A. 0.9, fits into a non-centering mount.

FIG. III.5.5. The phase contrast "universal" model microscope available from I. Koristka and Co. Courtesy of I. Koristka and Co. (1949).

The firm of Galileo (1949) provides phase accessories for its research stand equipped with a pancratic condenser system. The condenser proper is of the achromatic, aplanatic, immersion type, N.A. 1.40, and it is placed in a centering mount. The pancratic system of continuously variable power can change the effective numerical aperture of the condenser from 0.16 to 1.40. The pancratic system is located between
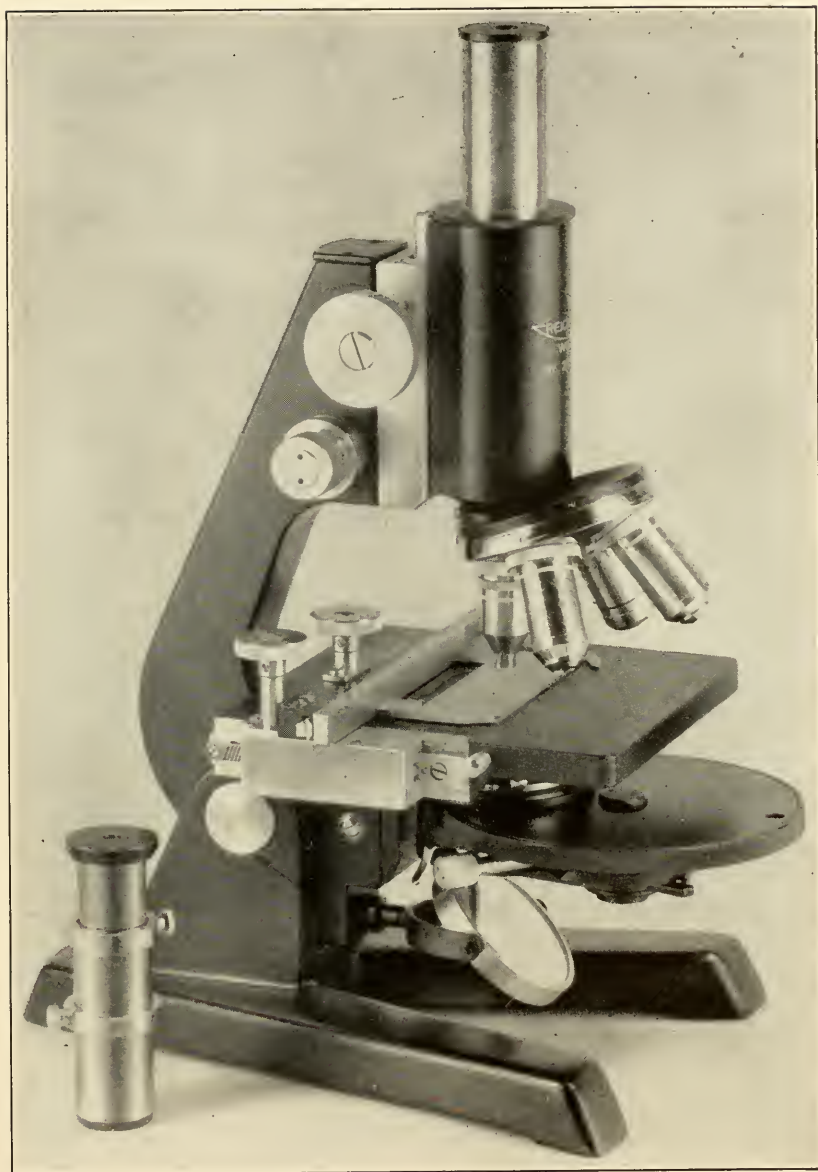
FIG. III.5.6.   Reichert phase contrast microscope.   Courtesy of Optische Werke
C. Reichert (1949).

the condenser proper and a rotatable turret arrangement which contains
a large free aperture, a smaller free aperture, and one centerable con-
denser diaphragm with an annular aperture for phase microscopy
(Fig. III.5.8).   The pancratic system forms an image of the annular
opening at the first focal plane of the condenser proper, and the magni-

FIG. III.5.7.   Zeiss-Winkel phase contrast microscope with turret changer plate
for diaphragms.   Courtesy of R. Winkel G.M.B.H. (1949).

fication of the pancratic system can be varied so that the size of the
image of the annular aperture can be changed to fit the conjugate area
of any of the phase objectives.   Zeiss, Jena (1949) provides phase
accessories also for the Lumipan stand with a pancratic condenser
system.

In order to meet the requirements of phase microscopy with slides of
greater than standard thickness or with specimens contained in small
cells or flasks, both the Bausch and Lomb Optical Co. and the American
Optical Co. supply, in addition to a N.A. 1.25 condenser, special phase
condensers which have a long working distance.   The Bausch and
Lomb long working distance condenser may be used with its series of
both the dry and the oil immersion achromatic objectives for phase

microscopy. The condenser mount is the single-unit type. The condenser diaphragm is located at the second surface of the bottom
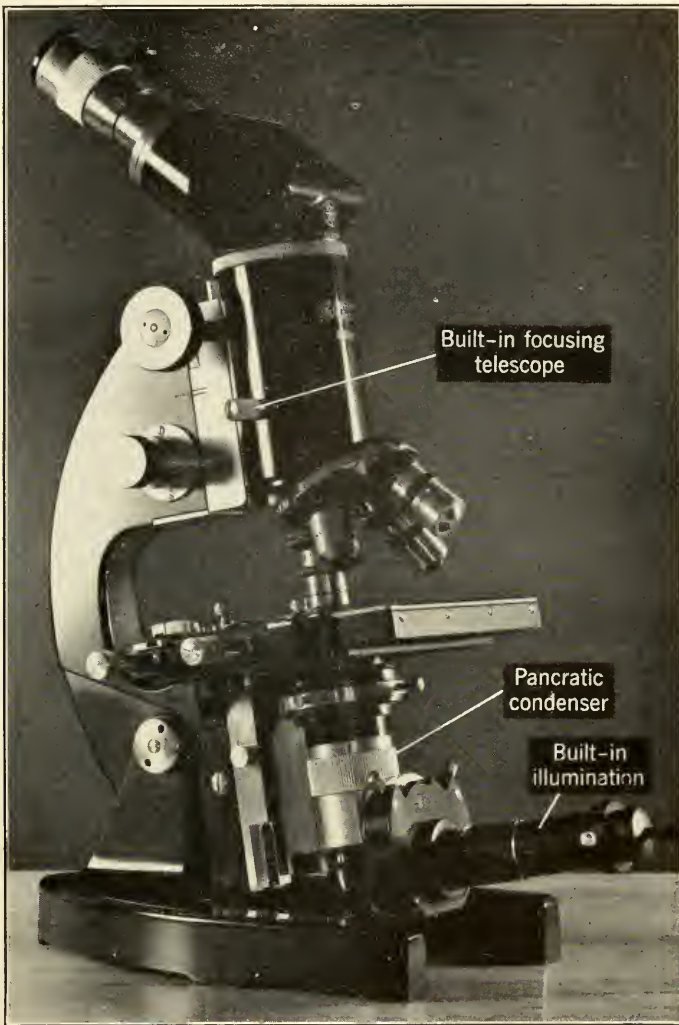
FIG. III.5.8.   Phase microscope with pancratic condenser system supplied by Officine Galileo.   Courtesy of Officine Galileo (1949).

element of the condenser. A separate bottom element with diaphragm is mounted in a plate and is inserted in the substage mount as required for working with one of the phase objectives. Each element is center-able in the substage mount. Figure III.5.9 shows a Bausch and Lomb
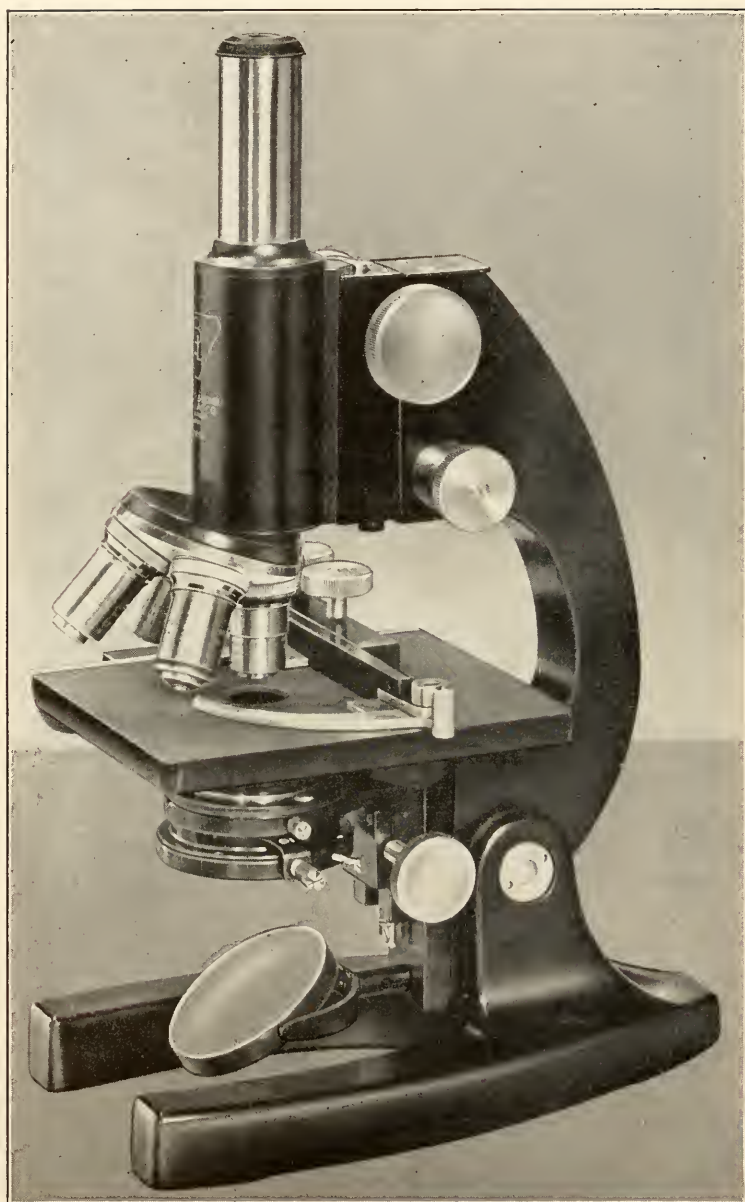
Fig. III.5.9.   Bausch and Lomb phase microscope with long working distance condenser fitted in single-unit type of mount.   Courtesy of Bausch and Lomb Optical Co. (1949).

phase microscope stand equipped with a long working distance condenser in the single-unit substage mount. This condenser permits a working distance in the range 9.5 mm to 10 mm in air (more in glass or water) when the condenser is adjusted for Köhler illumination.

The American Optical Co. supplies long working distance condenser elements and diaphragms which fit into its turret substage mount. A condenser consisting of two lenses is used with the phase objective of 4-mm focal length, and a working distance of approximately 7 mm in air is obtained. Only the bottom lens element of this condenser is retained with the phase objectives of 8-mm and 16-mm focal length, and the working distance is approximately 8 mm in air. This condenser lens is also the bottom element of the standard phase microscope condenser, N.A. 1.25. The diaphragms are contained in individual cells which screw into the rotatable changer plate of the turret mount. Of the phase microscope condensers supplied by various manufacturers as standard equipment with the rotatable disk type of substage condenser mount, some of the condensers having a numerical aperture of 1.0 or less are also suitable for slides of greater than standard thickness (e.g., five times the standard glass thickness). The phase microscope condensers made by Zeiss, Jena and by Cooke, Troughton and Simms, Ltd., are examples. Cooke, Troughton and Simms, Ltd., also offers a special condenser which permits a working distance of 6 mm in air. Koristka and Co. lists a special, long focal length condenser for its "simplified" phase microscope.

4.3. Centering telescopes

All manufacturers mentioned in the preceding part of this section, with the exception of Officine Galileo and I. Koristka and Co., supply separate, adjustable centering telescopes (long-focus microscopes, in fact) which can be inserted in the body tube in place of the eyepiece and focused on the coating of the diffraction plate. In the phase microscope made by the firm of Galileo, the eyepiece is not removed, and the user operates a knob on the body tube to place a lens in the path of light below the eyepiece. The eyepiece together with this lens forms the centering telescope. The knob also controls a focusing adjustment so that the centering telescope can be focused on the coating of the diffraction plate. In the Koristka phase microscope, a centering ocular replaces the eyepiece of the microscope and a knob is turned to move a second lens into the light beam so that these two components become the centering telescope.

5. SOME EFFECTS OF VARYING THE DIMENSIONS AND OPTICAL CHARACTERISTICS OF THE CONJUGATE AREA

The fact has been emphasized that a compromise decision must be made in choosing the dimensions of the conjugate area of the diffraction plate designed for general use. The elementary theory was developed in Chapter II to show the interdependence of the optical properties of the particle and those of the diffraction plate when the problem of optimum contrast is being considered. In Section 1 of this chapter this elementary theory was applied in an attempt to predict the range of usefulness of a diffraction plate with an optical path step equal to $\lambda/4$ between the complementary and the conjugate areas and with a lower energy transmission in the conjugate area than in the complementary area. The simple theory does not take into account either the shape of the object specimen or the area occupied by it, and this theory also does not include the effect on contrast of the size and location of the conjugate area of the diffraction plate.

In the previous general discussions statements have been made concerning whether a particle appears brighter or darker than its surround. However, observations with the phase microscope show that, when the area occupied by a particle of uniform optical path becomes large, the brightness at the center of the image of the particle is equal to that of the image of a comparatively remote region of the surround, and only the region near the boundary in the image of the particle appears darker or brighter according to the type of contrast being produced. Furthermore, it is also seen that the image of a particle is surrounded by a halo. A dark-contrast image is surrounded by a bright halo, and a bright-contrast image is surrounded by a dark halo. This halo is an artifact. Thus it is seen that phase contrast occurs only in the neighborhood of a rapid change in the optical properties of a particle relative to its surround. In order to achieve phase microscopy, the diffracted rays must be deviated sufficiently relative to the undeviated rays so that the deviated and undeviated bundles become fairly well separated at some plane within the microscope if a diaphragm is introduced below or within the substage condenser. The relative phase change introduced between the deviated and the undeviated light by the occurrence of diffraction lies in the neighborhood of 90° when the optical path difference between a transparent particle and its surround is a small fraction of a wavelength. The method of phase microscopy is not applicable for observing slow, gradual changes in optical path; in such cases interferometric means must be used. It is known, for example, that, when a particle is slightly smaller than the limit of resolution of an objective, the amount of light in the diffraction pattern diminishes rapidly with

distance from the discontinuity which causes the diffraction. It is not surprising, therefore, that phase contrast is produced only close to the boundary of a particle and that the more or less complementary halo is visible only in the neighborhood of the particle.

In order to study some of the effects resulting from varying the dimensions and transmission of the conjugate area of a diffraction plate, a specimen was prepared which had little internal detail so that the extent of the halo and the area over which contrast is produced could be more easily seen. The specimen was made by shielding some areas of a microscope slide with very thin iron filings while magnesium fluoride was evaporated on the slide. After the evaporation, the filings were wiped off the slide, and an oil having a refractive index of 1.47 was flowed underneath the cover slide. The specimen then consisted of a number of oil pools of different area surrounded by magnesium fluoride. The photomicrographs reproduced in Fig. III.7 show some of the oil pools as they appeared under the various conditions of the experiment. As a rule, a sharp shadow was not formed at the edge of the iron filings during the evaporation because the filings had not adhered closely to the slide over their entire area. The thickness of the magnesium fluoride film was such that the optical path difference between the oil pools and their surround was equal to or less than 0.065λ ($\lambda = 5461$ A) or $23.4°$. The oil pools will be referred to as the particles in the discussion of the observations made on them. The particles, then, differ in area, have an optical path greater than that of the surround, and may vary in thickness close to the edge. If no impurities are present, the edges cannot have an optical path exceeding that at the center of a particle.

These observations of changes in the image which resulted from varying the dimensions and transmission of the conjugate area included only diffraction plates that produced dark contrast. One photomicrograph of a bright-contrast image is shown for purposes of comparison. All the diffraction plates in this experiment were made with a coating of magnesium fluoride and Inconel such that the optical path difference between the conjugate area and the complementary area was $-\lambda/4$ ($\lambda = 5461$ A). The diffraction plates were separable from the objective and were mounted behind all the lenses so that the same objective remained in the optical system as different diffraction plates were substituted. A selected Spencer achromatic objective of 4-mm focal length, N.A. 0.66, was chosen. In the manufacture of such an objective, a separation between two lens components is adjusted to balance the objective as well as possible for spherical aberration. For Fig. III.7, the separation was chosen to give as good

definition of the edges of the oil pools as was feasible in the phase contrast image with the diffraction plate having a conjugate area limited by N.A. 0.52–N.A. 0.36 in the objective. Inspection of the objective itself in an interferometer illuminated by a narrow band of wavelengths in the neighborhood of $\lambda = 5461$ A showed the presence of one narrow fringe, due to spherical aberration, around the extreme edge of the aperture. The conjugate area of each diffraction plate lay well within the uniform area seen in the interferometer. The specimen was observed with white-light illumination, but the general results were still valid if any one of the Kodak series of Wratten M filters for photomicrography was placed in front of the lamp. The final magnification in the photomicrographs is $450\times$.

The size of the cone of light illuminating the specimen has some effect on the visibility of the specimen when no diffraction plate is present in the objective. Therefore, photomicrographs were also taken with the diffraction plate removed but with the condenser diaphragm remaining in position. When a photomicrograph was taken with a diffraction plate in the objective, the designation of the diffraction plate according to the notation in Section 2.5 is printed below each picture, and the range of numerical aperture included by the conjugate area of the diffraction plate is also given. If only the range of numerical aperture appears below a photomicrograph, this indicates that the diffraction plate had been removed from the objective but that the diaphragm corresponding to this plate remained at the first focal plane of the substage condenser. The photomicrographs obtained with such conical illumination are shown alongside the corresponding phase photomicrographs. For further comparison a photomicrograph, Fig. III.7.7, was taken with central conical illumination when the aperture of the condenser had been reduced to N.A. 0.36 and no diffraction plate was mounted in the objective. Neutral Inconel filters of different transmission were placed near the substage mirror and interchanged so that the same exposure time for each photomicrograph would result in negatives of closely the same background density.

The sketch of Fig. III.6 represents the system of particles as seen with a low-contrast phase objective at greater magnification than was produced by the objective of 4-mm focal length (see also Fig. III.7.22). Letters are placed near the image of a particle or group of particles in order to identify them. These particles fall into four groups of interest. The following comments apply only to the dark phase contrast images. Particles of the size and shape of A, B, C, and D never appear uniformly dark regardless of the characteristics of the conjugate areas of the diffraction plates. Whether particles such as E, F, and G appear

uniformly dark depends on the numerical aperture included in the
conjugate area of the diffraction plate as well as on the transmission of
the conjugate area.   Particles of the size and shape of those included
in groups H and P appear uniformly dark with all diffraction plates,
regardless of the size of the conjugate area.

FIG. III.6.   Drawing of the object specimen consisting of oil pools surrounded by a
film of magnesium fluoride.   The blackened areas indicate those regions of greatest
contrast which have been referrred to as inclusions.

In addition to these larger oil pools there is smaller detail such as
groups K (close to the upper right-hand edge of A), L (just to the left
of the upper edge of A), R, M, and N.   These groups contain particles
which are so small as to be sensitive to loss of resolution and which show
reversal of contrast when the absorption in the conjugate area is high.
The four particles K may not be visible in the reproduction of the phase
photomicrographs although they were in every case readily discernible

to the eye. With dark-contrast diffraction plates which do not have sufficient absorption in the conjugate area to cause reversal, detail K appears darker than the edge of A. Detail K also appears darker in the non-phase photomicrographs, and a question arises concerning the absorption and optical path of this detail as compared with the optical properties of the main body of oil pool A. Similarly, the non-phase photomicrographs and most of the phase photomicrographs show very small areas of higher contrast in groups L, M, N, H, P, and R, and there is the suggestion of some absorption in these areas. The difference in optical path between a particle and its surround as well as the relative transmission of the particle can be determined by means of a variable phase microscope which allows continuous variation both of the difference in optical path and also of the transmission ratio between the conjugate and complementary areas of the diffraction plate. The size and shape of the particle will also affect the amount of contrast in the image.

In the discussion to follow, these small areas of darkest contrast that are observed within the images of the oil pools will be referred to as inclusions although the observations reported in this section offer no conclusive evidence concerning whether the increase in contrast indicated a change in optical path alone or whether some absorption was also present within the so-called inclusions. It is possible that tiny pieces of iron became trapped under the magnesium fluoride film so that iron or iron oxide particles introduced some absorption. That the inclusions constituted areas of greater optical path only, with no absorption, can be accounted for by assuming that during the evaporation the iron filings adhered most closely to the slide over these areas and therefore shielded these regions more completely from the magnesium fluoride.

High-contrast diffraction plates were selected to observe changes in the extent of the halo around each particle and in the extent of the darkening in the image of a particle as the dimensions of the conjugate area were changed. If an object specimen contains an inclusion which appears darker than the remainder of a specimen when the diffraction plate in the objective produces a high-contrast, dark image of this specimen, it is sometimes possible to enhance the visibility of the inclusion with respect to the whole object specimen by substituting a diffraction plate which has a higher transmission in the conjugate area. Therefore photomicrographs were taken also to show the change in the visibility of the inclusions with respect to the edges of the oil pools as the energy transmission only of the conjugate area of the diffraction plate was changed.

Figure III.7.3 was obtained with diffraction plate $0.15\lambda - 0.25\lambda$, N.A. 0.52–N.A. 0.36, which produced a high-contrast image of the oil pools. With this plate particles K and the other inclusions appeared darker than the edges of the larger particles. When the energy transmission of the conjugate area of the diffraction plate was reduced to 6%, partial reversal of contrast in the image of particles K was observed, and the images of some of the small areas in groups P, R, and L showed reversal of contrast (Fig. III.7.11). There was no indication of reversal of contrast in the images of the edges of the oil pools. When the conjugate area of the diffraction plate contained no absorbing material, the inclusions again appeared dark and were more easily detected (Fig. III.7.9) than with the diffraction plate described by $0.15\lambda - 0.25\lambda$. However, particles K and the other small inclusions were even more clearly visible with the diffraction plate designated by $0.32\lambda - 0.25\lambda$. N.A. 0.52–N.A. 0.36 (Fig. III.7.10).

The simple theory would indicate that, since these inclusions appear darker than the edges of the oil pools with the diffraction plates having the higher transmissions in the conjugate area (in particular, even with the non-absorbing diffraction plate), the optical path through the inclusions is greater than the average thickness, in terms of optical path, of the edges of the larger oil pools. However, the simple theory does not exclude the possibility that the inclusions were also partially absorbing. When the bright-contrast diffraction plate $0.19\lambda + 0.25\lambda$, N.A. 0.52–N.A. 0.36, was inserted in the objective, the images of the oil pools and the inclusions were bright (Fig. III.7.8), and the areas which formerly were darkest (except when contrast reversal occurred with the $0.06\lambda - 0.25\lambda$ plate) now appeared brightest. According to the simple theory, this does not contradict the evidence that the inclusions had a greater optical path than did the edges of the larger oil pools, but again it also allows the possibility that some absorbing material is present in these small brightest areas. Thus the qualitative information obtained with this series of diffraction plates having a $\frac{1}{4}$-wavelength optical path step is not sufficient to determine conclusively whether the inclusions represent regions of greater optical path only or whether partial absorption is present.

As stated previously, the series of observations represented by the photomicrographs in Fig. III.7 was made chiefly to study the dependence of both the halo and the darkening of the images of the particles on the dimensions and energy transmission of the conjugate area. Because the halo is more pronounced when the amount of contrast is high, diffraction plates with relatively high absorption in the conjugate area were chosen for most of the observations. In any single phase
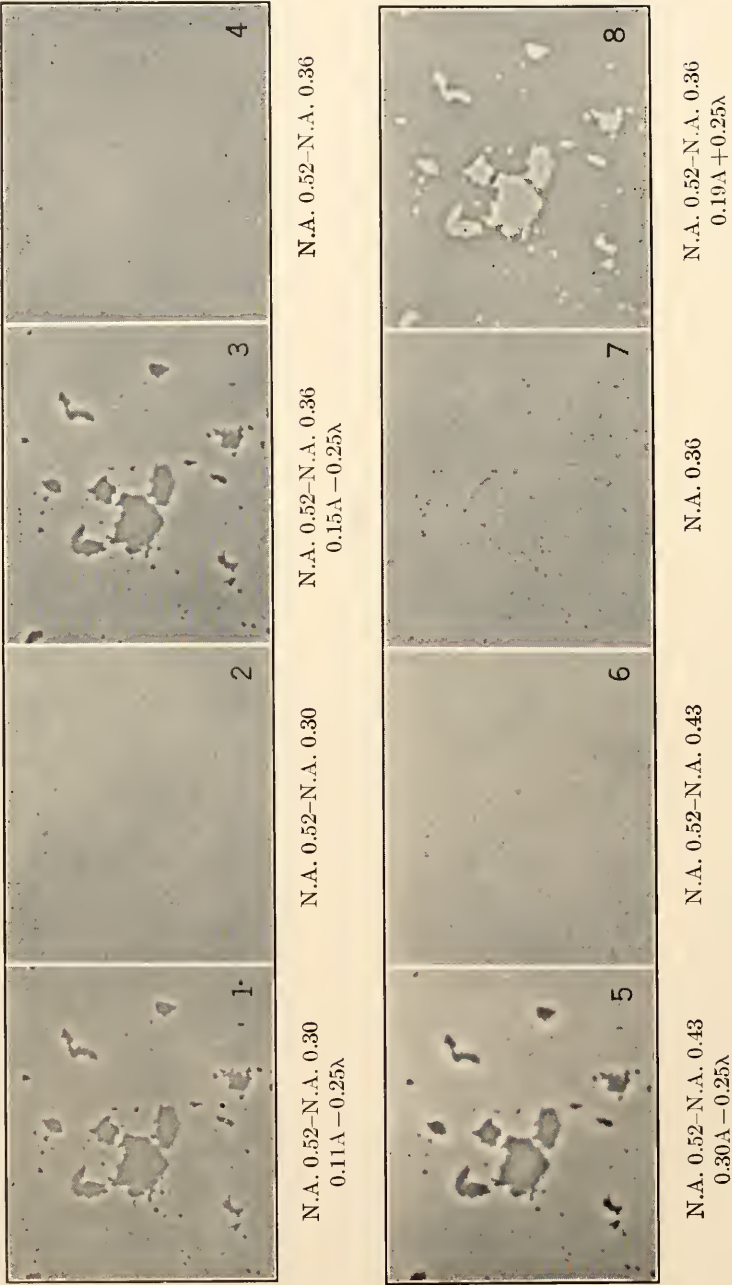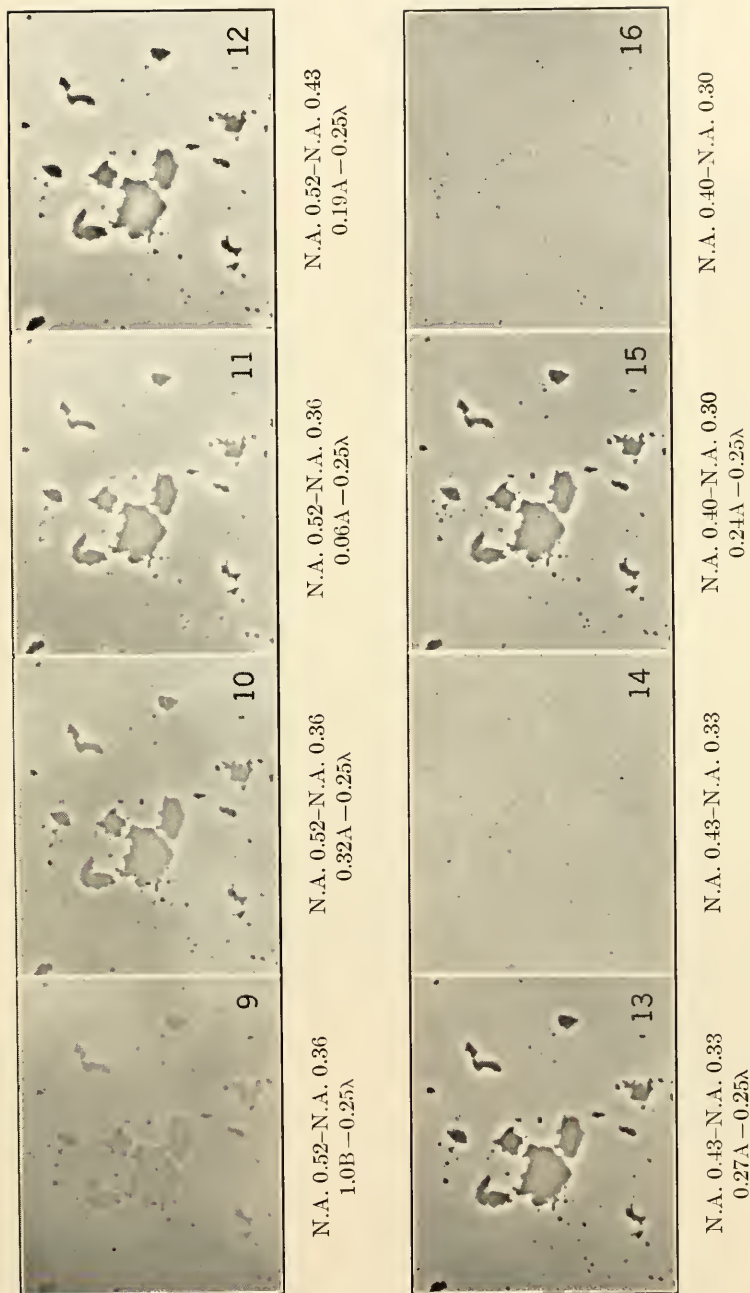
N.A. 0.52–N.A. 0.30   N.A. 0.52–N.A. 0.30   N.A. 0.52–N.A. 0.36   N.A. 0.52–N.A. 0.36
0.11λ − 0.25λ   0.15λ − 0.25λ

N.A. 0.52–N.A. 0.43   N.A. 0.52–N.A. 0.43   N.A. 0.36   N.A. 0.52–N.A. 0.36
0.30λ − 0.25λ   0.19λ + 0.25λ

Fig. III.7.   (Legend is on p. 137.)

N.A. 0.52–N.A. 0.36
1.0B – 0.25λ

N.A. 0.52–N.A. 0.36
0.32λ – 0.25λ

N.A. 0.52–N.A. 0.36
0.06λ – 0.25λ

N.A. 0.52–N.A. 0.43
0.19λ – 0.25λ

N.A. 0.43–N.A. 0.33
0.27λ – 0.25λ

N.A. 0.43–N.A. 0.33

N.A. 0.40–N.A. 0.30
0.24λ – 0.25λ

N.A. 0.40–N.A. 0.30

Fig. III.7.   (Legend is on p. 137.)

N.A. 0.40–N.A. 0.30
0.14A −0.25λ

N.A. 0.31–N.A. 0.17
0.13A −0.25λ

N.A. 0.31–N.A. 0.17

N.A. 0.26–N.A. 0.18
0.14A −0.25λ

N.A. 0.26–N.A. 0.18
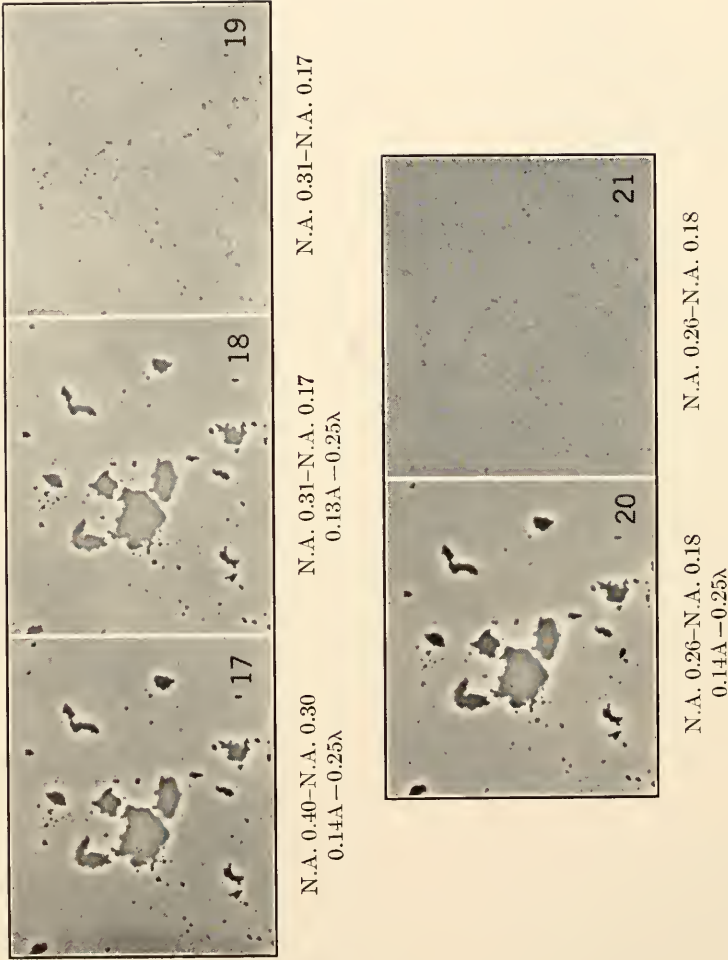
Fig. III.7.   (Legend is on p. 137.)
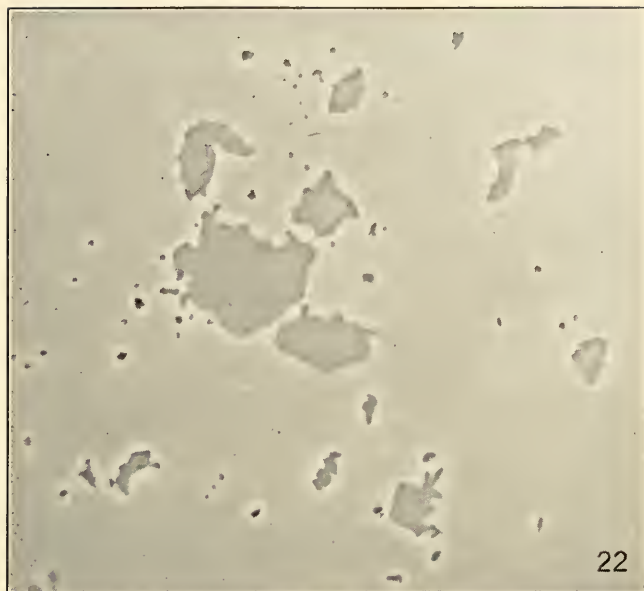
N.A. 0.79–N.A. 0.56
0.20A — 0.25λ

FIG. III.7. Photomicrographs of the object specimen consisting of oil pools in a surround of magnesium fluoride. The dark-contrast phase photomicrographs illustrate changes which occurred in the image when the dimensions or the transmission or both of the conjugate area were varied and δ remained fixed at δ = −λ/4 (λ = 5461 A). The ordinary photomicrographs show the effect on the image of changing the dimensions of the cone of light incident on the specimen. Figures 7.1–7.21, inclusive: 450×. Fig. 7.22: 1000×.

contrast photomicrograph it is evident that the brightness and the extent of the halo vary with the particle size or the amount of detail present. The halo is more pronounced around a large particle or in the neighborhood of a cluster of particles very close together than it is around a small, isolated particle. After an isolated particle has increased to a certain size, the brightness and the extent of the halo appear to remain constant, as does the extent of the darkest area within the image of the particle.

Figures III.7.1, III.7.3, and III.7.5 were obtained when the numerical aperture corresponding to the outer diameter of the conjugate area remained the same but the conjugate area was made narrower by increasing the inner diameter. As the conjugate area became narrower, the halo extended farther out into the image of the surround. Particles A, B, C, and D did not appear uniformly dark with any of these three diffraction plates, some part near the center of the images of the particles

always being brighter than the areas near the boundaries. (Unless explicit reference is made to inclusions, the variation in contrast caused by their presence is omitted from the general description of the appearance of the images of the larger oil pools.) The brightness at the center of the images of A, B, and C seemed to be approximately equal to the brightness of the image of the surround beyond the regions occupied by the halos. However, as the conjugate area became narrower, the dark region near the edge of the image of the particle extended farther toward the center. The manner in which the V-shaped lower edge of B darkened as the diffraction plate was changed is of interest. As the darker region extended farther toward the center of B, the darkening spread across the entire bottom corner, and in Fig. III.7.5 the darker border in the image does not follow the contour of B as closely as it does in the other two phase photomicrographs. This is an example of the fact that neighboring discontinuities in the optical path of the object specimen can interact to affect the amount of contrast present in an image formed by the phase microscope. Therefore caution must be used in trying to interpret amount of contrast in terms of relative optical path differences in the object specimen.

Particle E appeared clearly non-uniformly dark across its width when the diffraction plate with the widest conjugate area was in the objective. The diffraction plate having the conjugate annulus of intermediate width caused E to appear uniformly dark, and the narrowest conjugate annulus also made E appear uniformly dark. Particles G and F appeared uniformly dark only when the diffraction plate with the narrowest conjugate annulus was used. The particles in H, M, and N (inclusions excepted) appeared uniformly black with all three diffraction plates. The narrowest conjugate area produced partial reversal of contrast in the images of the small areas in P, R, and L that have been referred to as inclusions; otherwise particles in these groups appeared uniformly dark.

Figures III.7.9, III.7.10, and III.7.11 show the appearance of the oil pools when the dimensions of the conjugate area were given by N.A. 0.52–N.A. 0.36, as in Fig. III.7.3, but the energy transmission of the conjugate area was varied. As the transmission decreased, the halo around each image became more visible although it did not appear to change appreciably in area. Also, the area over which darkening occurred did not seem to be appreciably affected by the transmission of the conjugate area. The effect which this variation in the energy transmission had upon the small areas considered to be inclusions has already been discussed. Figure III.7.12 was obtained when the absorption in the conjugate annulus having the same dimensions as those indicated below Fig. III.7.5 was increased. There were no apparent changes in

the extent of either the halo or the darkening. A conjugate area having this included range of numerical aperture was not, in general, a satisfactory choice for this objective. A residual bluish haze, which could not be lessened by a different adjustment in separation between the lenses of the objective, made the definition seem poorer than when any of the other diffraction plates in this series were in the objective. The definition was made worse by placing a filter which transmitted blue light in front of the lamp, was improved somewhat by substituting a filter which transmitted green light, and was considerably improved by illuminating the specimen with red light.

If the corresponding non-phase photomicrographs in Figs. III.7.2, III.7.4, and III.7.6 are compared, it is not possible to decide whether the cone of light N.A. 0.52–N.A. 0.30 or the cone N.A. 0.52–N.A. 0.36 makes the specimen more visible. Those boundaries of the oil pools which contain no inclusions are hardly visible. The narrowest illuminating cone, N.A. 0.52–N.A. 0.43, caused the oil pools to appear in greater contrast than did the wider cones. When the phase condenser diaphragms were removed and the specimen was illuminated through a central opening corresponding to N.A. 0.36, the visibility of the oil pools and the inclusions was greatly increased (Fig. III.7.7) in comparison with the previous non-phase observations; however, a greater number of diffraction rings were visible around the smallest particles.

The rest of the phase photomicrographs included in Fig. III.7 show the change that occurred in the images of the oil pools when the outer diameter of the conjugate annulus became smaller. The conjugate area of the diffraction plate inserted in the objective to obtain Fig. III.7.13 was such that the outer diameter of the annulus coincided with the inner diameter of the conjugate area of the diffraction plates which are described under Figs. III.7.5 and III.7.12. The conjugate area related to Fig. III.7.13 was slightly wider than the conjugate area related to Figs. III.7.5 and III.7.12. The excessive haze which was apparent in the images of Figs. III.7.5 and III.7.12 disappeared. Diffraction plate $0.27A - 0.25\lambda$, N.A. 0.43–N.A. 0.33, produced a halo which was slightly less in extent than the halo observed with diffraction plate $0.15A - 0.25\lambda$, N.A. 0.52–N.A. 0.36. In Fig. III.7.13 particle E appears uniformly dark. A small region near the middle of the image of F and that of G was not so dark as the edges, but it was much darker than the image of the surround. The decrease in darkness from the boundary to the center of the images of particles F and G was less than that observed with the diffraction plate related to Fig. III.7.3. In Fig. III.7.13 there was no reversal of contrast in the image of particle groups K, L, M, N, R, and P. However, the diffraction rings around particles such as R

were a little more apparent than when diffraction plates with a conjugate annulus of greater outer diameter were substituted.

When the conjugate area was formed slightly closer (N.A. 0.40–N.A. 0.30) to the optical axis of the objective, Fig. III.7.15 was obtained. In the specimen being discussed, there was no noticeable difference in the image whether the diffraction plate related to Fig. III.7.13 or to Fig. III.7.15 was inserted in the objective except that the conjugate area having the smaller mean diameter increased, by a small amount, the visibility of the diffraction patterns around the smallest particles. . A more critical object specimen with closely spaced detail, such as the chromosome specimen shown in Fig. V.5, indicated that some loss of resolution had resulted from changing the dimensions of the conjugate area from N.A. 0.52–N.A. 0.36 to N.A. 0.40–N.A. 0.30. Figure III.7.17 shows the effect of decreasing the energy transmission of the annulus with the dimensions N.A. 0.40–N.A. 0.30. The contrast became greater, and the particles G and F appeared uniformly dark. There was no reversal of contrast in the images of the K, L, and R groups.

When the image produced with the addition of diffraction plate 0.13A − 0.25λ, N.A. 0.31–N.A. 0.17 (Fig. III.7.18), was compared with the image seen with the aid of diffraction plate 0.15A − 0.25λ, N.A. 0.52–N.A. 0.36 (Fig. III.7.3), it was observed that definition appeared better with the first diffraction plate because there was less haze over the field of view. However, the limitation of the cone of illumination to N.A. 0.31–N.A. 0.17 resulted in a noticeable loss of resolution. A greater number of diffraction rings were easily seen around particles in groups L, M, N, and R. The images of particles R resembled diffraction patterns consisting of a bright center and one dark outer ring. Narrow dark bands were visible within the region occupied by the halo around the image of particles as large as those in group H. The extent of the halo around the image of an oil pool in Fig. III.7.18 is most nearly like that shown in Fig. III.7.1. Particle E did not appear uniformly dark, but it appeared more nearly so with diffraction plate 0.13A − 0.25λ, N.A.0.31–N.A.0.17, than with diffraction plate 0.11A − 0.25λ, N.A.0.52– N.A. 0.30. The images of particles F and G were again non-uniform in brightness, as is seen in Fig. III.7.18.

The last phase photomicrograph in this series, Fig. III.7.20, was taken with diffraction plate 0.14A − 0.25λ, N.A. 0.26–N.A. 0.18, in the objective. The halo extended farther away from the boundary of the image of an oil pool than in Fig. III.7.18 but not quite so far as in Fig. III.7.5. Again, dark diffraction bands were clearly evident around the images of the particles in H, M, N, P, and R and within the region occupied by the halo. There was some indication that the distribution

of light in the halo around the images of the largest particles was being affected by the superposition of darker diffraction bands. The images of particles E, F, and G appeared uniformly dark, and the image of D was nearly so. This last diffraction plate produced a greater degree of uniformity in darkness across the image of particle A than did any of the other diffraction plates. Figure III.7.22 is included to show the particles at 1000×. It was obtained with an oil immersion phase objective of 1.8-mm focal length.

Figures III.7.14, III.7.16, III.7.19, and III.7.21 are non-phase photomicrographs showing the effect of changing the dimensions of the cone of illumination to correspond to the last four changes in the size of the conjugate area. The visibility of the oil pools was greater with the opening given under Fig. III.7.14 than with that cited under Figs. III.7.2 and III.7.4. Figure III.7.16 is similar to Fig. III.7.6. The two smallest annular openings in the condenser diaphragm resulted in an image similar to that formed with the central aperture N.A. 0.36, Fig. III.7.7. More diffraction rings could be counted around the smallest particles when the illuminating cones N.A. 0.31–N.A. 0.17 and N.A. 0.26–N.A. 0.18 were used than when the illuminating cones had a higher mean numerical aperture.

The influence of the residual aberrations of the objective on either the formation of the phase contrast image or on the appearance of the halo as the diffraction plates were changed is not known. If an objective contained a diffraction plate which had an annulus of the size N.A. 0.52–N.A. 0.36 and which produced medium or high dark contrast, then the addition of a corrector plate to decrease the spherical aberration of the objective did not improve noticeably the definition of a phase contrast image. However, if the diffraction plate produced low contrast, then less residual haze was apparent over the field of view when the corrector plate was inserted.

The phase photomicrographs of Fig. III.7 indicated the following trends. If the outer numerical aperture of the conjugate area remains constant, a narrower conjugate annulus forms an image in which the halo extends farther into the image of the surround and in which a wider area adjacent to the boundary (i.e., one that extends closer to the center of the object specimen) of a large, homogeneous, uniformly thick particle appears in either bright or dark contrast. If the magnitude of the difference in numerical aperture included within the conjugate annulus is fixed and small, then a conjugate area of lower mean numerical aperture can form an image in which a wider region adjacent to the boundary of the particle appears in dark or bright contrast. There was some evidence that the conjugate area of greater mean numerical

Undercorrection = −0.03-mm glass

Undercorrection = −0.07-mm glass

Undercorrection = −0.03-mm glass 0.15λ − 0.25λ

Undercorrection = −0.07-mm glass 0.15λ − 0.25λ

Overcorrection = +0.05-mm glass

Overcorrection = +0 08-mm glass

Overcorrection = +0.05-mm glass 0.15λ − 0.25λ

Overcorrection = +0.08-mm glass 0.15λ − 0.25λ
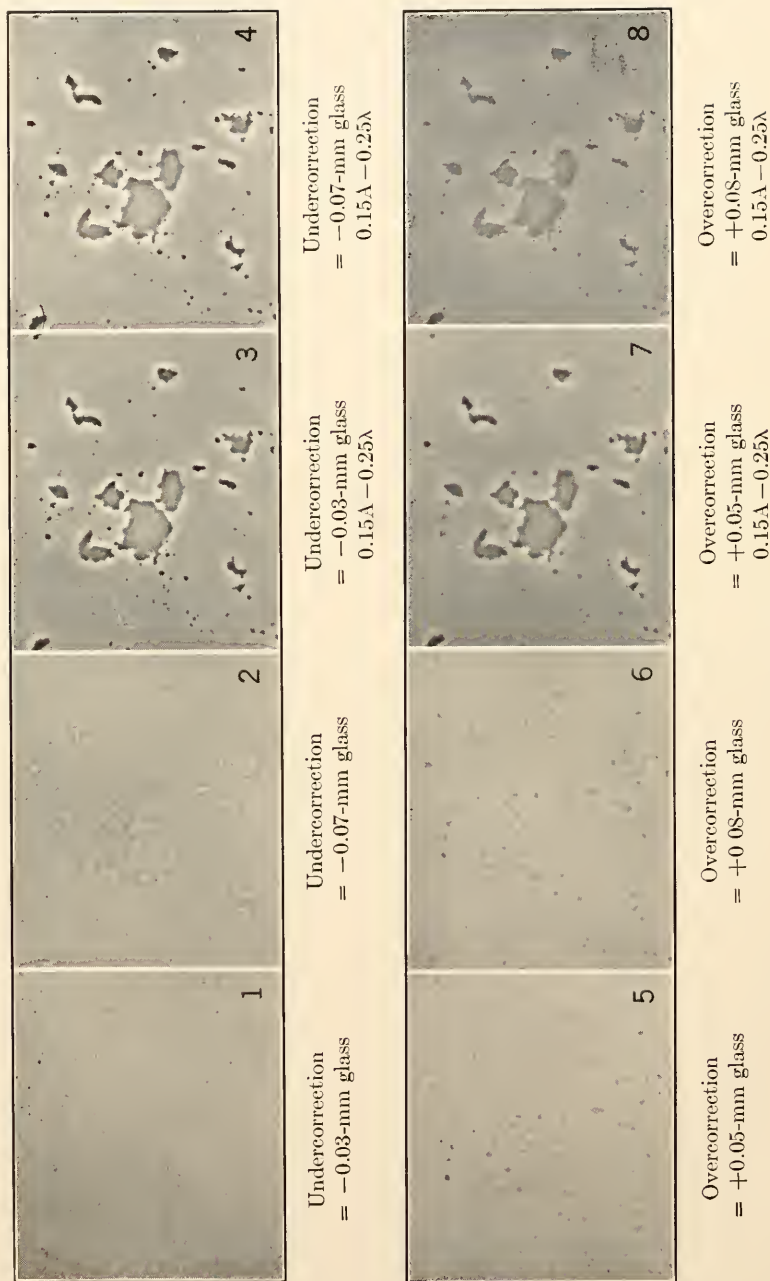
Fig. III.8.

aperture and given included difference in numerical aperture produced a halo that extended farther into the image of the surround, but the aberrations of the objective and the presence of pronounced diffraction patterns complicated the observations. The fact that the halo exists as an artifact does not limit the usefulness of phase microscopy. Care must be taken in trying to interpret amount of contrast in terms of optical path differences between the structural details within a specimen.

It has been explained that spherical aberration can affect the performance of a diffraction plate because the aberration also produces relative changes in phase over the wave front as it passes through the objective. The phase changes introduced by spherical aberration are not abrupt changes. However, if a condenser diaphragm with an annular opening is placed at the first focal plane of the substage condenser, it may be possible to introduce a net change in phase between the deviated and the undeviated light by sufficiently overcorrecting or undercorrecting the objective. Some degree of phase contrast should be observed in such a case although the definition may be less good than if a step-type diffraction plate is used in a well-corrected objective.

The photomicrographs reproduced in Fig. III.8 show the result of undercorrecting or overcorrecting the objective used to obtain Fig. III.7. The amount of spherical aberration introduced by altering the separation between two lens components in the objective is most easily described in terms of the equivalent effect that can be produced by leaving the objective adjusted according to design for a standard cover-glass thickness but by changing the thickness of the cover glass. The condenser diaphragm contained an annular opening described by N.A. 0.52–N.A. 0.36. The specimen consisted of the same group of oil pools photographed in Fig. III.7.

Fig. III.8. Photomicrographs illustrating changes produced in the image of the oil pool specimen by altering the spherical aberration of the objective. The cone of illumination was defined by N.A. 0.52–N.A. 0.36. The undercorrection or overcorrection is expressed in terms of a corresponding deviation from standard cover-glass thickness. (1) Undercorrection equivalent to a decrease of 0.03 mm in cover-glass thickness. (2) Undercorrection equivalent to a decrease of 0.07 mm in cover-glass thickness. (3) Undercorrection equivalent to a decrease of 0.03 mm in cover-glass thickness superimposed on diffraction plate $0.15\lambda - 0.25\lambda$. (4) Undercorrection equivalent to a decrease of 0.07 mm in cover-glass thickness superimposed on diffraction plate $0.15\lambda - 0.25\lambda$. (5) Overcorrection equivalent to an increase of 0.05 mm in cover-glass thickness. (6) Overcorrection equivalent to an increase of 0.08 mm in cover-glass thickness. (7) Overcorrection equivalent to an increase of 0.05 mm in cover-glass thickness superimposed on diffraction plate $0.15\lambda - 0.25\lambda$. (8) Overcorrection equivalent to an increase of 0.08 mm in cover-glass thickness superimposed on diffraction plate $0.15\lambda - 0.25\lambda$. $450\times$.

The result of undercorrecting the objective by an amount equivalent to a decrease of 0.03 mm in the thickness of the cover glass is seen in Fig. III.8.1. Figure III.8.2 shows the appearance of the oil pools when the objective was further undercorrected by an amount equivalent to an additional decrease of 0.04 mm in the thickness of the cover glass. The first adjustment indicated a tendency for bright contrast to occur when the objective was undercorrected, and the second adjustment produced a bright-contrast image. Inspection of the objective in an interferometer at the second stage of undercorrection showed that the part of the wave front which passed through the region corresponding to the conjugate area of the objective was retarded with respect to the part of the wave front passing through the center and outermost area of the objective.

Figures III.8.3 and III.8.4 were obtained by inserting diffraction plate $0.15A - 0.25\lambda$, N.A. 0.52-N.A. 0.36, in the objective at these two stages of undercorrection. The first step in undercorrection caused no visible deterioration in the definition of the edges of the oil pools (Fig. III.8.3). However, when the second step in undercorrection was introduced, the field was covered by some haze which was visible to the eye but which is only slightly evident in the photomicrograph, Fig. III.8.4, since the haze was superimposed on a high-contrast image. If more complicated structures are imaged in low contrast, such haze can obscure some of the detail. The contrast of the very small areas which have been considered as inclusions increased relative to the contrast of the edges of the oil pools as the two successive stages of undercorrection were superimposed on the diffraction plate. In fact, the inclusions were more distinct in the image corresponding to Fig. III.8.4 than they were in any of the images corresponding to the phase photomicrographs included in Fig. III.7. With an additional small amount of undercorrection when the diffraction plate was in the objective, the boundaries of the oil pools appeared blurred because of the overlying haze although the inclusions were still clearly evident.

Since it is to be expected that the choice of compromise focus differs as the spherical aberration of the objective is altered or as the objective is used with or without a diffraction plate coating, it is difficult to predict from the theoretical spherical aberration curves for the objective what effective phase difference is introduced between the deviated and undeviated bundles of rays when an objective is either undercorrected or overcorrected and then used either with or without a diffraction plate coating. It cannot be stated with certainty here that superimposing upon the diffraction plate the spherical aberration due to undercorrection had the effect of decreasing the magnitude of the optical path difference

δ between the conjugate and complementary areas and that the increased contrast of the images of the inclusions was due to a decrease in $|\delta|$. The two stages of undercorrection affected the appearance of the bright-contrast images produced with plate $0.19A +0.25\lambda$ in a similar way except that the contrast of the inclusions was not so greatly enhanced as the objective was undercorrected.

The diffraction plate was removed from the objective and the objective was overcorrected first by an amount equivalent to an increase of 0.05 mm in the thickness of the cover glass (as measured from the thickness of the standard cover glass for which the objective was initially adjusted to obtain Fig. III.7) and then by an amount equivalent to an increase of 0.08 mm in thickness from that of the standard cover glass. Figures III.8.5 and III.8.6 were obtained.   The oil pools then appeared in dark contrast and the definition was good.   It is interesting to compare Fig. III.7.9.   When the diffraction plate designated by $0.15A -0.25\lambda$, N.A. 0.52–N.A. 0.36, was placed in the objective at these two stages of overcorrection, the images seen in Figs. III.8.7 and III.8.8 were formed.   The superposition of the first step in overcorrection caused the particles K to appear in bright contrast and out of focus when the edges of the oil pools appeared sharpest, although all the images appeared blurred.   Superposition of the next step in overcorrection caused a blue haze to obscure much of the detail.   The overcorrection produced similar deterioration of the bright-contrast images formed when the diffraction plate $0.19A+0.25\lambda$ was placed in the objective at the two stages of overcorrection.   This illustrates the fact that the choice of the proper cover-glass thickness as well as the avoidance of a thick layer of mounting material between the specimen and the cover glass can be important for good image formation with a dry phase objective of relatively high numerical aperture.   It also follows that the correct tube length is then of consequence.

6. THE PHASE VERTICAL-ILLUMINATION MICROSCOPE

The method of phase microscopy has been adapted to vertical-illumination or incident-light microscopes for observing specularly reflecting specimens (Jupnik, Osterberg, and Pride, 1946, 1948; Cuckow, 1947, 1949; Taylor, 1949; Benford and Seidenberg, 1950).   Figure III.9 illustrates the optical system used by Jupnik et al. (1948) in their experimental test of the applicability of the method.   A diaphragm, D, having an annular opening served as the entrance pupil of an optical system consisting of a field lens, the microscope objective, and the reflecting surface of the specimen.   The light source was imaged on diaphragm D by the condenser lens.   The field lens and the objective

formed an image, D_1, of the diaphragm below the specularly reflecting surface of the object specimen. The light was reflected by the surface of the specimen and passed through the objective again to form a real image, D_2, of the diaphragm. Image D_2 became the exit pupil and therefore the location of the diffraction plate. In one trial, the optical
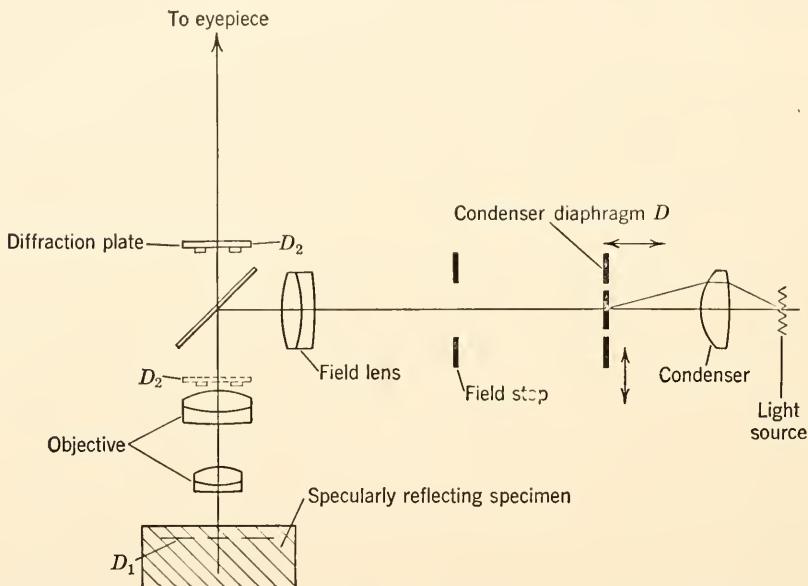
FIG. III.9. Optical system of the experimental phase contrast vertical-illumination microscope designed by Jupnik et al.

system was adjusted to form image D_2 below the beam splitter (broken lines), and in a second experiment image D_2 was formed above the beam splitter (solid lines). Locating the exit pupil between the beam splitter and the eyepiece, as in the second arrangement, minimized both the amount of stray light and losses of illumination. The diffraction plate for the phase vertical illuminator was a glass plate coated in the same way as the diffraction plate used in an objective for observing a transmitting specimen. Cuckow (1949) used a phase objective designed for transmission work to show that the phase vertical illuminator is a very useful tool in metallurgy. Taylor (1949) compressed the optical assembly consisting of the microscope objective lenses, the beam splitter, and the diffraction plate into the objective mount. The beam splitter was placed immediately above the lenses of the objective, and the image of the condenser diaphragm was formed on the diffraction plate located above the beam splitter.

Benford and Seidenberg (1950) introduced a projector system, analogous to the ordinary eyepiece of a microscope but better corrected for spherical and chromatic aberration, and mounted the diffraction plate at the conjugate aperture in the projector system. If the diaphragm is located at the aperture of the condenser system, an image of the diaphragm is formed at the exit pupil of the ocular of the microscope as well as at the back aperture of the objective. It has been shown (Osterberg, 1948a) that any one of the conjugate pupils which follows the entrance pupil of a phase microscope can serve as the location of the diffraction plate.

Whatever optical system is adopted, the surface of the specimen must be perpendicular to the optical axis of the microscope so that the image of the diaphragm is centered upon this optical axis when the condenser diaphragm has been centered. If the surface of the specimen diffuses the incident light completely, no image of diaphragm D is formed after the light passes through the objective the second time, and phase contrast cannot be obtained.

The phase vertical illuminator increases the contrast in the image of surface details which consist of elevations and depressions and which therefore give rise to small differences in optical path between rays reflected from neighboring areas at different heights on the surface of the specimen. If a well-polished, homogeneous specimen is being observed with the phase vertical illuminator and the diffraction plate is of the type $TA - 0.25\lambda$, a small elevation appears brighter than the surrounding area, and a depression, scratch, or hollow appears darker than the surrounding area, provided that the depression is not too deep. If the diffraction plate is of the type $TA + 0.25\lambda$, then a depression appears bright, and an elevation appears dark. When an image is to be observed in dark contrast, care must be taken that the optical path difference between the detail of interest and the surround is not too great. It should be noted that, since light is incident on the specimen and then reflected, the ray of light which is incident on the lower area travels through twice the optical path difference between the lower and higher regions before it re-enters the objective after reflection. Neighboring areas that introduce small differences in phase at reflection, areas that produce small optical path differences as a result of penetration and subsequent reflection of the incident light, and neighboring areas that show small differences in reflectivity or in absorption either with or without a small change in the relative phase also appear as areas of different brightness in the phase vertical-illumination microscope if the diffraction plate is suitably chosen.

In 1949 Cooke, Troughton and Simms, Ltd., began to supply phase

contrast accessories for their incident-illumination microscope. The phase objectives are a series of achromatic objectives which carry in the mount a beam splitter and a diffraction plate located above the
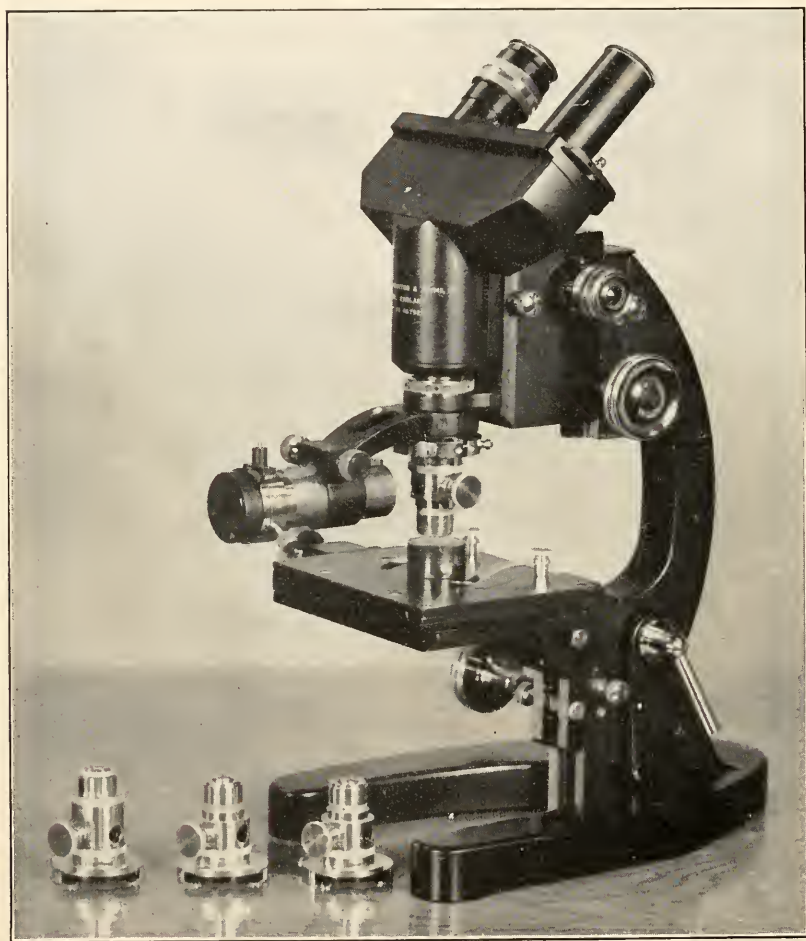
FIG. III.10. The phase contrast microscope available from Cooke, Troughton and Simms, Ltd., for vertical incident illumination. The aperture through which light is incident on the beam splitter is more easily seen in the mount of the objectives beside the stand. Courtesy of Cooke, Troughton and Simms, Ltd. (1949).

beam splitter (cf. Taylor, 1949) and which have been corrected for zero cover-glass thickness. The illuminator tube carries a single diaphragm with an annular aperture. Means are provided to move the condenser diaphragm in and out of action and to center it. The power

of the condensing lens system in the illuminator tube is variable, and the inner and outer diameters of the conjugate area of the diffraction plates contained in objectives of different power are made to a common ratio. Thus the correct match between the image of the condenser diaphragm and the conjugate area of the diffraction plate is produced by varying the magnification of the image of the single condenser diaphragm. Figure III.10 is a photograph of the Cooke, Troughton and Simms phase contrast incident-light microscope. This firm also
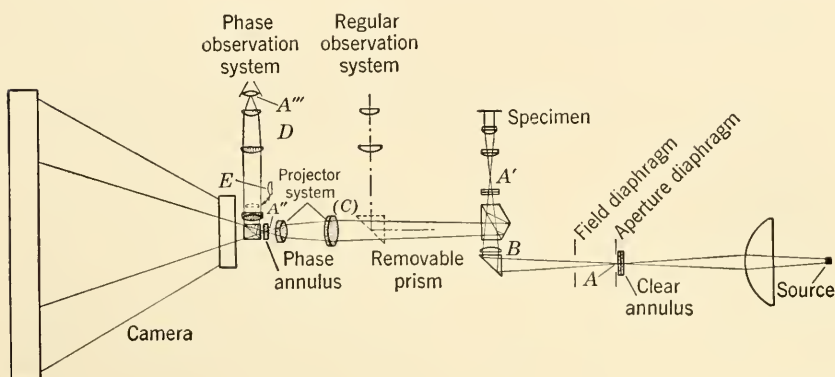
Fig. III.11. Layout of the Bausch and Lomb reflected-light microscope with phase contrast accessories. The phase accessories are shaded to differentiate them from the microscope proper. Courtesy of Bausch and Lomb Optical Co.

supplies (1949) phase contrast equipment for the Vickers projection microscope. The unit supporting the phase objective and the illuminator tube is attached to the instrument by means of a bayonet joint and is interchangeable with the universal illuminator. The phase objectives are achromatic objectives of a standard series of numerical apertures and powers and are adjusted for work with no cover glass at a tube length of 250 mm. Each objective is supplied with a beam splitter, a diffraction plate, and a magnetic centering mount.

The Bausch and Lomb Optical Co. has adopted the scheme reported by Benford and Seidenberg (1950). This system is illustrated in Fig. III.11. Advantage is taken of the fact that the size of the image of the condenser diaphragm (the clear annulus of Fig. III.11 is the condenser diaphragm) produced at the back focal plane of the objective remains substantially the same regardless of the focal length of the objective. The diffraction plate is placed at the exit pupil of the projector system. The same diffraction plate can be retained with the objectives of different power, and then only one condenser diaphragm is required. The

projector system is designed to minimize spherical and chromatic aberration in the plane of the exit pupil in which the diffraction plate is located. An ordinary ocular is not sufficiently well corrected to substitute for the projector system. A beam-splitting cube follows the projector system and diffraction plate. This cube allows a phase contrast image to be transmitted to the camera and also provides a reflected image for visual observation with an ordinary microscope eyepiece.

7. PHASE MICROSCOPY WITH ULTRAVIOLET AND INFRARED ILLUMINATION

In recent years there has been much interest in designing microscope and condenser systems for use with ultraviolet and infrared illumination. Such optical systems may include either refracting or reflecting components or both. The resolution of a given objective increases as the wavelength of illumination decreases. In addition to higher resolution, a further advantage may be gained with ultraviolet microscopy because many substances that are transparent to visible light absorb ultraviolet wavelengths selectively. The fact that many substances absorb infrared light selectively also makes infrared microscopy valuable. When small optical path differences and small amounts of absorption are present in the object specimen, a phase objective can increase the contrast in the image. However, determination of the absorption ratio between two parts of an object specimen, which in the general case contains both absorption and optical path differences, is a complicated procedure that requires a system of variable phase microscopy (Osterberg and Pride, 1950).

Bennett, Woernley, and Kavanagh (1948) have reported some initial work with an ultraviolet phase microscope. The light forming the image of the specimen passes through the diffraction plate. If the diffraction plate is of the transmission type, the same general design considerations hold as for visible illumination except that the high absorption of ultraviolet radiation by many materials may impose an additional limitation. If reflecting optics are contained in the objective, one of the reflecting surfaces can be altered to form a reflection type diffraction coating. If a coating is applied over part of the reflecting surface to form an abrupt step, then light reflected from the step and that reflected from the adjacent area travel through different lengths of path and a phase difference is introduced between such rays of light. The reflectivity of the step can be made different from that of the adjacent area, for example, by depositing coatings of different materials on the two regions, so that any ratio of the light energy reflected from the step to that reflected by the adjacent area can be obtained.

8. FRANÇON'S SYSTEM FOR PHASE MICROSCOPY

Françon (1950) devised a means for applying the method of phase microscopy without modifying the optical elements of the ordinary microscope. An intermediate image that is stigmatic and aplanatic is formed at unit magnification between the object specimen and the microscope objective. The optical assembly that forms the intermediate image contains the diffraction plate or its equivalent, and the ordinary microscope produces a magnified image of the intermediate
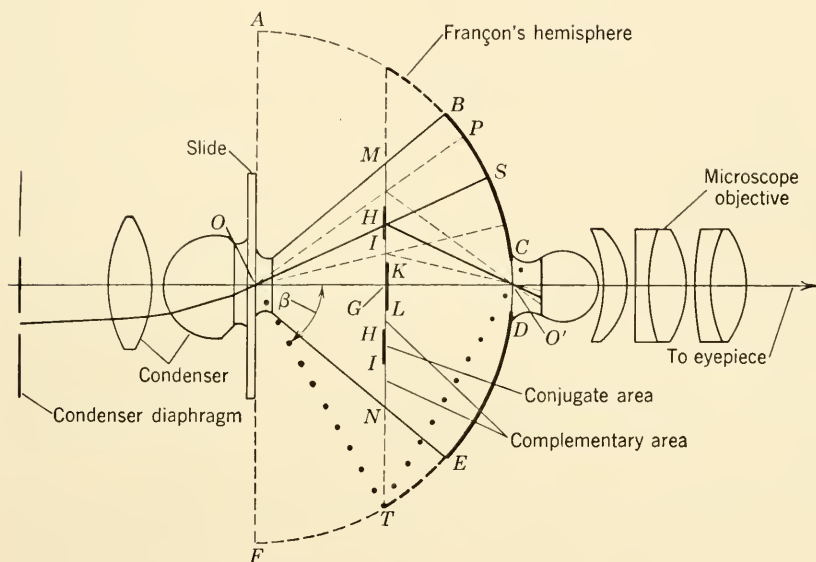
FIG. III.12. Schematic drawing of Françon's hemisphere for producing a phase contrast image.

phase contrast image. The numerical aperture of the microscope objective may be as high as 1.30.

The device proposed by Françon is placed between the specimen and the microscope objective. Figure III.12 illustrates this device and the manner in which the phase contrast image is formed. In Fig. III.12, BCDE represents the surface of a segment of a glass hemisphere cut into two parts along the plane MGN parallel to the base AOF of the hemisphere so that the distance OG is equal to one-half the radius of curvature of the hemisphere. O is the center of curvature of the hemisphere. The two surfaces which result from the cut along MGN are polished. The central circular area KL of the surface at MGN of the upper part of the hemisphere is opaque. A dielectric film having a

relatively high reflectivity is also applied over the upper face along
MGN. Françon used a film of titanium dioxide formed by means of
an evaporation process. The diffraction plate or its equivalent is placed
on the highly reflecting film and is centered on the optical axis of the
condenser-hemisphere-microscope system.

The conjugate area of the diffraction plate may have the shape of
either a disk or an annulus. The diffraction plate may be constructed
by any of the known procedures, such as evaporating a suitable com-
bination of metallic and dielectric films, cementing films of plastic or
gelatin at the interface MGN, or using polarizing or birefringent materials
or both as in systems of variable phase microscopy. In Fig. III.12
the conjugate area is designated by the letters III. After the dif-
fraction plate has been added, the two parts of the hemisphere are re-
combined. The hemispherical surface, or whatever portion of a
hemispherical surface is required, is silvered except over the small
circular aperture CD centered on the optical axis of the system. The
specimen is adjacent to the plane AOF and is centered at O. In order
to permit the use of a standard microscope preparation with a cover
glass 0.17 mm thick, the thickness of the lower part of the glass hemi-
sphere is reduced by 0.17 mm. For greater ease in moving the specimen
slide into the correct position and to prevent scratching, it is preferable
further to reduce the thickness of the lower part of the hemisphere by
0.1 or 0.2 mm and to use a film of oil between the slide and the hemi-
sphere, regardless of the numerical aperture of the microscope objective.
The cover glass and the oil film then complete the hemisphere.

In Fig. III.12 a ray of light emerging from the opening in the con-
denser diaphragm is incident on the specimen at the point O, the center
of curvature of the hemisphere. Part of the light is deviated by the
object specimen. The broken lines represent rays associated with the
light deviated by the specimen, and the solid line within the hemisphere
designates the ray associated with that part of the light which is not
deviated by the specimen. Consider the deviated ray OP. This ray
is partially reflected and partially transmitted (ideally, half the light
energy is transmitted) at the dielectric film applied over the face at
MGN. The reflected part of the light does not enter the microscope
objective. The transmitted portion incident at P is reflected by the
silvered surface back on itself to the interface MGN, and partial re-
flection again occurs at the highly reflecting dielectric film. The ray
arising from this last reflection passes through the opening designated
by CD. In the same way, the other rays which represent the deviated
light waves originating at O emerge through the aperture CD and inter-
sect at a point O'. Similarly, a part of the undeviated ray which passes

through O also crosses the point O' as it leaves the hemisphere. There-
fore O' is the image of O. Since the point O is at the center of curvature
of a spherical reflecting surface, the image at O' has a magnification
equal to unity, is free from both chromatic and spherical aberration,
and is free from coma. Although the object specimen is small, it has
some extent and therefore a small amount of astigmatism is present in
the image of a specimen centered at O. Françon has shown that with
a microscope objective of a given numerical aperture the proper selection
of the radius of curvature of the hemisphere can limit the astigmatism
to a tolerable amount.

From Fig. III.12 it can also be seen that either the deviated or the
undeviated rays which make a very small angle with the optical axis
would strike the non-metallized aperture CD of the hemisphere and
would, except for the small fraction reflected at the glass-air surface,
pass directly through the hemisphere. Such rays would not travel the
same length of optical path as do the rays making a greater angle with
the optical axis and would not be brought to a focus at O'. The opaque
region KL prevents any deviated or undeviated ray from passing
directly through the aperture CD without first being reflected by the
hemispherical surface. Therefore, because of the presence of the opaque
area KL, the deviated and undeviated rays travel equal lengths of
path in Françon's hemisphere except for the difference deliberately in-
troduced by means of the diffraction plate. Since the field of the micro-
scope system has some extent about O, the diameter of the area KL
should be at least equal to the diameter of the aperture CD. The
maximum angle of inclination β which a deviated ray that enters the
microscope objective can make with the optical axis of any hemisphere
in this arrangement is 60°. The dotted line OT in Fig. III.12 shows this
deviated ray. The largest section of a hemisphere required for this
device is delimited by the rays deviated 60° from the optical axis. If
the hemispherical section is made of glass with a refractive index of 1.52,
the numerical aperture of this intermediate image-forming system can
be made as great as 1.52 sin 60°, or approximately 1.32. This is suf-
ficient numerical aperture for almost all oil immersion objectives. In
Fig. III.12 the microscope objective is represented as being immersed.

Figure III.13 shows two methods of imaging the opening in the con-
denser diaphragm on the conjugate area of the diffraction plate. The
substage condenser is not shown. A illustrates the design common in
phase microscopy in which the condenser diaphragm is at the first focal
plane of the substage condenser. Any two rays that intersect at a point
in the plane of the condenser diaphragm emerge from the substage con-
denser as parallel rays. Such parallel rays which are not deviated by

the object specimen and which are partially transmitted by the highly
reflecting dielectric film at MGN form an image of the opening in the
condenser diaphragm on the conjugate area of the diffraction plate
after they have been reflected by the silvered portion of the surface
$BCDE$ since the diffraction plate is located at the focal plane of the
hemispherical section. These rays are again partially reflected at the
interface MGN and form a divergent bundle of light which passes
through the aperture CD. Thus the light which comes from a point in
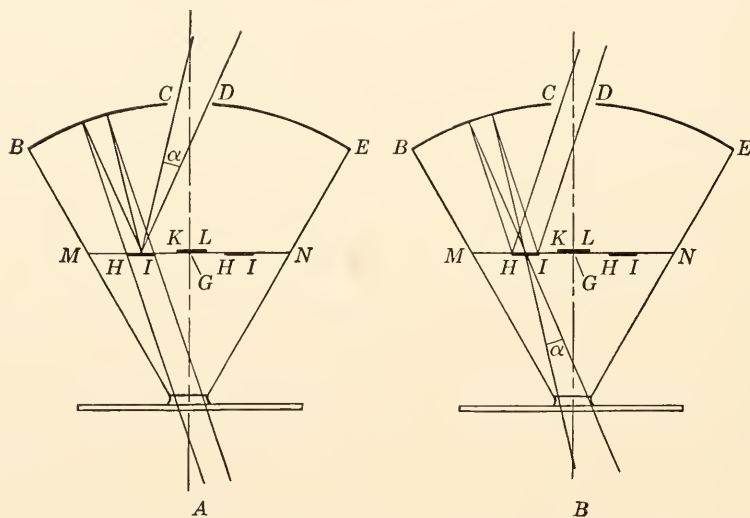
Fig. III.13. Formation of the image of the opening in the condenser diaphragm
on the conjugate area in Françon's hemisphere. A. The undeviated rays which enter
the hemisphere are parallel. B. The undeviated rays which enter the hemisphere
converge directly on HI.

the opening in the condenser diaphragm and which is not deviated by
the object specimen spreads over the field at CD and interferes with the
deviated light to form an image of the object specimen.

The substage condenser and the diaphragm can also be so arranged
that an image of the opening in the condenser diaphragm is formed
directly on the conjugate area of the diffraction plate as is shown in B.
The rays then diverge from the conjugate area until they strike the
silvered portion of the hemispherical surface and are reflected as a
bundle of parallel rays. After partial reflection at the interface MGN,
the parallel rays emerge from the aperture CD. The undeviated light
spreads over the image plane at CD and interferes with the deviated
rays to form an image of the object specimen. This bundle of parallel,

undeviated rays also forms a second image of the condenser diaphragm at the back focal plane of the microscope objective.

Either method of producing the image of the condenser diaphragm introduces some aberration in the rays passing through CD, but, since in practice the angle α is small, this aberration should not be troublesome. The presence of spherical aberration in the microscope objective will affect the quality of the final, magnified phase contrast image in the same way as if the diffraction plate were contained in the objective. If the microscope objective has been corrected for a cover glass 0.17 mm thick, then it is necessary to place a cover glass 0.17 mm thick, or its equivalent, over the image at O'. Françon found that a more practical solution was to form the image of O ⅓ mm above the aperture CD by displacing the interface MGN slightly toward the top of the hemisphere and then to cement over CD a planoconcave lens ½ mm thick (0.33 mm + 0.17 mm) and having the same radius of curvature as the hemisphere.

The device described by Françon can be expected to have several advantages. The image of the condenser diaphragm will be formed with less curvature of field in the plane of the diffraction plate within the hemisphere than within a microscope objective of short focal length. It will be easier to avoid parallax between the image of the opening in the condenser diaphragm and the conjugate area of the diffraction plate. The relatively intense undeviated beam that is present with most transparent specimens is weakened within the hemisphere, and there should be less loss of contrast produced by the scattering of light from the direct beam within the microscope. Françon's device is an example of the application of the multipupil principle to facilitate the practice of phase microscopy.

9. SYSTEMS OF VARIABLE PHASE MICROSCOPY

Throughout this section and its subdivisions the term phase difference will refer to the optical path or phase difference δ between the conjugate and complementary area of the diffraction plate or its equivalent, and the term amplitude ratio will refer to the ratio h of the amplitude transmission of the conjugate area to the amplitude transmission of the complementary area of the diffraction plate or its equivalent. The purpose of variable phase microscopy is to obtain continuous variation in the phase difference or in the amplitude ratio or in both. Although limited ranges of variation are useful, greatest flexibility is achieved when the phase difference is continuously variable from zero to 1 wavelength and when the amplitude ratio can be varied continuously from zero to infinity. When such a range of variation is available, it becomes

possible to adjust the microscope for optimum bright or dark contrast for a wide variety of object specimens. An important advantage of the continuously variable phase microscope is that quantitative information about the area and the optical properties of the particle can frequently be deduced from the h and δ setting required for producing optimum bright or dark contrast (Osterberg and Pride, 1950).

9.1. Polanret methods for phase microscopy

One of the methods for obtaining variable phase microscopy consists in replacing the diffraction plate by suitably chosen polarizing, analyzing, and birefringent retarding elements. This general method can be executed in a large number of ways. It is called, for brevity, the polanret method or polanret microscopy. Polanret methods can become simple both in principle and in practice when it suffices to vary either the phase difference only or the amplitude ratio only. However, when it is required that both the phase difference and the amplitude ratio be continuously and independently variable, a polanret system of high optical quality can become difficult to achieve with existing objective designs and with materials now available.

In one class of polanret systems the light passing through the conjugate area and that passing through the complementary area are polarized with different directions of vibration, preferably at right angles. This can be accomplished by replacing the diffraction plate by two zonal polarizers of high optical quality. One of these covers the conjugate area and the other covers the complementary area. After passing through the zonal polarizers, the deviated and undeviated bundles of rays remain separated physically because of their different directions of polarization until components of the deviated and undeviated bundles are subsequently brought into a common direction of vibration by passing the deviated and undeviated light through an analyzer. An important consequence of introducing zonal polarizers is that the phase difference and the amplitude ratio can be altered by the interaction of other polarizers and birefringent elements which do not have to be located adjacent to the zonal polarizers, that is, near the conjugate and complementary areas.

If only the zonal polarizers and the analyzer are included in the optical system, a continuously variable amplitude ratio is obtained. The amplitude ratio is varied by rotating the analyzer relative to the zonal polarizers, and the numerical value of the amplitude ratio is easily calculated from the angle of rotation of the analyzer. The amplitude ratio can assume practically any value from zero to infinity because the analyzer may be set, in the limiting cases, to block either the un-

deviated or the deviated bundles of rays.   Fixed phase differences may
be included by adding the correct thickness of a dielectric material over
the required area.   Polanret systems of this type are both relatively
simple in principle and relatively easy to construct with resultant good
optical performance.   A fixed phase difference may also be obtained by
placing a birefringent plate between the zonal polarizers and the
analyzer.   The fast or slow direction of vibration of the electric vector
in the birefringent plate should be parallel either to the direction of
vibration of the electric vector which emerges from the conjugate area
or to the direction of vibration of the electric vector which emerges from
the complementary area.

In order to obtain variable phase difference, a direct procedure, for
example, is to replace the plate with fixed birefringence by a variable
birefringent plate such as the Babinet-Soleil compensator or by a plate
the birefringence of which is varied electro-optically.   Although in-
corporating elements with variable birefringence into a polanret system
is sound in principle, such components form a cumbersome optical unit,
and several objections arise.   In these more direct methods of attack,
the amplitude ratio is altered preferably by rotating a polarizer which
is located either below or above the object specimen according as it is
desired that the specimen shall be illuminated by polarized or un-
polarized light.

9.2. A highly flexible polanret system

The polanret system illustrated in Fig. III.14 is capable of varying the
amplitude ratio and the phase difference continuously and independently
throughout the complete ranges of values that are of interest in phase
microscopy.   This method has been described by Osterberg (1947).
The phase variation is obtained by an indirect method which includes
simple optical components and which was discussed in an earlier paper
(Osterberg, 1946).

The conventional diffraction plate is replaced by the micoid disk.
This disk together with the rotatable analyzer and polarizer constitute
the essential elements of the polanret system.   The polarizer may be
located anywhere between the micoid disk and the source of light.   The
analyzer may be placed anywhere between the micoid disk and the eye
or viewing device.   Since lenses produce elliptical polarization, the
analyzer and the polarizer preferably are located adjacent to the micoid
disk, but in the usual phase microscope these locations are awkward for
mechanical reasons.   The micoid disk is composed of two zonal polarizers
which transmit electrical vibrations along the directions E_1 and E_2 over
the conjugate and complementary areas, respectively, and of a quarter-

wave retarding plate, the X direction of which is set at 45° with respect
to E_1 and E_2. X is the direction of vibration of the slow ray in the
quarter-wave plate. As explained by Osterberg (1947), the X direction
is the natural line of reference for measuring the angle θ of rotation of
the polarizer. θ is the angle between the X direction and the direction
of the electric vector transmitted by the polarizer. θ is positive in
the clockwise direction with respect to the observer as he looks into
the microscope. The light passes through the quarter-wave plate
before entering the zonal polarizers. Rotating the polarizer through
the angle θ serves only to introduce a phase difference $\delta = 2\theta$ between
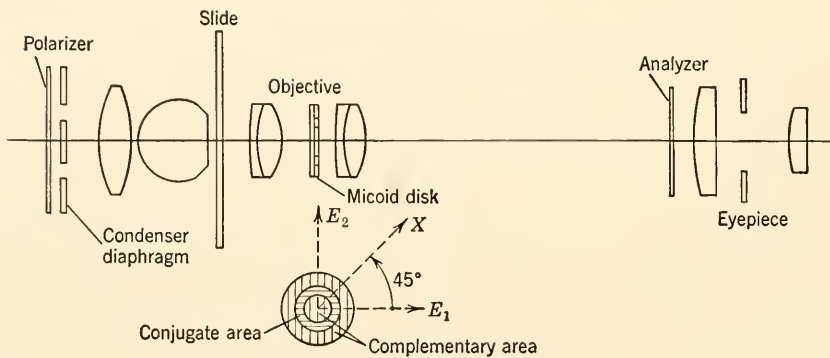
Fig. III.14.   A polanret system which permits the amplitude ratio h and the phase
difference δ to be varied continuously and independently.

the undeviated and deviated rays. It suffices to limit θ to the range
$-\pi/2 \leqq 0 \leqq \pi/2$. Let α denote the angle between E_2 and the direc-
tion of the electric vector transmitted by the analyzer. Rotation of
the analyzer varies only the amplitude ratio h between the undeviated
and deviated rays such that $h^2 = T = \tan^2 \alpha$. In principle, therefore,
the phase difference can be varied from $-\pi$ to π (one complete wave-
length) and the amplitude ratio can be varied from zero to infinity.

The zonal polarizers preferably are made of thin polarizing film of
high optical quality, but they may be constructed of left- and right-
handed elements of quartz which rotate the plane of polarization 45°.
The zonal polarizers can also be constructed of two half-wave retarding
plates. Thin polarizing films are preferred because they give rise to
fewer complications from troublesome phenomena due to birefringence
and because the polarizer may be omitted whenever it is unnecessary
to vary the phase difference, provided that the zonal polarizers are
polarizing sheets. On the other hand, thin polarizing films are difficult

to handle at present even when the Vectograph method is applied to making the zonal polarizer.

The polanret system illustrated by Fig. III.14 has been successfully incorporated into microscope objectives with relatively long focal length and low numerical aperture. Only moderate difficulties are encountered in objectives of 25-mm focal length, N.A. 0.17, and of 16-mm focal length, N.A. 0.25. Considerable development work will be required in adapting the method to oil immersion objectives. A practical solution may very well utilize the multipupil principle (Osterberg, 1948*a*) and, in particular, the multipupil system described by Françon (1950). (See also Section 8.)
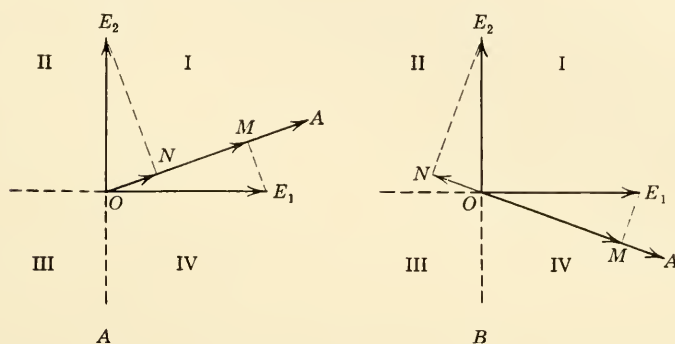
Fig. III.15. The neutral and anti-neutral quadrants. *A* denotes the transmission direction of the analyzer. E_1 and E_2 denote the positive direction of vibration of the undeviated and deviated waves respectively as these emerge from the micoid disk. The neutral quadrant is I or III. The anti-neutral quadrant is II or IV.

9.3. Neutral and anti-neutral quadrants in polanret systems

Polanret systems possess an important and advantageous peculiarity in that the phase difference between the undeviated and deviated waves undergoes a sudden jump of $\frac{1}{2}$ wavelength as the transmission direction of the analyzer is rotated out of the neutral quadrant. This phenomenon will be explained for the case in which the conjugate and complementary areas are polarized at right angles.

In Fig. III.15 let E_1 and E_2 be the positive directions of the electric vectors as they emerge from the conjugate and complementary areas, respectively. If the transmission direction A of the analyzer lies between E_1 and E_2 as in Fig. III.15*A*, the projections OM and ON of E_1 and E_2 upon A point along the A direction. In other words, the directions of the electric vectors which result from the interaction of E_1 and E_2 with the analyzer are alike. If the transmission direction A of the

analyzer falls outside the quadrant between E_1 and E_2, as in Fig. III.15B, the projections OM and ON upon A are opposite in direction, and it may be said that the directions of the electric vectors resulting from the interaction of E_1 and E_2 with the analyzer are now anti-parallel. The effect of rotating A out of the neutral quadrant between E_1 and E_2 is therefore to produce an apparent discontinuous phase change of $\frac{1}{2}$ wavelength between the undeviated and deviated waves which emerge from the conjugate and complementary areas. If the construction of Fig. III.15 is repeated for opposite quadrants, it can be verified that opposite quadrants are equivalent. Thus the neutral quadrants are I and III, and the anti-neutral quadrants are II and IV.

It is helpful to indicate the neutral quadrant on the scale of the analyzer. The neutral quadrant can be determined from a knowledge of the construction of the optical system, but it is usually easier to establish the location of the neutral quadrant by any one of several simple experimental procedures. First, the location of the four quadrants can be ascertained by removing the eyepiece and by rotating the analyzer to the angle of extinction of the light emerging from the conjugate area. Suppose, for example, that the observer has a slide containing non-absorbing particles, the optical path of which exceeds that of the surround by a small fraction of a wavelength. It is known that such particles appear in bright contrast with a $TA+0.25\lambda$ diffraction plate and in dark contrast with a $TA-0.25\lambda$ diffraction plate. Let the polanret system be of the type described in Section 9.2 and let θ be set at $+45°$ so that $\delta = 2\theta = +90°$ or $+\lambda/4$. When the microscope is focused on the particles, these particles appear brightest when the analyzer is rotated in the neutral quadrant and darkest when the analyzer is rotated in the anti-neutral quadrant. As a check for consistency, the experiment should be repeated with θ selected at $-45°$. The particles should then appear brightest or darkest according as the analyzer is rotated in the anti-neutral or neutral quadrants. The above procedure is applicable even when the quarter-wave plate has been omitted from the micoid disk and when a fixed phase difference of $\delta = \pm\lambda/4$ has been introduced between the conjugate and complementary areas by any one of the several possible methods. When the phase difference between the conjugate and complementary areas has been fixed at zero or $\frac{1}{2}$ wavelength, a suitable object specimen is a silvered slide containing pinholes. If $\delta = 0$ and if the objective is well corrected for spherical aberration, the center of the Airy disk in the sharply focused diffraction image of a small pinhole will appear brightest or darkest according as the analyzer is rotated in the neutral or anti-neutral quadrant. This situation is reversed when $\delta = \lambda/2$.

9.4. Polanret systems having continuously variable amplitude ratios

Systems of variable phase microscopy in which the amplitude ratio h is variable but the value of the phase difference remains fixed, for example $\delta = \lambda/4$, are likely to become important because of their utility and feasibility. Experience has shown that it is more important to be able to vary the amplitude ratio than the phase difference.

One class of systems is obtained by omitting the quarter-wave plate from the micoid disk shown in Fig. III.14. The undeviated and deviated waves which emerge from the conjugate and complementary areas are polarized at right angles. Consequently, the amplitude ratio h may be varied by rotating the analyzer. If the zonal polarizers of the micoid disk are formed of polarizing sheets, the uniform polarizer can be omitted. This polarizer is necessary, however, when the zonal polarizers consist of two left- and right-handed elements of quartz which rotate the plane of polarization 45° or when the zonal polarizers consist of two suitably oriented half-wave retarding plates. The fixed phase difference δ can be obtained by making one of the zonal polarizers slightly thicker than the other or by depositing a material such as magnesium fluoride upon one of the zonal polarizers or upon the conjugate or complementary area of one of the plates between which the zonal polarizers are cemented.

Suppose that $\delta = +\lambda/4$ so that the greater optical path belongs to the conjugate area. If the analyzer is rotated in the neutral quadrant, the equivalent of an infinite, continuous series of $TA+\lambda/4$ or $TB+\lambda/4$ diffraction plates is obtained. On the other hand, the equivalent of a continuous set of $TA-\lambda/4$ and $TB-\lambda/4$ diffraction plates is obtained by rotating the analyzer in the anti-neutral quadrant. T is continuously variable since $T = h^2$ and since h can be varied practically from zero to infinity. The limits zero and infinity will not be reached because perfectly polarizing materials do not exist. More generally, if the phase difference between the undeviated and deviated waves is δ_1 when these waves emerge from the zonal polarizers, the apparent phase difference between them is δ_1 when the analyzer is rotated in the neutral quadrant and is $\delta_1 \pm \lambda/2$ when the analyzer is rotated in the anti-neutral quadrant. The values $\delta_1 + \lambda/2$ and $\delta_1 - \lambda/2$ are equivalent in the practice of phase microscopy.

A method belonging to this class of polanret systems was discovered independently and described by Taylor (1947). In Taylor's system the zonal polarizers consist of left- and right-handed elements of quartz which rotate the plane of polarization 45°. The light incident upon the zonal polarizers was polarized linearly. A fixed phase difference of

$\delta = \lambda/4$ was introduced at the conjugate and complementary areas by means of an auxiliary diffraction plate. Phase differences of $\pm\lambda/4$ were thus obtained between the undeviated and deviated waves according as the analyzer was rotated in the neutral or anti-neutral quadrant. It is especially noteworthy that Taylor's objective was only 4 mm in focal length and produced excellent definition and contrast as demonstrated by the reproductions of his photomicrographs of the epithelial cell.

Kastler and Montarnal (1948) have described a scheme which uses half-wave retarding plates as zonal polarizers. The micoid disk in Fig. III.14 was constructed of two half-wave plates. One plate covered the conjugate area. The second plate covered the complementary area. The optical axis in the conjugate area was fixed at 45° with respect to the optical axis in the complementary area. If, in such a system, the transmission direction of the polarizer is parallel to the optical axis in the conjugate area, the electric vector of the light that emerges from the conjugate area vibrates along the direction of transmission of the polarizer whereas the electric vector that emerges from the complementary area vibrates at right angles to the direction of transmission of the polarizer. Therefore the amplitude ratio can be varied by rotating the analyzer in either the neutral or the anti-neutral quadrant. Variable amplitude ratios with a fixed phase difference δ can be obtained by depositing dielectric material upon the conjugate or complementary area or by choosing two half-wave plates with different optical path. If the half-wave plates are sheets of cellophane, it is possible to obtain half-wave plates of different optical thickness. As an alternative, the half-wave plates may be made of different crystalline materials, and the required phase difference may be obtained by a suitable choice of cement for retaining the half-wave plates between protecting plates of glass.

A simple method of adapting the half-wave plate has been described by Locquin (1948). Locquin omitted the half-wave plate over the complementary area and suggested that the half-wave plate covering the conjugate area be cemented between glass plates with a cement which produces the wanted phase difference. If, in such a scheme, the transmission direction of the polarizer is set at 45° with respect to the optical axis of the half-wave plate, the electric vector that emerges from the complementary area vibrates along the direction of transmission of the polarizer whereas the electric vector that emerges from the conjugate area vibrates at right angles to the direction of transmission of the polarizer. The amplitude ratio is varied by rotating the analyzer in the neutral or anti-neutral quadrant. Locquin emphasized that an advantage gained by his modification of the half-wave plate arrangement is that

auxiliary surfaces in the path of deviated rays are thus avoided. It is pointed out, however, that in the usual microscope a large number of surfaces lie in the path of the undeviated and deviated rays. The optical problem of polanret microscopy consists primarily of selecting and locating polarizing, analyzing, and retarding elements so that they produce the least possible injury to definition. A second important problem is to achieve polanret microscopy in spite of the elliptical polarization introduced by the lenses. An important advantage of Locquin's system is that the polarizer need not be rotated. Consequently, the polarizer can be cemented into the micoid disk which contains the half-wave plate. The light incident upon the half-wave plate is then linearly polarized in spite of the elliptical polarization introduced by the lenses. The polarizer may be included in the micoid disk also in the arrangements proposed by Taylor and by Kastler and Montarnal.

It has been pointed out with respect to the method by Osterberg that the quarter-wave plate in the micoid disk may be omitted together with the polarizer when only variations in the amplitude ratio are required. So doing results in the advantage that the zonal polarizers, if made of polarizing film, polarize the conjugate and complementary areas linearly or almost linearly for a relatively wide variation of the angle of incidence of the rays upon the micoid disk and for wide variations in the wavelength of the incident light. These are important properties of polarizing film which do not apply to the birefringent properties of retarding plates or to the rotatory properties of a quartz plate.

In another class of polanret systems for obtaining variable amplitude ratios with a fixed phase difference or with highly restricted variations in the phase difference, both the conjugate and the complementary area are not polarized linearly. A unique system of this class has been described briefly by Hartley (1947). In Hartley's method the micoid disk in Fig. III.14 consists of two quarter-wave birefringent elements. One of these covers the conjugate area; the other covers the complementary area. The direction of vibration of the fast ray in the conjugate area is fixed at 45° with respect to the direction of vibration of the fast ray in the complementary area. As in Fig. III.14, a substage polarizer and an analyzer complete the system. Suppose that the transmission direction of the polarizer is made parallel to the direction of vibration of the fast ray in the conjugate area. Then linearly polarized light emerges from the conjugate area whereas circularly polarized light emerges from the complementary area. Rotation of the analyzer varies the transmitted component of the undeviated light only such that the

amplitude ratio h falls in the range $0 \leqq h \leqq 1.0$.   In a similar manner, amplitude ratios in the range $1 \leqq h \leqq \infty$ are obtained by rotating the analyzer when the transmission direction of the polarizer is set parallel to the direction of vibration of the fast ray in the complementary area. If only the equivalent of A-type or B-type diffraction plates is wanted, it is advantageous to cement the polarizer into the assembly of the micoid disk.

A great number of polanret systems are possible, and several systems have already been suggested.   At the present time, polanret systems capable of varying both the amplitude ratio h and the phase difference δ can be successfully included in the standard microscope for objectives of relatively long focal length and of low numerical aperture.   Polanret systems which vary the amplitude ratio at fixed values of the phase difference present a less difficult optical problem and can be extended to objectives of shorter focal length and of higher numerical aperture. Multipupil systems afford an additional approach for introducing polanret devices into the microscope.

9.5. Application of Brewster's angle phenomenon to variable transmission phase microscopy

If ordinary light is incident on a dielectric so that the angle of incidence is equal to Brewster's angle, the light reflected by the dielectric is linearly polarized.   A fraction of only that component of the incident light which is vibrating perpendicular to the plane of incidence is reflected.   Therefore, if linearly polarized light is incident on the dielectric at Brewster's angle, then the amount of light reflected by the dielectric can be varied by rotating the plane of vibration of the incident light.   No light is reflected if the incident polarized light vibrates parallel to the plane of incidence, and the amount of reflected light is maximum when the incident light vibrates perpendicular to the plane of incidence.   Françon and Nomarski (1950a and 1950b) have applied this principle to vary the amount of light passing from the conjugate area of the diffraction plate into the rest of the microscope system.   Linearly polarized light illuminates the specimen, and the undeviated light is incident on the conjugate area of the diffraction plate at Brewster's angle.   Means are provided to rotate the plane of vibration of the light falling on the diffraction plate (for example, by rotating the polarizer placed in the light beam).   The diffraction plate designed to take advantage of this polarization phenomenon may reflect the light that forms the phase contrast image into the remainder of the optical system (Françon and Nomarski, 1950b), or it may be a transmission diffraction plate incorporated into Françon's hemispherical multipupil system for

producing a phase contrast image (Françon and Nomarski, 1950a). (See also Section 8 for a description of Françon's phase contrast system.)

9.6. Variable color-amplitude phase microscopy

Barer (1950) has suggested a modification of a system of variable phase microscopy in order to introduce color differences between the deviated and the undeviated light. The proposal is to replace the polarizer or analyzer with a type of dichroic filter or combination of such filters. A property of such a dichroic filter is that the spectral transmission varies with the plane of polarization of the light passing through it. For example, a combination of filters may be constructed such that if a polarizing element is also in the path of light, a band of wavelengths that appears green is transmitted with one orientation of the polarizer; but, if the polarizer is rotated 90°, the band of wavelengths appears red. For a given orientation of the polarizer with respect to the filter, the color of the transmitted light is the same whether the light is incident first on the polarizer or first on the filter. Therefore, if the diffraction plate contains zonal polarizers made of polarizing film oriented at 90° and if the filter described in the example is placed in front of the light source, the filter can be adjusted by rotation with respect to the zonal polarizers so that the light emerging from the conjugate area of the diffraction plate is red and the light emerging from the complementary area is green. A rotation of the filter through 90° causes a reversal in color between the two bands of wavelengths transmitted through the conjugate and complementary areas. The formation of a phase contrast image depends on the overlapping of wavelengths within the two bands of color. If light of the same wavelength is present in the bands emerging from the conjugate and complementary areas, then the deviated and the undeviated light of the wavelength interferes, as in the standard phase microscope, to form an image that is colored (bright contrast) or black (dark contrast). The remainder of the light from the complementary area, composed of wavelengths which cannot interfere with light from the conjugate area, superimposes an image that is colored and is analogous to the image formed with darkfield illumination. The remainder of the colored light from the conjugate area is spread over the field of the eyepiece. Similarly, if such a combination of dichroic filters replaces the analyzer instead of the polarizer, the polarized light emerging from the zonal polarizers is incident on the filter, and again rotation of the filter changes the composition of the band of wavelengths transmitted to the eyepiece by the filter from the conjugate and complementary areas.

THE TECHNICS OF
PHASE MICROSCOPY

The phase microscope utilizes absorption and optical path differences for the control of the contrast visible in the image. Increase or decrease of contrast, or reversal of bright and dark elements with increased or decreased contrast, facilitates the work of the microscopist. Phase microscopy is most valuable for specimens too transparent for effective examination with other types of microscopy. When the specimen detail consists of small differences in optical path due to variations in refractive index and thickness, regions of absorption, or both, the phase microscope should be used. Such specimens may be unstained living cells and tissues, suspensions and emulsions, glass, plastics, minerals, poorly stained or slightly pigmented objects, and similar materials. The phase microscope is used also in the orientation and preparation of specimens to be examined with the electron microscope.

When the image is brighter or lighter than its surround (Fig. IV.1C) it is described by the term bright contrast; dark contrast (Fig. IV.1D) designates a specimen darker than its surround. When the optical path of the specimen is greater than that of its surround the $A+$ diffraction plate will give bright contrast and the $A-$ and $B-$ diffraction plates dark contrast. When the surround has the greater optical path the specimen will show in dark contrast with the $A+$ and in bright contrast with the $A-$ diffraction plates. The contrast can be determined by focusing in the same direction slowly through the specimen. When the contrast is bright above the specimen, dark when in exact focus, and then bright on continued focusing, dark contrast is being observed. Likewise when the focus is dark as the specimen is approached, bright at exact focus, and then dark, the contrast is called bright.

Bright contrast is preferred, in general, for counting, for the study of motion, for very small specimens, for stereophotomicrography, and with optical staining. Dark contrast is preferred for measurement, for specimens to be compared with stained material from other methods, and for enhanced contrast with absorbing specimens. When appropriate the $B-$ dark contrast is useful for measurement. The Eberhard

effect in developing increases the contrast of the specimen edge and halo with dark contrast which aids measurement, although the same numerical results are obtained with both contrasts. With some specimens the same detail is shown with both contrasts and the choice becomes purely a matter of personal preference. Other specimens reveal detail with
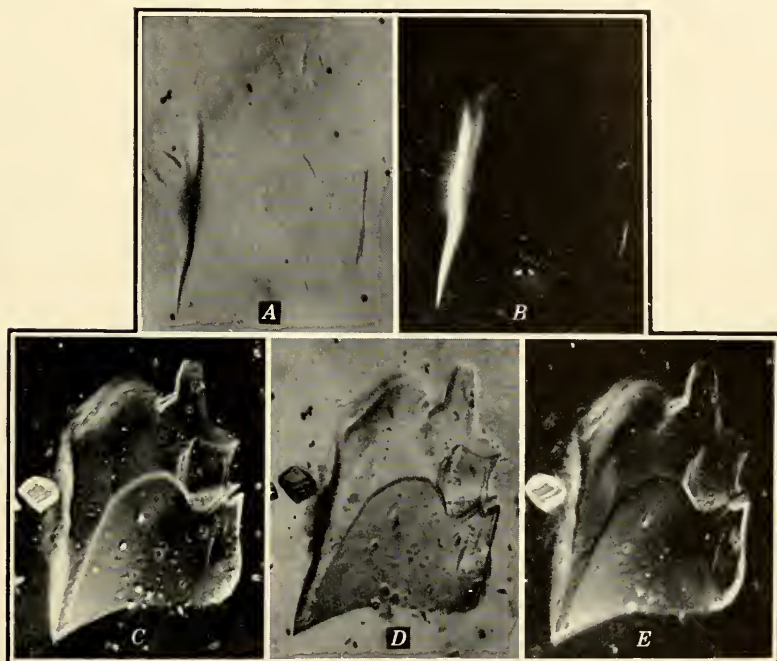
FIG. IV.1. Glass fragment mounted in balsam, 150×. (Refractive indices 1.52 and 1.54.) A, brightfield. B, darkfield. C, bright-contrast phase. D, dark-contrast (B−) phase. E, dark-contrast (A−) phase.

one contrast that is not seen equally well with the other contrasts, and several diffraction plates may be required to fully comprehend the nature of the specimen (Bennett et al., 1946; Oliver, 1948; Richards, 1947c). Of the two types of dark-contrast diffraction plates the B− is often better with slightly absorbing materials. Lower contrasts (20%) are better with larger specimens and higher contrast (7%) for smaller specimens. The quarter-wave retardation is frequently most useful, although more or less retardation may be required.

With the phase microscope the best focus is the exact focus, in contrast to the necessity in brightfield microscopy of defocusing to see specimens of low contrast (Linfoot, 1945). Also, the phase microscope

is operated at full aperture, and it is unnecessary partially to close the condenser diaphragm as must be done with the brightfield microscope in order to obtain enough edge diffraction to see such a specimen. In practical microscopy no decrease in resolution is noted with the phase microscope, and spurious images are less likely to occur. Examination of diatoms and other materials has confirmed this prediction. Oettlé (1950) has apparently confused halos with boundaries of cells.

The phase microscope has proved helpful when combined with other methods of microscopy. Within the resolving power of the light microscope, details can be seen in replicas which aid in interpretation and orientation when further study is to be made with the electron microscope. Ludford et al. (1948) reported that the phase microscope was useful in preparation of specimens for study with the ultraviolet microscope. Direct ultraviolet microscopy is possible with the phase microscope, as demonstrated by Bennett et al. (1948), and provides the advantages of greater resolution. The results will depend on how the specific absorptions at specific wavelengths combine with the optical path differences in the specimen. Photographic and photoelectric recording will make possible quantitative microspectrophotometry. Phase microscopy also is possible with long-wavelength infrared, and the specific absorptions may be used for microchemical analysis, even with specimens such as dark insect exoskeleta, red corals, and minerals that are opaque to light. Photoelectric translation is possible for direct vision with a 1P25 tube, as demonstrated by Bailly (1948), as with ordinary and polarization microscopy.

The marked clarity of image with great detail is the most impressive aspect of the phase microscope. Although the microscope is not difficult to operate, some knowledge and experience must be gained before it can be used at full efficiency.

1. COMPARISON OF PHASE MICROSCOPY WITH OTHER METHODS

When absorption is adequate and reasonably selective, the specimen may be examined with brightfield, ultraviolet, or infrared microscopes, depending on the region of the spectrum absorbed. When absorption is too weak, from inadequate staining or slight pigmentation, the phase microscope may add enough contrast to permit examination, and it may also reveal fine details that would be overlooked with brightfield methods on specimens of fairly low contrast.

Transparent specimens with internal detail due to differences in optical path may be examined with optical staining, darkfield, interference, polarizing, and phase microscopy. When the optical path differences are small, the phase microscope is preferable. With larger

differences in optical path the darkfield and ultramicroscope are preferable. A fragment of glass with a refractive index of 1.52 mounted in balsam with an index of about 1.54 is shown in Fig. IV.1. With brightfield (A) the path difference is so small that the fragment is nearly invisible and only the reflections from the longer slanting surfaces are visible with darkfield (B). With the phase microscope considerable detail is seen clearly with bright (C), B— dark (D), and A— dark (E) contrasts. Note the difference between dark-contrast phase microscopy (D, E) and darkfield (B) microscopy; these methods are complementary, one being appropriate when the other is not. Optical staining is often helpful in combination with phase microscopy (see Section 3.5). An annulus of greater aperture than that of the objective gives fairly good darkfield illumination (16-mm objective and 4- or 1.8-mm annulus) for comparison and is helpful for locating a transparent specimen.

The phase microscope promises to be more useful for internal specimen detail, and interference microscopy for the study of variation on the surface of the specimen. Both methods are too recent for other than broad generalizations. They may be used together or individually, depending on the object of the investigation and the nature of the specimen.

Anisotropic materials are revealed to advantage with the polarizing microscope. Two adjacent colorless, transparent, isotropic regions of small difference in path can be discovered only with the phase microscope. Materials that change the phase relations of the light passing through them may or may not be observed to advantage with the aid of polarized light in the phase microscope, as will be shown in Section 1 of Chapter VI. Ultimately, when the theory of phase and polarization microscopy is developed, prediction of the more useful method will become possible. The occasional gains justify trying the combination.

Rarely is a specimen found for which one, and only one, microscope method is entirely adequate. Usually the image formed is a result of the different properties of the specimen acting together on the radiant energy used for probing its content, and each method of microscopy will reveal additional information. The ideal microscope should be fitted for all methods. Since this is not practicable at the present time, the appropriate methods must be chosen with respect to the specimen and the objective of the investigation (Richards, 1950).

2. ILLUMINANTS

The most useful source of light is the research type of microscope illuminator with a focusable lens system, iris diaphragm, and filter

holder. A lamp with a CC–13 coiled-coil tungsten filament will, when properly focused, normally give greater and more uniform illumination than other types of coiled filaments, and a 100-watt T–8 50-hour projection lamp provides brighter illumination than a 200-hour G–16.5 lamp or a ribbon filament lamp. The uniformity of illumination of the ribbon filament offers slightly better definition although it is less bright.

The lamp should be positioned in the illuminator by adjusting it, or the reflector, until the reflected images of the coils are intermeshed with the direct image to give as uniformly illuminated an area as possible. This adjustment can be done by looking at the filaments directly after removing the lens system, or by closing the lamp iris and focusing the filaments on a nearby wall, or other convenient surface. (The mirror is usually omitted from the illuminator with a ribbon filament lamp, making this step unnecessary.) With both, it is important that the filament be centered to the lens.

Direct the light beam from the illuminator onto the center of the microscope mirror. (This is readily accomplished if the mirror is turned to reflect the beam on the lamp iris.) Turn the mirror to reflect the light into the microscope, and focus the lamp so that its filament image is in focus on either the annulus or the diaphragm of the microscope condenser. Focus the microscope condenser so that the lamp iris is in focus with the specimen, and open the lamp iris to illuminate the part of the field to be studied. If the light is too bright for comfortable vision, it may be reduced by placing neutral density filters between the lamp and the microscope. Since most glass filters are not quite neutral, a ground glass may be used in place of the neutral filter to reduce the illumination, and this is permissible for non-critical work. For the finest detail and best photomicrographs a ground glass should be avoided. Raising the microscope condenser slightly will diffuse out the pattern of the ground glass without unduly reducing the uniformity of illumination.

Illuminators consisting of a lighted surface with adequate intensity for comfortable vision may be used, although as good detail and contrast should not be expected as' from the illuminator with focusable lens system. Units with built-in illumination are adjusted according to instructions of the manufacturer. In all cases the field and aperture should be lighted uniformly and the image of the condenser annulus should match the corresponding part of the diffraction plate with no overlapping or leakage of light.

Strictly speaking, a diffraction plate has a given retardation only for the wavelength of radiation for which it is designed. A quarter-wave

plate for the 546-mμ mercury green line, for example, will be about 0.3 μ
at 400 mμ and 0.2 μ at 700 mμ, and for greatest contrast monochro-
matic light should be used. When color is not objectionable, the 546-mμ
line may be isolated with a Wratten No. 62, or equivalent, filter from a
mercury arc; or the sodium arc may provide monochromatic sources.
For visual observation, nearly as satisfactory results may be obtained
with an Interference Filter with a tungsten lamp (preferably one at
555 mμ, the peak sensitivity of the eye).

In actual experience the contrast is related to the absorption, the
retardation, and the width of the annulus of the diffraction plate (cf.
Sections 2–5 of Chapter III). With an annulus of sufficient width to
give adequate halftone detail in a properly adjusted objective the gain
from restricted wavelength is not so great as might be expected, and the
contrast and detail in the image do not vary a great deal with the use of
the usual medium broad-band photomicrographic filters such as com-
binations of the Wratten M filters, or their equivalents of other manu-
facture. Hence this is not a promising method for obtaining variable
phase. The result is partly explained by the decreased sensitivity of
the eye to wavelengths on either side of the yellow-green. With nar-
rower annular widths, less complete correction of the objective, or both,
restricting the light to a limited wavelength region (such as green) may
be desirable when such color limitation does not interfere with successful
observation. A more efficient filter with narrower transmission than
that of the Wratten B type would be appropriate. Phase microscopy
with slightly colored specimens or when color contrast is added to den-
siphase contrast precludes the use of color filters. No filter is required
by some makes of phase equipment. There is no objection to any
colored light that is pleasing to the microscopist and that does not de-
limit observation. Although maximum contrast can be obtained with
suitable monochromatic light, most visual phase microscopy can be done
with a standard microscope lamp and a daylight type of filter correct-
ing the light to a color temperature of about 4800° K.

For some applications very intense sources may be required. For
example, with bright contrast, the particle may be too small for the
resolving power of the instrument, and its discovery will depend on
having an illuminant bright enough to give a diffraction pattern illumina-
tion great enough to stimulate the eye or other recording medium.
Photomicrographic illumination will be discussed later in this chapter.

The increased detail and contrast of the phase microscope require
magnifications of about 1000 times the numerical aperture of the ob-
jective for full visibility with the average eye, and greater magnification

may be essential for some specimens when the illumination is good.   A 15× or 16× ocular is recommended, and spectacle wearers will find high eyepoint oculars comfortable and efficient.

3. GENERAL PRINCIPLES FOR APPLIED PHASE MICROSCOPY

3.1. Preparation methods

Many materials may be examined satisfactorily in water or in the liquid normally accompanying them. Such preparations should be quite dilute and, when the oil immersion objective is to be used, quite thin. One method places a small drop at the center of the slide of such size that it will spread to about half the area of the cover glass. A little petrolatum jelly, about equal in size to the shaft of a common pin, is spread along the four edges of the cover slip. The cover glass is inverted over the tiny drop and pressed into good contact by drawing a dissecting needle or other smooth small point around the periphery of the glass. This seals the preparation against evaporation and prevents its being dislodged when the preparation is moved during study. A less viscous immersion oil is preferable between the cover glass and the objective. By pressing the cover carefully into the sealing material the mount may be made as thin as desirable. Convection currents and motion are greatly restricted in such a thin preparation. White petrolatum jelly may be acid from bleaching, and fluids containing living material should not come in contact with it. When petrolatum jelly is not available, paraffin oil or Crown immersion oil may be used to seal a temporary preparation. A useful mount is the Rotocompressor of Wieterman (1940), especially an improved type with lower metal sides. Cover glasses 0.18 mm thick are essential for best results, as objectives are corrected to this standard. Other thicknesses decrease contrast, owing to added spherical aberration.

Hollow-ground cells and hanging drop mounts act also as lenses which prevent focusing the image of the annulus on the diffraction plate and are not suitable for phase microscopy. Hanging a small piece of cover glass on the hanging drop will often flatten it enough to make examination possible. Flat-bottomed depression slides are acceptable when the surface is good enough optically not to interfere with focusing the annulus image on the diffraction plate. If any wedge is present it will change the centration of the annulus as the preparation is moved during examination, and constant recentering with the aid of the telescope will be necessary to avoid loss of contrast. When the wedge effect is marked, it may be compensated for by placing a weak prism, such as a 2- to 5-Δ spectacle lens, over the condenser.

The standard phase microscope condenser is made for normal microscope slides 1.15 to 1.25 mm thick. Very thin slides may cause the oil contact to break between the slide and the condenser when the condenser is properly focused. This may be avoided by applying a more viscous immersion oil (e.g., Shillaber's Heavy) or by oiling a piece of cover glass to the top of the condenser.

For examination of thicker mounts two alternatives are possible. About 3 mm of the top lens of the condenser may be removed to allow the use of preparations up to that much thicker. For deeper mounts the top lens is removed from the condenser and an annulus for long focus is used. With a 16-mm objective a condenser working distance of about 18 mm is possible, and Carrel and roller tubes can be examined. Only the region of the top of the roller tube can be studied, as the curvature of the tube elsewhere prevents proper adjustment of the phase system. For 4-mm objectives the top lens of the condenser is replaced with that from a N.A. 0.66 condenser. The working distance is somewhat less at these magnifications. With such systems, frequent checking with the telescope is necessary to make sure that the annulus and the diffraction plate are concentric in order to obtain efficient phase microscopy. Moving the preparation usually necessitates recentering of the phase system. The above description applies to the Spencer equipment. A long-focus condenser with different lenses and annuli for longer working distances is also available from Bausch and Lomb Optical Co.

It is essential that the proper combination of annulus and objective be used, which is readily determined by noting whether the image of the annulus and diffraction plate superimpose when examined with the telescope. When the specimen is too dense, it may be moved to one side, and the checking done. A wedge effect will lessen the effectiveness of this substitute procedure, but adjustment may be made until the contrast is optimal as the specimen is watched. For best results the lamp iris should be focused with the microscope condenser onto the specimen before the annulus is matched with the diffraction plate.

Specimens of living matter should be mounted in appropriate physiological isotonic media, such as Ringer's or Locke's solution, to avoid distortion. Dalton et al. (1949) recommend cold 0.88 M sucrose, especially when the material will be examined later with the electron microscope. Albertini (1948) proposes the following solution, which he calls Tyrofusine KA, for histological and neoplastic cells: Na_3PO_4 0.05 gram, $NaHCO_3$ 5 grams, $NaCl$ 85 grams, KCl 4.2 grams, $CaCl_2$ 2.5 grams, $MgCl_2$ 0.05 gram, pure glucose 10 grams, HOH to 10 liters. This is sterilized for 1 hour with steam on successive days.

The thickness of specimen examinable with the phase microscope depends on its transparency and optical density. Dense tissues or materials up to about 4 μ thick may be seen, and less dense ones with thickness of 100 μ or more may be studied. Transparentizing an optically dense material may make examination possible (see Section 3.2). Larger specimens may be prepared for examination by the usual means of crushing, teasing, sedimentation, etc. Embedding and sectioning with a microtome is possible with many materials (Richards, 1949a). Frozen sections of tissues that are not thin enough for profitable examination may be further thinned by being squeezed under a cover glass or between two slides.

Smears of tissues or fluids make useful preparations. The smear should be thin and even. The usual technic for blood smears can be applied to other fluid specimens. The drop of material is placed near one end of a slide and is spread by touching it with another slide and letting it *follow* the movement of the spreader slide. Colloids and emulsions may be so treated, although dilution with a suitable fluid may be required. Touching the cut surface of an organ to a drop of fluid usually dislodges enough cells for study. A wet preparation should stand long enough for the solid components to settle out flat on the surface of the slide before examination. Flotation with albumin solutions has been used by Fawcett et al. (1950) for the separation of malignant cells from body fluids, and this method could be extended to other materials.

Opaque materials of high reflectivity may be polished and examined with the phase vertical illuminator (Section 8 of Chapter VI). Other opaque materials may be studied by making a replica of the surface and examining the replica. Cellulose acetate may be softened with a solvent and held against a metal surface until it hardens, as was done with a piston ring (Fig. IV.2). Thinner replicas such as those used with the electron microscope may be examined as made or after shadow-casting. (Barnes et al., 1945; Hershman, 1945; Scott and Wyckoff, 1949; and Wyckoff, 1947, describe methods.) Further discussion may be found in Section 8 of Chapter V and Section 8 of Chapter VI. Bright contrast (Fig. IV.3C) reveals the surface detail as contour lines. Replicas mounted on the 200-mesh screens can be seen only with difficulty with the phase microscope, because of the light reflected from the wires of the screen. A screen of flattened, oxidized or darker wire would be better when examination with both phase and electron microscopes is contemplated. With the 4-mm objective a cover glass should be placed over the preparation or the objective should be corrected for use without

a cover glass.   A cover glass will give clearer results with a regular 8-mm objective.

Since concentration gradients differ in refractive index, they may be seen with the phase microscope (Section 3.2).   Other technics that may
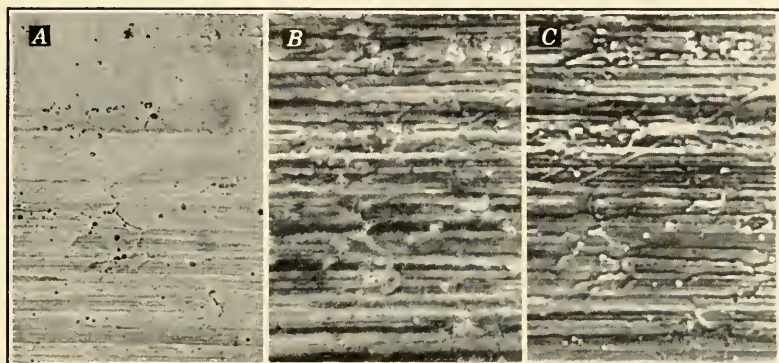
Fig. IV.2.   Replica of piston ring surface, 150×.   A, brightfield.   B, dark-contrast phase.   C, bright-contrast phase.
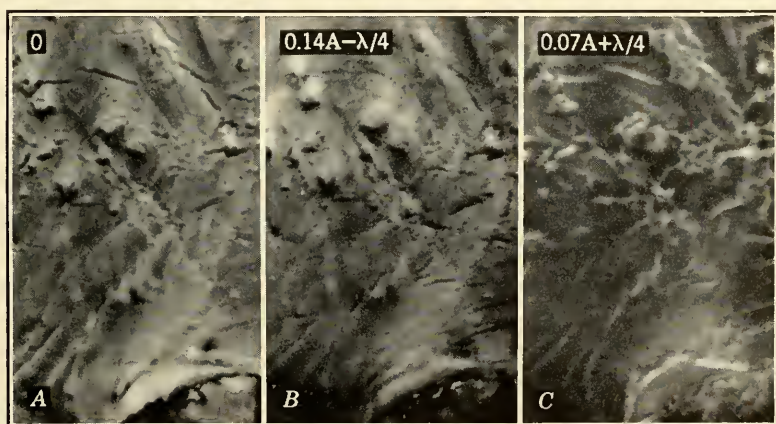
Fig. IV.3.   Chromium shadowcast silica replica of martensitic steel, 230×.   A, brightfield.   B, dark-contrast phase.   C, bright-contrast phase.

be helpful in the examination of materials with the phase microscope are: differential swelling (such as cellulosics with cuprammonium), stepwise dehydration with isopropyl or higher alcohols, incomplete salting out, and isothermal distillation.   Reactions in capillary tubes may be watched if the tube is immersed in a drop of fluid of the same

refractive index as the wall of the capillary and flattened by a cover glass on the surface of the immersion medium. These methods are helpful when it is necessary to determine whether a local difference in a specimen is due to a difference in thickness or in index (see Section 3.2).

Most of the mountants for permanent preparations have survived over a long period of years because they were good for stained preparations. Others have been devised to give large differences in index, as was necessary with brightfield methods (e.g., Hyrax for diatoms). Many of these are less applicable to phase microscopy, and we may expect discovery of a new series of materials, especially from the recently made plastic and synthetic materials. Glycerin jelly mounts are better with many biological materials for phase microscopy than balsam or damar. Tanning the exposed edges with bichromate solution and sealing with Gold Size or synthetic varnish will preserve such preparations for several years. (See Table IV.1C.)

3.2. Transparent specimens

Transparent specimens may be composed of regions differing from each other in size or in index of refraction; these regions can be examined with the phase microscope when they are above a minimum size (see Section 18 of Chapter II). The present discussion is confined to nearly colorless specimens. Lightly colored specimens will be considered later.

Since the optical path is the product of the thickness of the object and its refractive index, it is possible for regions of different size to have the same optical path. For example, one region of given thickness and index can have the same path as another of half the thickness and twice the refractive index. For these objects the phase microscope will show no difference unless appropriate changes are made in thickness or in mounting medium, or unless other treatment is applied that will affect one component more than the other. Fortunately such regions are not commonly adjacent in many properly prepared specimens. Nevertheless this possibility of misinterpretation should always be kept in mind.

The optical path differences of transparent specimens are shown in the phase microscope by shades of brightness or darkness. The greater the difference, within the limits of the method, the greater will be the contrast in the image. If the refractive index of the mounting medium is greater than that of the specimen, the specimen will appear dark with an A+ and bright with an A− diffraction plate, and vice versa when the refractive index of the mounting medium is less than that of the

specimen. When the refractive index and dispersion of the specimen and the mounting medium match, the specimen becomes invisible. Hence, if media of known index are available, the index of the specimen can be determined. In fact, the usual Becke line method is more sensitive when used with the phase microscope. Should this type of investigation be followed to the exclusion of other work, it would be desirable to have a narrow diffraction plate and corresponding annulus so that the observed contrast will be harsh, thereby further increasing the sensitivity of the method. As halftone detail would no longer appear, such a phase system would not be useful for general microscopy.

As one focuses a little above or below the specimen a bright line is seen to move along the edges of the specimen. This Becke line moves into the region of greater refractive index as the microscope is focused upward and into the region of lower index as the microscope is focused downward. It aids in determining refractive index and interpreting optical path differences.

When the mounting medium has no adverse effect on the specimen and a range of refractive indices is available, the contrast can be varied by changing the medium until visibility is optimal for the specimen under observation (Table IV.1, Fig. V.7).

It is possible to make one or more components of a mixture invisible while intensifying the appearance of another component under observation. Differences in refractive index of 0.05 or less are useful. Combined with dispersion staining (Section 3.5), all the advantages of ordinary differential staining become possible for transparent specimens with the phase microscope, without staining or damaging the specimen. This may be important when only microscopic amounts of material are available and the identification must be made without altering the specimen.

Table IV.1

Media for mounting specimens for microscopical examination

A. *Liquids*

	°C	n_D	Reference
Water	20	1.333	. . . . . .
Tyrode's solution	..	1.335	Thorell (1947)
Glycerin and water (equal parts)	..	1.40	. . . . . .
Perfluoro lube oil (du Pont)	..	1.335	Blout and Mellors (1949)
Silicone oil No. 9996-100	..	1.403	. . . . . .
Methyl cellosolve	..	1.403	. . . .
Dioxan	20	1.422	
Chamomile oil	..	1.447	
Glycerin	..	1.46±	
Corn syrup (Karo)	..	1.47±	
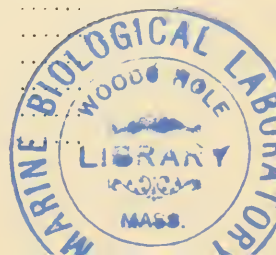
Table IV.1—*Continued*

Benzene, xylene, paraffin oil	..	1.49	......
Anisole	20	1.517	Duijn (1948)
Methyl benzoate	20	1.526	Duijn (1948)
Methyl salicylate	20	1.536	Duijn (1948)
Ethyl bromide	20	1.538	......
Nitrobenzene	20	1.553	......
Bromobenzene	20	1.56	......
Anethole	..	1.561	Haberman (1948)
Monobromonaphthalene	..	1.66	......
Methyl iodide	..	1.76	......

B. *Mixtures recommended for a series of indices*

	n_D	Reference
Aq. dest. and glycerin	1.33–1.44	......
Tributyl phosphate and triortho-cresyl phosphate	1.423–1.556	Groat (1941)
Paraffin oil with Arochlor dissloved in it	1.49–1.63	......
Paraffin oil and α-bromonaphthalene	1.49–1.62	......
α-Methylstyrene and castor oil	....	McCartney (1944)
Camphor dissolved in Santol	....	*Bull. Fr. Micr. Soc.* (1939, **8**: 34)
Diethylene glycol monobutyl ether and cinnemaldehyde	1.44–1.62	Crossmon (1948–1949)
Diethylene glycol monobutyl ether and α-chloronaphthalene	1.440–1.628	Crossmon (1948–1949)
Diethylene glycol monobutyl ether and Halowax oil	1.44–1.63	Crossmon (1948–1949)
α-Bromonaphthalene and Halowax oil	1.44–1.63	Crossmon (1948–1949)
α-Bromonaphthalene and methylene iodide	1.66–1.70*	Crossmon (1948–1949)
α-Bromonaphthalene and α-chloronaphthalene	1.632–1.656	Crossmon (1948–1949)
Methyl iodide and α-chloronaphthalene	....	Crossmon (1948–1949)
α-Bromonaphthalene and heptylic acid	1.4234–1.6582	Kunz and Spulnik (1937)
Mesitylene and ethyl propionate	1.3841–1.4981	Kunz and Spulnik (1937)
n-Butylphthalate and ethyl propionate	1.3841–1.4932	Kunz and Spulnik (1937)

* Not recommended for tissues.

C. *Solid permanent and semipermanent media*

	n_D	Reference
Glycerin jelly	1.47*	......
Vinylite from butyl alcohol	1.47	......
Haitinger's medium	1.44 on drying to 1.52	......

Table IV.1—*Continued*

Isobutylmethacrylate	1.477	O'Brien and Hance (1940)
Diaphane, Euparal	1.48–1.53	Coulston (1941) Garnett (1945)
Polyvinyl alcohol	1.49–1.53	Downs (1943)
Camsal	1.48	*Bull. Fr. Micr. Soc.* (1939, **8**: 134)
Lucite	1.50	. . . . . .
Siloxane silicone DC804	1.515	Spence (1948)
Damar	1.52 ±	. . . . . .
Balsam	1.53–1.54 ±	. . . . . .
Clarite	1.544	. . . . . .
Styrax	1.57–1.63	Spence (1941)
Bakelite	1.58–1.63	. . . . . .
Arochlor	1.63–1.65	. . . . . .
Hyrax	1.63–1.75	. . . . . .
Naphthrax	1.65–1.8	Fleming (1943)
Balsam of Tolu	1.52†	Spence (1941)
Realgar	2.5–2.6	. . . . . .

White Karo corn syrup 5 cc, Certo 5 cc, water 3 cc. Monk (1938).

Fructose syrup (1.43): 30 grams fructose (levulose) dissolved with gentle heat in 20 cc water.

Apathy medium (1.42–1.52): pure gum arabic 50 grams, pure cane sucrose 50 grams, water 50 cc, thymol 0.05 gram. Pantin (1946). Lillie (1948) uses instead 100 cc water and states that Highman adds 50 grams potassium acetate or 10 grams sodium chloride.

Dibutyl phthalate 5 cc, xylene 35 cc, polystyrene 10 grams.

Isobutyl methacrylate polymer and Arochlor can be dissolved in xylene to give media after hardening from 1.495 to 1.525. Bradfoot and Schwartz (1948).

Wright's medium: equal parts of phenol and camphor to which is added twice its volume of thin gum sandarac in isobutyl alcohol. Kenohan (1928).

Polyvinyl alcohol 2 grams, 70% acetone 7 ml, glycerin 5 ml, lactic acid 5 ml, water 10 ml. Acetone is slowly added to the resin and the liquids combined and stirred in drop by drop. Heat till clear (1.382). Gray and Wess (1950).

C-M medium (1.428): methyl cellulose 5 grams, Carbowax 4000 2 grams, diethylene glycol 1 ml, 95% EtOH 25 ml, lactic acid 100 ml, dist. water 75 ml. Methocel and EtOH mixed and added to the rest of the medium. Place in oven for 3–5 days until consistency is right. Clark and Morishita (1950).

Polyvinyl lactophenol: 56% by volume polyvinyl alcohol stock solution, phenol 22%, lactic acid 22%. Downs (1943).

Lillie (1950) describes a number of media, and Greco (1950) has published a table of refractive indices of the solutions of solid media.

* Can be modified to 1.41 and 1.75. Wotton and Zwemer (1935).

† with α-bromonaphthalene 1.73.

Notes: Values without references are from general sources. The indices will vary with temperature and the extent of evaporation of any solvent from the mixture. For accurate work the refractive index should be measured. These materials have been used in microscopy and are offered as suggestions for the microscopist.

Several series of liquids of varying refractive index are available commercially or may be made from directions given in the literature. They should not dissolve or alter the specimen, should be colorless or nearly so, and should have low vapor pressures so as not to change with age. Some useful materials are listed in Table IV.1. However, a change in temperature will usually change the refractive index, and it is desirable to keep temperature records to 0.1° C along with the observations. Solutions of a desired index may be made by mixing suitable materials according to the formula $V_x N_x = V_1 N_1 + V_2 N_2$, where V_x is the volume, N_x is the index desired, and the right-hand terms are the volumes and indices of the materials to be mixed. Such mixtures will not be overly accurate. To determine the exact refractive index it should be measured on a refractometer, or if solids of known index are available they may be put in the liquid and its index discovered (Chamot and Mason, 1939). Micro methods for determining refractive index have been proposed by Kirk and Gibson (1939), Alber and Bryant (1940), and Jelley (1949). Groat (1941) recommends tissue sections of 50-μ thickness for the determination of their refractive index. When the material is sectioned in paraffin the latter should be removed with xylene and several rinses made with the test liquid to remove the xylene before the index of the tissue is measured.

Most of the standard index series are oils or oily liquids. Therefore many materials must be dehydrated before their index may be measured. The dehydrated specimen often has a different index owing to concentration, or possibly to loss of materials extracted by the solvent, or to other chemical action occurring during the dehydrating process.

Three factors should be considered in choosing a mounting medium, assuming that it otherwise has no adverse effect on the specimen: (1) If color effects are to be avoided the medium should have about the same dispersion as the specimen; if optical dispersion staining is desired then the dispersions should have optimal relations to each other (Section 3.5). (2) Some materials make specimens appear more transparent than do others, even though the optical path differences are the same (e.g., tissues cleared in organic phosphates rather than in paraffin base liquids), and this difference may be important in examination with the microscope (Downs, 1943). (3) Other chemicals transparentize a specimen (as in making parchment) or have an effect, like that of phthalates, on paper and some fabrics. Dibutylphthalate is often so used in microscopy.

These well-known methods for microscopy are especially important for phase microscopy in which smaller path and intensity differences are clearly visible.

When the specimen is incompatible with or would be damaged by oily materials, it is necessary to devise aqueous or other mixtures. Some of these will be described under special applications of phase microscopy. For living materials the possibilities are more limited in that mountants must be non-toxic and not alter the specimen by osmotic or other effects. Some change in refractive index may be obtained by dissolving proteins or other materials of such large molecules that they are inactive osmotically in the mountant. Fortunately, small differences are more valuable in phase microscopy, and it may be possible to obtain differences in refractive index without damage to the specimen; e.g., change in index of blood serum is 0.00013 per degree C (du Noüy, 1929, 1933). Polyvinyl alcohol, methyl cellulose, gelatin, cooked starch, plastics, and other materials are possible mounting media in which the concentration can be varied to produce differences in refractive index.

Inhomogeneous specimens may be examined in several different media to obtain the best picture of each component. Mounting small known materials, microscopic glass spheres, threads, etc., with the specimen may make estimation of the path differences possible by direct observation or by photometering as suggested by Martin (1947). When variable phase becomes available it will be possible to investigate local gradients in specimens.

Aqueous and other mounting fluids change in refractive index with changes in temperature; the use of a warm stage with them provides small changes that are helpful in observing small details.

Establishing concentration gradients by flowing a more or less concentrated media under the cover glass brings out differences in some specimens. This is readily done by placing the drop in contact with one side of the cover glass and a piece of dry filter paper against the opposite side. Small changes in refractive index from slight differences in concentration are visible as a form of microschlieren.

3.3. Emulsions and suspensions

Suspensions of opaque pigments or strongly colored materials are seen to advantage with the brightfield microscope, but when they are colorless or relatively transparent they may be seen with the phase microscope even though invisible with other methods. Suspensions and emulsions may be prepared as wet mounts (diluting when necessary) or as dry smears. When a dry smear is to be examined a standard cover glass, 0.18 mm thick, should be placed over it; otherwise the spherical aberration introduced will degrade the image unduly. If uncovered preparations are to be routine, objectives corrected for use without a cover

glass are available.   A cover glass can be anchored with a bit of Scotch tape when the oil immersion objective is to be used.   Since the air between the specimen and the cover glass reduces the numerical aperture to about 0.9 there is little gain with an immersion objective at such decreased resolution.

These tiny specimens exhibit Brownian motion which interferes with clear observation.   When the choice of surrounding medium is not important, a more viscous mounting medium may be helpful.   When measurements are required, it is usually necessary to take a photomicrograph at a speed that will give a sharp picture and then measure the photomicrograph (see Section 3.6).

When the refractive indices of a two-phase system are known, it is possible to identify the inner and outer phases.   Particles of several sizes are examined with an $A+$ and $A-$ phase objective.   The phase of higher index will be bright with the $A+$ and dark with the $A-$ diffraction plates (see Section 9 of Chapter VI).   To avoid a possible ambiguous example it is well to pass judgment only after regions of several different sizes have been observed and all found to exhibit the same contrast behavior.

Degree of homogenization, uniformity of particle size, and presence of undissolved crystalloids can be determined by phase microscopy. With proper cells and electrodes electrophoretic charge and migration may be determined for otherwise transparent specimens.   Some caution should be exercised when inhomogeneous systems are examined, to avoid incorrect interpretation; e.g., it may not be possible to distinguish a spherical bacterium from a similar globule of fat in milk, when their path differences are the same.   Shape differences are diagnostic, and slight differences in path may be observed with diffraction plates of different transmissions.   Specific examples and recommendations will be cited in the following chapters.

3.4. Slightly absorbing specimens

The generalization of the theory for phase microscopy included both absorbing and retarding specimens and indicated that phase microscopy is useful with pigmented materials as well as with colorless ones (Bennett et al., 1946; Barer, 1949).   When the contrast from highly absorbing specimens is good, adding densiphase contrast may not make a noticeable difference, but, when the absorption contrast is low, the added contrast may be enough to make the specimen visible.   Even with contrasty preparations (metal-impregnated nervous tissue) the contrast added with phase brings out details that would be overlooked with brightfield

microscopy and shows more detail within the less dense parts of the specimen. Regions showing little detail, as the eosine-stained part of a spinal cord, may reveal added information, such as inclusion bodies, when examined with the phase system. Combined staining and mounting methods should also be helpful (Zirkle, 1940).

Since the eye is more sensitive to small bright regions on a dark background than to the reverse, it may be helpful to reverse a dark image to bright contrast with an $A+$ phase objective for detailed study. Some ray tracks in photographic emulsions show better in this manner (Section 9 of Chapter V).

In general, the phase microscope is most useful for studying absorbing specimens when their image is too weak for clear vision with brightfield methods. The $1B-0.25\lambda$ type of diffraction plate usually provides the best improved contrast, although the $2.5B-0.25\lambda$ plate may give greater visibility with some specimens. The $A+$ plate is useful when reversal of the contrast is desired or when the specimen has a lesser optical path than its surround. With a few absorbing materials the $A-$ type of diffraction plate gives better contrast than the others. Typical examples of the application of phase microscopy to stained materials are given in Table V.2, although the European work may need revaluation as they have the opportunity of using other than $A-$ diffraction plates.

Old, faded preparations may have enough stain left for good visibility with the phase microscope long after becoming invisible with the brightfield microscope. Thus some museum collections may have their value restored. Likewise light staining combined with phase contrast may reveal more detail than either method would alone. Dr. Jack Schultz reports that chromosomes slightly stained with light green have marked densiphase contrast. Lindegren (1947) obtained better visibility of yeast structure with a $B-$ phase objective with his acetoformol-toluidin blue chromosome stain. Barer (1947, 1948a, b) and Haselmann (1948a, b) report investigations under way with stained material. Interpretation of densiphase contrast is more difficult, because optical path differences may occur within the pigmented regions, as well as selective absorption of radiation of certain wavelengths. When bleaching of the absorbing material is possible without otherwise damaging the specimen, direct comparisons may be made. Measurement with phase before staining may yield pertinent information on the finer structure of specimens. Modern controlled staining methods should be combined with phase microscopy (Petrunkevitch, 1937; Stowell and Alber, 1943). Spectrophotometric methods offer further promise.

3.5. Adding color contrast to phase contrast

In the previous section the gain in contrast by phase microscopy with slightly absorbing specimens was considered in general terms.   When the specimen is sufficiently transparent and colored, color filters may enhance the visibility, as with brightfield microscopy.   A filter of complementary color between the lamp and the microscope will increase contrast, and one of nearly the same color will lessen contrast and often reveal greater detail.   Further results are possible with photographic recording, because the availability of emulsions of different color sensitivities makes possible effective color combinations that the specialized color sensitivity of the eye would not recognize (Evans, 1948).

Reversing the contrast of the specimen from dark to bright may make color contrast more effective.   Red stained wheat chromosomes (Fig. IV.4), examined in light from a Wratten A or an equivalent *red* filter, stand out in better contrast than with brightfield alone (Figs. V.2A–V.2D).   The same technic is useful with Ziehl-Neelsen stained acid-fast bacteria, which then appear as shining bright red rods against a dark background, the contrast almost as enhanced as in fluorescence microscopy.   Unfortunately any bacteria stained blue are also reversed in contrast and, when the staining is not dense, also appear in a translucent red.   The method is useful for locating the bacteria in the preparation, and further examination with dark-contrast phase, or with brightfield after swinging the annulus out of the phase system, will reveal whether or not they are acid-fast in nature.   This method of increasing contrast from reversing the image to bright contrast and examining it with light of the same, or nearly the same, color as the specimen may be used to advantage with other colored specimens, and the more transparent detail is particularly helpful in stereoscopic methods.

Optical dispersion staining may be combined with phase microscopy and may be more effective with diffraction plates giving bright or B − dark contrast.   The light-bending ability of transparent specimens is usually different for long and short wavelengths of light, and this difference in dispersion may be expressed as $v = (n_D - 1)/(n_F - n_C)$, where n_D, n_F, and n_C are the refractive indices for yellow, blue, and red light of those solar spectral lines.   When the specimen and its surround have nearly the same dispersion little color difference will be noticed; if their index is closely the same and their dispersions different the specimen will appear in colors.   In 1946 Richards found that dust mounted in nitrobenzene could be used for the approximation of its silica content as the quartz particles had enough difference in dispersion to appear violet when examined with the phase microscope in bright contrast with a $0.2\lambda + \lambda/3$ diffraction plate.   The color is helpful in

counting, and the phase system revealed smaller particles than could be seen by brightfield methods (see Section 2 of Chapter VI).

Dispersion has been important to mineralogists and used by them for many years, but only recently has it been explored and recommended
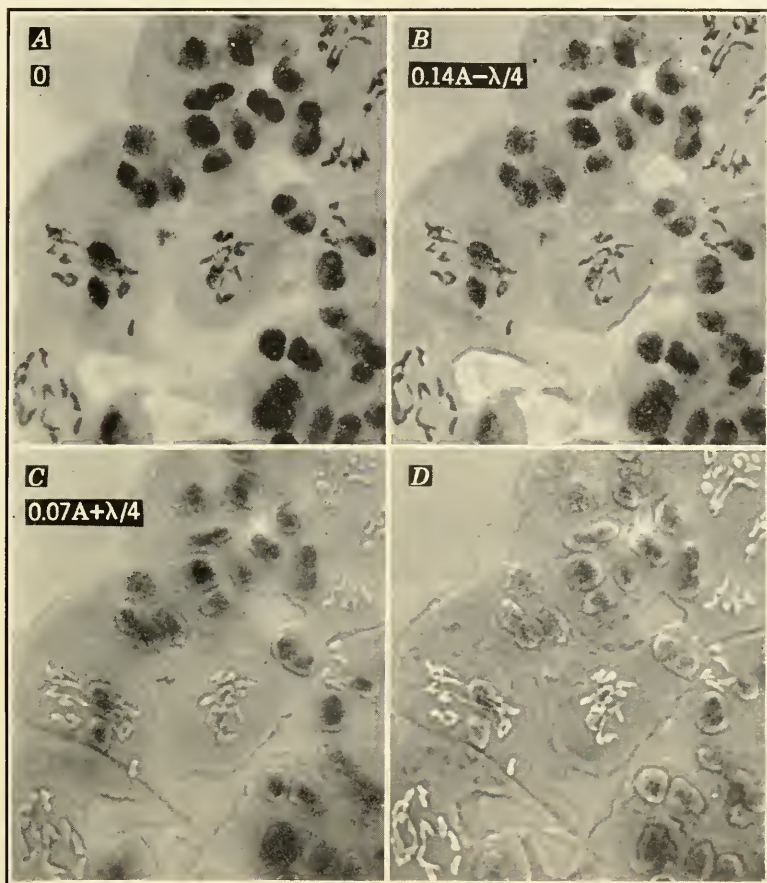
Fig. IV.4.   Wheat chromosomes stained with acetocarmine, 400×.   A, brightfield. B, dark-contrast (A−) phase.   C, high bright-contrast phase.   D, same as C, plus red filter.   Preparation courtesy of Professor Luther Smith.

for general application with transparent materials (Crossmon, 1948, 1949a).   For many specimens Crossmon recommends a medium of suitable dispersion, with a refractive index differing from that of the specimen by about 0.004 (see Table V.1).   He recommended a darkfield microscope to bring out the details of the specimen in color, but the same method may be even better with the phase microscope, because any

densiphase contrast present can be added to the color contrast for increased differential visibility. Dispersion staining is useful with colorless, or nearly so, specimens for bringing out detail and for evaluating impurities or contaminants within the specimen (see Section 2 of Chapter VI). Dispersion often explains the colors seen in some uncolored specimens under the phase microscope. The microscopist should be familiar with color theory and with the limited sensitivity of his own eye to avoid errors of interpretation when microscopy involves color (Evans, 1948).

3.6. Photomicrography

Photographic records are as easily made with the phase microscope by following the same rules and methods as in other photographic procedures. Nearly all the published papers on phase microscopy are illustrated with photomicrographs which attest this statement. Color may be recorded with color films when it is a part of the record.

The ability to see details and to follow physiological processes hitherto invisible in living organisms early brought out the value of making records with the motion picture camera. Grasshopper spermatogenesis was recorded in dark $(A-)$ contrast in a notable film by Michel (1941, 1950). Harrison et al. (1946) filmed the serological reactions of a green and a colorless species of *Paramecium bursaria* with Anscocolor motion picture film; color was important as a natural marker indicating the sensitized animals. In England, Hughes and his associates have filmed mitosis and have also combined phase and polarization microscopy for motion picture analyses of dividing cells (Hughes and Fell, 1949; Hughes and Preston, 1949, and Hughes and Swann, 1948). A phase motion picture of tumor cells was produced by Dr. G. O. Gey (Firor and Gey, 1947), and a tissue culture film of salamander lung cells was made by Dancs (1949). Farris (1947–1950) has made motion pictures of vertebrate spermatozoa. Films showing the growth and life histories of fungi should be available, and with long-focus methods that permit the use of normal cultures in Petri dishes they could be made under normal conditions of growth (Richards, 1947a, 1948b).

The phase microscope replaces the brightfield microscope, or phase accessories may be added to existing equipment. The slightly longer exposures are usually not a serious handicap as a 100-watt lamp has been found more than adequate for color film. Various kinds of equipment for this work are described in the *Journal of the Biological Photographic Association* (see the Cumulative Index **17**: 192, 1949; also Dragesco, 1948; Heard, 1932; and Richards, 1934). Hughes (1949) discusses

the problems of equipment, exposure, and materials in detail, and Ballerini and Scandone have described their 16-mm equipment.

Photomicrographs for reconstructions or models should be made with the objective of highest numerical aperture appropriate to the specimen in order to obtain optical sections having minimal depth of field. When thicker sections are to be photographed an objective with the lowest numerical aperture capable of giving the required resolution should be combined with higher power oculars to achieve the necessary magnification. A magnification of 1000 times the numerical aperture of the objective is often satisfactory. However, greater magnifications may be needed with the phase microscope to bring out the increased contrast and detail revealed. The ordinary classical Abbe theory of resolution is not adequate as a guide in photomicrography, and it is rarely applicable in practical microscopy in which extended objects are commonly observed rather than the separation of two adjacent geometrical image points. For example, the distance between the divided bacterial cells in Fig. V.1P and V.1Q is much less than the limit of resolution based on the Abbe formula ($\lambda/2$ N.A.), yet the edges are sharp and the greater resolution of the electron microscope confirms the record.

One of the main advantages of phase microscopy is that the sharp edges of the specimens are free from indefinite diffraction patterns. Measurements become possible, and this is important with living microorganisms and colloidal materials, wherein staining methods would so alter the size that the measurements could not be interpreted. However, such measurement is not often possible visually because of the motion of the specimen, and ordinary photomicrographic procedures do not permit exposures fast enough to avoid blurring from movement. This problem was solved in 1945 when Richards, Foster, and Wennemark took phase photomicrographs with an Edgerton type of electronic flash. The newer General Electric FT–230 flash tube has proved even more satisfactory (Richards, 1947b, Laporte, 1950). A lens system (Fig. IV.5) magnifies and images the electrodes of the tube on either side of the opening in the microscope condenser. Discharging an electrical condenser through the tube provides a rapid flash uniform enough to fill the aperture of the microscope and short enough to effectively stop Brownian and other motions of the specimen. It is necessary to add a source of continuous light for focusing the microscope. This is accomplished by focusing the aerial image of the filament of a small microscope illuminator between the electrodes of the FT–230 tube. This image is automatically focused in the microscope aperture and turned off before the high-speed flash exposure. The light is adequate for

good negatives on the high-speed black and white emulsions.   Photo-
micrographs have been made at 1800× with all contrasts of the Spencer
oil immersion phase objectives with loadings of 2 to 2.5 kv and 75 to
120 μf (150 to 250 watt-seconds).   The exposure duration was esti-
mated to be about 1/35,000 second by Mr. Frank Carlson (General
Electric Co.), to whom Richards is grateful for assistance and equip-
ment.   The flash tubes and power packs are available commercially, and
lens systems can be combined to illuminate the microscope.   By adding
a timing circuit to the timelapse motion picture equipment an elec-
tronic flash could be used although, as Carlson points out, the resulting
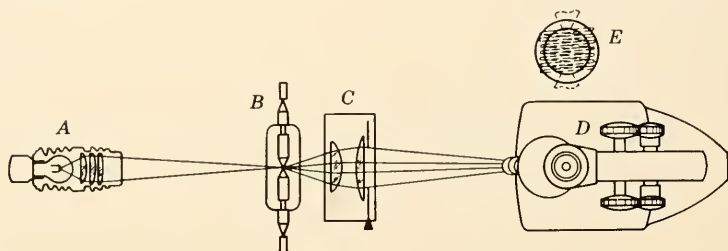
Fig. IV.5.   Diagram for electronic flash illumination for photomicrography.   A,
focusing light.   B, FT–230 flash tube.   C, condensing system.   D, microscope.   E,
image of focusing lamp filament and flash tube electrodes on underside of the micro-
scope condenser.

pictures may be so sharp as to appear jerky on projection.   (Figures
V.1P, V.1Q, V.4F, V.4H, VI.4, and VI.6 were made by electronic flash.)
    Film for the phase microscope is chosen according to the criteria
established for any other kind of photography.   A process or positive
type of emulsion is suitable when the specimen is uncolored and there is
enough light.   Richards favors a fine-grained type B panchromatic
film for general use such as Panatomic X or its equivalent, and develops
in DK–50 by time and temperature.   Others will get equally good
results with other materials and procedures.   When color is important
the emulsion suitable must be sensitive enough to record the color
directly or to give a correct rendering in black and white.   Cole (1949)
reports increased contrast with a Polaroid filter.
    With Spencer phase equipment, Richards (1947b) found that the
1B−0.25λ diffraction plate did not require increased exposure.   The
0.2A±0.25λ low-contrast diffraction plates usually took about the same
exposure as required by brightfield microscopy with the condenser
closed enough to give best contrast on the ground glass.   The higher
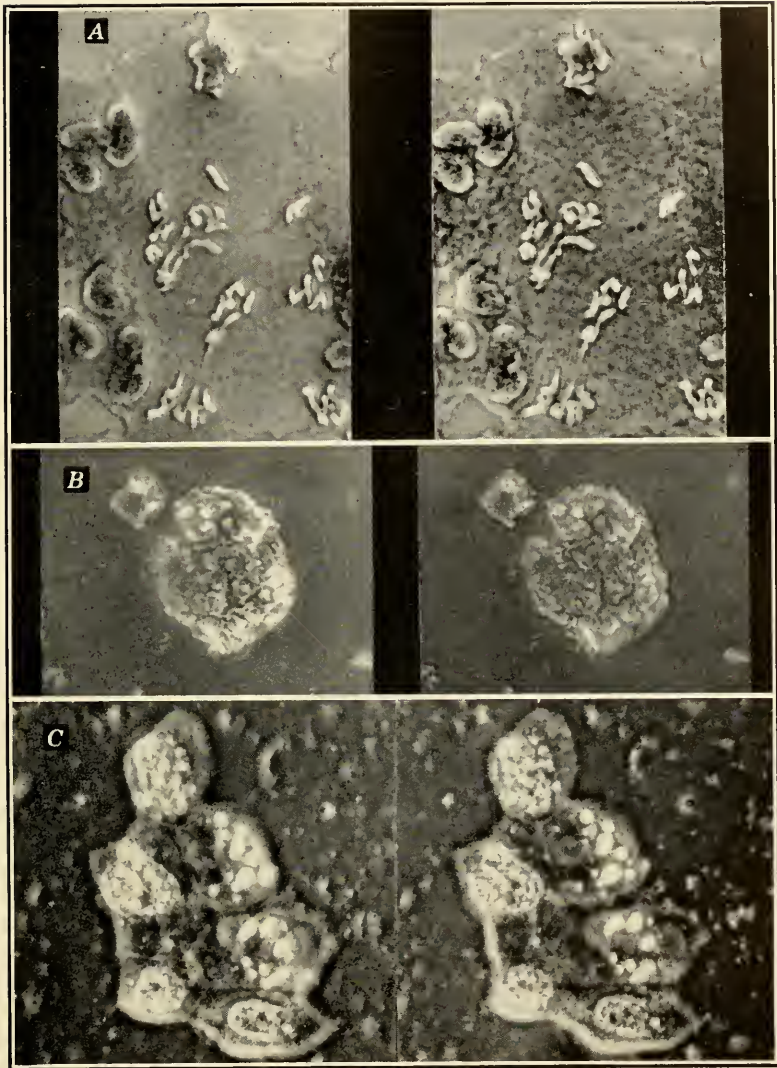
Fig. IV.6. Phase stereophotomicrographs. *A*, red-stained wheat chromosomes, 550×. *B*, β-naphthol crystals, 120×. *C*, epithelial cells from dorsum of an Axolotl tadpole, 400×.

contrast $0.14A\pm0.25\lambda$ and $0.07A\pm0.25\lambda$ plates often require two to four times the equivalent exposure required by brightfield. Other makes of phase equipment with narrower conjugate areas require correspondingly longer exposures. These figures are suggestive only and are given to assist the microscopist in determining the proper exposure. More exact exposures can be obtained with exposure meters appropriate for photomicrography (Maurer, 1944). With colored light and color filters the exposures are increased accordingly by the usual factors. Even with the best equipment some experience is necessary, and trial-and-error methods may be required for exposure determination.

Stereophotomicrographs are helpful in showing the third dimension of a specimen and may be made by several methods. With low powers the specimen may be tilted about 7° and one picture made, then tilted the same amount in the opposite direction and the second picture of the stereopair photographed. With higher magnifications there is not enough depth of field for this procedure, and the half-aperture method is satisfactory provided that the loss of half of the resolution is of no consequence. A piece of black Scotch tape is placed to cover one-half of the annulus, and the first picture made. The annulus is rotated 180°, or the tape is removed and placed on the opposite half of the annulus, and the second exposure is made. The simple condenser is more convenient for this than is the turret condenser. The two exposures of the pair should be processed together and mounted so that corresponding points are about 2.5 inches apart and so that horizontal lines in each are in line to avoid tilt. The mounted pair may be viewed with a stereoscope for study of the third dimension (Fig. IV.6) or, after some practice, fused on direct observation. The picture should be held so that by looking over it one may see some distant object. When the eyes are quickly dropped to the pictures, the pictures will fuse into one, with tridimensional depth. One should look through rather than at the pictures so that the accommodation will be relaxed.

The important precaution in phase photomicrography is to make sure by checking with the telescope that the image of the annular diaphragm is concentric with and superimposed on the diffraction plate. Any light leakage will markedly decrease the contrast in the photograph. Light leakage around the conjugate area will spoil the definition of the photomicrograph more than leakage around the outside of the objective, although both should be avoided. Glare from light leakage is additive in photography because the camera cannot focus and adapt like the eye. Proper alignment should not be neglected for efficient visual microscopy. For adequate photomicrography the condenser must be centerable and the annuli for the various apertures also must have individual centering

screws for correct alignment. Unless the equipment can be permanently aligned, it should be aligned immediately before taking a picture. Especial care must be taken with long-focus condensers (see Section 3.1 of Chapter IV).

Otherwise photomicrography with the phase microscope is the same as with other equipment, and the standard books on photography should be consulted (Jackson, 1948; Anon., 1944; Shillaber, 1944).

PHASE MICROSCOPY IN BIOLOGY AND MEDICINE

1. ORIENTATION

The phase microscope is particularly suited to the examination of cells, tissues, and organisms too transparent in their normal state to be seen with other methods of microscopy. With the proper choice of diffraction plates details may be seen with an optical equivalent of differential staining. Sharp boundaries are provided for measurement, adequate contrast for counting, with no loss of time for staining procedures (often important in clinical diagnosis) and with no question as to how much the preparation has altered the specimen. Slight absorption from small amounts of natural pigment, from failure to obtain adequate staining, and in faded preparations from old collections may be made visible with the phase microscope. Color contrast may be combined with phase contrast when desirable. The changes due to killing and fixing fluids or the effects of other chemical and physical agents may be seen, watched, and assessed. Digestive processes, sol-gel transformations, and other variations in concentration of materials also can be seen and evaluated with the aid of the phase microscope.

Because of these advantages for the biologist, the earlier articles on the phase microscope were illustrated mainly with biological specimens. Köhler and Loos (1941) demonstrated that phase microscopy provides greater and more useful visibility for urine sediments, blood cells, epithelial cells, trypanosomes, and an unstained kidney section. Pictures of living staphylococci, diphtheria bacteria, connective tissue, fibroblasts, mouse tumor, fungus, and yeast were shown by Loos (1941a, b). Michel (1941) examined the cells in the testis of *Oedipoda germinatica* and salivary gland chromosomes and made an unusual motion picture film showing sperm formation in the grasshopper. Spirochetes and epithelial cells were examined by Burch and Stock (1942) with a slit type rather than the annular form of diffraction plate. Photomicrographs of unstained, living lactic acid bacteria, yeast, Sarcina, mycelium, epithelial cells, chromosomes of *Chironomus*, trypanosomes, and brain-tissue sections in dark contrast were made by Bosshard (1944). Richards (1944) published pictures in bright and dark contrast of epithelial cells from the frog nictitating membrane and pointed out the advantage of choosing the diffraction plate giving the

optimal visibility from a series of diffraction plates of different contrasts and kinds, and the possibilities of phase microscopy with tissue cultures, microorganisms, fibers, surfaces, emulsions, homogenization of milk, and foods. The use of the phase microscope in bacteriology was discussed by Knoll (1944) including the saving to be gained from the elimination of staining procedures.

In 1945 a bacteriophage was seen and studied with the phase microscope by Hofer and Richards. Albertini (1945) discussed the importance of phase microscopy with fresh material, exudates, and frozen sections, and its applications in tumor diagnosis. Vital staining is aided with phase (Frauchiger, 1946), and Harrison et al. (1946) reported phase helpful in the study of serological reactions with protozoa and documented their results with a motion picture. Surface patterns of epithelial cells were seen by Albertini (1946a) and independently discovered by Ralph (1947). These patterns resembled the ridges of fingerprints.

The use of the Spencer phase microscope for some sixty specimens, its use with replicas for the study of surfaces, the combination of color and phase contrast, and the advantages of an optical equivalent of differential staining achieved by means of several different contrasts with the same specimen were described by Bennett et al. (1946). The clear detail revealed in emulsions and in living organisms was blurred by Brownian movement and movements of the specimen until Richards, in 1945, with an electronic flash produced photomicrographs sharp enough for measurement. A long-focus condenser was devised so that such studies could be made of cultures in Petri dishes, Carrel flasks, and other containers thicker than the microscope slide (Richards, 1946a, 1947a).

General articles by Taylor (1946), Martin (1947), Barer (1947, 1948b), and Magliozzi (1948) added applications with microfilaria, diatoms, urine sediments, *Chaoborus*, *Botryllus*, Purkinje, and muscle cells, seen with Cooke, Troughton and Simms and with Bausch and Lomb phase microscopes (dark A− contrast). Richards (1947c) reviewed biological phase microscopy. Most of the British and European contributions were made with dark-contrast (A−) equipment by Cooke, Troughton and Simms and by Zeiss, whereas the greater number in America have used Spencer equipment with all contrasts. The possibilities of phase microscopy in biology and medicine were by then reasonably clear, and the publications were becoming concerned more with the phase microscope as a means of solving problems. These contributions will be included in a systematic examination of the various fields of microscopy in the rest of this chapter.

2. TECHNIC

The ability of the phase microscope to reveal detail in unstained, living cells has placed emphasis on preparation methods which do not alter or damage the cells and tissues. Many of the technics described in the previous chapter are appropriate and will not be repeated here. Some cells and organisms will remain from a few hours to several days in a sealed mount with no apparent change, whereas others require an effectively constant environment for survival. The latter may be put in mounts through which nutrients may be flowed and excretion products washed out (Tinsley, 1938). Moment (1944) recommends polyvinyl alcohol for quieting protozoa and other small organisms.

Table V.1

A. *Biological materials*

	n_D	°C	Reference
Bacteria	1.33–1.54	15	Porter (1947)
Bacteria spores	>1.55	..	Porter (1947)
Trypanosoma balbiani flagella	1.56	..	Calkins and Summers (1941)
Mucor protoplasm	1.38	..	Heilbrunn (1937)
Phycomyces sporangiophore	1.38	..	Heilbrunn (1937)
Yeast protoplasm	1.38	..	Heilbrunn (1937)
Amoeba verrucosa	1.42–1.44	..	Frederikse (1933a, b)
Amoebocyte, *Lumbricus*	1.400	..	Calkins and Summers (1941)
Amoebocyte, *Lumbricus* hyaloplasm	1.364	..	Calkins and Summers (1941)
Amoebocyte, *Asterias*	1.446	..	Calkins and Summers (1941)
Amoebocyte, *Asterias* hyaloplasm	1.385	..	Calkins and Summers (1941)
Stentor cilia	1.51	..	Calkins and Summers (1941)
Sea urchin egg	1.39	..	Heilbrunn (1937)
Animal protein fibers	1.5–1.6	..	Schmitt (1944)
Blood protein, 1.736%	1.339	..	Schmitt (1944)
Blood protein, 10.48%	1.354	18	Schmitt (1944)
Blood, cell ghosts	1.504	..	Waugh and Schmitt (1940)
Blood, lipids	1.490	..	Waugh and Schmitt (1940)
Blood, hemaglobin	1.544	..	Waugh and Schmitt (1944)
Blood, hemaglobin from disks	1.525	..	Waugh and Schmitt (1944)
Serum	1.3466	..	Thorell (1947)
Serum	1.3495	17	0.0013/°C, du Noüy (1929)
Serum	1.34726	37	. . . . . .
Bone, fresh	1.481	..	. . . . . .
Bone marrow	1.3738	..	Thorell (1947)
Bone, human, dried	1.549–1.564	..	Antonio (1949)
Cell, fixed, cleared, strained	1.54	..	Pantin (1946)
Eye, aqueous and vitreous	1.337	..	American Optical Co. Chart
Eye, cornea	1.377	..	American Optical Co. Chart

Table V.1—*Continued*

Eye, lens	1.42	..	American Optical Co. Chart
Eye, retina, cow, dark adapted	1.3610 ± 0.0008	..	Ajo (1947)
Eye, retina, new-born calf	1.3621 ± 0.0012	..	Ajo (1947)
Eye, retina, pig	1.35733 ± 0.00167	..	Ajo (1947)
Muscle, deep back, of rat	1.537 ± 0.001	..	Groat (1941)
Histological sections	$1.536\pm$	..	Crossmon (1949)
Tooth enamel	1.627, 1.623	..	Crossmon (1949)
Tooth dentine	1.577 ± 0.003	..	Crossmon (1949)
Tooth cementum	1.560–1.570	..	Crossmon (1949)

B. *Some industrial and reference materials from various sources*

	n_D
Celluloid	$1.53\pm$
Cellulose	1.53 and 1.59
Cotton	1.56
Flax	1.56
Gelatin, dry	1.54
Hemp	1.56
Nylon	1.55
Ramie	1.56
Shellac	1.54
Silica, fused	1.46013
Silica, crystal	1.544 and 1.553
Silk	1.54 and 1.59
Silk, acetate	1.48 and 1.475
Silk, viscose	1 525 and 1.55
Sisal	1.53
Starch	1.53
Wool	$1.54+$ and $1.55+$
NH_4Cl	1.490
NH_4I	1.703
KCl	1.490
NaCl	1.544

Thinner preparations usually reveal more detail than thicker ones, which justifies the small amount of practice required to obtain good mounts with living materials. With many tissues, cells may be obtained by tapping the cut surface into a drop of fluid on a slide. Ciliated epithelial cells from the lung of a mouse are readily isolated in this way, providing a good teaching preparation as the beat of the cilia continues for some time in mammalian Ringer's or Locke's solution. Smooth muscle fibers isolated in 5% citric acid were examined by Magliozzi (1948). Some investigators force tumor or other tissues through a fine screen to break up the tissue and examine the resulting brie for isolated cells or cell groups. The classical experiment of disrupting a sponge and watching the reorganization might be repeated to advantage with the phase microscope. Microorganisms may be shaken apart for
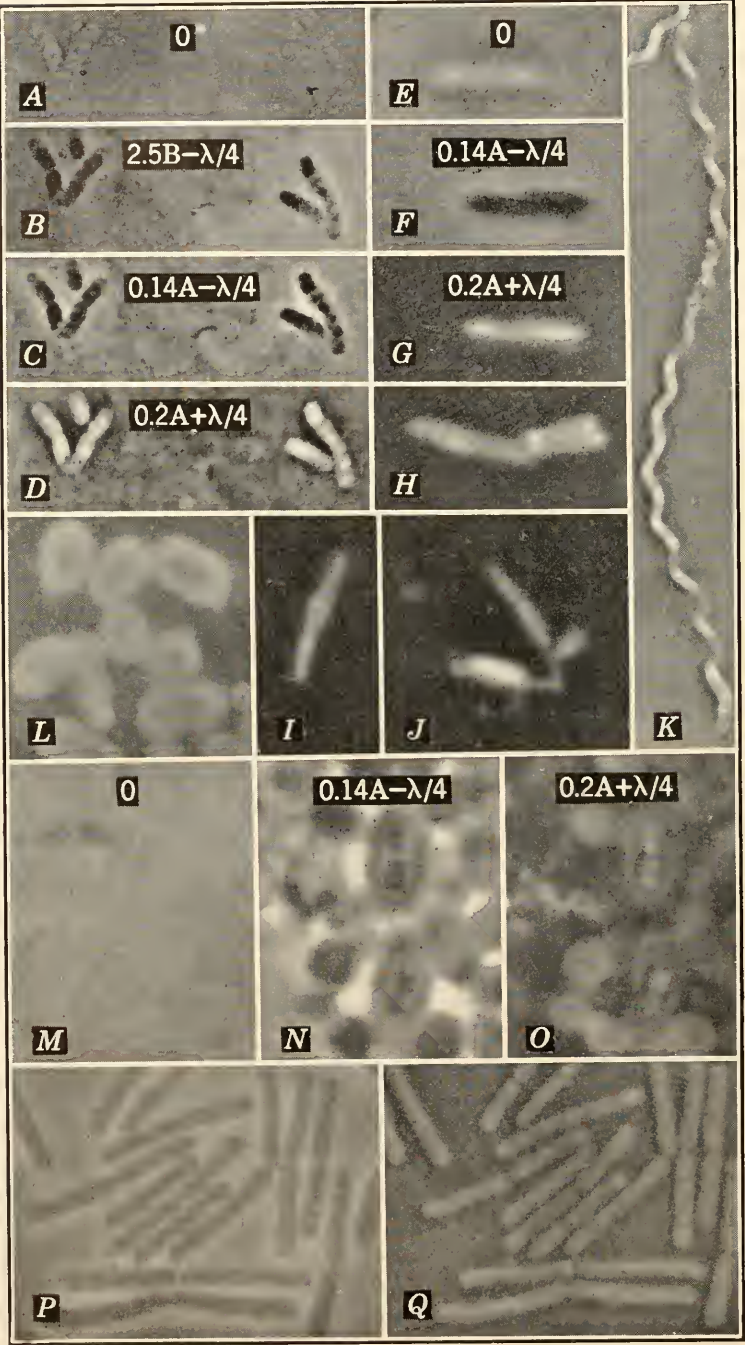
Fig. V.1

examination. Many body fluids contain cells or organisms and may be examined without further treatment. Serous fluids are useful mounting materials either as liquids or after clotting. When the optical path difference is not optimal for good visibility the refractive index of the mounting medium may be changed (Section 3.2 of Chapter IV) or other contrasts and types of diffraction plates tried. Table V.1 gives refractive indices of some specimens (see also Table IV.1).

Mounts of living organisms and wet mounts in general should be sealed with petroleum jelly, paraffin, or other suitable material to reduce movements from convection currents, to prevent evaporation and the consequent necessity of periodically adding water, and to hold the cover glass in place. When the aqueous preparation covers only the center three-fourths of the area, paraffin oil may be run under the cover to seal evaporation. Some immersion oils are sufficiently non-toxic and are preferable to paraffin oil as the index and dispersion are corrected for microscopy. Oxygen will dissolve and be carried through such a thin paraffin layer in adequate amounts for some microorganisms. Various types of mounts, cells, and compressors have been described in the earlier popular books on microscopy. These might well be revived for use with phase microscopy (Beale, 1870; Carpenter, 1901; Hogg, 1886; Quekett, 1852; or other editions).

3. MICROORGANISMS

3.1. Bacteria, phage, and virus

Bacteria should be examined in wet mounts (Fig. V.1). Heat fixation should be avoided whenever possible, because it shrinks and distorts the cells. The larger bacteria may be studied with the $0.2A \pm 0.25\lambda$ diffraction plates, although the $0.14A - 0.25\lambda$ may be found more useful than the $0.2A - 0.25\lambda$ plate. The smallest organisms require greater contrast, as do the internal details of the cell, and the $0.07A \pm 0.25\lambda$ plates are preferable. Bright contrast is usually chosen for locating and counting organisms, and dark contrast for measurement. The smaller structural details are more easily seen with bright contrast although the dark contrast resembles the appearance of

FIG. V.1. Bacteria. *A–D*, *Bacillus mycoides*, 1500×: *A*, brightfield. *B*, dark-contrast (B−) phase. *C*, dark-contrast (A−) phase. *D*, bright-contrast phase. *E–J*, *Mycobacterium lephrae*, 4000×: *E*, brightfield. *F*, dark-contrast phase. *G–J*, bright-contrast phase. *K*, giant spirochete, 1600×. Bright-contrast phase. *L–O*, pneumococci showing capsules, 3000×: *M*, brightfield. *N*, dark-contrast phase. *L*, *O*, bright-contrast phase. *P*, *Q*, *Bacillus cereus*, 2500×: *P*, dark-contrast phase. *Q*, bright-contrast phase.

stained preparations with the brightfield microscope. The B— diffraction plates are useful with stained organisms and often provide better contrast for fine detail with unstained organisms than the harsher A— type for dark contrast (Fig. V.1B).

With the long-focus condenser equipment it is possible to examine bacteria growing on agar in Petri dish cultures when the agar is not too thick, even with the oil immersion lens. A cover glass should be placed on the agar to prevent moisture from the preparation fogging the objective. The phase microscope shows more detail within organisms than the darkfield microscope, which reveals outlines or large inclusions. However, in the examination of exudates from sores the phase microscope makes the pus cells and other material likewise more visible, and the darkfield microscope is preferable for most observations of this type, e.g., finding spirochetes in smear preparations from syphilitic sores. Sputum smears with considerable amounts of mucus should be examined by fluorescence or staining methods rather than with the phase microscope, because the enhanced visibility of the mucus obscures any bacteria present. When the surrounding medium is not too full of extraneous material the phase microscope is useful for locating bacteria. Perry (1948) illustrated a spirochete in a tissue culture.

When the shape and optical path of a bacterium and material near it are the same, it may not be possible to tell them apart by phase microscopy. A single coccus often cannot be distinguished from a similar-sized fat globule in milk without other methods, but bacteria of other forms may be found and in some cases identified from their shape. Some organisms are too small to be seen, as unstained *Leptospira* in kidney tissue sections. The special stains add enough material (e.g., silver) to the organism to make it of size to be visible, and with these stains B— diffraction plates give still better contrast. For these the further development of phase microscopy may show that the $0.07\text{A}+0\lambda$ or $0.07\text{A}+0.4$–0.5λ diffraction plates are appropriate.

Although one of the advantages of phase microscopy is the saving of time and materials involved in staining procedures, the use of the phase microscope with stained materials is often advantageous, Table V.2 (see also Section 3.5 of Chapter IV). Eisenstark and McMahon (1949) have combined nigrosin negative staining with phase for study of the capsules of *Azotobacter*.

Phase and electronic flash have been used by Richards (1948b) to make very sharp pictures for accurate measurement of the size of bacteria (Fig. V.1, *P* and *Q*). A pure strain of *B. megatherium* had an average width of 1.0 μ ($\sigma = 0.06$ μ). For *B. cereus* an average width of 1.10 μ was obtained with bright-contrast phase and 1.05 μ with dark-contrast

Table V.2

Diffraction plates recommended for stained specimens

Stain	Specimen	Plate†	Reference
Acetoformol-toluidin blue	Yeast chromo-somes	$2.5B-0.25\lambda$	Lindegren (1947)
Bielschowsky	Nervous tissue	$A-$	Barer (1948b)
Fuelgen	Chromatin	$1B-0.25\lambda$	*
Light green	Chromosomes	$0.14A-0.25\lambda$	Schultz*
Machiavelli	Rickettsiae	$1B-0.25\lambda$	*
Orcein	Chromosomes	$0.14A-0.25\lambda$	*
Paschen's carbol-fuchsine	Fowl pox	$0.07A+0.25\lambda$ with red filter	*
Polychrome methylene blue	Blood (supravital)	$1B-0.25\lambda$	*
Soudan black	Mitochondria	$2.5B-0.25\lambda$	Jones (1947)
Toluidin blue	Cartilage	$1B-0.25\lambda$	*
Warthin-Starry method	Leptospira	$1B-0.25\lambda$	*

* Richards, unpublished observations.

† Commercial designations: $1B-0.25\lambda$ = low $B-$ contrast. $2.5B-0.25\lambda$ = medium $B-$ contrast. Of the $A+$ and the $A-$ plates 0.07 is high contrast, 0.14 is medium contrast, and 0.2 is low contrast. The $A-$ gives dark and the $A+$ bright contrast for specimens with greater optical path than that of their surround.

phase ($\sigma = 0.07$ and $0.05\ \mu$). The results agree with theory in that the same value was obtained with both contrasts within the error of measurement. The relation of these values to those in the literature are discussed in the original paper, although direct comparison was not possible since other methods (even negative staining) alter the size of the bacterium and brightfield microscopy does not provide an image sharp enough for measurement. The use of phase microscopy and motion picture recording should clarify some problems of growing bacteria and disputed life histories (Section 3.6 of Chapter IV).

Unstained bacteria show considerable detail (Fig. V.1). The outside wall does not show in most living, unstained organisms. With stained, mordanted *B. cereus* the $0.14A-0.25\lambda$ diffraction plate shows both wall and detail (Fig. V.2E). Unmordanted stained cells (Fig. V.2F) show nuclear detail as dark areas with a $0.15A+0.25\lambda$ plate. We are indebted to Dr. Robinow for the preparations from which Figures V.2E and V.2F were made. Increased contrast from reversal to bright contrast by means of a $0.07A+\lambda/4$ plate and red light from a Wratten A filter may be obtained with Ziehl-Neelsen stained bacteria (Fig. V.2, A–D). The limitations of this procedure were discussed in Section 3.5 of Chapter IV. Septa were observed at each full turn of the spiral in a giant spirochete by Dyar (1947) (Fig. V.1K). Leprosy bacteria have been studied with phase by Richards and Wade (1949). Haselmann
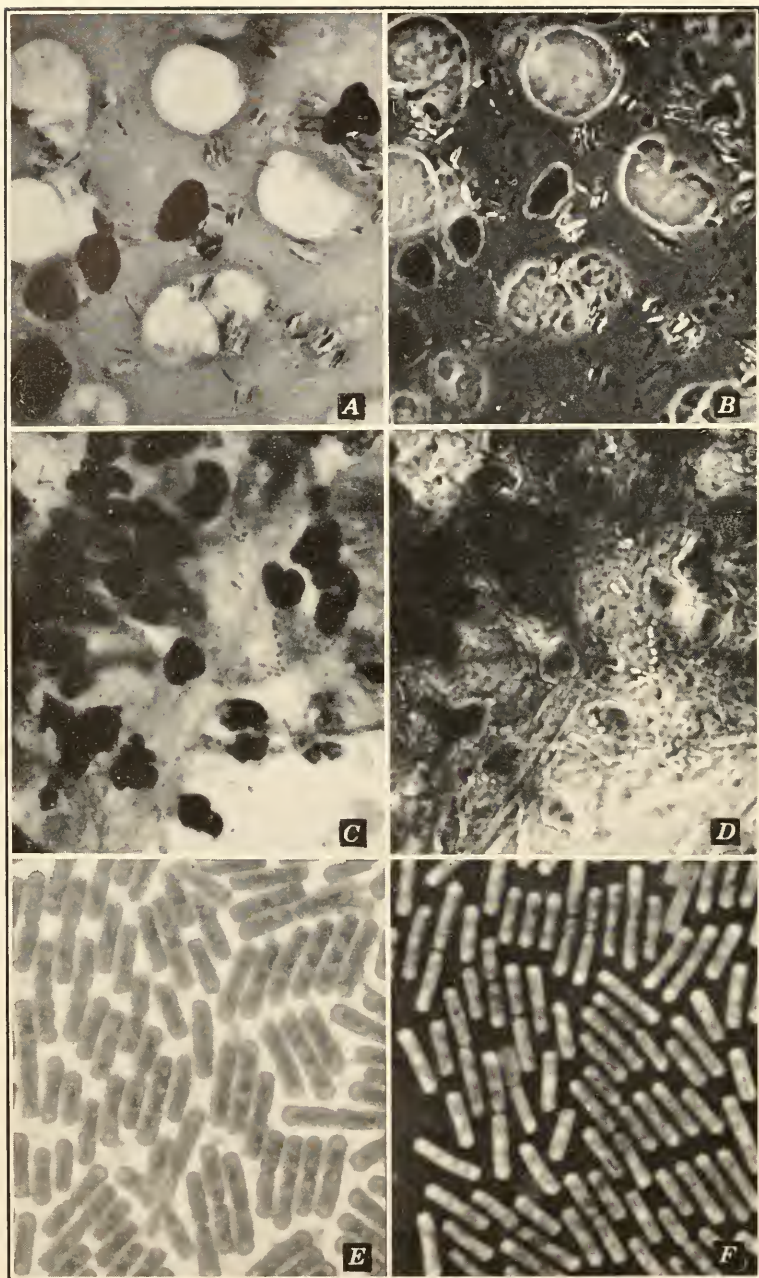
Fig. V.2. Bright contrast with red filter for Ziehl-Neelsen stained bacteria. *A, B,* leprosy; *C, D,* tuberculosis, 1000×. *A, C,* brightfield; *B, D,* high bright-contrast phase. *E, F, Bacillus cereus,* 1850×: *E,* stained without tannic acid. *F,* stained with tannic acid.

and Kappel (1949) found blue light and high-aperture phase objectives useful with gonococci.

A preparation of *Aerobacter* in glycerin jelly suggested the presence of a capsule, but the difference in optical path was not adequate for certain observation. A pneumococcus provided through the courtesy of Dr. Erwin Neter had good capsules, and the advantage of the phase microscope for observing these unstained living organisms in aqueous mounts is apparent when L, N, and O of Fig. V.1 are compared with M. Two cells, N and O of Fig. V.1, have been interpreted as either simple fission or as a possible reduction stage in sexual reproduction. Continuous observation or motion picture recording should answer such questions.

Swimming bacilli often show an undulating movement that Pijper has described and photographed with solar darkfield cinephotomicrography. Pijper (1949) reports seeing flagella on a large spirochete with phase microscopy. High-speed pictures of *proteus* and *subtilis* by Richards did not show flagella, nor did he see them in normal swimming. The addition of some Methocell to give a more viscous medium did suggest twirls similar to those seen by Pijper. Further study with both methods should provide the information needed to understand the motility of bacteria. The meagerness of information available and the details shown in the figures demonstrate the possibilities of phase microscopy in these fields.

Unstained fixed *Rickettsiae* may be seen with the $0.14A+0.25\lambda$ and the $1B-0.25\lambda$ diffraction plates, and the latter makes them even more visible when stained with the Machiavelli stain. The higher contrast may be preferable for the examination of small living organisms.

The action of the bacteriophage on *Rhizobium* was observed and reported by Hofer and Richards (1945). The ability to follow the changes in lysis in the living organisms assisted in understanding the process even though the resolution of the light microscope was not adequate for all the details on the phage. Barer (1948a) reported seeing the virus of psittacosis and of vaccinia. Inclusion bodies in unstained tissue sections of yellow fever (Fig. V 3, N and O), herpes simplex, fowl pox, and distemper were reported by Angulo et al. (1949), who found the $0.14A+0.25\lambda$ bright contrast most useful. They discussed the importance of phase microscopy for studies on the structure of inclusion bodies and the diagnosis of virus disease. Viral inclusion bodies have been seen in tissues from diseases of undetermined etiology (Angulo, 1949a). Another paper discusses inclusion bodies of rabies, vaccinia, wheat mosaic, yellow bean mosaic, mengiofeline- and mouse pneumonitis, and trachoma (Angulo, 1949b). Mumps virus has been seen with a high bright-contrast phase objective.
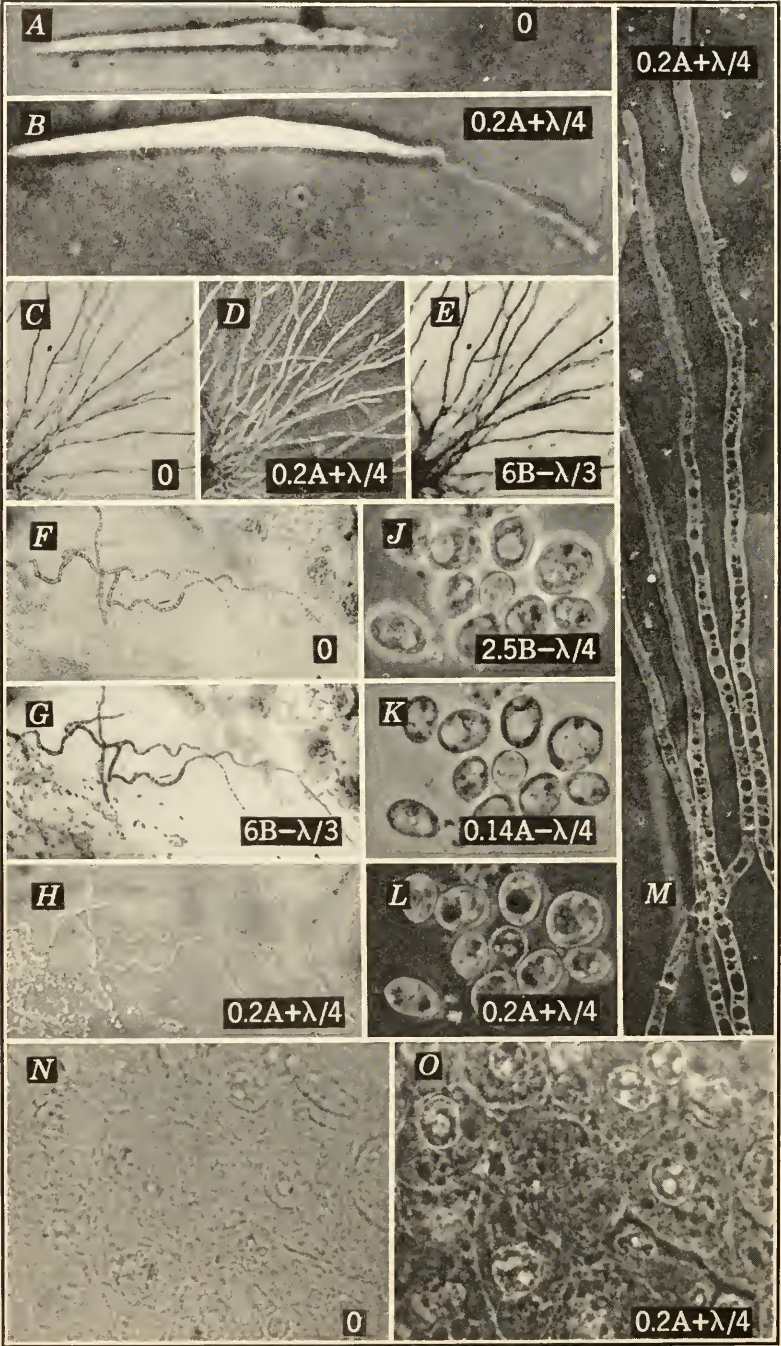
FIG. V.3

How small a virus particle may be seen depends on its path difference. For the *Rhizobium* phage better visibility was obtained with less retardation of a $0.17A+0.1\lambda$ diffraction plate, and other than the quarter-wave retardations should be tried with these materials. The possibilities of examining objects below the limit of resolution with the phase microscope, as discussed by Osterberg (1947b), offer promise. Also, with bright contrast the intensity of the light alone determines the smallness of particle that may be detected. Whenever the center of the diffraction pattern is bright enough to stimulate the receptor, it will be discovered.

Haselmann and Kappel (1949) recommend a high-aperture N.A. 1.4 phase objective for the study of living gonococci. Nuclear changes in *Rhodomicrobium* have been described by Murray and Douglas (1950). Tulasne (1949) is investigating nuclear and cytological detail in the division of bacterial cells. Even with such small cells the phase microscope is aiding in the understanding of living processes. These possibilities of the phase microscope should be explored by the bacteriologist and virologist.

3.2. Other fungi

The larger filamentous fungi may be seen with low-contrast phase objectives $(0.2A\pm0.25\lambda)$, and the smaller *Actinomycetes* can be seen with high contrast $(0.07A\pm0.25\lambda)$. Petri dish cultures may be observed with a long-focus phase condenser (Fig. V.3, *C–H*, and *M*). A cover glass should be placed over the area to be observed with the higher power objectives; otherwise the moisture collecting on the lens obscures the detail. Spores and spore formation show well with phase microscopy. A B− diffraction plate shows more detail within the mycelium, and it is preferable for pigmented fungi. Unless the pigmentation is very dense, more detail will be seen with phase than with brightfield microscopy.

Yeasts and yeast-like organisms show better with medium to high bright-contrast and with $2.5B-0.25\lambda$ dark-contrast phase (Fig. V.3, *J–L*). The B− permits focusing through the cell and seeing the

FIG. V.3. Fungi and viral inclusion bodies. *A, B, Ashbya gossypii*, brightfield fails to show the flagellum clearly seen with bright-contrast phase, 1000×. *C–E, Hormodendron*, and *F–H, Monilia*, growing on agar in a Petri dish, 67×: *C, F*, brightfield; *E, G*, high dark-contrast (B−) phase. *D, H*, bright-contrast phase. *J–L*, yeast, 700×: *J*, medium dark-contrast (B−) phase. *K*, dark-contrast (A−) phase. *L*, bright-contrast phase. *M, Hormodendron*, 750×, growing tip seen with oil immersion phase objective. *N, O*, yellow fever viral inclusion bodies, 700×: *N*, brightfield. *O*, bright-contrast phase. (Councilman body at the left of center.)

metachromatic and volutin granules, while the harsher contrast of the
A − type obscures the detail below the upper layers (Fig. V.3, J and K).
Nuclear behavior in stained and unstained yeast has been reported
by the Lindegrens (1947).

Pathogenic fungi in preparations from skin and hair may be seen to
advantage with the phase microscope. Alkali clearing is not always
necessary. Most pathologists working in this field have preferred the
medium dark contrast although the high bright contrast is useful for
locating bits of mycelium. The flagellum on the spore of Ashbya
(Fig. V.3, A and B) does not show with brightfield because the micro-
scope condenser has to be closed too much for resolution, but it does
show with the full aperture of the phase microscope.

Mycelium in tissues may or may not show with the phase micro-
scope, depending on the similarity of the optical paths. Granted equal
visibility with the tissue cells, identification of fungi is usually easier
because the granulation and other structure of the mycelium are clearly
seen. Sometimes light staining and the phase microscope are preferable
to brightfield microscopy.

A special diffraction plate $(5B − 0.15\lambda)$ and narrower annulus were
developed for counting mold fragments in tomato products. The
change in the annulus was necessary to reduce the numerical aperture
of the 16-mm objective to include the greater depth of the Howard
mold chamber. This was found helpful by the mycologists who depend
on the structure of the mycelium for identification, but others who
depend solely on the diffraction image of the mycelium could not use
phase because diffraction patterns were not visible.

3.3. Algae and higher plants

Considerable detail can be seen in living diatoms, desmids, and
similar forms and in some even after formalin fixation (Fig. V.4, C and E).
Mounted diatoms show better when differences in refractive index and
the siliceous shell are not too great (Bennett et al., 1946). For details
at the limit of resolution of the light microscope, electron microscopy
appears more promising. The phase microscope has been used by
Bonner (1950) in a study of polarity in a slime mold.

Different phase objectives are useful in studying the details of the
filamentous algae. In living *Spirogyra* the pyrenoids show better with
a $5B − 0.25\lambda$ diffraction plate, the protoplasmic strands with a high
bright-contrast $(0.07A + 0.25\lambda)$, and the vacuole with either a
$0.2A ± 0.25\lambda$ low-contrast diffraction plate. Chlorophyll-containing
regions usually reveal more detail with the B − diffraction plate, as do
algae living as symbionts within lichens or protozoa. Detail suggestive
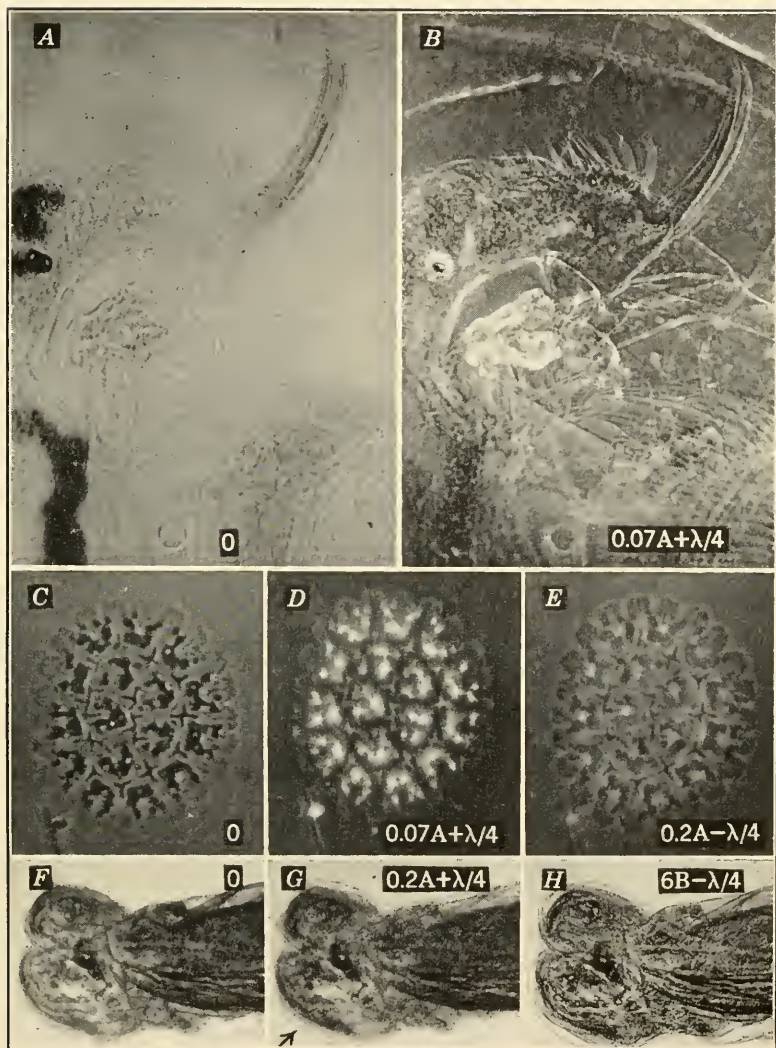
FIG. V.4. *Daphnia*, anterior end, 200×. *A*, brightfield. *B*, bright-contrast phase. *C–E*, *Pediastrum*, 750×: *C*, brightfield. *D*, high bright-contrast phase. *E*, dark-contrast phase. *F–H*, nematode head, 100×: *F*, brightfield. *G*, bright-contrast phase. *H*, high dark-contrast (B−) phase.

of nuclear behavior has been seen in a small blue-green alga resembling *Phormidium*.

Chromosomes and cytological detail in *Tradescantia* stamen hairs are better seen with the $0.2A+0.25\lambda$ bright and the $2.5B-0.25\lambda$ dark contrast, and this may be true generally for plant tissues. The middle lamella and other details in wood sections can be seen to advantage with the phase microscope, with or without staining. Farr (1946, 1949) has used phase microscopy on cotton structure. At present most of the work with these materials has been in the industrial field (see Section 10 of Chapter VI).

3.4. Protozoa and higher animals

With the larger protozoa different diffraction plates may produce the effect of differential staining. A series showing some of the possibilities with *Paramecium bursaria* was published by Richards (1947c). The nuclear and larger inclusions show better with low-contrast objectives, whereas the smaller details, cilia, and smaller Protozoa require the higher contrasts. Pigmented regions and symbiotic algae show best with B— diffraction plates in varying degrees of contrast.

Formation of a mucus-like material and clubbing of the ends of the cilia when locomotion is paralyzed by antisera in sensitized *P. bursaria* have been demonstrated by Harrison and Fowler (1946). Since colorless and green individuals were used as natural labeling for the sensitized animals, the motion picture showing the reaction was made with color film. Paralysis from serum and the changes following conjugation are visible. Micronuclear changes from ultraviolet radiation have been reported by Kimball (1949).

Large parasitic protozoa, such as *Balantidium coli*, usually show better with low bright contrast and require increased contrast for the internal details, and small ones like *Trichomonas vaginalis* need high bright contrast, although Zinser (1947) found the European dark (A—) contrast useful. Parasitic protozoa will be considered in some detail in Section 11. The malaria parasite of the duck shows well with the phase microscope (Trager, 1949).

The cells in *Hydra* are seen with low bright- or dark-contrast objectives, and the nematocysts show better with the high bright-contrast phase objective. The taxonomically useful details of gastrotrichs showed to advantage with a $0.07A+0.25\lambda$ bright and a $0.14A-0.25\lambda$ dark diffraction plate. Mites, such as *Byrobia*, are too nearly transparent when mounted in Clarite for brightfield microscopy but are readily seen with the $0.2A-0.33\lambda$ or a $0.2A-0.25\lambda$ plate in the 16-mm phase objective. Similar preparations of *Daphnia* required the high

bright contrast for the detail (Fig. V.4, *A* and *B*). A nematode was seen best with 5B -0.1λ and 0.2A $+0.25\lambda$ diffraction plates in the 16-mm objective (Fig. V.4, *F–H*). Chitwood (1949) found the phase microscope helpful in his revision of the nematode genus *Melodiogyne*. The hooks on an acanthocephalid showed about equally well with the A+ and the *B*− plates. Penetration glands in trematodes were investigated with phase by Reid (1948). Small insects and insect parts may be examined with the phase microscope, and the high bright-contrast plates may facilitate seeing details or finding the parts as contaminants in food. Gregoire and Florkin (1950) examined plasma coagulation of insect plasma.

Either the 0.2A$+0.33\lambda$ or the 0.2A-0.25λ diffraction plate shows the annulae of fish scales, whereas the *B*− is not so good for this application. A lower magnification than the 16 mm would be desirable for the larger scales. The same phase plates could be utilized for replicas from the scales.

The bat wing is only about 20 μ thick, too transparent for brightfield microscopy. However, when mounted with paraffin oil between glass, it shows considerable detail under the phase microscope. Low and medium contrast A$\pm$ diffraction plates proved useful at all magnifications. With long-focus condensers and suitable mounts, all magnifications of phase may be useful on transparent chamber preparations for the study of regenerating tissue and atypical growth. *B*− plates should be tried, as they are often better for these preparations. Details from higher animals will be discussed in following sections.

4. CYTOLOGY

The phase microscope shows detail in unstained, salivary gland chromosomes (Fig. V.5) (Michel, 1941, 1950; Richards, 1947*c*; Schultz, 1947). Slight staining with light green gave somewhat better results, according to Schultz. Polister and Leuchtenberger (1949) found purified methyl green specific for desoxypentose nucleic acid, and this staining might be used with phase microscopy. The effects of digestion and of electrolytes on chromosomes have been seen with phase microscopy by Kaufmann (1949). Salivary gland chromosomes of *Chironomus* were figured by Barer (1947*a*). Ludford et al. (1948) compared findings with ultraviolet microscopy and observed chromosome behavior. Michel's (1941) phase motion picture film of cell division in the grasshopper set a new level for cytological study (Duryee, 1948).

For chromosome study the 0.14A-0.25λ dark contrast has been preferred, probably because it more nearly resembles the picture seen with stained material. It is possible to see chromosomes in dividing cells in

preparations of the cornea of the frog and rat with a $0.2A - 0.25\lambda$ diffraction plate, although the overlying cells somewhat obscure the detail, even in an unstained preparation. Chromosome movements were measured by Hughes and Swann (1948) on biframe motion picture films made with phase microscopy to show the chromosomes and with polarized light to show the spindle. These films appear to support a traction theory of chromosome separation in embryonic cells of the chick. Enhanced contrast is possible from combining phase contrast with that of staining (Fig. IV.4). By combining phase and polarization cinemicroscopy Hughes and Fell (1949) were able to see both the chromosomes and the spindle during mitosis.
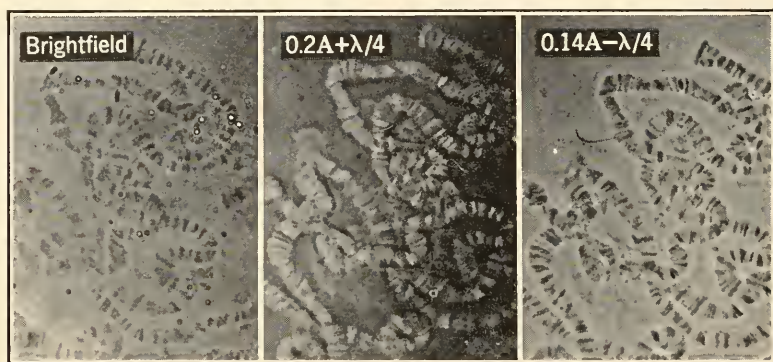
Fig. V.5. *Drosophila* salivary gland chromosomes, fixed unstained smear mounted in Clarite, 650×. *Left*, brightfield. *Center*, bright-contrast phase. *Right*, dark-contrast phase.

Mitochondria and tonofibrils were described by Albertini (1946b). Jones (1947c; 1948b) combined phase with staining methods for the analysis of mitochondrial behavior in embryonic blood cells of the rat. He preferred medium bright and dark $(A-)$ contrasts for unstained, fixed cells and the $2.5B - 0.25\lambda$ for Soudan Black stained preparations. Ludford et al. (1948) recommended phase for observing mitochondria. The mitochondria of flattened tissue culture cells show especially well (Firor and Gey, 1947).

The Golgi apparatus shows in enlargements of the epithelial tissue figured by Richards (1944b). Brice et al. (1946) discovered this apparatus in smears from the seminal vessicle of *Lumbricus*, and Oettlé (1948) saw it in the testicular cells of man. Jones (1947a, 1948b) and Corti (1948) reported seeing the Golgi apparatus, but Zollinger (1948c) failed to find it. Baker (1949) preferred dark $(A-)$ contrast for the examination of this and recommends calling it, instead, the Golgi
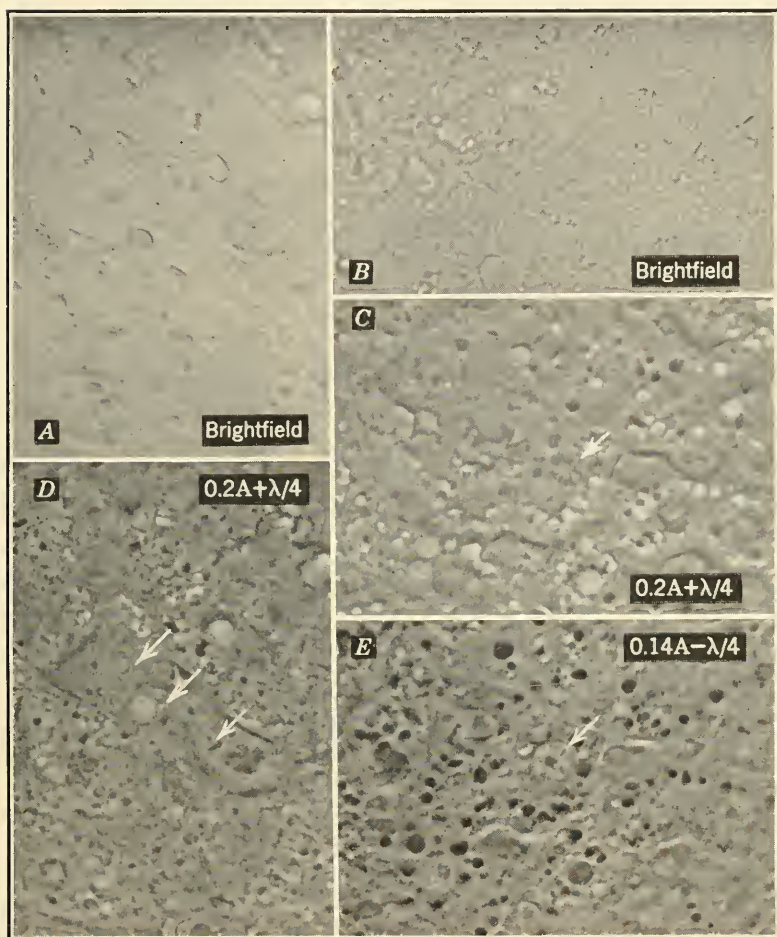
FIG. V.6. Liver tissue, unstained, deparaffined section mounted in damar, 750×.
Arrows mark inclusion body in nucleus (C, E) that does not show in brightfield (B),
and comparable details in A and D.

element.   Gatenby and Moussa (1949) have studied this in dorsal root ganglia.

Thorell (1947) used the phase microscope with an auxiliary lens for the measurement of cell thickness.   Jones (1947c) recommends phase microscopy for optical sectioning to determine in which layer of a cell the inclusions are arranged.   A pattern resembling the ridges of finger-prints was found on the surface of epithelial cells by Albertini (1946b), Baud (1947), and Ralph (1947).   Bejdl (1949) interprets these as the remains of intercellular bridges, as did Chambers and de Rényi (1925). Richards (1949d) exibited phase stereophotomicrographs of these ridges and of various kinds of cells showing the three-dimensional distribution of cellular content of nerve fibers and capillaries in tissues.   Nissl bodies have been studied by Hoessley (1947) and Albertini (1948) (see also Section 6).   Cellular details seen with phase and ultraviolet micros-copy have been compared by Ludford et al. (1948).   Dedifferentiation of cells has been reported by Albertini (1946b).

Details may be seen in tissue sections (Fig. V.6) when the section is not too thick.   If the material is embedded in paraffin it is necessary to remove it before examination (see also Fig. VI.1).   Albumen embed-ding proposed by Wilson (1942) should be useful in phase microscopy.

A most impressive application of the phase microscope for the elucida-tion of cellular structure and behavior is seen in the motion pictures of Michel (1941), Firor and Gey (1947), Fell and Hughes (1949), Hughes and Preston (1949), and Hughes and Swann (1948).   The changes in the chromatin as the chromosomes form and divide and of the cyto-plasmic constituents show clearly in Michel's film.   Unfortunately the dark (A−) contrast did not show the spindle fibers.   Other types may do so and should be tried.   A film combining phase and polarization microscopy in successive frames and showing both chromosomes and spindle fibers is reported by Hughes and Swann (1948).   Gey reports special advantage from study with phase of the cell membrane during division.

5. KILLING AND FIXATION

For many years microscopists have differed as to how well the usual killing and fixing technics retain the detail of the living cell, or whether artifacts are produced.   The transparency of living cells prevented clear observation of them by brightfield methods in most cases.   Buchsbaum (1947, 1948) examined salamander macrophages in living tissue cultures with the phase microscope and then studied the changes after fixation and staining.   Photomicrographs were made for record.   Acetic acid containing fluids (Bouin's and Carnoy's) caused cytoplasmic distortion.

Formalin, especially neutral or alkaline (10%), was better, and the Zenker-formol-osmic fluids gave fixed images resembling the living cell most closely. Hoessley (1947) investigated killing agents. Chromosome changes with fixation were described by Schultz (1947).

Oliver (1948) watched the fixation of isolated cells and reported a sharpening of detail in the structure as the protoplasmic elements became denatured. He also stated that ". . . it can be definitely observed while the process is occurring under the eye that no structures similar to rods or droplets result as artifacts or products of fixation . . ." with weak formalin treatment. Barer (1948b) shows photomicrographs of living and fixed salamander testis. Crawford and Barer (1949) used formalin fixation of living, teased cells from *Salamandra maculosa* and reported shrinkage first, followed by swelling and exudation of bubbles. The addition of saline reduced the swelling. Whether the same condition prevails in blocks of tissue is uncertain. Detailed studies on cellular death were reported by Zollinger (1948d). (See also Peters et al., 1950.)

Haselmann (1948b) believes that better detail can be seen in fibrils and membranes with the phase microscope after staining. This, he states, may be due to luminescence, refraction, or total absorption of the dye. Observations with diffraction plates other than those available in the Zeiss equipment should clarify these relations. With very small specimens, as with bacteria, staining procedures, especially metal impregnation methods, increase the size of the organism and may make observation possible with the light microscope. Combined fixing, staining, and mounting media (Zirkle, 1940) should be tried both with and without the stain.

6. EMBRYOLOGY AND HISTOLOGY

6.1. Embryology

The structures of spermatozoa, usually revealed by staining, may be seen in unstained living cells with the phase microscope. Study of motion and counting may be done to advantage with medium bright contrast, and structure may be observed with dark contrast. Farris (1947, 1948a, b) has made motion pictures of normal and atypical sperm and their locomotion which provide basic information for alleviating human infertility. An early sperm phase photomicrograph is to be found in Smith (1946).

Fertilization and early development of the rat has been studied by Austin and Smiles (1948) and by Odor and Blandau (1949). At the 1949 meeting of the American Association of Anatomists, Odor and Blandau exhibited remarkable photographs showing the sperm within the egg. Albertini (1947) reported phase microscopy helpful in the

examination of mesoderm formation in the guinea pig.   Photographic records of the development of nerve cells of the 5-day chick embryo were made by S. C. Williams (1949*a, b*) over a 2-week period.

6.2. Histology

The epithelial cells of the tongue and the inner lining of the cheek have been the regular test object for phase microscopy because of their un- limited availability and ease of preparation.   Almost all the earlier papers have pictured them, either with or without bacteria, but owing to the differences in the reproductions (screen and paper quality) it is not possible to compare the efficiencies of the various methods from the published illustrations (see Section 4 of Chapter V).   Richards (1944) examined the epithelium from the nictitating membrane of the frog, which is easily prepared and offers more detail than the squamous epi- thelial cells from the mouth.   Improved resolution with ultraviolet phase microscopy was demonstrated by Bennett et al. (1948).   Chase and Smith (1949) reported the B— dark contrast valuable for study of pig- ment in hair.   Zahn and Haselmann (1950) have examined the middle membrane in hair.

Frauchiger (1946) examined the choroid plexus in Tyrode's solution and concluded that the phase microscope should be useful in neurology and, with toluidin blue, should help to explain the function of the plexus.   Brain tissue of several animals was studied by Hoessley (1947) with brightfield, phase, and ultramicroscopy.   He believed that all the methods would provide new conclusions.   A structure was reported to appear after death that resembled the Nissl body and might be a pre- cursor of it.   Fixation changes were also investigated.   Gatenby and Moussa (1949) have examined dorsal root ganglion cells, and Peters et al. (1950) have studied dendrites.   Thomas (1947) described a beaded appearance observed in the motoneurones of *Helix* that was disturbed on fixation and found very small granules which he proposes calling microneurosomes.   He believes that one of the prime advantages of the phase microscope is the revelation of smaller granules than can be seen with other microscopical methods. S. C. Williams (1949*a, b*) followed nerve-cell development of chick embryo tissue.   (See also Section 6.1.) The islet tissue of Langerhans has been examined by Hartroft (1950).

The middle and Krause's membranes of unstained muscle fibers were seen by Albertini (1946*b*), and Ralph (1949) has photographed even smaller details within the muscle cell with the phase microscope.   Con- nective tissue was examined early in the history of phase microscopy by Loos (1941*a*).   A diffraction plate of greater contrast $(0.1\mathrm{A}-0.25\lambda)$ shows the elastic and gelatin-containing fibers better than the usual

transmission. Cartilage shows organized structure when unstained and considerably more detail after light staining with toluidin blue. The 1B—0.25λ phase objective is preferable for stained connective tissue. Bensley (1950) has a phase picture of the intercellular substance in loose connective tissue.

Blood may be examined without staining as the phase microscope shows fine detail in the leucocytes and transition cells. Hematologists prefer a medium dark (A—) diffraction plate for fresh smears, but the 1B—0.25λ plate shows better color contrast and detail in supravitally stained blood. Brecher (1948, 1949) used phase microscopy for the examination of reticulocytes, and Hoffman and Rottino (1950) discuss the progressive cytolysis undergone by reticulocytes in Hodgkin's disease leading to Sternberg-Reed cells. Radiation effects on blood were studied by Dickie and Hempelmann (1947). Phase microscopy is helpful in counting platelets in a shallow 0.05-mm hemocytometer using Feissly's (1948) diluting fluid of cocaine HCl 3 grams, NaCl 0.20 gram, in 100 cc Aq. dest. (See also Ralph, 1950.) Jones (1947a, b, c, 1948a, b) has made effective use of the phase microscope in the study of blood-cell development of the rat embryo with especial reference to mitochondria and nuclear details. Moeschlin (1949), on comparing phase microscopy with the usual methods of examination of stained blood smears, concluded that the former yields new information of diagnostic importance. Bessis (1949a, b) and Bessis and Bricka (1949) have published an atlas of blood-cell phase pictures. They have also combined phase microscopy with shadowcasting technics to increase contrast. Ludin (1947, 1948, and in the discussion of Moeschlin, 1949) has found phase microscopy useful for study of motion of cells and of dividing cells such as neuterophil leucocytes and megaloblasts. Feissly and Ludin (1949) discuss hemolysis and the transformation of thrombocytes as seen with phase microscopy. Bolen's method has been examined by Lind and Ashley (1950). Other possibilities with the phase microscope for tissue structure will be discussed under pathology. Köhler and Loos (1941) and Crossmon (1950) recommend phase for counting cells in a hemocytometer.

The ash from microincineration of a tissue section is distinctly more visible with medium bright or low B— contrast phase objectives.

Very transparent tissues, like the vitreous body of the eye, are seen with the phase microscope to be composed of fibers, cells, and media of different optical densities. Very fresh corneas show the epithelium and mesothelium but little detail in between. The tissue soon deteriorates, as an isosmotic mounting fluid for the epithelium is not correct for the mesothelium, and then fibers and nerve cells may be seen as the tissue
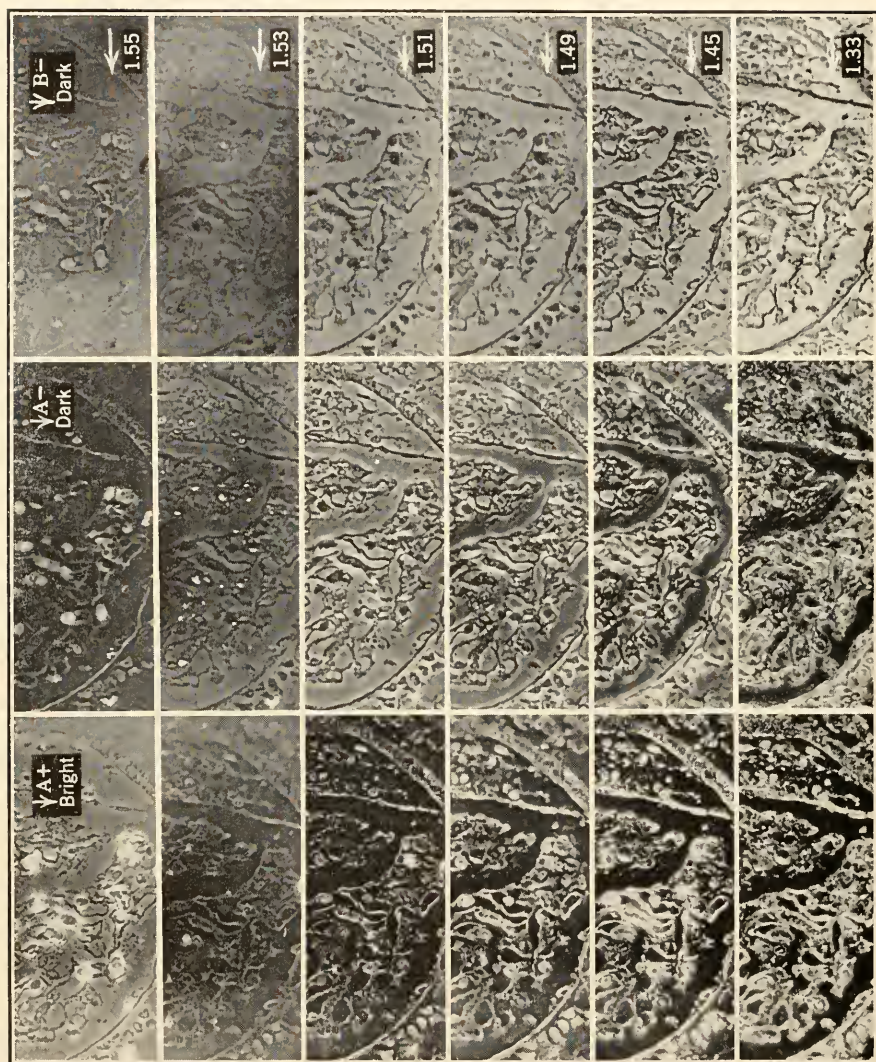
Fig. V.7.   Kidney tissue in mounting media of different refractive index, 400×.
Note reversal in 1.55 index fluid.   (See text.)

changes. The phase microscope is appropriate for preserved as well as for unstained living tissues, because poorly staining fibers to the lens are readily seen in mounted sections.

The information obtained with phase microscopy on unstained preparations has included much that was known previously, and in addition an histology of living tissues is evolving. By changing the refractive index of the mounting medium, the contrast may be controlled so that certain features show well while the visibility of others is suppressed (see Section 3.2 of Chapter IV). Some of the changes possible are shown in Fig. V.7. Several diffraction plates may be required to fully comprehend a specimen. Referring to the nephron, Oliver (1948, p. 188) wrote: ". . . these illustrations emphasize the necessity of the use of varying phase contrasts in the examination of a tissue if one is to feel confident that he has seen all of the structural detail within the specimen."

7. TISSUE CULTURE

The cells of tissue cultures are especially well suited for examination with the phase microscope because they are too transparent for brightfield and the path differences are rather small for darkfield. Preparations can be studied in many of the standard culture dishes with a long-focus microscope condenser. Hollow-ground slides are contraindicated. Because of the curvature, only the cells at the top of roller tubes can be seen clearly. With the thicker vessels more care is required in centering the equipment because of the wedge effect caused by local surface irregularities and lack of parallelism of the sides of the flasks (see Section 3.1 of Chapter IV).

Living spirochetes of syphilis in tissue cultures of testicular cells have been seen with phase by Perry (1948). The increased detail seen with the phase microscope is most effectively demonstrated in the motion pictures by Firor and Gey (1947) and by Danes (1949), which were discussed in Section 4 of Chapter V.

For the 16-mm objective the $0.2A+0.33\lambda$ diffraction plate has been preferred for the examination of tissue cultures. With the 4-mm objective, low and medium $A\pm$ contrast and low $B-$ contrast have been chosen for this application. Some investigators would add the high bright contrast $(0.07A+0.25\lambda)$ to the list for the oil immersion objective. (See also Ludford and Smiles, 1950; Sylvén, 1950.)

8. EXAMINATION OF SURFACES

Opaque materials including some tissues can be examined with the phase vertical illuminator when they have good reflectivity (see Section 8

of Chapter VI). Other surfaces can be examined indirectly with the ordinary phase microscope by first preparing a replica of the surface (Section 3.1 of Chapter IV). Large specimens like fossils, teeth, etc., can be polished and thick cellulosic replicas obtained. Thinner and more delicate living materials require a thinner membrane technic like that used by Wolf (1948) and by Fishbein (1950). Considerable detail may be seen, and such study is often helpful before turning to the higher resolution of the electron microscope for finer detail. Replicas of
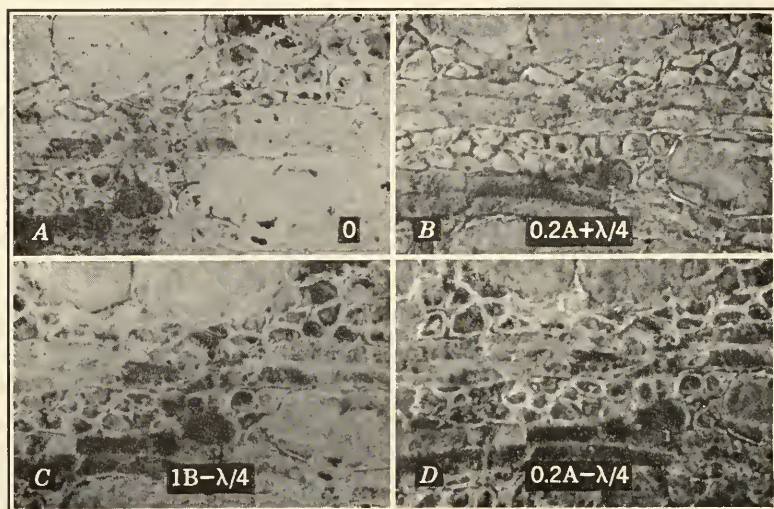
FIG. V.8. Replica from fossil wood, 135×. A, brightfield. B–D, phase photomicrographs.

fish scales should show more detail by phase microscopy. The study of hair will be considered later (Section 10 of Chapter VI).

A cellulose acetate replica of a polished piece of fossil wood obtained through the courtesy of Dr. H. N. Andrews from the Missouri Botanical Garden is shown in Fig. V.8. Brightfield shows detail due to the adherence of microscopic bits of the rock. The pigmented parts show better with the $1B - 0.25\lambda$ diffraction plate, and the cellular details appear dark with the $A+$ and bright with the $A-$ diffraction plates because the material of the replica was of lesser refractive index than the Clarite mounting medium. The woody structure is quite clear. Further polishing and making of replicas will make serial sectioning possible, and the detail can be kept by the replicas even though the original specimen is destroyed by the preparation method.

9. RAY TRACKS AND RADIOAUTOGRAPHS

The tracks in a developed photographic emulsion after exposure to cosmic or other radiation consist of fine lines of silver grains. Since there is usually considerable contrast between the dark silver grains and the rest of the emulsion, less increase of contrast might be expected from phase microscopy. The short side paths of proton tracks and other regions of slight silver deposit do show better with a $0.14A-0.25\lambda$ or a $1B-0.25\lambda$ diffraction plate. Some investigators prefer to reverse the contrast of the silver particles from dark to bright with an $A+$ phase objective, because the eye is more sensitive to small bright regions on a dark background than to dark regions on a bright background. When yeast, bacteria, or other organisms are included in the emulsion they show better with phase than with a brightfield microscope.

A radioautograph, or autoradiograph, is formed when a section of tissue containing radioactive materials is placed in contact with a photographic emulsion in the dark for a period of time and subsequently developed. The ray tracks show in the emulsion, and the problem is to locate their origin with reference to the tissue elements. The development process in strong alkaline solution tends to lessen the visibility of the tissue, and the decreased visibility of the tracks in the emulsion under a stained tissue is undesirable. Tissues mounted in balsam are too transparent for analysis, and in glycerin jelly and other aqueous media the contrast is so great that the tracks are not seen with the phase microscope. The dilemma is resolved by means of a transparentizing medium of the proper refractive index to reveal the tissue pattern and yet not obscure the ray tracks. One solution is Groat's organic phosphate mixtures described in Section 3.2 of Chapter IV; for example, a mixture of about 1.528 refractive index was satisfactory for kidney tissue.

The 8-mm objective is preferable as it has enough resolving power to show the organization of the tissue and enough depth of field to show both the tissue and track levels. The medium dark $A-$ contrast has been found useful (Fig. V.9). With $15\times$ to $20\times$ oculars, or by subsequent enlargement of a photomicrograph, adequate magnification may be obtained. With objectives of greater aperture the depth of field may not be adequate to show the tissue and the tracks simultaneously. Photomicrographs can be made also by divided exposure. Expose at the tissue layer for one-half to two-thirds of the total exposure required, turn the fine adjustment the amount previously determined to focus at the track level, and expose for the remainder of the required time. Since the path of the rays in the emulsion is often not parallel with the surface, stereophotomicrographs with bright or dark contrast phase may be
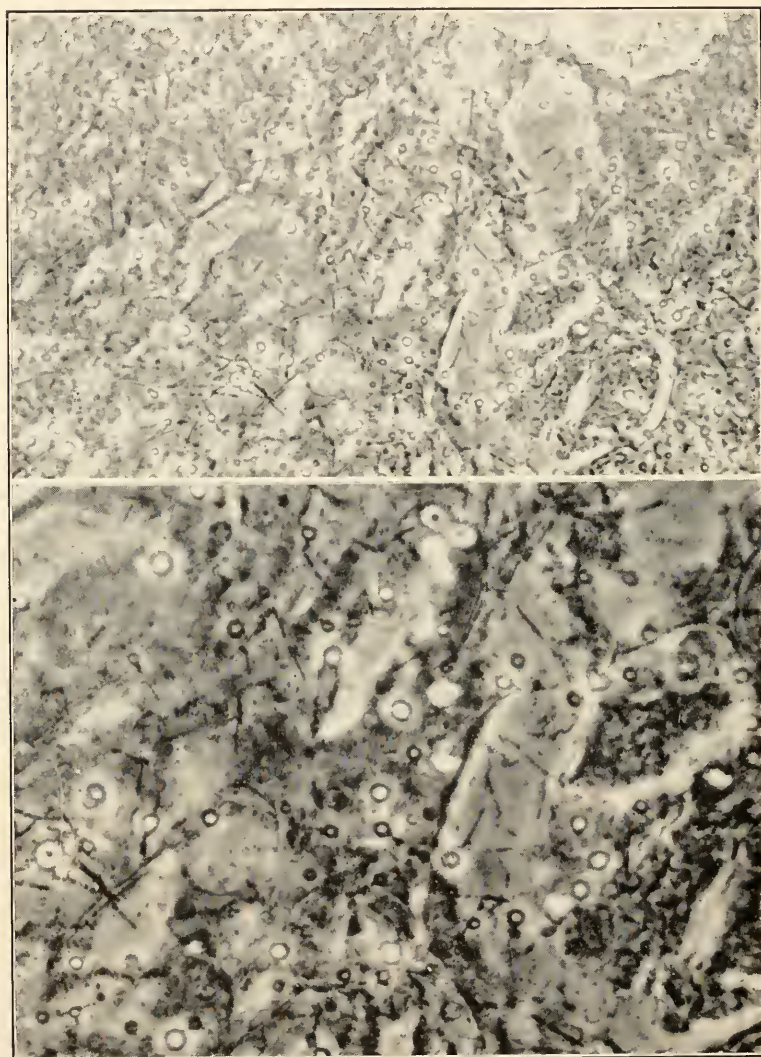
FIG. V.9.   Radioautographs of polonium in tissue, 250× and 500×.   Preparation courtesy of George A. Boyd and the Atomic Energy Project.

required. Viewing a picture made with an objective of high resolution of the tissue superimposed on a picture of the tracks with a stereoscope may be helpful. Another method is to combine two pictures, one at the tissue and the other at the track level (Boyd, 1947; Herz, 1950).

10. PHYSIOLOGICAL APPLICATIONS

The increased visibility with phase microscopy makes possible many experiments with living processes that were not possible with brightfield methods. One of the most spectacular teaching demonstrations is the cyclosis of the cells of the epithelium from the inner scales of an onion bulb. With the $0.2\lambda \pm 0.25\lambda$ diffraction plate one can see the plastids, mitochondria, and other cell constituents pass in review. The use of other materials like *Elodea* and *Nitella* are possible although the green chlorophyll obscures the more transparent constituents. Amoeboid movement is of interest because the ecto-endoplasm boundaries show clearly. Protozoa or cells from the clam gill are suitable for ciliary motion study. Changes from paralysis by sensitive serum have been described for *P. bursaria* (Section 3.2). The effects of drugs and other agents on motion may be followed under the phase microscope.

Sol-gel reversals and concentration gradients may also be observed. Starch hydrolysis and other digestive changes can be studied. The changes in fibers between feed and feces may be seen. Chemical and vitamin effects may be observed. Growth changes in microorganisms can be followed in permanent records when phase motion picture films are made. Microorganisms may be used in testing the potency of drugs for pharmacology. Evaluation of radiation effects is aided by phase microscopy (X-ray, Chase and Smith, 1949; ultraviolet, Kimball, 1949). In fact, a broad field is opened by phase microscopy for the study of function.

11. MEDICAL APPLICATIONS

No sharp distinction is possible between experimental biology and medicine other than the aim of the investigation. Much of what has been written before, especially on microorganisms and histology, is of equal interest to those in the field of medicine. Yet certain types of microscopy are more apt to be selected with respect to disease. These will now be considered.

Much of the laboratory work of clinical diagnosis can be lightened by phase microscopy. Urine sediments and casts can be seen more clearly with the phase microscope (Gradwohl, 1948; Magliozzi, 1948). Vaginal smears can be examined without staining, as suggested by Albertini (1948), by Culiner and Gluckman (1948b), and by Runge et al. (1949).

Zinser (1947) recommends phase microscopy for the diagnosis of trichomonas in fresh mounts of vaginal secretion. Fertility problems involving sperm are aided by information obtained with the phase microscope (Farris, 1948, 1950).

Many parasites such as fungus mycelium in skin scrapings, *trypanosomes*, and other organisms, can be seen to advantage with the phase microscope. Large uncencysted forms, like *B. coli*, show better with low bright contrast, and smaller ones with medium or high contrast. The sporozoites of malaria can be seen in the stomach of the mosquito *Aëdes egypti* with a medium bright $A+$ contrast phase oil immersion objective (Fig. V.10E), and trophozoites show in human blood smears (Fig. V.10F), with this and with the dark-contrast objectives (Richards, 1947). *Endamoeba histolytica* and *Endolimax nana* can be seen with low contrast $A\pm$ diffraction plates although the protoplasm of the parasitic forms is denser and they do not show as well as free living Protozoa. Encysted forms are more easily found with the $2.5B-0.4\lambda$ dark and the $0.07A+0.25\lambda$ bright contrasts, and for some of these the $A-$ dark contrast is unsatisfactory (Fig. V.10, A and D).

The phase microscope was used early by Albertini (1946–1948) for the investigation of tumors. He even devised a suitable mounting fluid for the study of cells from tumors (Section 3.2 of Chapter IV) and reported that the same details could be seen in the unstained living cells with phase as after staining with brightfield microscopy. In addition fresh material was preferred for diagnostic procedures. Cells were found in body fluids and exudates. Albertini described dedifferentiation, disorganization and regenerative processes.

Oliver et al. (1947) and Paff et al. (1947) examined tumor scrapings and tissue cultures of tumor materials. With the phase microscope granules could be followed in the living cells which they believe are concerned with heparin formation. The material came from a spontaneous mast cell tumor in a dog. The same granules were seen in tissue cultures from such tumors.

Zollinger (1948a) compared findings with brightfield and phase microscopy and began a series of studies on normal and atypical tissues. Blister formation, called potocytolysis, was reported along with observations on the cell membrane (Zollinger, 1948b). The effects of fixing agents and other chemicals were tested on resting and dividing cells. Formalin, acids, alcohol, and acetone caused the nucleus to appear brilliant (more refractile), whereas alkali, M NaCl, and distilled water turned it hazy. The nuclear membrane was thought not to be dissolved during mitosis. In another paper Zollinger (1948c) investigates
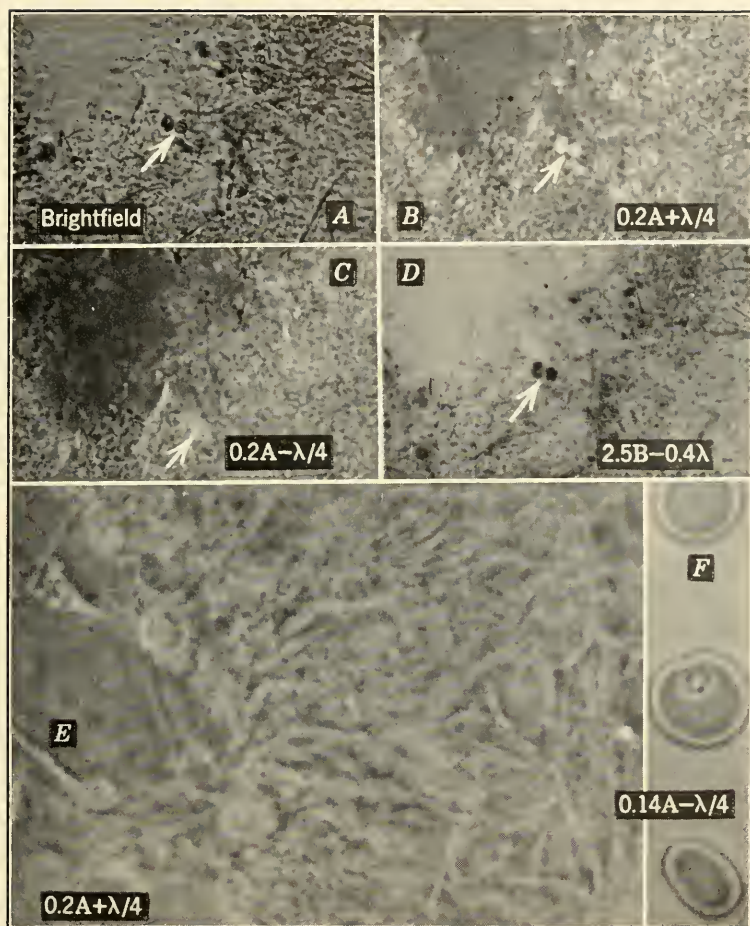
Fig. V.10. *A–D*, cysts of *Giardia lamblia*, 1000×. *E*, malaria in tissue of mosquito stomach, 500×. *F*, malaria in human red blood cell, 1250×. All unstained.

cytology of dying and dead cells, especially with respect to the nuclear changes. Cole (1948) discussed the value of the phase microscope in the investigation of the osteopathic lesion. Flotation methods are described by Fawcett et al. (1950) for separating malignant cells from blood and serous fluids.

Larger tumor cells and cytoplasmic detail are seen best with $0.35A\pm0.25\lambda$ to $0.2A\pm0.25\lambda$, smaller cells and nucleoli with 0.2–$0.14A\pm0.25\lambda$, mitochondria with $0.07A+0.25\lambda$, and small granules with $0.2A+0.1\lambda$ diffraction plates.

Leprosy bacteria from treated cases appear different from those from florid cases, and aggregations of bacteria in globi are described by Richards and Wade (1949). Phase microscopy in hematology was discussed in Section 4 of this chapter. Its application in pathological cytology is promising as demonstrated by Dustin (1949) for pycnonecrosis or nuclear destruction studies, as well as in showing changes from irradiation and radiomimetic poisons. The pathologist can examine small cellular granulations, especially with the B — dark-contrast phase objectives, and can often distinguish autolysis from degeneration.

Thus, the use of the phase microscope in investigative medicine promises the development of improved methods that will become routine in clinical, forensic, and laboratory medicine.*

* Dustin (1949, p. 84) has also predicted: "Il nous paraît que la microscope de phase deviendra un outil d'utilization courante, tant dans la recherche qu'en practique médicale."

INDUSTRIAL APPLICATIONS OF PHASE MICROSCOPY

The technics and materials of industry no longer are separated from those in other fields. Although this chapter concerns materials from an industrial viewpoint much of it will be of interest to others; likewise, parts of the previous two chapters will be useful to industrial microscopists. All three chapters should be read for a complete understanding.

The visualization of transparent materials with small differences in refractive index, or of slight absorption or pigmentation, is helpful in industrial microscopy for the identification of materials and impurities therein, for the control of processing, such as salting-out, homogenization, solution, dispersion, polishing, and for the examination of surfaces and changes in them from weathering and abrasion.

1. CHEMICALS, CRYSTALS, AND MINERALS

Transparent, uncolored crystals having a slight difference in refractive index from their surround, or mother liquor, may be seen clearly with the phase microscope when they are too transparent for brightfield microscopy. Because of the increased visibility, form and size may be determined to a degree of smallness beyond the capability of the bright-field microscope. Larger crystals show better with low-contrast $(0.2A\pm0.25\lambda)$ and the smallest visible ones with high-contrast $(0.07A\pm0.25\lambda)$ diffraction plates. Both bright and dark contrast are useful, and the choice usually depends on the conditions and needs of the examination (see the suggestions in Chapter IV).

Microcrystals of paraffin from isopropyl alcohol (Fig. VI.1, E and F) are of interest. Since the crystals are very small, only the rolled edges show with polarized light, and these were mistakenly interpreted to be acicular crystals. With phase they appear as thin plaques with a hexagonal symmetry, which is more suitable for waxing paper and other materials. The thin plates of β-naphthol are readily seen (Bennett, 1946), and stereophasephotomicrographs of them showed small spicules of interest in filtration procedures (Fig. IV.6B).

Emulsions of other than densely pigmented materials show well with

223
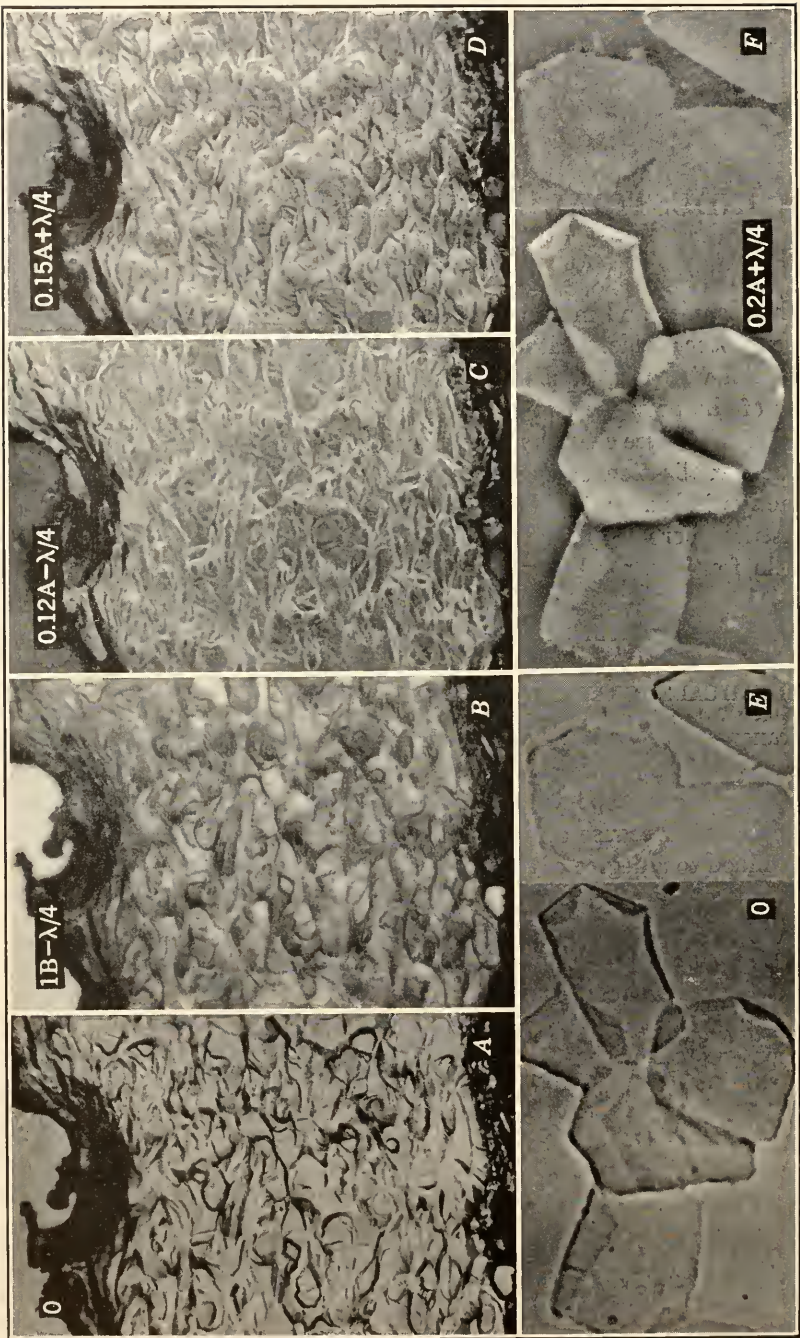
Fig. VI.1

the phase microscope. Water-in-oil emulsions are generally revealed with $0.2A+0.25\lambda$ and $0.14A-0.25\lambda$ diffraction plates in the oil immersion objective, and oil-in-water emulsions are often seen better with $0.2A+0.25\lambda$ and $2.5B-0.25\lambda$ diffraction plates. In some cases, especially when measurement is to be made, the $0.14A-0.25\lambda$ plate is preferable. To arrest the Brownian and other movements usually encountered with these preparations, photomicrographs are required and the measurements made on the photographs. Suggestions for making preparations are given in Sections 3.3 and 3.6 of Chapter IV (see also Section 3 of this chapter). Phase identification is possible and sol-gel reversals may be examined with the phase microscope.

Refractive index determination is more sensitive when a phase objective is used. Differential visual contrast may be obtained by mounting the specimen in a medium of proper index (see Section 3.2 of Chapter IV).

Smithson (1946, 1948) found phase microscopy to have the following advantages in mineralogy: index differences of less size were visible, relief was improved, and heterogeneity was shown. The phase microscope did not show strain. Adding a Polaroid polarizer to the condenser showed "twinkling" with less birefringence, inclusions, and intergrowths, such as one feldspar with another. Using a polarizer and an analyzer with phase sometimes was helpful and other times not, depending on the nature of the specimen. Zoning was shown better in plagioclase feldspar, as was the relation of the zoned regions to the surrounding feldspar. Smithson points out that path differences arising from differences in thickness, differences in compensation, and, with polarized light, differences in refractive index arising from optical orientation are made visible with the phase microscope; but it may be difficult to determine which are involved, especially when roughness of the specimen is also part of the problem.

Stereophotomicrographs should assist in evaluating the roughness factor, and replica technics also should be helpful. When two colorless isotropic substances with only slight differences in refractive index are intermingled, the phase system is the only effective microscopical method for observation. For example, a phyllite of silica and feldspar clearly showed boundaries with a $0.2A+0.25\lambda$ diffraction plate when the index difference was only 1 in the fourth decimal place.

The mathematical analysis of the combined effects of phase and polar-

FIG. VI.1. A–D, paraffin crystals supporting a thin tissue section, 135×: A, brightfield. B, dark-contrast (B−) phase. C, dark-contrast (A−) phase. D, bright-contrast (A+) phase. E–F, paraffin microcrystals from isopropyl alcohol, 1250×: E, brightfield. F, bright-contrast phase.
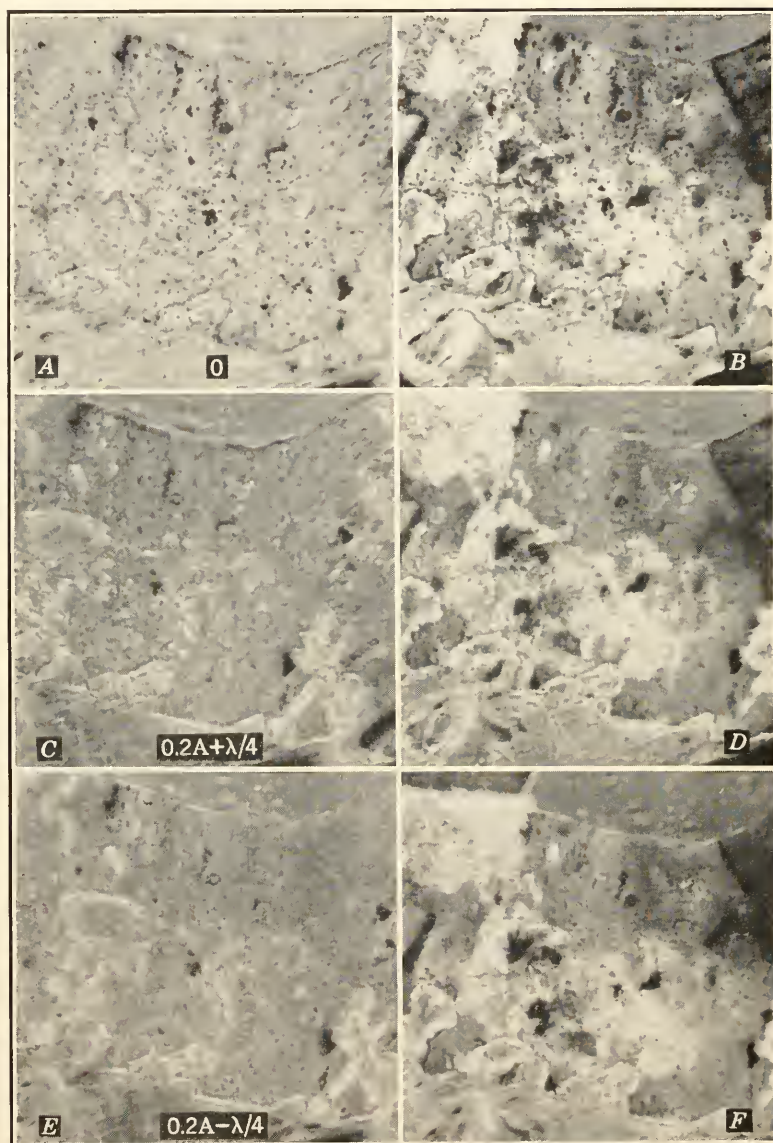
Fig. VI.2.   Microgranite, 75×.   A, brightfield.   B, polarization.   C, bright-contrast phase.   D, bright-contrast phase plus polarization.   E, dark-contrast (A —) phase.   F, dark-contrast phase plus polarization.

ization with various shaped anisotropic specimens is very complicated and incompletely known at present. With such specimens the addition of a polarizer, an analyzer, or both may give either appreciably better detail or may lessen the contrast. This can be done easily with pieces of Polaroid (sextant grade H is recommended) and is worth trying on an empirical basis. The pictures of microgranite (Fig. VI.2) illustrate some of the possibilities of combined phase and polarization microscopy.

2. CLAY AND DUST

Samples of clays usually contain a considerable range of particle sizes, and more than one diffraction plate may be necessary for the complete observation of the sample. The larger particles usually show better with $0.2A \pm 0.25\lambda$ and the smaller ones with $0.07A \pm 0.25\lambda$ diffraction plates. When the range of sizes is too great, the particles may be separated by sedimentation. Some specimens may be examined to advantage with $B-$ diffraction plates. By altering the refractive index of the mounting medium, contrast may be changed to give optimal visibility. In fact, it is possible to make some components invisible with a mounting medium of the same refractive index as the unwanted grains, thereby facilitating the examination of the other particles. Visibility is improved with counting chambers having the lines ruled into the glass (Köhler and Loos, 1941; Magliozzi, 1948).

By varying the dispersion difference between the specimen and its surround by means of an appropriate mounting medium, it is possible to add color contrast to the densiphase contrast from the phase microscope. Dust containing silica mounted in nitrobenzene ($n_D = 1.55$) reveals the silica as violet-colored particles when a $0.2A + 0.255\lambda$ or a $0.2A + 0.35\lambda$ phase objective is used. This simplifies finding the smaller particles and provides differentiation when counts are made to estimate the relative composition of a sample. Bright-contrast $(A+)$ phase objectives are preferable, because they show the colors better than the dark contrasts, and the eye sees small bright objects on a darker field more easily than dark ones on a bright field (see Section 3.3 of Chapter IV).

Dust counts made with a phase microscope will be more accurate because of the increased visibility of the particles and more complete because smaller particles will be seen. These differences should be kept in mind when counts made with the phase microscope are compared with those made with a brightfield microscope. With proper choice of mounting or dispersing medium, differential dust counting will be possible for components of the sample that look alike with the brightfield microscope.

3. FOODS, DRUGS, AND PHARMACEUTICALS

The phase microscope is useful in identifying foods, revealing impurities, and evaluating and controlling processing methods. Homogenization, which is important for milk and for salad dressings, may be evaluated with a $0.2A+0.25\lambda$ diffraction plate in a 4- or 1.8-mm objective. Emulsions for salad dressings usually show well with this or with a $1B-0.25\lambda$ or $0.14A-0.25\lambda$ diffraction plate. As pointed out in Section 3.1 of Chapter V, it is usually not possible to identify a single coccus bacterium or distinguish it from a fat globule of the same size. Bacteria of other sizes and shapes or of different optical density may be seen and the number present determined. Inorganic particles such as undissolved crystals are made visible in mayonnaise and in similar materials.

Small changes resulting from processing foods may be seen, such as the hydrolysis of starch, or the results of cooking. With a $0.14A+0.25\lambda$ diffraction plate, partially hydrolyzed starch shows the changes in the grains when mounted in Crown Immersion Oil. Another specimen was seen better in a water mount with a medium, rather than the low, dark $(A-)$ contrast. Some experimentation is necessary to determine the most appropriate procedures. The effect of digestion may be studied with a phase microscope by comparing the feed and the feces.

Insect parts that are relatively transparent are readily revealed with the phase microscope, which makes it valuable in discovering and identifying such filth in dirty food. Transparentizing the specimen with a suitable mounting medium will assist in finding the extraneous matter (see Section 3.2 of Chapter IV). The problem of mold counting in tomato products was discussed in Section 3.2 of Chapter V.

Many applications of the phase microscope are possible in the drug and pharmaceutical industry. The purity of cultures used in making biologicals can be determined, the nature of emulsions and the degree of inhomogenization can be seen, and impurities may be found and identified. The components of preparations containing paraffin oil, agar, yeast, and similar materials and their relation to each other are easily seen. The $0.14A+0.25\lambda$ is the most useful single phase objective for such a specimen, although the $2.5B-0.25\lambda$ is better for yeast and the $1B-0.25\lambda$ is better for smallest visible oil globules and agar plaques. The dark-contrast $(A-)$ phase objectives are also useful for emulsions (see Section 3.3 of Chapter IV and Section 1 of this chapter). The 8-mm objective will be helpful for many specimens which do not require the highest resolution, because of its longer working distance and larger field of view.

4. FAT, GREASE, OIL, AND SOAP

Mixtures of these materials reveal their general character with a $0.2\lambda+0.33\lambda$ or a $0.2\lambda-0.25\lambda$ diffraction plate in a 16-mm objective. At higher magnifications the 0.2 or $0.14\lambda\pm0.25\lambda$ plate usually gives adequate contrast. The number of phases in the system and the approximate amounts are readily determined with the phase microscope, also the presence of liquid crystals, or other aggregates. Polarized light sometimes is helpful with phase contrast (see Section 1).

Microcrystals of paraffin were considered in the first section of this chapter. The structure within a wax is often important and may be revealed with the phase microscope. Figure VI.1, A–D, shows the appearance of the paraffin part of a section of liver embedded in a paraffin block with the different contrasts. For adequate support when thin sections are to be cut, the crystals must be small enough to fill all gaps around and within the tissue. These sections were cut with a microtome, mounted, and observed before the paraffin was removed.

The structure of a grease is important as well as its composition. This can be seen in a direct sample, a melted sample, or after working the grease between two microscope slides. Liquid crystals in soft soaps may be seen, and some shampoo soaps make good demonstrations.

5. PAINT AND PIGMENTS

Very dense fine colored pigments may be seen better with the brightfield microscope, but the less opaque pigments show better with the phase microscope. It is possible to evaluate grinding and disperison by direct examination of the product, likewise emulsification when liquid components are dispersed in the product. The shape of colorless, or slightly colored, materials may be seen within the limits of the optical microscope. This may be important when the particles can become orientated later from spreading by the paint brush, or roller.

Sections of painted or varnished wood or other material may be examined and the surface protective layers measured with the phase microscope. The nature of enamel surfaces and the effects of abrasion and weathering have been studied with the aid of ethylcellulose replicas by Richmond and Francisco (1949). The phase microscope reveals more detail in replicas than the brightfield microscope, and low to medium contrast phase objectives in either bright or dark contrast are appropriate. When reflection from the surface is adequate, phase vertical illumination should be considered. (See Section 8.)

6. GLASS AND PLASTICS

Glass surfaces have proved one of the most interesting and difficult microscopical specimens. However, slight differences in thickness from minute surface irregularities change the phase of light passing through them and may therefore be seen with the phase microscope. Loos et al. (1941) reported phase useful for the study of the polishing of glass surfaces. Circular polishing marks and stains not visible with other
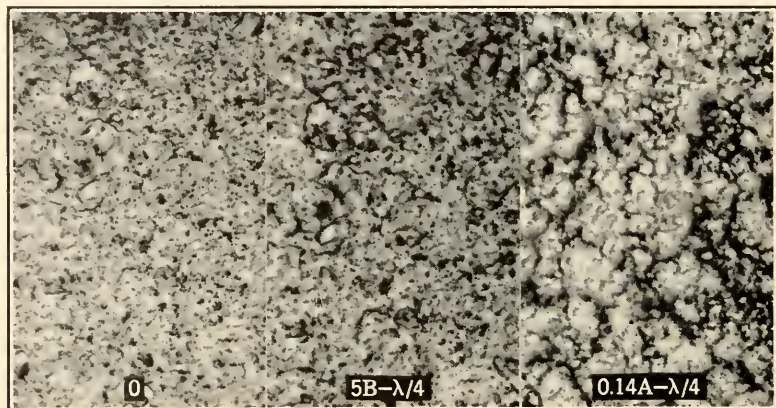
Fig. VI.3. Fine ground glass, 400×. *Left*, brightfield. *Center*, dark-contrast (B−) phase. *Right*, dark-contrast (A−) phase.

microscopical methods were photographed and described by Bennett et al. (1946), and Lyot and Françon (1948) examined faults from polishing glass by phase microscopy using stereoscopic technic. Since there is no satisfactory explanation of the nature of polishing of optical glass surfaces, phase microscopy promises information of both heuristic and practical value. Bright contrast reveals very small defects in the glass surface, and the $0.2A+0.33\lambda$ plate has been found best for the 16-mm objective. Slight deposits of metals on the surface are also revealed. On the other hand, for the examination of fine ground surfaces (Fig. VI.3) the $5B-0.25\lambda$ reveals more detail than the bright $(A+)$ plate, and the dark $(A-)$ contrast is not useful for this application. The picture shows a finely ground surface in air with an 0.18-mm cover glass placed over it to maintain the correction of the 4-mm objective.

Smaller fragments of glass may be examined in immersion oil or other suitable mounting fluid (Fig. IV.1). Seeds such as occasionally plug the spinneret of fiber-making equipment may be studied with the phase microscope for identification and structure, and the information gained should suggest means for minimizing the numbers per melt. Like other

specimens, small glass particles require higher contrast objectives than
larger ones, and the contrast can be adjusted for the best visibility by
choosing the proper kind and contrast of diffraction plate and the proper
immersion medium.

Transparent plastics may be examined for regions of inhomogeneity
and for impurities. Cotton fibers in the sheet can be recognized with a
5B −0.25λ objective. The "dope" may be examined before processing,
and the processed product examined either directly or after sectioning to
obtain preparations thin enough for microscopic examination. With a
long-focus condenser, sheets up to about $\frac{1}{2}$ inch in thickness may be
examined. The 0.2A+, 0.14A+, and 5B −0.25λ diffraction plates are
preferable for this. Further information for rayons will be given below.
The extent of dyeing of cellophane-like materials may be determined
from the examination of cross sections. Medium contrast A+, A −, or
B − are suitable, depending on the material and the pigment.

Replica technics may be applied to the examination of glass and plastic
surfaces, and some of these surfaces have enough reflectivity to make
the phase vertical illuminator worth while (see Section 8).

7. PAPER

The phase microscope is useful to show the breakdown and condition
of the fibers, freedom from lignin and other undesirable materials, and
for examination and size determination of baryta and other materials
for smoothing the surface finish. The color reactions of the special dyes
are more useful for fiber identification and show better in brightfield.
Typical changes in two common types of papers with different kinds of
phase objectives are illustrated in Fig. VI.4.

Sections of paper may be examined for a study of composition and
for the measurement of ink penetration below the surface. Low-
contrast (0.2A±0.25λ) and high-contrast (5B −0.25λ) objectives are
helpful in paper microscopy.

8. METAL SURFACES

Two methods are available with the phase microscope. When the
surface has considerable specular reflection, the vertical phase il-
luminator may be used. The replica technic is applicable to metal as
well as to other surfaces. Marx and Diehl (1948) have used phase
microscopy with replicas from anodized aluminum.

Jupnik et al. (1946, 1948) described a phase vertical illuminator
equipped with both bright- and dark-contrast diffraction plates and the
examination of metals with it. With monochromatic green light from the
mercury arc, considerable detail could be seen on specularly reflecting
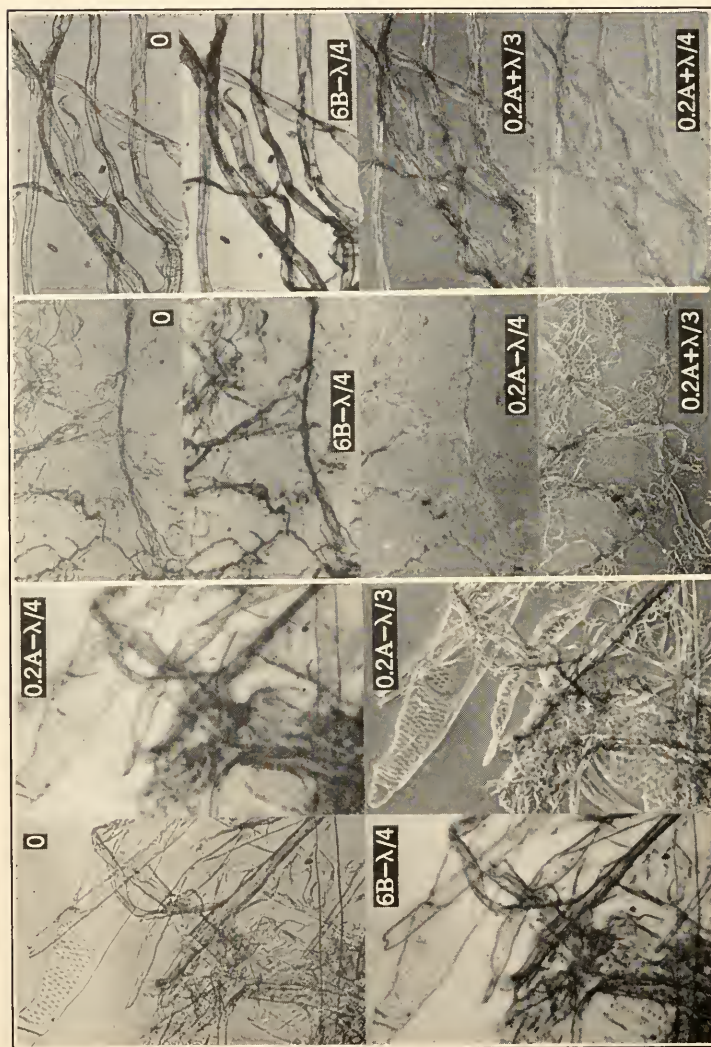
Fig. VI.4.   Paper fibers, 50 ×: *Left set*, Kraft wrapping paper. *Center panel*, filter paper pulp, dried. *Right set*, same in wet mount.   0 indicates brightfield; the others were taken with the phase objectives indicated.

surfaces. Any diffusion of the incident light precluded this method. Scratches and sleeks showed well in bright contrast with a 0.12A+0.25λ diffraction plate. Grain boundaries were made more visible in high-speed steels, and carbide segregation showed with bright and with dark (0.12A−0.25λ) contrast. Stains, etching, and polishing effects could be studied by this means.

In England, Cuckow (1947, 1949) concluded, after examination of metals, that more information is revealed by the phase vertical illuminator than by the study of replicas. He found it particularly good for the assessment of surface levels. Martensite and transformed
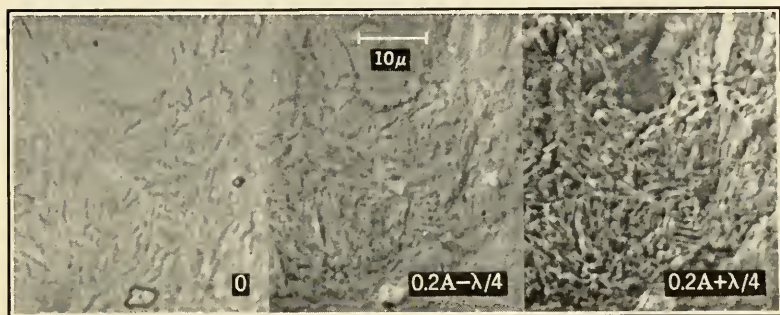
FIG. VI.5. Silica replica from a steel surface, showing pearlitic structure, ca. 1000×: Left, brightfield. Center, dark-contrast (A−) phase. Right, bright-contrast phase.

austenite showed well. For some problems he believed it to be more valuable than replica methods would be with the electron microscope, in general, more convenient to use, and sometimes a helpful guide to aid in understanding the very fine detail revealed by the electron microscope. Taylor (1949) has described the Cooke vertical phase illuminator and recommends it for metallurgy and mineralogy. Crystal boundaries could be seen as well as slight differences in level from etching and polishing.

Coarse detail may be studied in relatively thick replicas (Fig. IV.2). Finer detail requires thinner replicas, and for the usual Formvar replica prepared for the electron microscope the 0.05A+0.25λ and 0.2A+0λ plates are very good, and the 0.2A±0.25λ plates are useful. For fine detail such as dots, the 0.07 transmission is useful. Increased detail can be obtained with the phase microscope if the replicas are shadowcast with a dielectric. Very fine detail of replicas can be seen with the phase microscope, such as the differences from path differences of 40 to 50 A thickness in Formvar produced by lightly etched metal surfaces. Pearlitic structure in a silica replica is shown in Fig. VI.5. Replicas for

the study of surface roughness (Hershman, 1945) should be easier seen and evaluated with the phase microscope.

9. RUBBER

The phase microscope is useful for the investigation of the homogeneity of rubber and for the examination of fillers. With the 1.8-mm phase objective it is possible to distinguish five different phases in one specimen. Fillers, such as carbon, channel and chrome blacks, silica, etc., may be examined within the limits of the light microscope, and
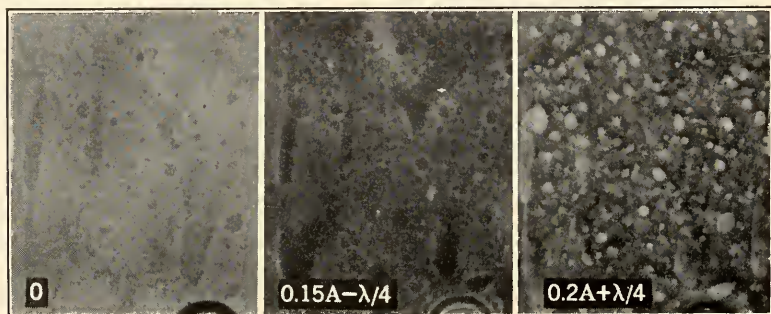
Fig. VI.6.   Emulsion of rubber and resin, 800×.   *Left*, brightfield.   *Center*, dark-contrast (A−) phase.   *Right*, bright-contrast phase.

for this the 0.07A+0.25λ diffraction plate in an oil immersion objective is recommended, although the same transmission in an A− plate would be appropriate when dark contrast is preferred. Lesser transmissions are not so good for such fine detail.

In a two-phase system (Fig. VI.6) it is possible to identify the continuous and the dispersed phases when their refractive index is known. As was pointed out in Chapter IV the greater path is bright with an A+ and dark with an A− diffraction plate. In this specimen the two phases show with brightfield because the inner phase was slight amber in color. Examining a number of the inner-phase globules we note that they are bright with the A+ and dark with the A− objective, which indicates that the inner phase is of the higher refractive index. In this case it was known that the resin had a higher index than the rubber and therefore this is a *resin-in-rubber emulsion*. To avoid possible ambiguities, particles of several sizes should be examined for consistent behavior in reversing contrast.

10. TEXTILES

A Zeiss phase microscope placed at the disposal of the Höchst works of I. G. Farbenindustrie led to early trial and discovery of its utility in

this field (Remuth, 1947).   Phase microscopy was reported for observing bacterial and enzymatic decomposition of wool, fine detail in 1- to 3-μ cross sections of wool, bacteria and fungi on unstained fibers, fine structure in thin sections, inclusions, turbid portions and samples with small density differences, thickening pastes and their penetration, liquid crystals in liquid soaps and lubricants, solid crystals and thin plates, particles embedded in fibers such as silicates, and fissures in fibers due to laundering.   Objections to the method included failure with thick objects, failure with large differences in index such as between a fiber and a delusterizing agent, and failure with pigments and with oblique light.   Modern equipment with long working distance condensers and phase objectives with various kinds and types of diffraction plates have met many of these objections.

Royer and Maresh (1947, 1949) also summarized many of the applications of phase microscopy in this field through a discussion of thickness variations, rayon cross sections, pigments, emulsions and dispersions, and thin coatings on textiles, paper fibers, leather, and pigments.

The scales on wool show well without stain with a medium A $-$ dark-contrast phase objective.   Lanaset coating on the wool scales may be seen with a $0.07A+0.25\lambda$ diffraction plate (Calco, 1947; Royer and Maresh, 1947).   Hairs may be studied when not too pigmented; the medium dark-contrast A $-$ and high bright-contrast A $+$ plates have usually been found preferable for the lighter ones and the $5B-0.25\lambda$ for darker pigmented hairs (Chase, 1949).   Pigmented hairs are usually examined with the aid of a replica of their surface, and the phase microscope will improve the visibility of details seen in the replicas.   For a nigrosine method like that of Koonz and Strandine (1945) the $1B-0.25\lambda$ plate would be preferable, and for transparent replicas such as described by Hardy and Plitt (1940) either bright- or dark-contrast low or medium $(0.14-0.2A\pm0.25\lambda)$ phase objectives would be useful.

Farr (1946, 1949) has shown the value of the phase microscope in determining the structure of cotton fiber and related materials.   These fibers may be examined as found and then during or after treatment with solvents such as cuprammonium, or with macerating agents.   Bright contrast offers some advantage in the study of fibers.   For single fibers the phase microscope is useful in assessing maturity, but for masses of fibers the conventional staining technics are better.

"Dopes" may be examined for gel inclusions and for undissolved fibers.   The $0.07A+0.25\lambda$ plate is better for the former and the $0.14A-0.25\lambda$ and $1-2.5B-0.25\lambda$ plates for the latter, depending on their size.   Rayon yarn fibers and their cross sections (Fig. VI.7) may be examined when mounted in paraffin oil.   The extent of the skin shows, and when mineral or oil globules have been added for delusterification
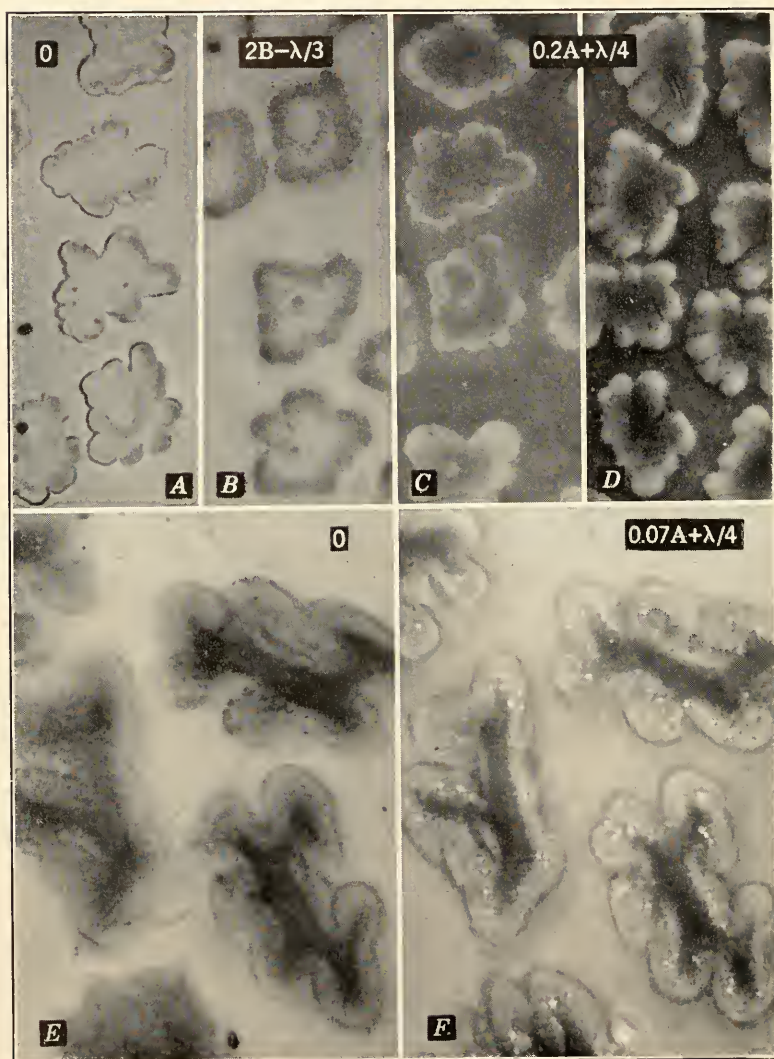
FIG. VI.7. Rayon fibers in cross section.   A, brightfield.   B, dark-contrast (A−) phase.   C, D, bright-contrast phase, 1000×: E, F, fibers containing oil droplets for delusterification, 1100×.   E, brightfield.   F, bright-contrast phase.

their location may be seen in the fiber. Thin sections are preferable (especially for photomicrographs) because of the limited depth of field of the oil immersion objective. Irregularities and marks on the surfaces of the fibers may also be observed.

For the more birefringent synthetic fibers the high bright contrast $(0.07\lambda+0.25\lambda)$ usually shows more detail than does the $A-$ or $B-$ diffraction plates. By a proper choice of phase and mounting medium it is possible to examine the details of the fiber, including any surface patterns present. Refractive indices of some textile fibers are given in Table V.1B. Special mounting media have been devised by Bradfoot and Schwartz (1948) for textile microscopy (see also Table IV.1).

Fewer papers have been published in the industrial field, probably because publication usually is deferred until the product has been marketed. More applications may be expected with more general application of the phase microscope. The discussion in this chapter points the way.

CHAPTER VII

APPENDIX: THE DIFFRACTION THEORY
OF PHASE MICROSCOPY WITH
KÖHLER ILLUMINATION

1. INTRODUCTION

The following diffraction theory of image formation in the microscope
will be derived under the suppositions that the illuminating beam is
unpolarized and that the microscope has been adjusted as in Köhler
illumination. The phenomena of phase microscopy are different with
Köhler and with critical illumination but can become highly similar
under conditions that are well satisfied in the normal usage of the
typical microscope. Even the theory for Köhler illumination becomes
cumbersome when the integrations for the total energy density in the
image are referred to the radiating atoms in the source of light. Sim-
plicity of argument will be obtained by supposing that the virtual image
of the source as imaged by the combined lamp and substage condensers
acts for the purposes of microscopy as a self-luminous source. This
supposition can be justified with at least fair approximation when the
speeds of the lamp and substage condensers are high and when the
opening in the diaphragm of the substage condenser is not too narrow.
The effect of closing down the field stop in Köhler illumination is to
decrease the speed of the lamp condenser and thus to spread the diffrac-
tion image of a point in the source over a greater area at the condenser
diaphragm. If the supposition as to the self-luminous character of the
virtual image of the source is to be valid, the field stop should be opened
far enough so that the diffraction image of a point in the source is small
compared with the width of the opening in the diaphragm of the sub-
stage condenser. We note that simplifications occur also when the
field stop is closed to point dimensions, but a discussion of this specialized
case will not be included.

In integrating over the virtual image of the source, we shall obtain
additional simplicity of argument by omitting a summation procedure
which leads to a generalized statement of Lambert's law. The effect
of introducing Lambert's law into the diffraction integrals will, however,

238

be stated. Curiously enough, Lambert's law leads to a simplification of the diffraction integral for the total energy density in the image.

The laws of microscopy may be derived from two different lines of attack which lead to substantially the same conclusions. The first attack was outlined by Abbe but was not formulated analytically by him. In Abbe's attack one selects an arbitrary point in the source of light and computes the amplitude and phase distribution produced over the plane conjugate to the source of light (the plane of the diffraction plate) by the coherent light radiated from the selected point. This computation or formulation takes into account the modifications which result from the passage of the light through the object specimen. The corresponding amplitude and phase distribution produced over any selected image plane is now determined with the aid of Kirchhoff's law from the known amplitude and phase distribution over the plane of the diffraction plate. The selected image plane is not necessarily conjugate to the object plane. The *partial energy density* is defined as the distribution of energy density produced over the selected image plane by the coherent light radiated from the selected point in the source of light. The partial energy density is proportional to the square of the absolute value of the amplitude and phase distribution produced over the image plane. Since different points in the source of light act as independent radiators, the *total energy density* produced over the image plane by all points in the source of light can be found by summing or integrating the partial energy densities produced by all points in the effective area of the source of light. Whereas Abbe's procedure can be outlined with ease, it can become very cumbersome to formulate analytically unless the effective area of the source of light is small and is centered upon the optical axis. Abbe's procedure, moreover, gives more than the required amount of information because the amplitude and phase distribution produced over the plane of the diffraction plate is rarely of direct interest.

We shall formulate the following attack because it is simpler and more amenable to analysis than the attack outlined by Abbe. Beginning with the coherent light radiated from an arbitrary point in the effective area of the source of light, we state the amplitude and phase distribution over the light wave as it emerges from the object plane. We then apply a transfer property of the primary diffraction integral to formulate directly the corresponding amplitude and phase distribution produced over the selected image plane. The partial energy density is proportional to the square of the amplitude and phase distribution produced over the image plane. The total energy density produced over the image plane by all points in the effective area of the source of light is obtained by integrating the partial energy density with respect to the

elements of area over the effective area of the source of light. If the amplitude and phase distributions are expressed as complex numbers, the partial and total energy densities are automatically the time average of the instantaneous partial and total energy densities. For this and other reasons of mathematical convenience, we prefer to express the laws of microscopy in terms of complex numbers. It should be noted that this attack is general enough to include the essential laws of both phase and ordinary microscopy as well as the laws of image formation in a variety of other optical and non-optical systems. Furthermore, the method of attack includes the combined effects of the source of light, of the object specimen, and of the optical system upon the image of the object specimen.

The method can be adapted to either Köhler or critical illumination. We shall discuss the adaptation to Köhler illumination since optical systems are most frequently adjusted for Köhler illumination or other equivalent forms of illumination.

It is emphasized that the following theory applies primarily to the case in which the light is transmitted by the object specimen. In applying the theory to microscopy with vertical illumination, great caution has to be exercised in constructing the appropriate object function. This is because the modifications of the amplitude and phase of the illuminating wave can become more complicated when the wave is reflected by the object specimen than when the wave is transmitted by the object specimen. Thus with vertical illumination the incident wave may be reflected from one or both surfaces of the specimen and from particles or layers within the specimen. By taking advantage of the dissimilarity of the phenomena of transmission and reflection, the ordinary or the phase microscope can be made to yield additional information about the object specimen.

In deriving the diffraction integrals governing image formation, we shall apply Kirchhoff's laws as they have been reformulated by Luneberg (1944). Consequently, the theory will be limited in generality by the restrictions stated by Luneberg. The most fruitful problem is not, however, to evolve a theory that is free from limiting restrictions but rather to construct a theory whose integrals can be solved by methods of the present or of the near future. To this end the primary diffraction integral will not be applied in its most general form as given by Luneberg. Instead, we shall be content to evaluate the primary diffraction integral by integrating over the rays in the axial bundle. This procedure involves the determination of the imagery for off-axial points in terms of the data which belong to a suitably chosen axial point.

2. THE PRIMARY DIFFRACTION INTEGRAL

An integral which we shall call the primary diffraction integral has been reformulated from fundamental considerations by Luneberg (1944). We shall begin with the form of this integral as presented by Luneberg and shall modify it for the purpose of rendering it more suitable to the theory of phase microscopy.
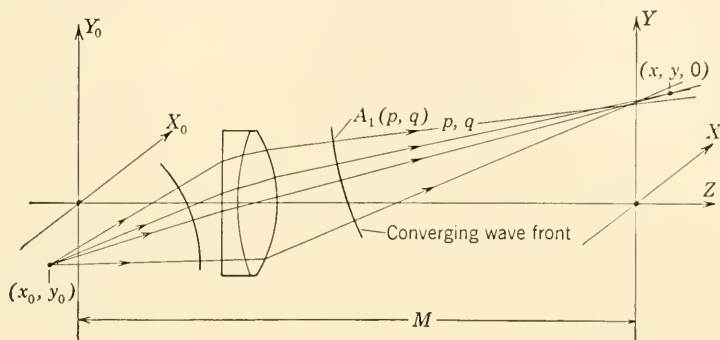
FIG. VII.1. Notation with respect to the most general formulation of the primary diffraction integral.

Let X_0Y_0 and XY denote a conjugate pair of object and image planes, as in Fig. VII.1. A point (x, y, z) falls in the conjugate (sharply focused) image plane only when $z = 0$. Suppose that an "unpolarized" dipole radiator of strength unity is located at the object point x_0, y_0 and that it is desired to find the amplitude and phase distribution $U(x - Mx_0, y - My_0, z)$ produced by the unpolarized dipole and the optical system. Then in accordance with Luneberg we set

$$U(x - Mx_0, y - My_0, z) \equiv F(x, y, z); \tag{2.1}$$

$$U(x - Mx_0, y - My_0, z) = \frac{1}{2\pi} \iint \phi(p, q) e^{ik(W+px+qy+sz)} \, dp \, dq \tag{2.2}$$

in which the integral extends over the optical direction cosines p, q of the normals to the converging wave front (Fig. VII.1) in the image space whose refractive index is n. By definition,

$$k \equiv \frac{2\pi}{\lambda} ; \tag{2.3}$$

$$s \equiv (n^2 - p^2 - q^2)^{\frac{1}{2}}; \tag{2.4}$$

$$W = W(x_0, y_0, z_0; p, q) \tag{2.5}$$

is Hamilton's mixed characteristic. Furthermore, if $A_1(p, q)$ denotes the amplitude variation over the converging wave front,

$$\phi(p, q) = \frac{A_1(p, q)}{(n^2 - p^2 - q^2)^{\frac{1}{2}}} \qquad (2.6)$$

when the converging wave front does not depart appreciably from a sphere. Both $A_1(p, q)$ and Hamilton's mixed characteristic can be determined by triangulating rays through the optical system and may be regarded as known properties of a given system.

Let all distances be measured in number of wavelengths. x_0, y_0, z_0, x, y, and z are then dimensionless. Equation 2.2 assumes the form

$$U(x - Mx_0, y - My_0, z) = \iint \phi(p, q)e^{2\pi i(W + px + qy + sz)} \, dp \, dq. \qquad (2.7)$$

Since z_0 is simply a parameter which determines the location of the object plane, we may take $z_0 = 0$ without essential loss of generality.

In order that the primary diffraction integral shall be amenable to simplified mathematical transformations as well as to simplified computations, we shall assume that Abbe's sine condition is obeyed and we shall replace the integration over the optical direction cosines of the normals to the wave front by an integration over the optical direction cosines of a set of factitious axial rays which become real axial rays when the object point x_0, y_0 is located upon the optical axis and when the objective is free of spherical aberration. Hamilton's mixed characteristic W now reduces to the form (Luneberg, 1944, p. 226)

$$W = W_0(p, q) - pMx_0 - qMy_0 \qquad (2.8)$$

in which M is the constant magnification ratio between the object and image planes and $W_0(p, q)$ is the usual integral over the lateral spherical aberration. $W_0(p, q)$ is to be evaluated from the data of the object point $x_0 = y_0 = 0$ upon the supposition that the reference sphere of Fig. VII.2 has been chosen so as to coincide with the axial wave front in the paraxial region. This means physically that the reference sphere will be chosen so that

$$W_0(O, O) = 0. \qquad (2.9)$$

We now introduce Eq. 2.8 into Eq. 2.7 and write

$$U(x - Mx_0, y - My_0, z)$$
$$= \iint \phi(p, q)e^{2\pi iW_0(p,q)}e^{2\pi i[p(x-Mx_0)+q(y-My_0)+sz)]} \, dp \, dq \qquad (2.10)$$

in which the optical direction cosines p, q refer to the factitious rays of

the axial bundle as in Fig. VII.2 and are limited by the numerical aperture of the objective such that

$$p^2 + q^2 \leqq n^2 \sin^2 \vartheta_m \equiv n^2 \rho_m{}^2 \qquad (2.11)$$

where ϑ_m is defined together with ρ_m in Fig. VII.2. By means of Eq. 2.10 the amplitude and phase distribution $U(x - Mx_0, y - My_0, z)$ is computed in terms of the axial data of the objective. The results obtained by means of Eq. 2.10 will therefore be highly accurate for
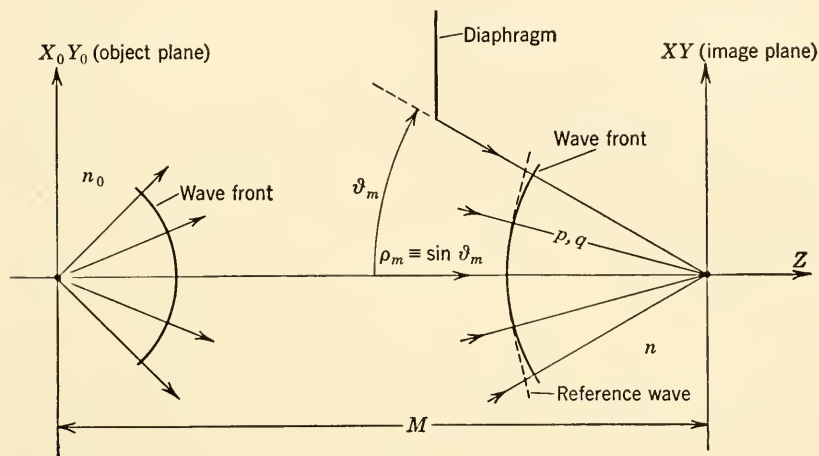
FIG. VII.2. The axial, spherical wave of reference.

object points x_0, y_0 which fall in the paraxial region and will be less accurate when x_0, y_0 lies in the extra paraxial region.

It is convenient to define the *pupil function* $P(p, q)$ such that

$$P(p, q) \equiv \phi(p, q)e^{2\pi i W_0(p,q)} = \frac{A_1(p, q)e^{2\pi i W_0(p,q)}}{(n^2 - p^2 - q^2)^{\frac{1}{2}}}. \qquad (2.12)$$

Then from Eqs. 2.12 and 2.10

$$U(x - Mx_0, y - My_0, z)$$
$$= \iint P(p, q)e^{2\pi i [p(x - Mx_0) + q(y - My_0) + sz]} \, dp \, dq; \qquad (2.13)$$

$$p^2 + q^2 \leqq n^2 \rho_m{}^2; \qquad (2.13a)$$

$$s = (n^2 - p^2 - q^2)^{\frac{1}{2}}. \qquad (2.13b)$$

Finally, it is convenient and significant to define the *afocal pupil function* $P_z(p, q)$ such that

$$P_z(p, q) \equiv P(p, q)e^{2\pi i z(n^2 - p^2 - q^2)^{\frac{1}{2}}}. \qquad (2.14)$$

Hence

$$U(\zeta, \eta, z) = \iint P_z(p, q)e^{2\pi i(p\zeta + q\eta)} \, dp \, dq; \tag{2.15}$$

$$\zeta \equiv x - Mx_0; \quad \eta \equiv y - My_0; \tag{2.15a}$$

$$p^2 + q^2 \leqq n^2\rho_m{}^2. \tag{2.15b}$$

It should be noted that $P_z(p, q) = P(p, q)$ when $z = 0$.

For purposes of analysis it is frequently convenient to require that

$$P_z(p, q) = 0 \tag{2.16}$$

when $p^2 + q^2 > n^2\rho_m{}^2$ and that $P_z(p, q)$ is given by Eq. 2.14 when $p^2 + q^2 \leqq n^2\rho_m{}^2$. Equation 2.16 is simply the statement that the pupil function is zero for rays that are blocked by the aperture of the objective. It follows from Eqs. 2.15 and 2.16 that $U(\zeta, \eta, z)$ and $P_z(p, q)$ are related as the pair of Fourier transforms

$$U(\zeta, \eta, z) = \int_{-\infty}^{\infty} \int_{-\infty}^{\infty} P_z(p, q)e^{2\pi i(p\zeta + q\eta)} \, dp \, dq; \tag{2.17}$$

$$P_z(p, q) = \int_{-\infty}^{\infty} \int_{-\infty}^{\infty} U(\zeta, \eta, z)e^{-2\pi i(p\zeta + q\eta)} \, d\zeta \, d\eta; \tag{2.18}$$

in which z is regarded as a parameter.

The presentation of the theory of phase microscopy will be simplified with the aid of the following observation. Suppose that one has constructed a theory which involves operations upon the primary diffraction integral $U(\zeta, \eta, 0) \equiv U(\zeta, \eta)$ given by

$$U(x - Mx_0, y - My_0)$$
$$= \int_{-\infty}^{\infty} \int_{-\infty}^{\infty} P(p, q)e^{2\pi i[p(x - Mx_0) + q(y - My_0)]} \, dp \, dq. \tag{2.19}$$

Then the theory for out-of-focus planes which are located z wavelengths away from the conjugate XY plane can be obtained from the theory based on Eq. 2.19, in which $z = 0$, by replacing $P(p, q)$ by $P_z(p, q)$. For simplicity of presentation we shall therefore state the laws of phase microscopy in terms of the primary diffraction integral as given by Eq. 2.19 with the understanding that $P(p, q)$ is to be replaced by $P_z(p, q)$ whenever the plane of observation is displaced from the conjugate image plane by z wavelengths. A summary of the primary diffraction integral and of the manner in which the pupil function $P(p, q)$ is to be computed will be given in the next section.

The following properties of the primary diffraction integral have been demonstrated by Luneberg (1944) and will be restated here in order to

avoid confusion as to the physical meaning of the primary diffraction integral $U(x - Mx_0, \; y - My_0)$. The complex imaginary function $U(x - Mx_0, \; y - My_0)$ is of direct physical significance in the sense that $|U(x - Mx_0, \; y - My_0)|^2$ gives the distribution of energy density produced in the image plane by an unpolarized dipole radiator. An unpolarized dipole radiator may be regarded as one that changes its orientation in a random manner in a period of time which is short compared with the smallest interval of time that can be distinguished by the receptor of the energy density, or it may be regarded as a group of independent dipole radiators oriented at random in an element of area or volume which can be considered as being infinitesimally small. $|U(x - Mx_0, \; y - My_0)|^2$ is the distribution of energy density produced by these unpolarized, that is, randomly oriented, dipole radiators. It is important to appreciate that, whereas the phase and amplitude distribution produced by a polarized radiator is physically real, the phase and amplitude distribution produced by an unpolarized radiator and hence by $U(x - Mx_0, \; y - My_0)$ is fictitious. A logically complete exposition of the theory of microscopy should therefore begin with polarized radiation and should expose in detail those considerations which lead to the laws for unpolarized radiation. A presentation of the complete theory would add a prohibitive amount of material to this Appendix and would increase the reader's difficulties in mastering the essential elements of a more general theory of microscopy. For these reasons the primary diffraction integral as given by Eq. 2.13 is sufficient for determining the energy density in the image plane when the source of light is unpolarized. Furthermore, the conclusions reached with the aid of Eq. 2.13 agree closely with the conclusions resulting from the more complete theory which takes into detailed account the effects of randomly polarized radiation. We shall continue to call $U(x - Mx_0, y - My_0)$ an amplitude and phase distribution, but we shall not claim that either it or the amplitude and phase distributions derived from it are real amplitude and phase distributions. This distinction as to the fictitious nature of the amplitude and phase distribution associated with the primary diffraction integral is usually ignored or is implied tacitly.

We remark finally that the use of the primary diffraction integral is not limited to radiating dipoles as object specimens but applies also to illuminated pinholes in an opaque slide or, more generally, to illuminated elements of area in the plane of the object specimen.

3. THE PUPIL FUNCTION $P(p, q)$ IN PHASE MICROSCOPY

The pupil function $P(p, q)$ is to be computed from the data of the axial bundle. For a more detailed statement of the method of computation and of the physical significance of the pupil function so com-

puted, the reader should consult a recent publication by Osterberg and
Wilkins (1949).   Unit spheres are drawn about the axial points O_0 and
O in the object and image space of the objective, respectively, as in
Fig. VII.3.   The unit sphere about the point O_0 is regarded as the inci-
dent wave front of reference whose amplitude is taken as the constant
unity with unpolarized light.   The unit sphere about the point O is
regarded as the locus of the corresponding spherical wave converging
upon O.   This spherical wave of reference is a wave front, and its
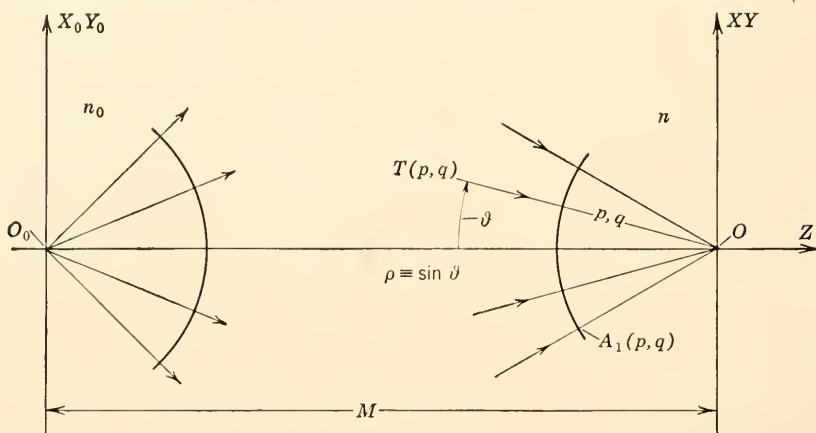
Fig. VII.3.   The reference unit spheres.

normals with optical direction cosines p, q are real rays only when
spherical aberration is absent and when the diffraction plate is either
uncoated or is coated uniformly. $A_1(p, q)$ is defined as the amplitude
variation over the spherical wave. $A_1(p, q)$ depends on the zonal
properties of the diffraction plate and on the manner in which the axial
rays are converged by the objective.   Both $A_1(p, q)$ and the phase
variation over the spherical wave can be determined by triangulating
rays from O_0 into the neighborhood of point O.   In performing this
triangulation of the axial bundle of rays, we adopt the convention that
the supporting plate (if any) which bears the coating material of the
diffraction plate is to be considered as one of the elements of the ob-
jective and that the supporting plate shall be considered as uncoated.
The usual integral over the lateral spherical aberration (Luneberg, 1944,
p. 224) determines $2\pi W_0(p, q)$, the phase variation over the spherical
reference wave.   Triangulation of the bundle of axial rays in accordance
with the above convention serves also to determine $T(p, q)$, the am-
plitude transmission along the axial rays.   Since the spherical reference

wave converges upon O and since this wave is a wave front in the paraxial region, $W_0(0, 0) = 0$. $T(p, q)$ shall be normalized such that $T(0, 0) = 1$. It has already been assumed in stating the primary diffraction integral that the objective satisfies Abbe's sine condition. When the bundle of axial rays is converged in accordance with Abbe's sine condition, there is introduced over the spherical reference wave (Osterberg and Wilkins, 1949) an amplitude variation $k(\rho)$ given by

$$k(p, q) \equiv k(\rho) = \frac{(1 - \rho^2)^{\frac{1}{4}}}{[1 - (nM\rho/n_0)^2]^{\frac{1}{4}}} ; \tag{3.1}$$

$$\rho \equiv \frac{(p^2 + q^2)^{\frac{1}{2}}}{n} ; \tag{3.1a}$$

in which n_0 and n are the refractive indices in the object and image space, respectively, and M is the magnification ratio between the object and image planes.   Hence

$$A_1(p, q) = T(p, q)k(p, q) \tag{3.2}$$

is the normalized amplitude variation over the spherical reference wave in the absence of coating material upon the diffraction plate. $2\pi W_0(p, q)$ is the corresponding phase variation in radians over the spherical reference wave.
   Let

$$\psi(p, q) \equiv \frac{A_1(p, q)e^{2\pi i W_0(p,q)}}{(n^2 - p^2 - q^2)^{\frac{1}{2}}} . \tag{3.3}$$

Then the pupil function $P(p, q)$ is given by

$$P(p, q) = c(p, q)\psi(p, q) \tag{3.4}$$

in which $c(p, q)$ is a complex coating function which specifies the amplitude and phase transmission of the coating material on the diffraction plate.   Let $c(p, q)$ be written in the form

$$c(p, q) = |c(p, q)|e^{i \, \arg c(p,q)}. \tag{3.4a}$$

The amplitude transmission, $|c(p, q)|$, is to be taken along the direction in which the axial rays pass through the coating material.   The phase angle, $\arg c(p, q)$, is to be determined from the optical path along the normal to the coating material when the diffraction plate is perpendicular to the optical axis.
   It is often expedient to replace the optical direction cosines p, q by the polar angles ϑ and the azimuthal angles ϕ.   It follows from the

notation of Fig. VII.4 that

$$p = -n \sin \vartheta \cos \phi \equiv -n\rho \cos \phi;$$

$$q = -n \sin \vartheta \sin \phi \equiv -n\rho \sin \phi;$$

$$\rho = \sin \vartheta = \frac{(p^2 + q^2)^{\frac{1}{2}}}{n}. \tag{3.5}$$
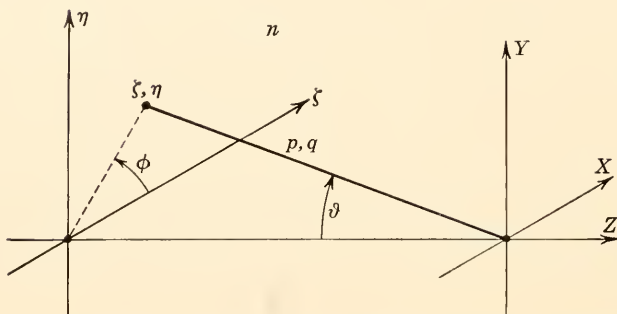
FIG. VII.4.   Geometrical relations among the optical direction cosines p, q, the polar angle ϑ, and the azimuthal angle ϕ.

In microscopy the refractive index n is always unity in the image space. Henceforth we shall therefore set

$$n = 1. \tag{3.6}$$

ρ is the zonal numerical aperture of the objective with respect to the image space.   Furthermore,

$$\rho_m = \sin \vartheta_m \tag{3.7}$$

is the maximum numerical aperture of the objective with respect to its image space. ρ_m is related to the numerical aperture, N.A., of the objective in accordance with the equation

$$|M| \, \rho_m = \text{N.A.} \tag{3.8}$$

For optical systems that are symmetrical about their optical axis, it follows at once that

$$T(p, q) \equiv T(\rho);$$

$$k(p, q) \equiv k(\rho);$$

$$W_0(p, q) \equiv W_0(\rho); \tag{3.9}$$

$$c(p, q) \equiv c(\rho);$$

$$\psi(p, q) \equiv \psi(\rho).$$

Hence

$$P(p, q) \equiv P(\rho) = c(\rho)\psi(\rho). \tag{3.10}$$

In detail,

$$\psi(\rho) = \frac{T(\rho)e^{2\pi i W_0(\rho)}}{(1 - \rho^2)^{\frac{1}{4}}[1 - (M\rho/n_0)^2]^{\frac{1}{4}}}. \tag{3.11}$$

In the conventional microscope $\rho_m < 0.04$ with $0 \leqq \rho \leqq \rho_m$. Therefore with excellent approximation

$$(1 - \rho^2)^{\frac{1}{4}} = 1 \tag{3.12}$$

in Eq. 3.11. Consequently, it suffices to take $\psi(\rho)$ in the simpler form

$$\psi(\rho) = \frac{T(\rho)e^{2\pi i W_0(\rho)}}{[1 - (M\rho/n_0)^2]^{\frac{1}{4}}}. \tag{3.13}$$

Furthermore, with objectives of relatively low numerical aperture

$$T(\rho) \rightarrow 1;$$

$$\left[1 - \left(\frac{M\rho}{n_0}\right)^2\right]^{\frac{1}{4}} \rightarrow 1; \tag{3.14}$$

so that

$$\psi(\rho) \rightarrow e^{2\pi i W_0(\rho)}. \tag{3.15}$$

If, in addition, the objective is free of spherical aberration, $W_0(\rho) = 0$ and

$$\psi(\rho) = 1; \tag{3.16}$$

$$P(\rho) = c(\rho); \quad 0 \leqq \rho \leqq \rho_m. \tag{3.17}$$

It should be noted that in the paraxial region, where ρ approaches zero,

$$\psi(\rho) = 1;$$

$$P(\rho) = c(\rho); \tag{3.18}$$

irrespective of the spherical aberration.

From Eqs. 2.14, 3.5, and 3.6,

$$P_z(p, q) = P_z(\rho) = P(\rho)e^{2\pi i z(1 - \rho^2)^{\frac{1}{2}}}. \tag{3.19}$$

We have seen that in a microscope $\rho_m < 0.04$ with $0 \leqq \rho \leqq \rho_m$. Hence with excellent approximation

$$(1 - \rho^2)^{\frac{1}{2}} = 1 - \frac{\rho^2}{2} \tag{3.20}$$

so that

$$P_z(\rho) = e^{2\pi i z} P(\rho) e^{-i(\pi z \rho^2)/2}. \tag{3.21}$$

The phase factor $e^{-i(\pi z \rho^2)/2}$ will be recognized as the classical zonal phase factor associated with an observation plane which is displaced z wavelengths from the conjugate image plane.

In summary, the primary diffraction integral $U(x - Mx_0, y - My_0)$ is given by

$$U(x - Mx_0, y - My_0)$$
$$= \int_{-\infty}^{\infty} \int_{-\infty}^{\infty} P(p, q) e^{2\pi i [p(x-Mx_0)+q(y-My_0)]} \, dp \, dq \qquad (3.22)$$

in which the pupil function $P(p, q)$ is given by

$$P(p, q) = 0 \qquad (3.23)$$

when

$$p^2 + q^2 > \rho_m^2 \qquad (3.23a)$$

and by

$$P(p, q) = P(\rho) = \frac{c(\rho) T(\rho) e^{2\pi i W_0(\rho)}}{[1 - (M\rho/n_0)^2]^{\frac{1}{4}}} \qquad (3.24)$$

when

$$0 \leqq p^2 + q^2 = \rho^2 \leqq \rho_m^2. \qquad (3.24a)$$

The coating function $c(p, q) = c(\rho)$ specifies in accordance with the convention of Eq. 3.4a the amplitude and phase transmission of the coating material of the diffraction plate. $T(p, q) = T(\rho)$ is the amplitude transmission along the axial rays in the absence of coating material on the diffraction plate. $2\pi W_0(p, q) = 2\pi W_0(\rho)$ radians is determined from the integral over the lateral spherical aberration of the axial rays in the absence of coating material on the diffraction plate. $W_0(\rho)$ is to be considered as negative when it represents a reduction of the optical path with respect to the spherical reference wave. n_0 and n are, respectively, the refractive indices of the object and image space with $n = 1$. M is the magnification ratio between the conjugate object and image planes. When $n = 1$, p and q are the direction cosines of the normals to the spherical reference wave of the image space. Furthermore, p and q are related to the polar angle ϑ and to the azimuthal angle ϕ of these normals in accordance with Eqs. 3.5. All distances are to be measured as numbers of wavelengths. Equations 3.22 and 3.24 contain the assumption that the objective satisfies the Abbe sine condition. The primary diffraction integral of Eq. 3.22 applies to the conjugate object and image planes but holds also for observation planes which are displaced by z wavelengths from the conjugate image plane when the pupil function $P(p, q)$ is replaced by the afocal pupil function

$$P_z(p, q) = P_z(\rho) = e^{2\pi i z} P(\rho) e^{-i(\pi z \rho^2)/2}. \qquad (3.25)$$

The functions P, T, W_0, and c are expressed in terms of the direction cosines p, q when the optical system is not symmetrical axially but can be expressed in terms of the zonal numerical aperture ρ of the image space when the optical system does possess axial symmetry.   Finally, the inequalities of Eqs. 3.23 and 3.24, which serve as limits of integration in Eq. 3.22, have been written explicity for objectives having circular apertures.   These inequalities are easily modified for application to objectives having rectangular apertures.

4. SPECIFICATION OF THE COATING FUNCTION $c(p, q)$ IN PHASE MICROSCOPY

The following conventions will be used in specifying the coating function $c(p, q)$ in a Zernike system of phase microscopy.   In Zernike's method the conjugate and complementary areas of the diffraction plate are coated differently with substantially uniform coatings.

Let $c_0(p, q)$ and $c_1(p, q)$ denote the amplitude and phase transmission of the coating material on the conjugate and complementary areas, respectively.   We set

$$c_0(p, q) = h_0(p, q)e^{i\delta_0};$$

$$c_1(p, q) = h_1(p, q)e^{i\delta_1}. \tag{4.1}$$

The amplitude transmissions h_0 and h_1 are to be specified along the direction in which the axial rays pass through the coating material. The phase transmissions δ_0 and δ_1 are to be determined from the optical paths along the normal to the coating material. δ_0 and δ_1 may be taken as independent of p, q because the amount of spherical aberration associated with the passage of the axial rays through the extremely thin coating materials of the diffraction plate is secondary and therefore negligible.

In a conventional microscope $0 \leqq p^2 + q^2 \leqq \rho_m{}^2$ with $\rho_m < 0.04$.   If the diffraction plate is located well away from the object space of the objective, the range in p, q becomes so small that $h_0(p, q)$ and $h_1(p, q)$ are substantially constant.   Whenever this is true, we let

$$he^{i\delta} \equiv \frac{c_0(p, q)}{c_1(p, q)} = \frac{h_0}{h_1} e^{i(\delta_0 - \delta_1)}. \tag{4.2}$$

h is physically the ratio of the amplitude transmission of the coating material on the conjugate area to the amplitude transmission of the coating material on the complementary area. δ is determined from the optical path difference in radians between the conjugate and complementary areas and is considered as positive when the optical path

through the conjugate area exceeds that through the complementary area.

Since $c_1(p, q) \neq 0$, no essential loss of generality is obtained by setting

$$c(p, q) = c_1(p, q) = 1 \qquad (4.3)$$

for points (p, q) of the complementary area and by setting

$$c(p, q) = he^{i\delta} \qquad (4.4)$$

for points (p, q) in the conjugate area.

In phase microscopy the conjugate area is so narrow that the variation introduced into $h_0(p, q)$ by the allowable range in p, q is negligible. Since $h_1(p, q) \equiv 1$ when the absorbing material is placed upon the conjugate area, Eqs. 4.3 and 4.4 apply with excellent approximation to all A-type diffraction plates, irrespective of the location of the diffraction plate. This is not necessarily true for B-type diffraction plates which are used in conjunction with oil immersion objectives. With B-type diffraction plates it may in some instances become necessary to return to Eqs. 4.1. If the conjugate area is narrow, one may, however, introduce the simplification

$$c_0(p, q) = h_0 e^{i\delta_0} \qquad (4.5)$$

in which h_0 is specified by $h_0(p_m, q_m)$ where p_m and q_m are the median values of p and q in the narrow conjugate area.

5. THE PRIMARY DIFFRACTION INTEGRAL WITH AIRY-TYPE OBJECTIVES

An Airy-type objective is defined as one for which the aberration function

$$\psi(p, q) = 1. \qquad (5.1)$$

Real objectives have the property that $\psi(p, q)$ approaches unity at low numerical aperture. Whenever the objective obeys or approximates closely the condition

$$\psi(p, q) = 1, \qquad (5.2)$$

$$P(p, q) = c(p, q) \qquad (5.3)$$

so that the pupil function is numerically equal to the coating function. If the diffraction plates of such objectives are uncoated, $c(p, q) = 1$ and $P(p, q) = 1$. Equations 5.2 and 5.3 are of theoretical and practical importance because they are often approximated by well-corrected objectives of relatively high numerical aperture. Whenever approximate solutions are acceptable, the pupil function is given with sufficient accuracy by the simplified statement of Eq. 5.3.

Suppose that Eq. 5.3 is satisfied, that $c(p, q) = 1$, and that the object point is located at $x_0 = y_0 = 0$. Then the primary diffraction integral reduces to

$$U(x, y) = \iint e^{2\pi i(px+qy)} \, dp \, dq \tag{5.4}$$

for points x, y of the conjugate image plane. From Equations 3.5 and 5.4, with $n = 1$,

$$U(x, y) = \int_0^{\rho_m} \int_0^{2\pi} e^{-2\pi i\rho(x \cos\phi + y \sin\phi)} \rho \, d\phi \, d\rho;$$

$$U(x, y) = 2\pi \int_0^{\rho_m} J_0[2\pi\rho(x^2 + y^2)^{\frac{1}{2}}]\rho \, d\rho;$$

$$= \pi\rho_m^2 2 \frac{J_1[2\pi\rho_m(x^2 + y^2)^{\frac{1}{2}}]}{2\pi\rho_m(x^2 + y^2)^{\frac{1}{2}}} ; \tag{5.5}$$

in which J_0 and J_1 are Bessel functions of zero and first order, respectively. Introducing

$$r = (x^2 + y^2)^{\frac{1}{2}}, \tag{5.6}$$

one finds that

$$U(x, y) \equiv U(r) = \pi\rho_m^2 \frac{2J_1(2\pi r\rho_m)}{2\pi r\rho_m} . \tag{5.7}$$

Since the energy density $E(r)$ is proportional to $|U(r)|^2$,

$$\frac{E(r)}{\pi^2\rho_m^4} = 4 \left[\frac{J_1(2\pi r\rho_m)}{2\pi r\rho_m} \right]^2. \tag{5.8}$$

Equation 5.8 describes the classical energy distribution produced over the image plane by the coherent light emitted by an object point which is located upon the optical axis. The discovery of this distribution law is attributed to Airy. We see therefore that $|U(x, y)|^2$ describes an Airy type of diffraction image when the objective is of the Airy type.

By introducing ρ_m from Eq. 3.8 into Eq. 5.8, we find that

$$\frac{M^4 E(r)}{\pi^2(\text{N.A.})^4} = 4 \left[\frac{J_1(2\pi r \text{ N.A.}/|M|)}{2\pi r \text{ N.A.}/|M|} \right]^2. \tag{5.9}$$

Since the first positive root of $J_1(z) = 0$ occurs at $z = 3.8317$, the first zero value of $E(r)$ occurs at

$$\frac{r}{|M|} = \frac{3.8317}{2\pi \text{ N.A.}} = \frac{0.6098}{\text{N.A.}} \text{ wavelengths.} \tag{5.10}$$

It follows from a criterion which is often attributed to Airy that two object points are just resolvable when their separation in the object space is equal to $r|M|$ wavelengths as determined by the classical Eq. 5.10. To those who have not had the opportunity of studying Luneberg's derivation of the primary diffraction integral, Eqs. 5.7, 5.8, and 5.10 will serve to demonstrate that the primary diffraction integral includes the classical behavior of diffraction images.

Airy-type objectives may become important in adapting the phase microscope to the measurement of the properties of an object particle. It is pointed out that an objective not normally of the Airy type may be rendered of the Airy type by placing upon the diffraction plate or upon an adjacent plate a second coating material whose auxiliary coating function $a(p, q)$ is related to the aberration function $\psi(p, q)$ by the equation

$$a(p, q)\psi(p, q) = 1. \tag{5.11}$$

Then

$$P(p, q) = c(p, q)a(p, q)\psi(p, q) = c(p, q). \tag{5.12}$$

6. A TRANSPORT PROPERTY OF THE PRIMARY DIFFRACTION INTEGRAL

Suppose that the object plane has been illuminated in any suitable way which causes Huygens' wavelets to leave elements of area $dx_0\, dy_0$ of the object plane with a coherent amplitude and phase distribution described by some "civilized" but otherwise arbitrary function $\chi(x_0, y_0)\, dx_0\, dy_0$. The function $\chi(x_0, y_0)$ is then equivalent to the existence of χ unpolarized dipoles of unit strength per unit area. Since each unpolarized dipole produces the amplitude and phase distribution $U(x - Mx_0, y - My_0)$ in the conjugate image plane, the assembly of χ unpolarized dipoles in the element of area $dx_0\, dy_0$ produces the amplitude and phase distribution

$$\chi(x_0, y_0)U(x - Mx_0, y - My_0)\, dx_0\, dy_0 \tag{6.1}$$

in the conjugate image plane. The physical meaning of this amplitude and phase distribution is subject to the reservations described at the end of Section 2. We may say that the phase and amplitude $\chi(x_0, y_0)\, dx_0\, dy_0$ of the wavelets which leave an element of area $dx_0\, dy_0$ of the object plane is transported to the image plane as the product of $\chi(x_0, y_0)\, dx_0\, dy_0$ and the primary diffraction integral.

The coherent distributions (Eq. 6.1) which are produced from different elements of area $dx_0\, dy_0$ of the object plane overlap at any point x, y of the image plane. The resultant amplitude and phase so produced at point x, y is therefore the sum or integral of the products (Eq. 6.1) over

all elements of area of the object plane.   Let $F(x, y)$ denote this resultant amplitude and phase distribution.   Then

$$F(x, y) = \int_{-\infty}^{\infty} \int_{-\infty}^{\infty} \chi(x_0, y_0) U(x - Mx_0, y - My_0)\, dx_0\, dy_0 \quad (6.2)$$

in which $\chi(x_0, y_0)$ is required to be zero beyond the field of view of the optical instrument and in which all dimensions are to be measured as numbers of wavelengths.   Hence we may say that the coherent amplitude and phase distribution $\chi(x_0, y_0)$ of the object plane is transported to the image plane as the coherent amplitude distribution $F(x, y)$.
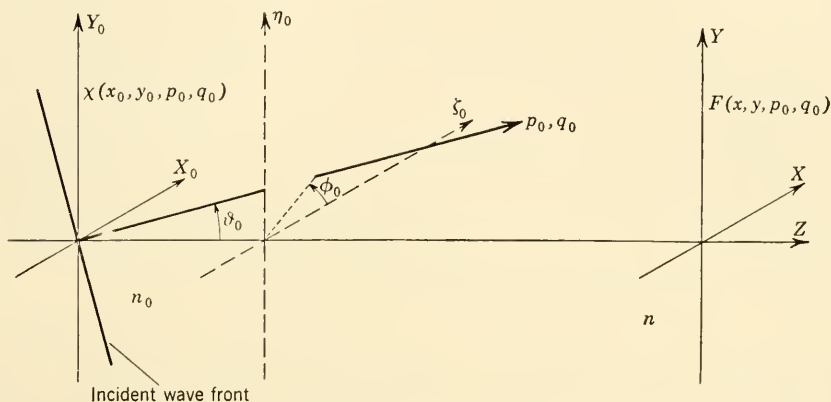
Fig. VII.5.   Coherent illumination of the object plane $X_0 Y_0$.

7. THE MOST GENERAL STATEMENT OF THE DIFFRACTION INTEGRALS OF PHASE MICROSCOPY

Suppose that a substantially plane wave front whose normals have the optical direction cosines p_0, q_0 is incident (as in Fig. VII.5) upon the object plane.   The light in this incident beam originates at an infinitesimally small area in the source of light and may be regarded as coherent.   From a knowledge of p_0, q_0 and of the physical properties of the object specimen, one can construct a function $\chi(x_0, y_0, p_0, q_0)\, dx_0\, dy_0$ which gives the amplitude and phase of the wavelets which leave an element of area $dx_0\, dy_0$ of the object plane.   The difficulties of constructing $\chi(x_0, y_0, p_0, q_0)$ can become great even with relatively simple object specimens, and the difficulties of integrating the expressions in which $\chi(x_0, y_0, p_0, q_0)$ appears can readily become insurmountable. Except with very simple object specimens, considerable ingenuity will be required in finding a good approximation to $\chi(x_0, y_0, p_0, q_0)$ and in integrating the resulting diffraction integrals with satisfactory approxi-

mation. When $\chi(x_0, y_0, p_0, q_0)$ has been found, the amplitude and phase distribution $F(x, y, p_0, q_0)$ produced over the image plane by the coherent light in the incident wave front whose normals have the optical direction cosines p_0, q_0 is given according to the transport property of the primary diffraction integral by the equation

$$F(x, y, p_0, q_0) = \int_{-\infty}^{\infty} \int_{-\infty}^{\infty} \chi(x_0, y_0, p_0, q_0)$$
$$\times U(x - Mx_0, y - My_0) \, dx_0 \, dy_0 \quad (7.1)$$

in which χ is required to be zero for points x_0 y_0 which lie beyond the field of view of the objective. Equation 7.1 will be most accurate for points x, y which fall near the optical axis. Consequently, the object specimen should be placed upon or near the optical axis whenever its imagery is to be interpreted with the aid of the diffraction integrals of phase microscopy.

Let $E(x, y, p_0, q_0)$ denote the energy density produced over the image plane by the light in the incident wave front whose normals have the optical direction cosines p_0, q_0. We shall call $E(x, y, p_0, q_0)$ the *partial energy density*. It is produced by the light from an infinitesimally small portion of the source and is proportional to $|F(x, y, p_0, q_0)|^2$.

$$E(x, y, p_0, q_0) \; : \; |F(x, y, p_0, q_0)|^2. \quad (7.2)$$

Let $G(x, y)$ denote the *total energy density* produced in the image plane by light from all the effective elements of area in the source. $G(x, y)$ can be obtained by integrating over the effective area of the source or by integrating over the optical direction cosines p_0, q_0 of the total beam of rays which are incident upon the object plane. We know that there must exist a positive function $S(p_0, q_0)$ such that

$$G(x, y) = \iint \frac{S(p_0, q_0)}{n_0^2 - p_0^2 - q_0^2} |F(x, y, p_0, q_0)|^2 \, dp_0 \, dq_0 \quad (7.3)$$

in which the limits of integration extend over the optical direction cosines p_0, q_0 of the family of rays which are incident upon the object plane. This family of rays, and hence p_0, q_0, is limited by the opening in the diaphragm of the substage condenser. Since $S(p_0, q_0)$ must be proportional to the energy radiated in the p_0, q_0 direction, $S(p_0, q_0)$ will be proportional to the intensity of the source. Furthermore, $S(p_0, q_0)$ must be expected to be proportional to

$$\cos \vartheta_0 = \frac{1}{n_0} (n_0^2 - p_0^2 - q_0^2)^{\frac{1}{2}} \quad (7.4)$$

because the normal to the aperture of the objective makes the angle

ϑ_0 with the rays which enter the objective in the object space. If the source obeys Lambert's law and is uniformly bright, the intensity of the source is proportional to $\cos \vartheta_0$. For simplicity of presentation, we take the combination of proportionality factors as unity and assert that with Lambertian sources of uniform brightness

$$G(x, y) = \iint |F(x, y, p_0, q_0)|^2 \, dp_0 \, dq_0 \tag{7.5}$$

in which the integral extends over the optical direction cosines p_0, q_0 of the rays which are incident upon the object plane. Except when it is demonstrable that the more general expression of Eq. 7.3 can or should be used, Eq. 7.5 suffices for the purpose of computing the variation in the total energy density over the image plane of a phase microscope or of an ordinary microscope.

A remarkable simplification occurs when the opening in the diaphragm of the substage condenser is small. In this case the variation in p_0, q_0 is so small over the restricted range of p_0, q_0 that the integrand in Eq. 7.3 remains sensibly constant. Then

$$G(x, y) = \frac{S(p_0, q_0)}{n_0{}^2 - p_0{}^2 - q_0{}^2} |F(x, y, p_0, q_0)|^2 \iint dp_0 \, dq_0$$

so that

$$G(x, y) = K |F(x, y, p_0, q_0)|^2 \tag{7.6}$$

wherein K is a parameter which depends on the size and location of the opening in the condenser diaphragm. With Lambertian sources of uniform brightness K will depend only upon the size of the opening in the condenser diaphragm. Of course, K increases with the strength of the source of light. Equation 7.6 applies to the types of illumination which were treated by Abbe. More specifically, it applies to narrow cones of either axial or oblique illumination.

8. THE DIFFRACTION INTEGRALS IN TERMS OF THE OBJECT FUNCTION $f(x_0, y_0, p_0, q_0)$

There exists a broad class of object specimens for which the function $\chi(x_0, y_0, p_0, q_0)$ of the last section can be written in the form

$$\chi(x_0, y_0, p_0, q_0) = C e^{2\pi i (p_0 x_0 + q_0 y_0)} f(x_0, y_0, p_0, q_0). \tag{8.1}$$

C is a complex number not depending on (x_0, y_0, p_0, q_0). The exponential is a phase factor due to the incidence of an inclined wave front. The *object function* $f(x_0, y_0, p_0, q_0)$ may be interpreted as the change produced in the amplitude and phase transmission of the object plane

by the presence of the object specimen.   Equation 8.1 is most readily
applied to object specimens which can be subdivided into areas of
practically constant optical path.   Equation 8.1 is not the most con-
venient way of formulating the function χ in the case of spherical
particles (more generally, lens-like particles).

   We shall now derive Eq. 8.1 on the supposition that the virtual image
of the source of light as formed by the combined lamp and substage
condensers behaves as a self-luminous source.   Because the condenser
diaphragm is located at or slightly inside the first focal plane of the
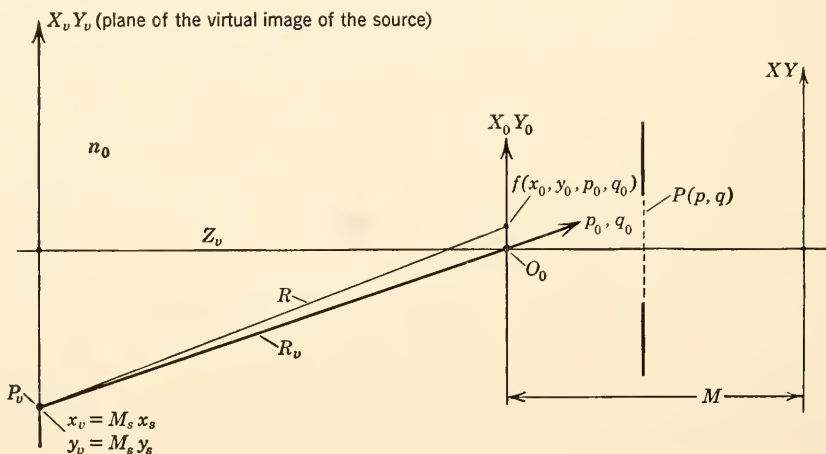
FIG. VII.6.   Relative locations of the object plane X_0Y_0 and the plane X_vY_v which
is occupied by the virtual image of the source of light.   The distance Z_v will be great.

substage condenser, the plane X_vY_v of the virtual image is located far
to the left of the object plane X_0Y_0 of Fig. VII.6.   The luminous portion
of the X_vY_v plane is limited to the image formed in this plane of the
opening in the condenser diaphragm.

   Wavelets from a point P_v within the luminous portion of the distant
X_vY_v plane expand according to the law $e^{2\pi i n_0 R}/R$.   For points belonging
to the object plane

$$R = [(x_0 - x_v)^2 + (y_0 - y_v)^2 + Z_v^2]^{\frac{1}{2}}$$
$$= [R_v^2 + x_0^2 + y_0^2 - 2(x_0 x_v + y_0 y_v)]^{\frac{1}{2}}; \tag{8.2}$$

wherein

$$R_v \equiv (x_v^2 + y_v^2 + Z_v^2)^{\frac{1}{2}}. \tag{8.3}$$

When Z_v is large enough, $R_v^2 \gg x_0^2 + y_0^2$.   Then with excellent

approximation

$$R = R_v - \frac{x_0 x_v + y_0 y_v}{R_v} \; ; \tag{8.4}$$

$$\frac{e^{2\pi i n_0 R}}{R} = \frac{e^{2\pi i n_0 R_v}}{R_v} \, e^{-2\pi i n_0 \frac{x_0 x_v + y_0 y_v}{R_v}} . \tag{8.5}$$

With reference to Fig. VII.6, the rays originating at point P_v are incident upon the object plane along the direction $P_v O_0$ as Z_v approaches infinity. Let p_0, q_0 be the optical direction cosines of rays which are parallel to the direction $P_v O_0$. Then from the trigonometric meaning of a direction cosine

$$p_0 = \frac{-n_0 x_v}{R_v} \; ; \qquad q_0 = -n_0 \frac{y_v}{R_v} . \tag{8.6}$$

Let p_0, q_0 from Eq. 8.6 be substituted into Eq. 8.5. We learn, accordingly, that the plane wave originating at point P_v induces upon the object plane $X_0 Y_0$ the amplitude and phase distribution

$$\frac{e^{2\pi i n_0 R_v}}{R_v} \, e^{2\pi i (p_0 x_0 + q_0 y_0)} \tag{8.7}$$

in which p_0, q_0 are the optical direction cosines of the normals to the wave front. If $f(x_0, y_0, p_0, q_0)$ denotes the change produced in the amplitude and phase transmission of the object plane by the presence of the object specimen, we see that the wavelets from point P_v emerge from the object plane with an amplitude and phase distribution $\chi(x_0, y_0, p_0, q_0)$ which is given by

$$\chi(x_0, y_0, p_0, q_0) = \frac{e^{2\pi i n_0 R_v}}{R_v} \, e^{2\pi i (p_0 x_0 + q_0 y_0)} f(x_0, y_0, p_0, q_0). \tag{8.8}$$

It will be noted that Eq. 8.8 agrees with Eq. 8.1 and specifies the complex number C.

As in Eq. 7.1, let $F(x, y, p_0, q_0)$ denote the amplitude and phase distribution produced in the image plane by the incidence upon the object plane of a wave front whose normals have the optical direction cosines p_0, q_0. Then

$$F(x, y, p_0, q_0) = \frac{e^{2\pi i n_0 R_v}}{R_v} \, F_0(x, y, p_0, q_0) \tag{8.9}$$

where

$$F_0(x, y, p_0, q_0) \equiv \int_{-\infty}^{\infty} \int_{-\infty}^{\infty} e^{2\pi i (p_0 x_0 + q_0 y_0)}$$

$$\times f(x_0, y_0, p_0, q_0) U(x - M x_0, y - M y_0) \, dx_0 \, dy_0. \tag{8.10}$$

The object function $f(x_0, y_0, p_0, q_0)$ is required to be zero beyond the field of view of the objective. All distances are dimensionless because they are to be measured in wavelength numbers. As we shall see presently, $F_0(x, y, p_0, q_0)$ is the function of most significance to the theory of microscopy. We shall call $F_0(x, y, p_0, q_0)$ the amplitude and phase distribution of the image plane even though F_0 differs from F by the factor of Eq. 8.9.

The partial energy density $E(x, y, p_0, q_0)$ is given by

$$E(x, y, p_0, q_0) = \left| F(x, y, p_0, q_0) \right|^2 = \frac{1}{R_v^2} \left| F_0(x, y, p_0, q_0) \right|^2. \quad (8.11)$$

Let

$$S(p_0, q_0) \equiv S(x_v, y_v, x_0, y_0); \qquad x_0 = y_0 \equiv 0 \quad (8.12)$$

be an energy function which is proportional to the energy radiated from point P_v (Fig. VII.6) in the p_0, q_0 direction and which is subsequently *accepted* by the projected area of the objective. If $G(x, y)$ denotes the total energy distribution in the image plane,

$$G(x, y) = \iint \frac{S(x_v, y_v, x_0, y_0)}{R_v^2} \left| F_0(x, y, p_0, q_0) \right|^2 dx_v \, dy_v \quad (8.13)$$

in which the integral extends over the luminous area of the $X_v Y_v$ plane, that is, over that portion of the $X_v Y_v$ plane which is occupied by the image of the opening in the diaphragm of the substage condenser. x_0, y_0 in Eq. 8.13 refers to the particular point $x_0 = 0$, $y_0 = 0$, with reference to which p_0 and q_0 are determined by Eq. 8.6.

From Eq. 8.6

$$x_v = -\frac{R_v}{n_0} p_0 = -\frac{Z_v p_0 / n_0}{(n_0^2 - p_0^2 - q_0^2)^{\frac{1}{2}}};$$

$$\qquad (8.14)$$

$$y_v = -\frac{R_v}{n_0} q_0 = -\frac{Z_v q_0 / n_0}{(n_0^2 - p_0^2 - q_0^2)^{\frac{1}{2}}}.$$

Hence

$$J\left(\frac{x_v, y_v}{p_0, q_0}\right) = \frac{R_v^2}{n_0^2 - p_0^2 - q_0^2} \quad (8.15)$$

where J is the Jacobian of the indicated variables. If, therefore, the variables x_v, y_v in Eq. 8.13 are transformed to the variables p_0, q_0 in accordance with Eqs. 8.14, it follows that

$$G(x, y) = \iint \frac{S(p_0, q_0)}{n_0^2 - p_0^2 - q_0^2} \left| F_0(x, y, p_0, q_0) \right|^2 dp_0 \, dq_0 \quad (8.16)$$

in which the integral extends over the range of optical direction cosines p_0, q_0 of the rays which are incident upon the object plane. This range is limited by the opening in the diaphragm of the substage condenser.

In summary, the total energy density $G(x, y)$ in the image plane is given by Eq. 8.16 in which $F_0(x, y, p_0, q_0)$ is determined by Eq. 8.10. Furthermore

$$U(x - Mx_0, y - My_0) = \int_{-\infty}^{\infty} \int_{-\infty}^{\infty} P(p, q)e^{2\pi i [p(x - Mx_0) + q(y - My_0)]} \, dp \, dq;$$

(8.17)

$$P(p, q) = 0$$

when

$$p^2 + q^2 > \rho_m{}^2; \tag{8.18}$$

$$P(p, q) = P(\rho) = \frac{c(\rho)T(\rho)e^{2\pi i W_0(\rho)}}{[1 - (M\rho/n_0)^2]^{\frac{1}{2}}}$$

when

$$0 \leqq p^2 + q^2 = \rho^2 \leqq \rho_m{}^2. \tag{8.19}$$

For out-of-focus image planes $P(p, q)$ is to be replaced by the afocal pupil function $P_z(p, q)$ as in Eq. 3.25.

The properties of the optical system which are peculiar to phase microscopy are contained in the modification of the pupil function $P(p, q)$ by the coating function $c(p, q)$ and in the restriction of the range of the optical direction cosines p_0, q_0 by the choice of opening in the diaphragm of the substage condenser.

The problem of integrating Eq. 8.16 becomes formidable since Eqs. 8.10 and 8.17 have to be combined with Eq. 8.16.

For reasons already stated in Section 7, $G(x, y)$ is given with good approximation by

$$G(x, y) = \iint |F_0(x, y, p_0, q_0)|^2 \, dp_0 \, dq_0 \tag{8.20}$$

when the source of light is Lambertian. If the opening in the diaphragm of the substage condenser is very small, Eq. 7.6 applies again, provided that F_0 is determined by Eq. 8.10.

9. THE OBJECT FUNCTION $f(x_0, y_0, p_0, q_0)$ FOR PLATE-LIKE OBJECT PARTICLES

If the object particle is of uniform thickness and refractive index, the incident rays which have like optical direction cosines p_0, q_0 pass

through the object specimen in the manner illustrated by Fig. VII.7. The rays that pass through the surround continue uninterrupted except at the cover glass or other discontinuities which are of secondary interest and which need not be considered here. The rays that pass through the interior of the particle suffer a lateral displacement but emerge parallel to their original course. Rays that pass through the edge e of the particle suffer both displacement and deviation. The magnitude of the displacement and deviation depends on the physical properties at the
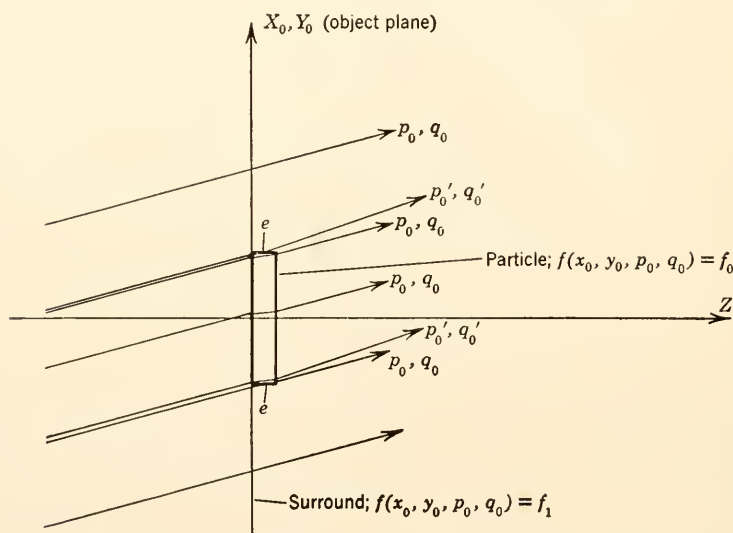
FIG. VII.7.   Passage of rays through plate-like particles.

edge of the particle.   As a result, the rays that emerge from the edge of a relatively thick particle may form a brush of rays p_0', q_0'.   If the particle becomes very thin, this brush effect becomes weak and, finally, negligible. Herein lies an important difference between thick and thin plate-like particles.

Suppose first that the particle is so thin that the brush effect may be neglected.   For points x_0, y_0 in the surround we may set

$$f(x_0, y_0, p_0, q_0) = f_1(p_0, q_0) = |f_1(p_0, q_0)| \, e^{i \arg f_1(p_0, q_0)}. \qquad (9.1)$$

For points x_0, y_0 in the particle, we may set

$$f(x_0, y_0, p_0, q_0) = f_0(p_0, q_0) = |f_0(p_0, q_0)| \, e^{i \arg f_0(p_0, q_0)}. \qquad (9.2)$$

The amplitude transmissions $|f_0(p_0, q_0)|$ and $|f_1(p_0, q_0)|$ are to be determined along the direction in which the rays pass through the

particle and the surround for equal thicknesses of particle and surround. However, arg $f_0(p_0, q_0)$ and arg $f_1(p_0, q_0)$, the phase transmissions, are to be determined from the optical path along the normal to the particle and for equal thicknesses of particle and surround. It is assumed that the plane of the particle is practically normal to the optical axis. The phase transmissions arg $f_0(p_0, q_0)$ and arg $f_1(p_0, q_0)$ do not depend on p_0, q_0 because phase variations due to p_0, q_0 are automatically included except for secondary effects due to the object specimen in the spherical aberration function $W_0(p, q)$.

If the surround is opaque,

$$f_1(p_0, q_0) = 0. \tag{9.3}$$

If the surround is not opaque, as is usual in microscopy, one may set

$$f_1(p_0, q_0) = 1 \tag{9.4}$$

and write

$$f_0(p_0, q_0) = g(p_0, q_0)e^{i\Delta} \tag{9.5}$$

in which Δ is the optical path difference between the particle and an equal thickness of the surround with Δ considered positive when the optical path of the particle exceeds that of the surround. $g(p_0, q_0)$ is the ratio of the amplitude transmission of the particle to the amplitude transmission of an equal thickness of the surround. Now in systems of phase microscopy the conjugate area of the diffraction plate is ordinarily narrow. Consequently the range of p_0, q_0 is limited. Since amplitude transmissions are slowly varying functions of p_0, q_0, it suffices to take

$$g = g(p_{0m}, q_{0m}) \tag{9.6}$$

where (p_{0m}, q_{0m}) are the median values of (p_0, q_0). Hence

$$f_0(p_0, q_0) = ge^{i\Delta}; \tag{9.7}$$

$$f_1(p_0, q_0) = 1 \tag{9.8}$$

express the object function $f(x_0, y_0, p_0, q_0)$ for thin plate-like particles in a transmitting surround. The amplitude transmission ratio g is to be computed for the median value of p_0, q_0 of the bundle of rays incident upon the object plane. If, for example, the opening in the condenser diaphragm is a small hole centered upon the optical axis, the median values of p_0, q_0 are $p_0 = q_0 = 0$. g is then the amplitude transmission ratio between particle and surround for rays that pass through the object plane along the normal to the object plane.

Suppose next that the particle is so thick that the brush effect at its edge cannot be neglected. Equations 9.7 and 9.8 still hold for points x_0, y_0 which are located within the edge and beyond the edge of the

particle, respectively. For incident rays p_0, q_0 that pass through the edge of the particle the object function f will depend upon x_0, y_0, p_0, q_0 in a manner which is related to the geometry of the edge and to the relative optical properties of the particle and surround. It is to be presumed that when the brush effect is included in the object function $f(x_0, y_0, p_0, q_0)$, Equations 8.16, 8.10, and 8.17 are capable of interpreting imagery at the edge of a thick particle as a function of z when the pupil function $P(p, q)$ is replaced by the afocal pupil function $Pz(p, q)$. Calculations of this type are extremely difficult and tedious and have not been attempted to the knowledge of the writers. Such calculations are, however, necessary to a complete interpretation of imagery near the edge of a relatively thick particle such as a cubic crystal of salt.

The above methods for writing the object function are readily extended to several plate-like particles or to periodic structures whose elevations and troughs are plate-like. If such structures are so thin that the brush effect can be neglected, it suffices to introduce into the diffraction integrals of phase microscopy an object function which is formally independent of the optical direction cosines p_0, q_0 and which is a stepped function of the object coordinates x_0, y_0.

10. PHASE MICROSCOPY WITH OBJECTS OF PERIODIC STRUCTURE

The theory of Section 8 will now be applied to objects of periodic structure whose object function $f(x_0, y_0, p_0, q_0)$ can be represented by

$$f(x_0, y_0, p_0, q_0) = f(x_0, y_0). \tag{10.1}$$

This equation applies with high precision to simple or crossed grating structures whose troughs and elevations are shallow and do not focus the incident light. The troughs and elevations of Fig. VII.8 may represent optical path differences between the adjacent portions of the periodic structure, amplitude transmissions of these adjacent portions, or both optical path differences and amplitude transmissions. If $2l$ and $2m$ are the grating spacings along X_0 and Y_0, respectively, the object function can be expressed by the Fourier series

$$f(x_0, y_0) = \sum_{\nu = -\infty}^{\infty} \sum_{\mu = -\infty}^{\infty} f_{\nu,\mu} e^{i\pi \left(\frac{\nu x_0}{l} + \frac{\mu y_0}{m} \right)} \tag{10.2}$$

in which the Fourier coefficients $f_{\nu,\mu}$ depend upon the details of the periodic structure.

From Eqs. 8.10 and 10.2

$$F_0(x, y, p_0, q_0) = \sum_{\nu} \sum_{\mu} f_{\nu,\mu} \int_{-\infty}^{\infty} \int_{-\infty}^{\infty} e^{i\pi \left(\frac{\nu x_0}{l} + \frac{\mu y_0}{m} \right)} e^{2\pi i (p_0 x_0 + q_0 y_0)}$$
$$\times\ U(x - Mx_0, y - My_0)\ dx_0\ dy_0 \tag{10.3}$$

where $F_0(x, y, p_0, q_0)$ is the amplitude and phase distribution produced over the image plane XY by the incidence upon the object plane of a
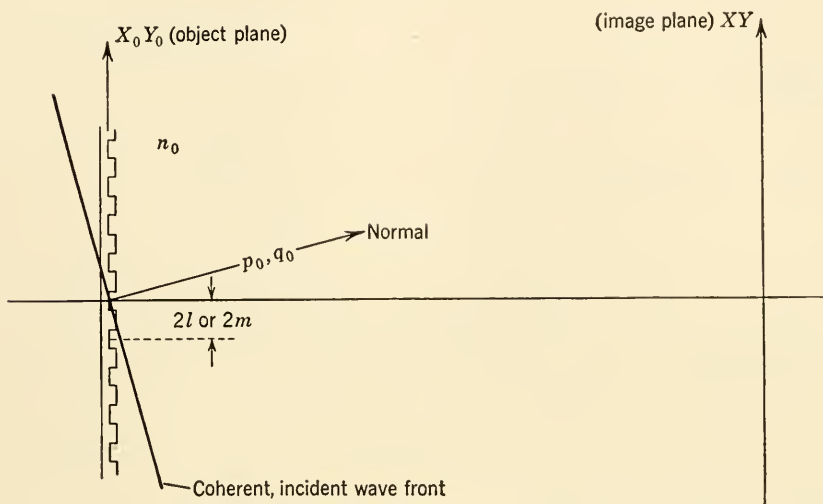
FIG. VII.8. Object specimens of periodic structure.

wave front whose normals have the optical direction cosines p_0, q_0. Introduce into Eq. 10.3 the change of variable

$$x_1 = x - Mx_0; \quad y_1 = y - My_0; \tag{10.4}$$

then

$$M^2 F_0(x, y, p_0, q_0) = e^{\frac{2\pi i}{M}(p_0 x + q_0 y)} \sum_\nu \sum_\mu B_{\nu,\mu} f_{\nu,\mu} e^{\pi i \left(\frac{\nu x}{Ml} + \frac{\mu y}{Mm} \right)}; \tag{10.5}$$

$$B_{\nu,\mu} \equiv \int_{-\infty}^{\infty} \int_{-\infty}^{\infty} e^{-i\pi \left[x_1 \left(\frac{\nu}{Ml} + \frac{2p_0}{M} \right) + y_1 \left(\frac{\mu}{Mm} + \frac{2q_0}{M} \right) \right]} U(x_1, y_1) \, dx_1 \, dy_1. \tag{10.6}$$

Equations 10.3, 10.5, and 10.6 contain the assumption that the field of view extends over a great number of wavelengths and over a large number of the grating spacings. The limits $-\infty$ to $+\infty$ in the integration with respect to $dx_0 \, dy_0$ or to $dx_1 \, dy_1$ now comprise an excellent approximation to the truth.

The coefficients $B_{\nu,\mu}$ can be stated more simply from the following considerations. Since

$$U(x_1, y_1) = \iint P(p, q) e^{2\pi i(px_1 + qy_1)} \, dp \, dq, \tag{10.7}$$

$$B_{\nu,\mu} = \iiint_{-\infty}^{\infty} \int_{-\infty}^{\infty} P(p, q)e^{2\pi i(px_1 + qy_1)}$$
$$\times e^{-i\pi\left[x_1\left(\frac{\nu}{Ml} + \frac{2p_0}{M}\right) + y_1\left(\frac{\mu}{Mm} + \frac{2q_0}{M}\right)\right]} dx_1\, dy_1\, dp\, dq. \quad (10.8)$$

Integrating with respect to $dx_1\, dy_1$, we obtain

$$B_{\nu,\mu} = \lim_{\substack{x_1 = \infty \\ y_1 = \infty}} \iint P(p, q)\, \frac{\sin\left[2\pi x_1\left(p - \frac{p_0}{M} - \frac{\nu}{2Ml}\right)\right]}{\pi\left(p - \frac{p_0}{M} - \frac{\nu}{2Ml}\right)}$$

$$\times \frac{\sin\left[2\pi y_1\left(q - \frac{q_0}{M} - \frac{\mu}{2Mm}\right)\right]}{\pi\left(q - \frac{q_0}{M} - \frac{\mu}{2Mm}\right)} dp\, dq; \quad (10.9)$$

$$p^2 + q^2 \lesseqgtr n^2\rho_m{}^2. \quad (10.10)$$

Since the Dirichlet integral

$$\lim_{\alpha = \infty} \int_{-a}^{a} f(x)\, \frac{\sin \alpha(x - t)}{\pi(x - t)}\, dx = f(t); \quad (10.11)$$

$$-a < t + a; \quad (10.12)$$

successive integration with respect to dp and dq in Eq. 10.9 yields

$$B_{\nu,\mu} = P\left(\frac{p_0}{M} + \frac{\nu}{2Ml}, \frac{q_0}{M} + \frac{\mu}{2Mm}\right). \quad (10.13)$$

Discontinuities in the pupil function $P(p, q)$ may be ignored in the theory of phase microscopy because such discontinuities are limited to a small finite number of loci.

In summary: Given the periodic object function

$$f(x_0, y_0) = \sum_{\nu}\sum_{\mu} f_{\nu,\mu} e^{i\pi\left(\frac{\nu x_0}{l} + \frac{\mu y_0}{m}\right)} \quad (10.14)$$

the corresponding amplitude and phase distribution $F_0(x, y, p_0, q_0)$ in the conjugate image plane is given by

$$F_0(x, y, p_0, q_0) = \frac{e^{\frac{2\pi i}{M}(p_0 x + q_0 y)}}{M^2} \sum_{\nu}\sum_{\mu} B_{\nu,\mu} f_{\nu,\mu} e^{i\pi\left(\frac{\nu x}{Ml} + \frac{\mu y}{Mm}\right)} \quad (10.15)$$

in which

$$B_{\nu,\mu} = P\left(\frac{p_0}{M} + \frac{\nu}{2Ml}, \frac{q_0}{M} + \frac{\mu}{2Mm}\right). \qquad (10.16)$$

Furthermore,

$$P\left(\frac{p_0}{M} + \frac{\nu}{2Ml}, \frac{q_0}{M} + \frac{\mu}{2Mm}\right) = 0 \qquad (10.17)$$

when

$$\left(\frac{p_0}{M} + \frac{\nu}{2Ml}\right)^2 + \left(\frac{q_0}{M} + \frac{\mu}{2Mm}\right)^2 > \frac{(N.A.)^2}{M^2} \qquad (10.18)$$

wherein N.A. is the numerical aperture of the objective and M is the magnification ratio between the object and image planes.

The amplitude and phase distribution of the light entering the image plane may now be compared with the amplitude and phase distribution of the light leaving the object plane. From Eq. 8.9 it will be seen that the phase factor $e^{2\pi i n_0 R_v}/R_v$ is not included in the function $F_0(x, y, p_0, q_0)$. For purposes of direct comparison we therefore exclude this phase factor from $\chi(x_0, y_0, p_0, q_0)$ as given by Eq. 8.8 and write

$$\chi_0(x_0, y_0, p_0, q_0) \equiv e^{2\pi i(p_0 x_0 + q_0 y_0)} f(x_0, y_0). \qquad (10.19)$$

We call $\chi_0(x_0, y_0, p_0, q_0)$ the *composite object function*. It may be interpreted as the amplitude and phase distribution of the coherent light which leaves the object plane. $e^{2\pi i(p_0 x_0 + q_0 y_0)}$ is in fact a phase factor which specifies the phase distribution induced upon the object plane by the incidence of a wave front whose normal has the optical direction cosines (p_0, q_0). Hence the equations

$$\chi_0(x_0, y_0, p_0, q_0) = e^{2\pi i(p_0 x_0 + q_0 y_0)} \sum_\nu \sum_\mu f_{\nu,\mu} e^{i\pi\left(\frac{\nu x_0}{l} + \frac{\mu y_0}{m}\right)}; \qquad (10.20)$$

$$F_0(x, y, p_0, q_0) =$$

$$\frac{e^{2\pi i\left(p_0 \frac{x}{M} + q_0 \frac{y}{M}\right)}}{M^2} \sum_\nu \sum_\mu B_{\nu,\mu} f_{\nu,\mu} e^{i\pi\left(\frac{\nu x}{Ml} + \frac{\mu y}{Mm}\right)} \qquad (10.21)$$

describe the amplitude and phase distributions which leave the object plane and enter the image plane, respectively. Suppose that $B_{\nu,\mu} \equiv 1$. Since points x_0, y_0 of the object plane are imaged into points x, y of the image plane such that $x = Mx_0, y = My_0$, it follows that

$$\chi_0 = M^2 F_0 \qquad (10.22)$$

when

$$B_{\nu,\mu} = 1. \qquad (10.23)$$

Equations 10.22 and 10.23 are nothing but Lummer's theorem. The image is similar to the object, provided that all $B_{\nu,\mu}$ are equal to unity or any other constant. We have seen in Section 5 that $P(p, q) = 1$ for an uncoated Airy-type objective. It follows from Eqs. 10.16–10.18 that $B_{\nu,\mu} \equiv 1$ for an idealized Airy-type objective of infinite numerical aperture. Fourier series have the property

$$f_{\nu,\mu} \to 0 \qquad (10.24)$$

as ν and μ become large. Hence

$$\chi_0 \to M^2 F_0 \qquad (10.25)$$

as ν and μ become large with Airy-type objectives.

Equation 10.25 expresses Lummer's theorem in its more useful form. It states that the object and image approach similarity as the number of spectral orders reaching the image is increased.

A study of Eqs. 10.16–10.18 shows also that the resolution formula for the (ν, μ)th spectral order is

$$\frac{4lm}{(\nu^2 m^2 + \mu^2 l^2)^{\frac{1}{2}}} \geqq \frac{2}{\text{N.A.}_{\text{objective}} + \text{N.A.}_{\text{condenser}}} \text{ wavelengths.} \quad (10.26)$$

The resolution formula for simply periodic structure whose spacing is $2l$ wavelengths along the X_0 direction is obtained by setting $m = \infty$ in Eq. 10.26. Thus

$$2l \geqq \frac{|\nu|}{\text{N.A.}_{\text{objective}} + \text{N.A.}_{\text{condenser}}} \text{ wavelengths.} \qquad (10.27)$$

The choice of the greater-than sign in Eqs. 10.26 and 10.27 gives the necessary condition for resolution of the (ν, μ)th spectral harmonic. The choice of the equality sign gives the physical limit of resolution. The physical limit may be approached but never attained. Abbe's resolution formula for the first spectral order is obtained by setting $\nu = \pm 1$ in Eq. 10.27.

The above phenomena are consistent with well-known experimental and theoretical facts about the image formation with periodic structure in the ordinary microscope. Hence the formulation of Section 8 yields predictions consistent with known facts.

That the formulation is capable of explaining phase microscopy with periodic structures will now be demonstrated in a general manner from Eqs. 10.20 and 10.21. Note that the composite object function χ_0 is determined by the Fourier coefficients $f_{\nu,\mu}$ of the object function whereas the image function F_0 is determined by the Fourier coefficients

$$F_{\nu,\mu} \equiv B_{\nu,\mu} f_{\nu,\mu} \qquad (10.28)$$

in which the *pupil coefficients* $B_{\nu,\mu}$ are numerically equal to the value of the pupil function $P(p, q)$ at the points $(p = p_0/M + \nu/2Ml, q = q_0/M + \mu/2Mm)$. It follows from Eq. 3.24 that the values $B_{\nu,\mu}$ can be altered at will by the choice of coating function $c(p, q)$. Hence the Fourier coefficients $F_{\nu,\mu}$ of the image function can be altered at will with respect to the Fourier coefficients $f_{\nu,\mu}$ of the object function. Since a function described by a Fourier series depends on the Fourier coefficients, it follows that the image function can be made quite different from the composite object function. In particular, we should expect to be able to increase or decrease and to reverse contrast in the image. In a Zernike system of phase microscopy, the coating material of the diffraction plate is distributed so as to modify $B_{0,0}$ together with a highly restricted set of the remaining pupil coefficients $B_{\nu,\mu}$. In fact, it can be shown that the points $(p = p_0/M, q = q_0/M)$ belong to the conjugate area of the diffraction plate. Consequently, $P(p_0/M, q_0/M)$ is the value of the pupil function for points in the conjugate area. Hence with respect to Eq. 10.16 only a highly restricted set of points $(p = p_0/M + \nu/2Ml, q = q_0/M + \nu/2Mm)$ will fall in the conjugate area.

If the conjugate area is narrow, it can happen that *all* $(p = p_0/M + \nu/2Ml, q = q_0/M + \mu/2Mm)$ fall in the complementary area of the diffraction plate when $\nu \neq 0$ or $\mu \neq 0$ or both. In this case $B_{0,0}$ will be said to be *uniformly altered* with respect to the pupil coefficients $B_{\nu,\mu}$ of the higher spectral orders. Since the zero-order coefficient $B_{0,0}$ is almost uniformly altered with respect to the higher ordered coefficients $B_{\nu,\mu}$ in a Zernike system of phase microscopy, it will not be possible to change the image function $F_0(x, y, p_0, q_0)$ arbitrarily with respect to the composite object function $\chi_0(x_0, y_0, p_0, q_0)$. Indeed, it can be shown that the effect of altering $B_{0,0}$ uniformly with respect to $B_{\nu,\mu}$ of the higher spectral orders is mainly to alter contrast in the image. Consequently, the Zernike system of phase microscopy is happily chosen so as to enable one to alter contrast in the image without introducing artifact beyond that already present in the ordinary system of microscopy. In making this assertion, it is assumed that the conjugate and complementary areas are coated uniformly and differently.

With $F_0(x, y, p_0, q_0)$ determined by Eq. 10.21, the total energy density $G(x, y)$ in the plane of the image is given in accordance with Eq. 8.16 by the relation

$$G(x, y) = \iint \frac{S(p_0, q_0)}{n_0^2 - p_0^2 - q_0^2} |F_0(x, y, p_0, q_0)|^2 \, dp_0 \, dq_0. \quad (10.29)$$

If the source of illumination is Lambertian, one may set

$$\frac{S(p_0, q_0)}{n_0{}^2 - p_0{}^2 - q_0{}^2} = 1. \tag{10.30}$$

The following formulation is equivalent to Eq. 10.29 and is more convenient for some theoretical and practical purposes. It may be derived from certain transformations which exist among the various diffraction integrals of phase microscopy. These transformations are not included in order to conserve space. Let

$$I(p_0, q_0) \equiv \frac{S(p_0, q_0)}{n_0{}^2 - p_0{}^2 - q_0{}^2}, \tag{10.31}$$

a quantity which may be set equal to unity with Lambertian sources. Then it can be shown that

$$M^4 G(x, y) = \sum_{\nu} \sum_{\mu} \sum_{s} \sum_{t} f_{\nu,\mu} \tilde{f}_{s,t} Q_{\nu,\mu,s,t} e^{i\pi \left[\frac{x}{Ml}(\nu - s) + \frac{y}{Mm}(\mu - t) \right]} \tag{10.32}$$

in which the integers ν, μ, s, and t range from $-\infty$ to $+\infty$; in which $f_{\nu,\mu}$ is conjugate to $\tilde{f}_{\nu,\mu}$; in which

$$Q_{\nu,\mu,s,t} \equiv \iint I(p_0, q_0) B_{\nu,\mu} \bar{B}_{s,t} \, dp_0 \, dq_0; \tag{10.33}$$

$$B_{\nu,\mu} = P\left(\frac{p_0}{M} + \frac{\nu}{2Ml}, \frac{q_0}{M} + \frac{\mu}{2Mm} \right); \tag{10.34}$$

$$\bar{B}_{s,t} \equiv \bar{P}\left(\frac{p_0}{M} + \frac{s}{2Ml}, \frac{q_0}{M} + \frac{t}{2Mm} \right); \tag{10.35}$$

and in which the integration with respect to $dp_0 \, dq_0$ extends over the optical direction cosines of the rays incident upon the object plane.

It can be shown from Eqs. 10.31–10.35 that the resolution formulas 10.26 and 10.27 hold irrespective of the source function $I(p_0, q_0)$ and of the pupil function $P(p, q)$, provided only that the source function is continuous and that $P(p, q)$ is nowhere equal to zero within the circle $p^2 + q^2 = \rho_m{}^2$. In a phase microscope the numerical aperture of the condenser is equal to the product $n_0 \rho_{0m} = n_0 \sin \vartheta_{0m}$ where ϑ_{0m} is the angle made with the optical axis by the most steeply inclined ray which is incident upon the object specimen. n_0 is the refractive index of the object space. If, for example, the opening in the condenser diaphragm is annular, the numerical aperture of the condenser corresponds to the numerical aperture of the outermost edge of the annular opening. The physical limit of resolution is therefore somewhat larger with the phase microscope than with the ordinary microscope in viewing periodic

structure. For highest resolution the conjugate area should extend to the edge of the clear aperture of the phase objective in viewing periodic structure. On the other hand, the physical limit of resolution will be approached more closely by the phase microscope than by the ordinary microscope for those periodic structures which appear with poor contrast in the ordinary microscope. This statement follows from Eq. 10.26 because the left-hand member must exceed the right-hand member by greater amounts for those systems of microscopy which reveal the object in poorer contrast. Since the denominator of the right-hand member of Eq. 10.26 is only slightly different with phase and ordinary microscopes and since the physical limit can be approached more closely by the phase microscope, there may exist periodic structures that are resolved better by the phase microscope than by the ordinary microscope. Periodic structures whose troughs and elevations represent slight optical path differences belong to this category of object specimens.
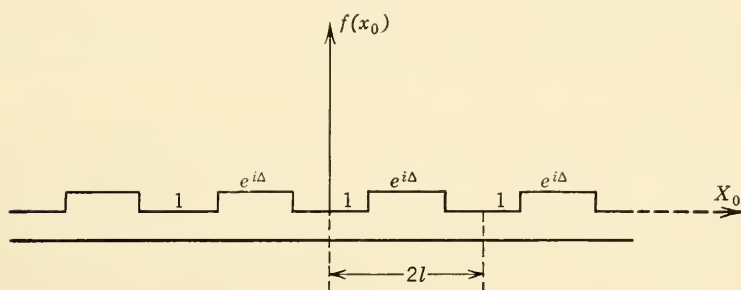
Fig. VII.9. Simply periodic, pure phase gratings as object specimen. The grating spacing is $2l$ along the X_0 direction. The troughs and elevations are supposed to be equal in width.

10.1. Phase gratings whose higher orders are altered uniformly

A simple, pure phase grating is a simply periodic structure whose troughs and elevations represent differences in optical path only. Let the troughs and elevations be arranged across the X_0 direction as in Fig. VII.9. The object function $f(x_0, y_0) = f(x_0)$ is taken as unity over the troughs and as $e^{i\Delta}$ over the elevations. Δ is the optical path difference between the elevations and the troughs and is considered positive when the optical path through the elevations exceeds that through the troughs. This object function is expressed as the Fourier series

$$f(x_0) = \sum_{v=-\infty}^{\infty} f_v e^{i\pi(vx_0/l)} \qquad (10.1.1)$$

in which

$$f_0 = \tfrac{1}{2}(1 + e^{i\Delta});$$

$$f_\nu = f_{-\nu} = \frac{1}{\pi\nu} \sin \frac{\nu\pi}{2} (1 - e^{i\Delta}). \qquad (10.1.2)$$

Then from Eqs. 10.15–10.18

$$F_0(x, y, p_0, q_0) = \frac{e^{(2\pi i/M)(p_0 x + q_0 y)}}{M^2}$$

$$\times \sum_{\nu=-\infty}^{\infty} P\left(\frac{p_0}{M} + \frac{\nu}{2Ml}, \frac{q_0}{M}\right) f_\nu e^{i\pi(\nu x/Ml)}. \qquad (10.1.3)$$

For simplicity, let us consider the special case of narrow-coned, axial illumination. The opening in the condenser diaphragm is a small hole centered on the optical axis, and, correspondingly, the conjugate area of the diffraction plate is a small spot centered on the optical axis. The hole in the condenser diaphragm shall be made so small that one is willing to accept the approximation

$$P\left(\frac{p_0}{M} + \frac{\nu}{2Ml}, \frac{q_0}{M}\right) = P\left(\frac{\nu}{2Ml}, 0\right) \equiv P\left(\frac{\nu}{2Ml}\right). \qquad (10.1.4)$$

From Eqs. 10.1.3 and 10.1.4

$$M^2 F_0(x, y, p_0, q_0) = e^{(2\pi i/M)(p_0 x + q_0 y)} \sum_\nu P\left(\frac{\nu}{2Ml}\right) f_\nu e^{i\pi(\nu x/Ml)}. \qquad (10.1.5)$$

Since $P(p, q) = 0$ when $p^2 + q^2 > \rho_m{}^2$, the largest value of ν for which $P \neq 0$ is given by

$$\left|\frac{\nu}{2Ml}\right| = \frac{N}{2|M|l} \leqq \rho_m = \frac{\text{N.A.}}{|M|}. \qquad (10.1.6)$$

With the integer N determined by Eq. 10.1.6, ν ranges from $\nu = -N$ to $\nu = +N$ in Eq. 10.1.5.

As in Eq. 7.6, the total energy density $G(x, y)$ over the image plane in the case of narrow-coned axial illumination obeys the law

$$G(x, y) = K|F_0(x, y, p_0, q_0)|^2 = \frac{K}{M^4}\left|\sum_{\nu=-N}^{N} P\left(\frac{\nu}{2Ml}\right) f_\nu e^{i\pi(\nu x/Ml)}\right|^2 \equiv G(x). \qquad (10.1.7)$$

The constant K is proportional to the intensity of the source and to the area of the opening in the condenser diaphragm. Whereas the amplitude

and phase distribution over the image plane is a function of both x and y, the total energy density is a function of x alone.

Let

$$S(x) \equiv \sum_{\nu=-N}^{+N} P\left(\frac{\nu}{2Ml}\right) f_\nu e^{i\pi(\nu x/Ml)}. \tag{10.1.8}$$

Then $G(x) = 0$ when $S(x) = 0$, and $G(x)$ is maximum when $S(x)$ is maximum. Hence it suffices to consider the simpler function $S(x)$ in determining the magnitudes and locations of the maxima and minima in the total energy density $G(x)$.

From Eqs. 10.1.2 and 10.1.8

$$S(x) = \frac{1}{2}(1 + e^{i\Delta})P(0) + \frac{2}{\pi}(1 - e^{i\Delta})\sum_{\nu=1}^{N}\frac{1}{\nu}\sin\frac{\nu\pi}{2}P\left(\frac{\nu}{2Ml}\right)\cos\frac{\nu\pi x}{Ml};$$

$$= \frac{2}{\pi}(1 - e^{i\Delta})P(0)\left\{\frac{\pi}{4}\frac{1 + e^{i\Delta}}{1 - e^{i\Delta}} + \sum_{\nu=1}^{N}\frac{1}{\nu}\sin\frac{\nu\pi}{2}\frac{P\left(\dfrac{\nu}{2Ml}\right)}{P(0)}\cos\frac{\nu\pi x}{Ml}\right\};$$

$$P(0) \neq 0. \tag{10.1.9}$$

We introduce at this point the supposition that the zero order shall be altered uniformly with respect to the higher spectral orders; i.e., only the zero spectral order ($\nu = 0$) passes through the conjugate area. This supposition implies tacitly that the objective is of the Airy-type so that $P(p, q) = c(p, q)$ and that the conjugate and complementary areas of the diffraction plate are coated uniformly and differently. It follows from Section 4 that

$$\frac{P(\nu/2Ml)}{P(0)} = \frac{c(\nu/2Ml)}{c(0)} = \frac{e^{-i\delta}}{h}. \tag{10.1.10}$$

Let Eq. 10.1.10 be introduced into Eq. 10.1.9 together with the trigonometric identity

$$\frac{1 + e^{i\Delta}}{1 - e^{i\Delta}} = i\cot\frac{\Delta}{2}. \tag{10.1.11}$$

$$S(x) = \frac{2}{\pi}(1 - e^{i\Delta})P(0)\left(i\frac{\pi}{4}\cot\frac{\Delta}{2} + \frac{e^{-i\delta}}{h}\sum_{\nu=1}^{N}\frac{1}{\nu}\sin\frac{\nu\pi}{2}\cos\frac{\nu\pi x}{Ml}\right). \tag{10.1.12}$$

Δ is the optical path difference between the elevations and the troughs, as in Fig. VII.9, with Δ considered positive when the greater optical path is associated with the elevations. δ is the optical path difference

between the conjugate and complementary areas and is considered positive when the greater optical path belongs to the conjugate area of the diffraction plate. h is the ratio of the amplitude transmission of the conjugate area to the amplitude transmission of the complementary area.

Let us derive the relation which must exist among Δ, δ, and h in order that $S(x)$, and hence $G(x)$, shall be zero at the particular points $x = 0, \pm n2Ml$, in which n is an integer. From Eq. 10.1.12 this relation is

$$0 = i\frac{\pi}{4} \cot \frac{\Delta}{2} + \frac{e^{-i\delta}}{h} \sum_{\nu=1}^{N} \frac{1}{\nu} \sin \frac{\nu\pi}{2}. \tag{10.1.13}$$

Accordingly,

$$\delta = sgn \left(\cot \frac{\Delta}{2} \right) \frac{\pi}{2}; \tag{10.1.14}$$

$$h = \frac{4}{\pi} \left| \tan \frac{\Delta}{2} \right| \sum_{\nu=1}^{N} \frac{1}{\nu} \sin \frac{\nu\pi}{2} \tag{10.1.15}$$

in which $sgn(z) \equiv z/|z| = \pm 1$. Other solutions of δ exist, but these differ from the values of Eq. 10.1.14 by $\mu 2\pi$, where μ is an integer. These solutions are not of practical interest in phase microscopy. The center of the troughs will appear darkest provided that δ and h are related to Δ and the optical properties of the objective in accordance with Eqs. 10.1.14 and 10.1.15. In conclusion, regions of greater optical path will appear dark when $\delta = -\pi/2$ whereas regions of lesser optical path will appear dark when $\delta = +\pi/2$. It is important to observe that, when the zero spectral order is altered *uniformly* with respect to the higher orders, the minimizing δ values are $\delta = \pm\pi/2$. Whereas the minimizing δ values are independent of the numerical value of Δ (that is, $|\Delta|$), the minimizing h values depend on the numerical values of Δ. Physically, therefore, extreme contrasts in the image of pure phase gratings will be produced by the choice of diffraction plates for which $\delta = \pm\pi/2$ when *all* of the higher spectral orders pass through the complementary area. Equation (10.1.15) shows that h will be small with small values of Δ but can become very large as Δ approaches 180°. The elementary theory indicated that h values greater than 2 are not particularly useful. This is not in accord with Eq. 10.1.15 as Δ approaches 180°. The point of demarcation between A- and B-type diffraction plates is given by

$$h = 1 = \frac{4}{\pi} \left| \tan \frac{\Delta}{2} \right| \sum_{\nu=1}^{N} \frac{1}{\nu} \sin \frac{\nu\pi}{2} \tag{10.1.16}$$

for equally spaced, pure phase gratings illuminated by narrow cones of axial illumination.

10.2. Absorption gratings viewed under narrow-coned illumination

The main thesis of this subsection is to demonstrate theoretically that phase microscopy is useful not only for improving contrast in the image of pure phase gratings (object specimens whose adjacent portions differ only in optical path) but also for improving contrast in the image of pure absorption gratings (object specimens whose adjacent portions differ only in amplitude transmission). This theoretical prediction has led to the use of the phase microscope in observing weakly stained biological
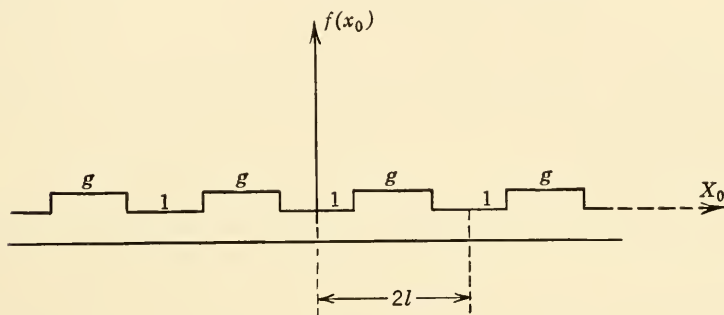
Fig. VII.10. Simply periodic, pure absorption gratings as object specimen. The grating spacing is $2l$ along the X_0 direction. The troughs and elevations are taken as equal in width.

specimens. The method of this section and of Section 10.1 can be extended to show also that the phase microscope is useful for improving contrast in the image of object specimens whose adjacent portions exhibit differences in both optical path and amplitude transmission. The utility of the phase microscope in observing pure phase or pure absorption specimens has been established in Chapter II on the elementary theory but can, of course, be established more conclusively with the aid of the more general theory.

It is pointed out that with the use of narrow-coned, axial illumination all the higher spectral orders will pass through the complementary area except with object gratings that have unusually large spacings $2l$. For most practical purposes the zero order will therefore be altered uniformly with respect to the higher orders when the specimen is observed under narrow-coned, axial illumination.

In the simple, equally spaced grating of Fig. VII.10 let the amplitude

transmission of the troughs be taken as unity and let the amplitude transmission of the elevations be taken as g. Physically, g is the ratio of the amplitude transmission of the elevations to the amplitude transmission of the troughs. Then

$$f(x_0) = \sum_{\nu=-\infty}^{\infty} f_\nu e^{i\pi (\nu x_0/l)}; \qquad (10.2.1)$$

in which

$$f_0 = \frac{(1+g)}{2}; \qquad f_\nu = f_{-\nu} = \frac{(1-g)\sin(\nu\pi/2)}{\nu\pi}. \qquad (10.2.2)$$

As in Eqs. 10.1.7 and 10.1.8,

$$G(x) = \frac{K}{M^4} |S(x)|^2; \qquad (10.2.3)$$

$$S(x) \equiv \sum_{\nu=-N}^{N} P\left(\frac{\nu}{2Ml}\right) f_\nu e^{i\pi (\nu x/Ml)}. \qquad (10.2.4)$$

From Eqs. 10.2.2, 10.2.4, and 10.1.10

$$S(x) = \frac{2}{\pi} P(0)(1-g) \left(\frac{\pi}{4} \frac{1+g}{1-g} + \frac{e^{-i\delta}}{h} \sum_{\nu=1}^{N} \frac{1}{\nu} \sin\frac{\nu\pi}{2} \cos\frac{\nu\pi x}{Ml} \right) \qquad (10.2.5)$$

wherein N is given by Eq. 10.1.6.

The condition under which the total energy $G(x)$ shall be zero at the points $x = 0$, $\pm n2Ml$, where n is an integer, is therefore

$$0 = \frac{\pi}{4} \frac{1+g}{1-g} + \frac{e^{-i\delta}}{h} \sum_{\nu=1}^{N} \frac{1}{\nu} \sin\frac{\nu\pi}{2}. \qquad (10.2.6)$$

Hence

$$e^{-i\delta} = -sgn(1-g).$$

Consequently

$$\delta = \pm\pi, \qquad g < 1;$$

$$\delta = 0, \qquad g > 1. \qquad (10.2.7)$$

$$h = \frac{4}{\pi} \frac{|1-g|}{1+g} \sum_{\nu=1}^{N} \frac{1}{\nu} \sin\frac{\nu\pi}{2}. \qquad (10.2.8)$$

Equations 10.2.7 and 10.2.8 are the relations which must hold among h, δ, g, and the properties of the objective in order that the centers of the troughs of Fig. VII.10 shall have zero energy density. These conditions can be satisfied by the proper choice of diffraction plate. However, h becomes very small as the amplitude transmission of the troughs approaches

the amplitude transmission of the elevations.   As an example, suppose that the grating spacing is chosen relative to the numerical aperture of the objective such that three of the higher spectral orders are transmitted.   Suppose that the energy transmission of the elevations (Fig. VII.10) is 81% of the energy transmission of the troughs.   Then $N = 3$ and $g = (0.81)^{\frac{1}{2}} = 0.9$.   Such a grating will be seen in fair to poor contrast in the ordinary microscope.   From Eq. 10.2.7 $\delta = \pi$ radians or 0.5 wavelength.   From Eq. 10.2.8

$$h = \frac{4}{\pi} \frac{0.1}{1.9} \sum_{\nu=1}^{3} \frac{1}{\nu} \sin \frac{\nu\pi}{2} = 0.05808; \qquad h^2 = 0.0034.$$

Hence an $0.0034A \pm 0.5\lambda$ diffraction plate will cause the centers of the troughs to appear black.   On the other hand, an $0.0034A \pm 0.0\lambda$ diffraction plate will cause the centers of the elevations to appear black.

An examination of Eq. 10.2.8 shows that the choice of B-type diffraction plates is hardly to be expected with gratings of the present section since h will usually be less than unity.   However, B-type diffraction plates are required theoretically with other types of object specimens. Equation 10.2.7 shows that the optimum δ value of a diffraction plate is either 0 or $\lambda/2$ for observing equally spaced, purely absorbing structures, all of whose higher spectral orders pass through the complementary area.

10.3. Phase gratings whose zero order is altered non-uniformly with respect to the higher orders

It was seen in Section 10.1 that the optimum δ values of the diffraction plate are $\pm \pi/2$ radians when all the higher spectral orders pass through the complementary area.   It will be the thesis of this section to demonstrate that the optimum δ values are not necessarily $\pm \pi/2$ radians with pure phase gratings when some of the higher spectral orders pass through the conjugate area.   This conclusion is of sufficient importance to phase microscopy that a general demonstration of its truth would be appropriate.   Up to the present time a general demonstration does not appear to have been published.   The conclusion has, however, been demonstrated in a number of special cases.   Let us consider the special case in which the pure phase grating is arranged as in Fig. VII.9 and in which the grating spacing $2l$ has been chosen so that the complete first order passes through the objective and so that only one branch of the third spectral order passes through the diffraction plate.   We suppose that the first order passes through the complementary area but that the transmitted branch of the third order passes through the conjugate area.

The even orders are absent with equally spaced object gratings. We suppose that all orders higher than the third fail to reach the plane of the image.

In order to formulate a problem which can be solved with relative ease, we suppose further that the condenser diaphragm is opaque except
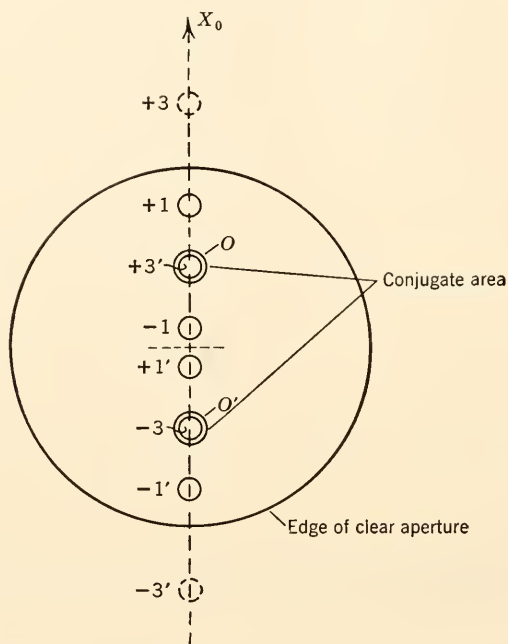
Fig. VII.11. Arrangement of the spectral orders at the plane of the diffraction plate. The $+3$ and $-3'$ branches of the third order are blocked. The first orders pass through the complementary area. The zero orders O and O' and the branches $+3'$ and -3 of the third spectral orders pass through the conjugate area.

for two small holes whose centers are arranged on a line perpendicular to the lines of the grating. The grating is therefore illuminated by two narrow cones of oblique illumination. The holes in the condenser diaphragm shall be chosen so small that one is willing to accept the approximation

$$P\left(\frac{p_0}{M} + \frac{\nu}{2Ml}, \frac{b_0}{M}\right) = P\left(\frac{p_0}{M} + \frac{\nu}{2Ml}\right). \qquad (10.3.1)$$

The optical direction cosine p_0 is of opposite sign for the light issuing from the two holes. If one looks down the body tube of the microscope after removing the eyepiece, the arrangement of the spectral orders will have the appearance of Fig. VII.11. The actual conjugate area of

the diffraction plate consists of two spots which coincide with the images produced by the oppositely inclined zero orders.

The object function is described by Eqs. 10.1.1 and 10.1.2. The amplitude and phase distribution over the plane of the image is given by Eq. 10.1.3 but with the pupil function subject to Eq. 10.3.1. Since two narrow cones of light are incident upon the object plane, an argument similar to that which leads to Eq. 10.1.7 shows that

$$G(x) = \frac{K}{M^4} \left| \sum_{\nu=-3}^{3} P\left(\frac{p_0}{M} + \frac{\nu}{2Ml}\right) f_\nu e^{i(\pi \nu x/Ml)} \right|^2$$

$$+ \frac{K}{M^4} \left| \sum_{\nu=-3}^{3} P\left(\frac{-p_0}{M} + \frac{\nu}{2Ml}\right) f_\nu e^{i(\pi \nu x/Ml)} \right|^2. \quad (10.3.2)$$

Let

$$S_1(x) \equiv \sum_{\nu=-3}^{3} P\left(\frac{p_0}{M} + \frac{\nu}{2Ml}\right) f_\nu e^{i(\pi \nu x/Ml)}; \quad (10.3.3)$$

$$S_2(x) \equiv \sum_{\nu=-3}^{3} P\left(\frac{-p_0}{M} + \frac{\nu}{2Ml}\right) f_\nu e^{i(\pi \nu x/Ml)}. \quad (10.3.4)$$

Let $P = P_0$ or P_1, according as the point $p = (\pm p_0/M + \nu/2Ml)$ falls in the conjugate or in the complementary area. Thus $P = P_0$ when $\nu = 0$;

$$P\left(\frac{p_0}{M} - \frac{3}{2Ml}\right) = P\left(\frac{-p_0}{M} + \frac{3}{2Ml}\right) = P_0;$$

$$P\left(\frac{\pm p_0}{M} + \frac{\pm 1}{2Ml}\right) = P_1;$$

$$P\left(\frac{p_0}{M} + \frac{3}{2Ml}\right) = P\left(\frac{-p_0}{M} - \frac{3}{2Ml}\right) = 0.$$

These statements follow directly from the arrangement of the spectral orders of Fig. VII.11. Since $f_\nu = f_{-\nu}$, we obtain

$$S_1(x) = f_0 P_0 + 2P_1 f_1 \cos \frac{\pi x}{Ml} + P_0 f_3 e^{-i(3\pi x/Ml)}; \quad (10.3.5)$$

$$S_2(x) = f_0 P_0 + 2P_1 f_1 \cos \frac{\pi x}{Ml} + P_0 f_3 e^{i(3\pi x/Ml)}. \quad (10.3.6)$$

At the points $x = 0, \pm n2Ml$, in the centers of the troughs

$$S_1(\pm n2Ml) = S_2(\pm n2Ml) = f_0 P_0 + 2P_1 f_1 + P_0 f_3; \quad (10.3.7)$$

$$n = 0, 1, 2, 3, \text{etc.}$$

Hence $G(x) = 0$ at the centers of the troughs (Fig. VII.9), provided that

$$0 = P_0 \left(f_0 + 2 \frac{P_1}{P_0} f_1 + f_3 \right) ; \quad P_0 \neq 0. \qquad (10.3.8)$$

Introducing f_0 and f_ν from Eq. 10.1.2 and introducing

$$P_0 / P_1 = h e^{i\delta}, \qquad (10.3.9)$$

we obtain the zero condition in the form

$$0 = \frac{2}{\pi} P_0 (1 - e^{i\Delta}) \left(\frac{\pi}{4} \frac{1 + e^{i\Delta}}{1 - e^{i\Delta}} + \frac{e^{-i\delta}}{h} - \frac{1}{6} \right).$$

Consequently the total energy density is zero at the centers of the troughs if

$$0 = i \frac{\pi}{4} \cot \frac{\Delta}{2} + \frac{e^{-i\delta}}{h} - \frac{1}{6}. \qquad (10.3.10)$$

Equation 10.3.10 is true only when the real and imaginary parts of its right-hand member are both zero.   Accordingly

$$\sin \delta = \frac{h\pi}{4} \cot \frac{\Delta}{2} ; \qquad \cos \delta = \frac{h}{6} \cdot \qquad (10.3.11)$$

This equation is easily solved for δ and h.   In summary, the energy density is zero at the centers of the troughs provided that h and δ have the values

$$h = \left(\frac{\pi^2}{16} \cot^2 \frac{\Delta}{2} + \frac{1}{36} \right)^{-\frac{1}{2}} ; \qquad (10.3.12)$$

$$\sin \delta = \frac{\pi}{4} \cot \frac{\Delta}{2} \left(\frac{\pi^2}{16} \cot^2 \frac{\Delta}{2} + \frac{1}{36} \right)^{-\frac{1}{2}} ;$$

$$\cos \delta = \frac{1}{6} \left(\frac{\pi^2}{16} \cot^2 \frac{\Delta}{2} + \frac{1}{36} \right)^{-\frac{1}{2}} \cdot \qquad (10.3.13)$$

These zero conditions differ from the zero conditions of Eqs. 10.1.14 and 10.1.15 in two important respects.   The solution for δ depends on the optical path difference Δ between the elevations and the troughs. The δ values will depart from $\pm\pi/2$.   In the present specialized case the departure of δ from $\pm\pi/2$ will not be large.   This is due to the fact that only one branch of one spectral order passes through the conjugate area. In conclusion, the phase difference δ between the conjugate and complementary areas of the diffraction plate must in general be chosen different from $\pm\lambda/4$ in order to obtain optimum contrast in the image of a pure phase grating when some of the higher spectral orders pass through the

conjugate area. We see from the physical argument of this section that the required departure of δ from $\pm\lambda/4$ depends on Δ, on the grating spacing $2l$, on the numerical aperture of the objective, and on the size and shape of the conjugate area of the diffraction plate. A more general argument which includes spherical aberration of the objective would show that δ depends on the character and magnitude of the spherical aberration.

The following property of Eqs. 10.3.13 is typical not only of the special case studied in this section but also of most, if not all, of the cases in which some of the higher spectral orders from a pure phase grating pass through the conjugate area of the diffraction plate. Suppose that Δ becomes so small that

$$\sin\Delta = \Delta; \qquad \cos\Delta = 1. \tag{10.3.14}$$

If the optical path differences Δ between the elevations and the troughs are small, Eqs. 10.3.12 and 10.3.13 reduce to the simpler relations

$$h = \frac{2|\Delta|}{\pi} ; \tag{10.3.15}$$

$$\sin\delta = \text{sgn}\left(\cot\frac{\Delta}{2}\right) = \text{sgn}(\Delta);$$

$$\cos\delta = \frac{|\Delta|}{3\pi}. \tag{10.3.16}$$

Hence δ will fall in the interval $-\pi/2 \leqq \delta \leqq \pi/2$ and very near the upper and lower bounds of this interval. The center of the troughs will appear dark when the optical path difference δ of the diffraction plate is $+\lambda/4$ or $-\lambda/4$ according as $\Delta > 0$ or $\Delta < 0$. By definition, $\delta > 0$ when the optical path of the conjugate area exceeds that of the complementary area, and $\Delta > 0$ when the optical path of the elevations (Fig. VII.9) exceeds that of the troughs. Since $h < 1$ in Eq. 10.3.15, we reach again the familiar result that regions of lesser optical path appear in optimum dark contrast with $\Lambda+\lambda/4$ diffraction plates and that regions of greater optical path appear in optimum dark contrast with $\Lambda-\lambda/4$ diffraction plates. The most interesting conclusion to be drawn from this paragraph is that the δ values for optimum contrast are again $\pm\lambda/4$, even when some of the higher spectral orders pass through the conjugate area, *provided that Δ is so small that sin $\Delta = \Delta$.*

Sections 10.1 and 10.3 demonstrate that the phenomena of phase microscopy become more complicated when some of the light which is deviated by diffraction at the object passes through the conjugate area. In fact unpublished studies of special cases have shown that unusual

phenomena can take place when both branches of the first spectral order pass through the conjugate area. In general, the passage of the complete first order through the conjugate area is to be avoided.

A comparison of Sections 10.1 and 10.3 with Section 10.2 shows that δ values near $\pm\lambda/4$ are useful for enhancing contrast in the image of pure phase gratings, but that δ values near 0 or $\lambda/2$ are useful for enhancing contrast in the image of pure absorption gratings. An actual grating may present differences both in absorption and in phase transmission. Hence several diffraction plates having different h and δ values are required for obtaining optimum contrast in the image of different periodic structures. The same conclusion applies to non-periodic object structures but is more difficult to demonstrate theoretically.

11. THE IMAGE FUNCTION $F_0(x, y, p_0, q_0)$ FOR A UNIFORM OBJECT PARTICLE IN A LARGE FIELD OF VIEW

The field of view of a microscope often extends over a very large field of view as measured in wavelengths and often contains an assembly of particles each of which may be regarded as substantially uniform in amplitude and phase transmission. The amplitude and phase transmission of the surround will be assumed to be substantially uniform. In considering the assembly of particles, it is sufficient to construct a theorem which applies to a single particle. This theorem is easily generalized to more than one particle.

Let the object function $f(x_0, y_0, p_0, q_0) = f_1 = 1$ for points x_0, y_0 of the surround and let $f(x_0, y_0, p_0, q_0) = f_0$ for points x_0, y_0 which fall within the particle. We suppose that the surround extends over a practically infinite number of wavelengths. The location, size, and shape of the particle are not restricted. However, the particle should be located near the optical axis and shall be thin. Equation 8.10 now assumes the form

$$F_0(x, y, p_0, q_0) = F_u(x, y, p_0, q_0) + F_d(x, y, p_0, q_0) \qquad (11.1)$$

in which F_u and F_d are defined as

$$F_u(x, y, p_0, q_0) \equiv \int_{-\infty}^{\infty} \int_{-\infty}^{\infty} e^{2\pi i(p_0 x_0 + q_0 y_0)}$$
$$\times U(x - Mx_0, y - My_0) \, dx_0 \, dy_0; \qquad (11.2)$$

$$F_d(x, y, p_0, q_0) \equiv \int \iint_{\text{area of the particle}} e^{2\pi i(p_0 x_0 + q_0 y_0)}$$
$$\times U(x - Mx_0, y - My_0) \, dx_0 \, dy_0; \qquad (11.3)$$

$$f \equiv f_0 - f_1 = f_0 - 1 = ge^{i\Delta} - 1. \qquad (11.4)$$

$F_0(x, y, p_0, q_0)$ describes the amplitude and phase distribution produced

over the plane of the image by the incidence upon the object plane of a wave front whose normals have the optical direction cosines p_0, q_0. For the present F_u and F_d are merely definitions, but we shall see later that they correspond, respectively, to the undeviated and deviated waves which reach the plane of the image.

Let U from Eq. 2.19 be introduced into Eq. 11.2.   Then

$$F_u = \iiint_{-\infty}^{\infty} \int_{-\infty}^{\infty} P(p, q) e^{2\pi i(px+qy)} e^{2\pi i[x_0(p_0-Mp)+y_0(q_0-Mq)]} \, dx_0 \, dy_0 \, dp \, dq;$$

$$= \lim_{\substack{x_0 = \infty \\ y_0 = \infty}} \iint P(p, q) e^{2\pi i(px+qy)}$$

$$\times \frac{\sin [2\pi x_0(p_0 - Mp)]}{\pi(p_0 - Mp)} \frac{\sin [2\pi y_0(q_0 - Mq)]}{\pi(q_0 - Mq)} \, dp \, dq.$$

Successive integration with respect to $d(Mp) \, d(Mq)$ gives, in view of Eq. 10.11, the result

$$F_u(x, y, p_0, q_0) = \frac{1}{M^2} e^{(2\pi i/M)(p_0x+q_0y)} P\left(\frac{p_0}{M}, \frac{q_0}{M}\right). \qquad (11.5)$$

Discontinuities in the pupil function are ignored because they appear at isolated loci which do not usually exceed three in number.   We recall that the points ($p = p_0/M$, $q = q_0/M$) belong to the conjugate area of the diffraction plate.   The amplitude and phase of F_u is therefore modulated by the coating function at the conjugate area.   Hence F_u must represent the wave which has passed through the conjugate area and must in fact be the undeviated wave.   This conclusion is furthermore consistent with the fact that the phase multiplier of the infinite integrals of Eq. 11.2 is the phase and amplitude transmission factor $f_1 = 1$ of the surround.   It is interesting to note that the undeviated wave of the more general theory is substantially the same as the undeviated wave as given by Eq. 7.3 in Chapter II of the elementary theory.   However, Eq. 7.4 of Chapter II is far too simple to describe adequately the deviated wave F_d.

Introduce into Eq. 11.3 the change of variable

$$\zeta = x - Mx_0; \qquad \eta = y - My_0. \qquad (11.6)$$

Then

$$F_d(x, y, p_0, q_0) = \frac{f}{M^2} e^{(2\pi i/M)(p_0x+q_0y)} \iint e^{-(2\pi i/M)(p_0\zeta+q_0\eta)} U(\zeta, \eta) \, d\zeta \, d\eta$$

$$(11.7)$$

in which the integration with respect to $d\zeta \, d\eta$ extends over the area of the *geometrical image* of the particle.

From Eqs. 11.1, 11.4, 11.5, and 11.7

$$F_0(x, y, p_0, q_0) = \frac{e^{(2\pi i/M)(p_0 x + q_0 y)}}{M^2}$$

$$\times \left[P\left(\frac{p_0}{M}, \frac{q_0}{M}\right) + (ge^{i\Delta} - 1) \iint e^{-(2\pi i/M)(p_0 \zeta + q_0 \eta)} U(\zeta, \eta) \, d\zeta \, d\eta \right]. \quad (11.8)$$

The double integral extends over the area of the geometrical image of the particle. It is important to bear in mind that, since ζ, η are defined by Eq. 11.6, the origin for the coordinates ζ, η is located at the point x, y of the image plane. The point x, y may fall within or outside of the geometrical image of the particle. The double integral is consequently a function of x and y. $F_0(x, y, p_0, q_0)$ is the amplitude and phase distribution produced over the image plane by the incidence upon the object plane of a wave front whose normals have the optical direction cosines p_0, q_0. g is the ratio of the amplitude transmission of the particle to the amplitude transmission of the surround. Δ is the optical path difference in radians between the particle and its surround. Δ is considered positive when the particle has the greater optical path. U is the primary diffraction integral associated with the objective. It is given by the equation

$$U(\zeta, \eta) = \iint P(p, q) e^{2\pi i(p\zeta + q\eta)} \, dp \, dq \quad (11.9)$$

where $p^2 + q^2 \leqq n^2 \rho_m{}^2 = \rho_m{}^2$ when $n = 1$ in the image space. The first term within the square brackets is the contribution of the undeviated wave. The second term involving the double integral is the contribution of the deviated wave.

It will be noted that the phase factor $e^{(2\pi i/M)(p_0 x + q_0 y)}$ is common to both the undeviated and the deviated waves. This factor represents the phase variation introduced by the inclination of the incident wave front. We may say that this phase variation is transported to the image plane in accordance with Lummer's theorem. Since this phase factor does not alter the partial or the total energy densities, it is of no practical importance to microscopy.

From Eqs. 8.16 and 11.8 the total energy density $G(x, y)$ in the plane of the image obeys the law

$$M^4 G(x, y) = \iint I(p_0, q_0) \left| P\left(\frac{p_0}{M}, \frac{q_0}{M}\right) \right.$$

$$\left. + (ge^{i\Delta} - 1) \iint e^{-(2\pi i/M)(p_0 \zeta + q_0 \eta)} U(\zeta, \eta) \, d\zeta \, d\eta \right|^2 dp_0 \, dq_0. \quad (11.10)$$

$$I(p_0, q_0) \equiv \frac{S(p_0, q_0)}{n_0{}^2 - p_0{}^2 - q_0{}^2} \qquad (11.11)$$

and may be set equal to unity with Lambertian sources of light. Since ζ and η are measured from the point (x, y), G is in fact an implicit function of x, y. The integration with respect to $dp_0\, dq_0$ extends over the range of optical direction cosines of the rays incident upon the object plane. Equations 11.8 and 11.10 are of great importance to the theory of phase microscopy with non-periodic objects. These equations may be used with considerable confidence when the field of view in the object space extends over 50 or more wavelengths and when the particle is located well within the field of view. When smaller fields are encountered, the validity of the approximation afforded by Eqs. 11.8 and 11.10 should be investigated or one should return to the more general equations from which Eq. 11.8 has been specialized. Smaller fields of view are permissible with objectives having the higher numerical aperture.

12. CRITERION FOR ISOLATED PARTICLES

Upon looking into a phase microscope, one is impressed by the rapidity with which the energy density in the surround approaches a substantially constant value as the point of observation recedes from the edge of a particle. One is impressed also by the slight effect which one particle exerts upon the image of another unless the particles are tightly packed. The cause of these phenomena will now be treated in a semirigorous manner.

With reference to Eq. 11.8, it has already been stated that the phase factor $e^{(2\pi i/M)(p_0 x + q_0 y)}$ is of no practical interest to microscopy. We shall therefore omit it and write

$$M^2 F_0(x, y, p_0, q_0) = P\left(\frac{p_0}{M}, \frac{q_0}{M}\right)$$
$$+ (g e^{i\Delta} - 1) \iint e^{-(2\pi i/M)(p_0 \zeta + q_0 \eta)} U(\zeta, \eta)\, d\zeta\, d\eta. \quad (12.1)$$

The meaning of the double integral is clarified by Fig. VII.12. As the point x, y recedes from the edge of the geometrical image of the particle, the double integral decreases for two reasons. First, the exponential in the integrand oscillates more rapidly as $(\zeta^2 + \eta^2)^{\frac{1}{2}} = D$ increases. The rapidity of these oscillations increases with the inclination p_0, q_0 of the incident wave front. Hence the double integral of Eq. 12.1 decreases more rapidly as the point x, y recedes from the edge of the

geometrical image of the particle when the annular opening in the condenser diaphragm is increased in numerical aperture. Second, the
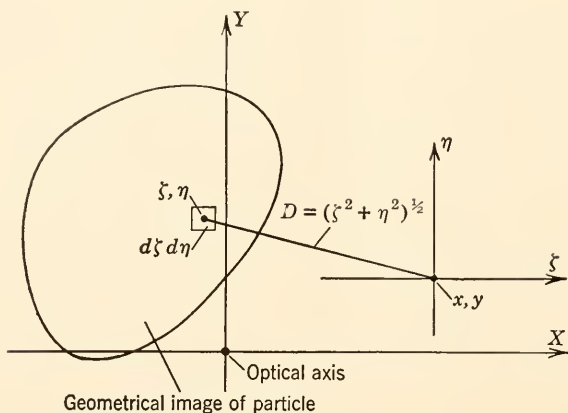
FIG. VII.12.   Relation of the coordinates ζ, η to a point x, y which is exterior to the geometrical image of the particle.

primary diffraction integral $U(\zeta, \eta)$ decreases rapidly with D and is an oscillatory function of D.   Approximately,

$$U(\zeta, \eta) \;=\; \pi\rho_m{}^2 2 \frac{J_1(2\pi\rho_m D)}{2\pi\rho_m D} \;=\; \pi\rho_m{}^2 2 \frac{J_1(\beta D_a)}{\beta D_a} \qquad (12.2)$$

wherein $\beta \equiv 3.8317$ and

$$D_a \equiv \frac{D}{r_a}\,; \qquad r_a \equiv \frac{0.6098}{\rho_m} = \frac{0.6098\,|M|}{\text{N.A.}} \text{ wavelengths.} \quad (12.3)$$

N.A. is the numerical aperture of the objective.   To fix the order of magnitudes, we note that $2J_1(\beta D_a)/\beta D_a = 1$ when $D_a = 0$ and that $2|J_1(\beta D_a)|/\beta D_a < 0.02$ when $D_a > 5$ Airy units r_a.   Furthermore, $\rho_m < 0.04$ so that $\rho_m{}^2 < 16 \times 10^{-4}$.   Since the integrand of the double integral oscillates with $D_a = (\zeta^2 + \eta^2)^{\frac{1}{2}}/r_a$, we must expect that the second right-hand member of Eq. 12.1 will be negligible as compared with $P(p_0/M, q_0/M)$, whose absolute value is usually greater than 0.3, when the point x, y is located 5 or more Airy units away from the edge of the geometrical image of the particle.   Observations in the microscope show that this statement is conservative.

For points x, y that fall in the distant portions of the surround one can show rigorously that

$$\iint e^{-(2\pi i/M)(p_0\zeta+q_0\eta)} U(\zeta, \eta) \, d\zeta \, d\eta = 0; \qquad (12.4)$$

whence

$$M^2 F_0(x, y, p_0, q_0) = P\left(\frac{p_0}{M}, \frac{q_0}{M}\right) = h e^{i\delta}; \qquad (12.5)$$

$$M^4 G(x, y) = \text{constant} = h^2 \iint I(p_0, q_0) \, dp_0 \, dq_0. \quad (12.6)$$

Thus

$$G_s = \frac{h^2}{M^4} \iint I(p_0, q_0) \, dp_0 \, dq_0 \qquad (12.7)$$

is physically the energy density in the image of the surround at points well removed from the *nearest* geometrical image of a particle. For brevity we shall call G_s the energy density of the surround. G_s is proportional to the energy transmission h^2 of the conjugate area and vanishes, as in the Schlieren method, when the conjugate area is opaque. In conclusion, the energy density at any point x, y in the image of the surround approaches G_s when the nearest geometrical image of any one of the particles is located 5 or more Airy units r_a from the point x, y.

As a corollary, one particle will not disturb appreciably the image of another provided that the edges of their geometrical images are separated by 5 or more Airy units. Accordingly, particles whose geometrical images are separated by at least 5 Airy units are said to be *isolated*. It follows from Eq. 12.3 that particles are more likely to be isolated with objectives having the higher numerical aperture.

13. THE ENERGY DENSITY IN THE FAR INTERIOR OF A LARGE PARTICLE

Suppose first that the particle is very large and is located in a much larger field of view. For points x, y located well in the interior of the geometrical image of the particle the argument leading to Eq. 11.5 may be repeated with F_d of Eq. 11.3 to show that

$$F_d(x, y, p_0, q_0) = \frac{f}{M^2} e^{(2\pi i/M)(p_0 x + q_0 y)} P\left(\frac{p_0}{M}, \frac{q_0}{M}\right). \qquad (13.1)$$

Then from Eqs. 11.1, 11.4, 11.5, and 13.1 we obtain almost directly the result

$$F_0(x, y, p_0, q_0) = \frac{e^{(2\pi i/M)(p_0 x + q_0 y)}}{M^2} g e^{i\Delta} P\left(\frac{p_0}{M}, \frac{q_0}{M}\right). \qquad (13.2)$$

The total energy density $G(x, y)$ at points x, y which are located in the far interior of a large particle obeys therefore the law

$G(x, y) = \text{constant} \equiv G_p$

$$= \frac{g^2}{M^4} \iint I(p_0, q_0) \left| P\left(\frac{p_0}{M}, \frac{q_0}{M}\right)\right|^2 dp_0\, dq_0. \qquad (13.3)$$

If the objective is of the Airy type and if the conjugate and complementary areas of the diffraction plate are coated uniformly and differently, $P(p_0/M, q_0/M) = he^{i\delta}$. For this specialization to a Zernike system of phase microscopy

$$G_p = \frac{g^2 h^2}{M^4} \iint I(p_0, q_0)\, dp_0\, dq_0 = g^2 G_s \qquad (13.4)$$

where G_s is the total energy density of the surround as in Eq. 12.7. If the amplitude transmission of the particle is equal to that of the surround, $g = 1$ and $G_p = G_s$, irrespective of the optical path difference Δ between the particle and the surround. This means physically that with such particles the brightness of a far interior point in the image of the particle will be the same as the brightness of the surround. This phenomenon is familiar to users of the phase microscope.

If the particle is not large or if the point x, y approaches the edge of the geometrical image of a large particle, the evaluation of Eq. 11.7 becomes difficult. No relatively simple generalizations can be made at the present time beyond the observation that the solution can become quite different from that of Eq. 13.1. Some interesting conclusions can be drawn, however, in the specialized case in which the object is illuminated by narrow-coned axial illumination. These conclusions will form the subject matter of Sections 14 and 15.

Experiment reveals a halo near the edge of the geometrical image formed of a particle by a phase microscope. Explanation of this halo for thin plate-like particles involves the formidable task of evaluating Eq. 11.7 at points x, y near the edge of the geometrical image.

14. CONDITIONS FOR REDUCTION TO THE ELEMENTARY THEORY

The predictions of the elementary theory of phase microscopy of Chapter II are characterized by the fact that the variation in the energy density between particle and surround is a step function. The level of illumination is sensibly uniform over the entire image of the particle and changes abruptly at the edge of the geometrical image of the particle to another uniform level over the image of the surround. The laws that govern the difference between these two levels of illumination are derived in Chapter II. An abrupt change in the level of illumination is

not possible from the general theory, but we shall see that under severe restrictions as to the size of the conjugate area it is possible for the levels of illumination to approach the properties of a step function.

From Eq. 11.8

$$M^2 F_0(x, y, p_0, q_0)$$

$$= e^{(2\pi i/M)(p_0 x + q_0 y)} \left[P\left(\frac{p_0}{M}, \frac{q_0}{M}\right) + (ge^{i\Delta} - 1)H_p(x, y, p_0, q_0) \right] \quad (14.1)$$

in which

$$H_p(x, y, p_0, q_0) = \iint e^{-(2\pi i/M)(p_0\zeta + q_0\eta)} U(\zeta, \eta) \, d\zeta \, d\eta; \quad (14.2)$$

$$U(\zeta, \eta) = \iint P(p, q)e^{2\pi i(p\zeta + q\eta)} \, dp \, dq; \quad (14.3)$$

$$p^2 + q^2 \leqq \rho_m{}^2. \quad (14.4)$$

The double integral for H_p extends over the area of the geometrical image of the particle. The coordinates ζ, η are to be measured from a point x, y within the geometrical image. The suffix p is attached to H to indicate that H depends on the size and shape of the particle.

If the objective is of the Airy type and if the conjugate and complementary areas are coated uniformly and differently,

$$P\left(\frac{p_0}{M}, \frac{q_0}{M}\right) = he^{i\delta}. \quad (14.5)$$

Let us assume that it is possible to select a pupil function $P(p, q)$ and a set of optical direction cosines p_0, q_0 such that

$$H_p(x, y, p_0, q_0) = 1 \quad (14.6)$$

for points x, y which occupy an extended region within the geometrical image of the particle. Denote this region by A. We show that the relative energy densities of this area A of the geometrical image of the particle and of the surround obey the laws of the elementary theory of phase microscopy.

From Eqs. 14.1, 14.5, and 14.6

$$M^2 F_0(x, y, p_0, q_0) = e^{(2\pi i/M)(p_0 x + q_0 y)} (he^{i\delta} + ge^{i\Delta} - 1) \quad (14.7)$$

for points x, y which belong to the region A. Correspondingly the total energy density $G(x, y)$ in the plane of the image obeys the law

$$G(x, y) = \text{constant} \equiv G_A = K_1 |he^{i\delta} + ge^{i\Delta} - 1|^2; \quad (14.8)$$

$$K_1 \equiv \frac{1}{M^4} \iint I(p_0, q_0) \, dp_0 \, dq_0. \quad (14.9)$$

Comparison of Eq. 14.8 above with Eq. 8.4 of Chapter II shows that the total energy density over the region A of the geometrical image of the particle obeys the law derived from the elementary theory. The consequences of this law have been discussed in detail in Chapter II.

The necessary conditions for the derivation of Eq. 14.8 are given by Eqs. 14.5 and 14.6. In addition, Eq. 14.1 involves the supposition that the field of view extends over a great number of wavelengths.

15. CONDITIONS UNDER WHICH $H_p = 1$ OVER AN EXTENDED AREA

It has been shown in Section 14 that, if there exists within the geometrical image of the particle an area A for which $H_p(x, y, p_0, q_0) = 1$, the contrast relations between this area and the image of the surround obey the simple laws of the elementary theory. The problem of this section is to determine under which physical conditions the area A can be made to extend over a substantial portion of the geometrical image of the particle in a Zernike system of phase microscopy.

It is known that

$$\lim_{c = \infty} \int_a^b e^{icx} f(x) \, dx = 0 \tag{15.1}$$

for "civilized" functions $f(x)$. Hence it is to be suspected that the oscillations of the exponential phase factor in the integrand of Eq. 14.2 may lead to difficulties in finding an extended region A for which $H_p = 1$. For this reason we shall require that p_0 and q_0 are restricted to values so small that $e^{-(2\pi i/M)(p_0\zeta + q_0\eta)}$ is substantially unity when

$$(\zeta^2 + \eta^2)^{\frac{1}{2}} \leqq R \tag{15.2}$$

where R is the radius of the largest circle which can be inscribed in the geometrical image of the particle about the point x, y as center (see Fig. VII.13). The optical direction cosines p_0, q_0 can be restricted in this manner with the use of a very narrow cone of axial illumination. We suppose for definiteness that the hole in the condenser diaphragm is small, circular, and centered upon the optical axis. The conjugate area is a corresponding small, circular spot centered on the optical axis. Let the numerical aperture of the conjugate area and of the objective be ρ_1 and ρ_m, respectively, with respect to the image space of the objective. Introducing into Eq. 14.3 the changes of variable

$$p = -\rho \cos \phi; \qquad \zeta = r \cos \theta;$$
$$q = -\rho \sin \phi; \qquad \eta = r \sin \theta; \tag{15.3}$$

together with the facts that $P(p, q) = 1$ in the complementary area and

Boundary of geometrical image of particle
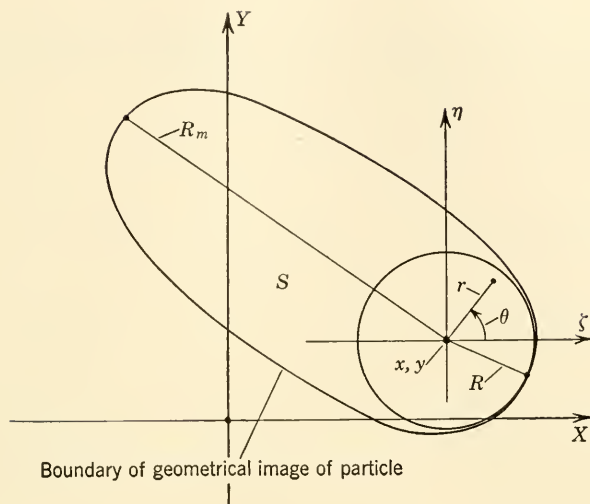
FIG. VII.13. The area S and the inscribed circle of greatest radius R which can be drawn about a point x, y in the interior of the geometrical image of the particle.

that $P(p, q) = he^{i\delta}$ in the conjugate area, one finds that in a straight-forward manner

$$U(r) = \int_0^{\rho_m} \int_0^{2\pi} e^{-2\pi i r \rho \cos (\phi - \theta)} \rho \, d\phi \, d\rho$$

$$+ (he^{i\delta} - 1) \int_0^{\rho_1} \int_0^{2\pi} e^{-2\pi i r \rho \cos (\phi - \theta)} \rho \, d\phi \, d\rho;$$

$$= 2\pi \rho_m{}^2 \frac{J_1(2\pi r \rho_m)}{2\pi r \rho_m} + 2\pi \rho_1{}^2 (he^{i\delta} - 1) \frac{J_1(2\pi r \rho_1)}{2\pi r \rho_1}. \quad (15.4)$$

From Eq. 14.2

$$H_p(x, y, 0, 0) \equiv H_p(x, y) = \iint U(\zeta, \eta) \, d\zeta \, d\eta \quad (15.5)$$

in which the integral extends over the area of the geometrical image of the particle with ζ, η measured from the point x, y as in Fig. VII.13. Consequently,

$$H_p(x, y) = H_R(x, y) + H_S(x, y) \quad (15.6)$$

where

$$H_R(x, y) \equiv \iint_R U(\zeta, \eta) \, d\zeta \, d\eta = 2\pi \int_0^R U(r) r \, dr; \quad (15.7)$$

$$H_S(x, y) \equiv \iint_S U(\zeta, \eta) \, d\zeta \, d\eta = \iint_S U(r) r \, d\theta \, dr. \quad (15.8)$$

S denotes the portion of the area of the geometrical image which is unoccupied by the inscribed circle of radius R. All dimensions are to be measured as numbers of wavelengths.

From Eqs. 15.7 and 15.4

$$H_R(x, y) = 1 - J_0(2\pi\rho_m R) + (he^{i\delta} - 1)[1 - J_0(2\pi\rho_1 R)] \qquad (15.9)$$

because

$$\int_0^R \frac{J_1(ar)}{ar} \, r \, dr = -\frac{1}{a^2} \int_0^{aR} d[J_0(z)] = \frac{1}{a^2}[1 - J_0(aR)].$$

With a large particle it will be possible to find an extended region of points x, y for which R is so large that

$$J_0(2\pi\rho_m R) \to 0. \qquad (15.10)$$

Moreover, as the numerical aperture of the objective is increased, this region of points creeps toward the edge of the geometrical image of the particle. With R so determined, it will also be possible to choose a conjugate area (and hence ρ_1) so small that

$$1 - J_0(2\pi\rho_1 R) \to 0. \qquad (15.11)$$

Hence with a suitably chosen small conjugate area there will exist an extended region A of points x, y for which

$$H_R(x, y) = \text{constant} \to 1. \qquad (15.12)$$

This region of points x, y is an increasing function of the numerical aperture of the objective and is a decreasing function of the numerical aperture $|M|\rho_1$ of the conjugate area.

From Eqs. 15.8 and 15.4

$$H_S(x, y) = 2\pi\rho_m{}^2 \times$$
$$\left[\int\int_S \frac{J_1(2\pi\rho_m r)}{2\pi\rho_m r} \, r \, d\theta \, dr + \frac{\rho_1{}^2}{\rho_m{}^2}(he^{i\delta} - 1)\int\int_S \frac{J_1(2\pi\rho_1 r)}{2\pi\rho_1 r} \, r \, d\theta \, dr \right] \qquad (15.13)$$

in which

$$r = (\zeta^2 + \eta^2)^{\frac{1}{2}} > R. \qquad (15.14)$$

The first double integral in the right-hand member will be negligible when R satisfies Eq. 15.10. Except for a negligible term

$$H_S(x, y) = (he^{i\delta} - 1)\rho_1 \int\int_S J_1(2\pi\rho_1 r) \, d\theta \, dr. \qquad (15.15)$$

whence

$$|H_S(x, y)| < 2\pi\rho_1 |he^{i\delta} - 1| \left| \int_S J_1(2\pi\rho_1 r) \, dr \right|. \qquad (15.16)$$

Let R_m be the greatest distance from the point x, y to any point on the geometrical boundary as in Fig. VII.13. With few exceptions, in phase microscopy $\left|he^{i\delta} - 1\right| < 1$. Furthermore, $\left|J_1(2\pi\rho_1 r)\right| < 0.52$. Therefore

$$\left|H_S(x, y)\right| < 2\pi\rho_1(R_m - R)0.52. \qquad (15.17)$$

The condition which ρ_1 must satisfy in order that $H_S(x, y)$ shall be negligibly small as compared with $H_R(x, y)$ of Eq. 15.12 is

$$\pi\rho_1(R_m - R) \ll 1. \qquad (15.18)$$

Larger values of ρ_1 are of course tolerable, but the largest tolerable values are difficult to estimate.

In conclusion, a point x, y belongs to the region A provided that it is possible to draw about the point x, y (Fig. VII.13) an inscribed circle whose radius R is so large that

$$J_0(2\pi\rho_m R) \rightarrow 0,$$

provided also that the conjugate area is chosen so small that

$$J_0(2\pi\rho_1 R) \rightarrow 1,$$

and provided that ρ_1 is so small that

$$\pi\rho_1(R_m - R) \ll 1$$

where R_m is the greatest distance in wavelengths from the point x, y to any point on the boundary of the geometrical image of the particle. $|M|\rho_m$ is the usual N.A. of the objective. As the numerical aperture of the objective is increased, the region A creeps toward the edge of the geometrical image of the particle. $|M|\rho_1$ is the numerical aperture of the conjugate area with respect to the object space of the objective. As ρ_1 is decreased, the region A spreads throughout the interior of the geometrical image of increasingly larger particles. For points x, y of the region A the function $H_p(x, y)$ of Eq. 15.6 is practically unity and the total energy density G_A is given by Eq. 14.8 of the elementary theory of phase microscopy.

When the required hole in the condenser diaphragm assumes pinhole dimensions, it is preferable to discard the lamp and substage condensers and to illuminate the object directly by means of a distant zirconium arc, etc. The question as to the self-luminous character of a virtual image is thus avoided.

Osterberg and Pride have performed experiments with polanret systems involving narrow-coned axial illumination and have found that the above predicted A region exists. In one of the polanret systems

$\rho_1 = 0.0033$, $\rho_m = 0.033$, and $|M|\rho_m = $ N.A. $= 0.14$.   Despite the fact that the value $\rho_1 = 0.0033$ was much larger than the conservative theoretical values required by Eqs. 15.11 and 15.18, the observed A region extended throughout large portions of relatively large particles. Moreover for the A region, the h and δ values producing extreme contrast between the A region and the surround were in substantial accord with the elementary theory.

When the method of this section is applied to diffraction plates having annular conjugate areas, as in the usual practice of phase microscopy, an A region is found to exist.   This region is increased by increasing the numerical aperture of the objective and by decreasing the width of the conjugate area.   It is, however, difficult to form an estimate of the size of the A region.   Whereas the function $H_R(x, y)$ is of character permitting an extended A region, the function $H_S(x, y)$ is not readily amenable to the purpose of relating the size of the A region to the properties of the particle and of the optical system.   Experiments performed by Dr. H. Jupnik and described briefly by her in Section 5 of Chapter III are at least consistent with the conclusion that the A region increases with decreasing width of the annular conjugate area.

In summary, the geometrical image of the particle can exhibit three distinctly different regions of contrast.   In the A region the contrast with respect to the image of the surround obeys the laws of the elementary theory of phase microscopy.   The A region is usually surrounded by the B region which may extend 5 or more Airy units beyond the boundary of the geometrical image of the particle.   The energy density may change rapidly in the B region.   The halo near the edge of the geometrical image belongs, for example, to the B region.   The C region occurs only in the far interior of relatively large particles.   The energy density of the C region is equal to that of the surround when the amplitude transmission of the particle is equal to that of the surround.   The C region is brighter or darker than the surround according as the particle has higher or lower light transmission than its surround.   Except for the fact that the energy density of the C region is proportional to the energy transmission of the conjugate area of the diffraction plate, the C region is unaffected by a Zernike system of phase microscopy.   All three regions are predicted by the general theory, but only the A region together with the region of the surround is predicted by the elementary theory of phase microscopy.   Experiment indicates the existence of all three regions in the image of relatively large particles.   The system of microscopy described by Dyson (1949) is a method for avoiding the C region.

16. CRITICAL VERSUS KÖHLER ILLUMINATION

Phase microscopy occurs in a Zernike system whether the microscope is adjusted for Köhler or for critical illumination. The following simple considerations indicate that it is remarkable that the two systems of illumination should produce under any circumstances similar contrasts in the image. In Köhler illumination the coherent light from a point in the condenser diaphragm emerges from the substage condenser as a substantially plane wave which extends over the entire object plane and which subsequently forms in the image plane an "Abbe" picture of the *entire* field of view. The complete picture of the object is formed by the superposition of the Abbe pictures produced by the light from the various points in the opening of the condenser diaphragm. On the other hand, with critical illumination, the coherent light from a point in the source is focused in a highly localized manner upon a small portion of the object plane. The object plane is the scene of a localized, circular diffraction image of the point in the source. This diffraction image is reprojected by the objective into the plane of the eyepiece as a modulated, but still localized, diffraction image of the point in the source. Consequently the image of the object is constructed in a *piecewise* manner by the light emanated from the various points in the source.

Some consideration will show that the elementary theory of phase microscopy does not apply to critical illumination. Suppose, for example, that the object is a ruled grating. Since the coherent light from a point in the source is concentrated upon one or more of the rulings and not upon all of the rulings, the deviated and undeviated waves which leave the grating will be vastly different from the case of Köhler illumination. Hence the usual simplified vector models for phase microscopy fail.

A general theory for phase microscopy with critical illumination can, however, be formulated. This theory shows that the total energy density in the image plane can become similar with critical and Köhler illumination provided that the source of illumination is broad and fairly uniform, provided that a large field of view is illuminated, and provided that the speeds of the lamp and substage condensers are high. These conditions are well fulfilled in the normal usage of a microscope. To the extent that one or more of these three conditions are violated, phase microscopy with critical and Köhler illumination will produce different distributions of energy density in the plane of the image. The fact that the phenomena of phase microscopy are not necessarily similar with Köhler and critical illumination is an advantage rather than a dis-

advantage because the versatility of the phase microscope is thus increased. That the appearance of the image becomes similar with critical and Köhler illumination when the above-mentioned conditions are fulfilled can be verified by introducing a ribbon filament illuminator and adjusting the phase microscope for critical illumination.

BIBLIOGRAPHY

Ajo, A., 1947. On the refractive index of the retina. *Acta Physiol. Scand.* 13:130–149.

Alber, H. K., and J. T. Bryant, 1940. Determination of the refractive index of liquids. *Ind. Eng. Chem., Anal. Ed.* 12:305–307.

Albertini, A. von, 1945. Zur Anwendung der Phasenkontrastmikroskopie in der pathologischen Histologie. *Schweiz. Z. Path. u. Bakt.* 8:298–310.

1946a. Pflasterepithelzellen im Phasenkontrastbild. *Acta Anat.* 1:463–466.

1946b. Erfahrungen und Ergebnisse mit dem Phasenkontrastverfahren in der normalen und pathologischen Histologie. *Praxis, Schweiz. Rund. Med.* 35:107–112.

1946c. Cytologische Exudatbefunde mit dem Phasenkontrastverfahren. *Schweiz. Z. Path. u. Bakt.* 9:701–706.

1947. Vergleichende histologische Geschwulstuntersuchungen mit dem Phasenkontrastverfahren. *Schweiz. Z. Path. u. Bakt.* 10:1–29.

1948a. La méthode du contraste de phases en histologie. *Rev. hématol.* 3:139–153.

1948b. Ueber die Bedeutung von Dissociationserscheinungen in Krebszellen. *Schweiz. med. Wochenschr.* 78:1–10.

Albertini, A. von, and M. Aufdermaur, 1947. Zell- und Strukturstudien am embryonalen Bindegewebe. *Schweiz. Z. Path. u. Bakt.* 10 (*Suppl.*):1–11.

A.L.E.B., 1949. A new outfit for phase contrast microscopy. *Micr. & Ent. Mon.* 7:204–208.

Angulo, J. J., 1949a. The inclusion bodies from diseases of undetermined etiology and from apparently healthy animals as seen unstained with the phase microscope. *J. Infect. Dis.* 85:243–250.

1949b. Demonstration of viral inclusion bodies in unstained tissue sections with the aid of the phase microscope. *Arch. ges. Virusforsch.* 4:118–129.

Angulo, J. J., O. W. Richards, and A. L. Roque, 1949. Demonstration of viral inclusion bodies in unstained tissue sections with the aid of the phase microscope. I. The inclusion bodies of yellow fever, herpes simplex, fowl pox, and distemper. *J. Bact.* 57:297–303.

Anon., 1934. Report of paper [by Zernike] on the phase-contrast method. *J. Quckett Micr. Club* 1:75–76.

Anon., 1944. *Photomicrography.* Eastman Kodak Co., Rochester, N. Y. 14th ed. 174 pp.

Anon., 1947. *Cooke phase contrast microscope.* Cooke, Troughton and Simms. York, England. 7 pp.

Anon., 1947. *Phase contrast with Bausch and Lomb accessories.* Bausch and Lomb Optical Company, Rochester, N. Y. 4 pp.

Anon., 1948. *AO Spencer phase microscopes.* American Optical Co., Buffalo, N. Y. 20 pp.

Anon., 1949. *Beck phase contrast apparatus.* R. and J. Beck, London. 10 pp.

Anon., 1949. *Bausch & Lomb phase contrast accessories.* Bausch and Lomb Optical Company, Rochester, N. Y. 16 pp.

Anon., 1949. *Gebrauchsanweisung Phasenkontrast-Einrichtung.* 4 pp. *Zeiss-Winkel Phasenkontrast.* 12 pp. R. Winkel, G.m.b.H., Göttingen.

Anon., 1949. *Phase contrast.* R. Winkel, G.m.b.H., Göttingen. 19 pp.

Anon., 1949. Refractive index and phase microscopy. *Educ. Focus* 20:13–15.

Anon., n.d. *Microscopio a contrasto di fase.* Fratelli Koristka. Micro N. 130.
    8 pp. Same title, suppl. 4 pp. Milan.

Anon., n.d. *Wild microscopes.* General catalog Mi501e, pp. 38–39. *Wild phase
    contrast accessories.* Mi502e, 4 pp. *Phasenkontrast-Ausrüstung und Ge-
    brauchsanweisung.* Mi503d, 12 pp. Heerbrugg, Switzerland.

Antonio, A., 1949. Quantitative researches on the optical properties of human bone.
    Nature 163:604.

Austin, C. R., and J. Smiles, 1948. Phase-contrast microscopy in the study of
    fertilization and early development of the rat egg. *J. Roy. Micr. Soc.* 68:13–19.

Bachrach, M., 1946. Method for observing surface structure. *J. Biol. Photogr.
    Assoc.* 14:157–162.

Bailly, R., 1948. A new tool for infrared studies. *Science* 108:143.

Baker, J. R., 1949. Further remarks on the Golgi element. *Quart. J. Micr. Sci.*
    90:293–307.

Baker, J. R., D. A. Kempson, and P. C. J. Brunet, 1949. A simple method for phase-
    contrast microscopy: improvements in technique. *Quart. J. Micr. Sci.* 90:323–
    329.

Ballerini, L., 1948. Teoria elementare del microscopio a contrasto di fase. *Galileo
    News* 1948(1):14–20. *Nuovo Cimento* 5:121–132.

Ballerini, L., and F. Scandone, 1949. Microcinématographie en contraste de phase.
    Microscopie (Paris) 1:M162–M164.

Barer, R., 1947. Some applications of phase-contrast microscopy. *Quart. J. Micr.
    Sci.* 88:491–500.

    1948*a*. Phase-contrast microscopy of viruses. *Nature* 162:251.

    1948*b*. Recent advances in microscopy; phase-contrast microscopy. *Brit. Sci.
        News* 1(9):10–13.

    1949. Phase-contrast microscopy in anatomy. *J. Anat.* (London) 83:61.

    1949. Variable colour-amplitude phase-contrast microscopy. *Nature* 164:1087–
        1088.

Barnes, R. B., C. J. Burton, and R. G. Scott, 1945. Electron microscopical replica
    techniques for the study of organic surfaces. *J. Appl. Phys.* 16:730–739.

Baud, C. A., 1947. Structure microscopique et inframicroscopique de la membrane
    des cellules épithéliales pavimenteuses. *Compt. rend. acad. sci.* (Paris) 225:590–
    592.

Beale, L. S., 1870. *How to work with the microscope.* 4th ed. Lindsay and Blakiston,
    Philadelphia. xvii+383 pp.

Bejdl, W., 1949. Beobachtungen an Plattenepithelzellen im Phasenkontrast-
    mikroskop und mit anderen Methoden. *Mikroskopie* (Wien) 4:28–40.

Benford, James R., and Richard L. Seidenberg, 1950. Phase contrast microscopy
    for opaque specimens. *J. Opt. Soc. Am.* 40:259; 314–316.

Bennett, A. H., 1944. Phase-difference microscopy for transparent objects. *Anat.
    Rec.* 89:547.

    1946. Phase microscopy, its development and utility. *Sci. Month.* 63:191–193.

    1948. The phase contrast microscope. *J. Washington Acad. Sci.* 38:30.

Bennett, A. H., H. Jupnik, H. Osterberg, and O. W. Richards, 1946. Phase micros-
    copy. *Trans. Am. Micr. Soc.* 65:99–131.

Bennett, A. H., D. L. Woernley, and A. J. Kavanagh, 1948. Ultraviolet phase
    microscopy. *J. Opt. Soc. Am.* 38:739–740.

Bensley, S. H., 1950. Histological studies of the reactions of cells and intercellular
    substances of loose connective tissue to the spreading factor of testicular extracts.
    Ann. N. York Acad. Sci. 52:983–988.

Berti, L., 1948. Teoria della microscopia in contrasto di fase. *Nuovo Cimento* 5:133–139. *Ottica* (*N.S.*) 2:29–33.

Bessis, M., 1949*a*. Études sur les cellules sanguines au microscope à contraste de phase et par la méthode de l'ombrage. *Rev. hématol.* 4:294–349.

1949*b*. Études sur les cellules des leucémies et des myélomes au microscope à contraste de phase et par la méthode de l'ombrage. *Rev. hématol.* 4:364–394.

Bessis, M., and M. Bricka, 1949. Études sur l'étalement des leucocytes du sang humain au microscope à contraste de phase et par la méthode de l'ombrage. *Rev. hématol.* 4:350–363.

Blout, E. R., and R. C. Mellors, 1949. Infrared spectra of tissues. *Science* 110:137–138.

Bonner, J. T., 1950. Observations on polarity in the slime mold *Dictyostelium discoideum*. *Biol. Bull.* 99:143–151.

Bosshard, E., 1944. Phasenkontrast-Mikroskopie. *Schweiz. Brauerei-Rund.* 55:131–136.

Bouyer, R., 1950. Sur le contraste de phase. *Microscopie* (Paris) 2:11–14.

Boyd, G. A., 1947. The physical principles and techniques of autoradiographs. *J. Biol. Photogr. Assoc.* 16:65–77.

Boyd, G. A., and A. I. Williams, 1948. Stripping film technics for histological autoradiographs. *Proc. Soc. Exptl. Biol. and Med.* 69:225–232.

Bratuscheck, K., 1892. Die Lichtstärke-Aenderungen nach verschiedenen Schwingungsrichtungen in Linsensystemen von grossem Oeffnungswinkel mit Beziehung zur mikroskopischen Abbildung. *Z. wiss. Mikroskopie* 9:145–160.

Brecher, G., 1948. The structure of unstained reticulocytes. *Pro. Soc. Exptl. Biol. and Med.* 69:89–90.

1949. Phase microscopy in the study of reticulocytes. *Bull. Int. Assoc. Med. Museums* 30:99–105.

Brice, A. T., R. P. Jones, and J. D. Smyth, 1946. Golgi apparatus by phase contrast microscopy. *Nature* 157:553–554.

Brice, A. T., and P. H. Keck, 1947. Most favorable absorption of the phase plate in phase contrast microscopy. *J. Opt. Soc. Am.* 37:647–651.

Broadfoot, H. H., and E. R. Schwarz, 1948. An improved permanent mounting medium for textile fibers. *Textile Res. J.* 18:756–758.

Buchsbaum, R., 1947. Individual cells observed under phase microscopy during fixation. *Anat. Rec.* 99:640.

1948. Individual cells under phase microscopy before and after fixation. *Anat. Rec.* 102:19–35.

Burch, C. R., 1934. On the phase-contrast test of F. Zernike. *Roy. Astron. Soc. M. N.* 94:384–399.

Burch, C. R., and J. P. P. Stock, 1942. Phase-contrast microscopy. *J. Sci. Instrum.* 19:71–75.

Calco, 1947. *Dyelines and Bylines.* February.

Calkins, G. N., and F. M. Summers, 1941. *Protozoa in biological research.* Columbia University Press, New York. xli+1148 pp. (see p. 85).

Carini, A., 1948. The phase-contrast microscope. VFC. *Galileo News* 25–33.

Carpenter, W. B., 1901. *The microscope and its revelations.* Revised by W. H. Dallinger. J. & A. Churchill, London. 1181 pp.

Chambers, R., and G. S. de Rényi, 1925. The structure of the cells in tissues as revealed by microdissection. 1. The physical relationships of the cells in epithelia. *Am. J. Anat.* 35:385–402.

Chamot, E. M., and C. W. Mason, 1938, 1940. *Chemical Microscopy.* John Wiley and Sons, New York. I. xiii+478 pp.; II. xi+438 pp.

Chase, H. B., and V. W. Smith, 1949. X-ray induced greying in the mouse with reference to melanoblasts. *Anat. Rec.* 105:533–534.

Chitwood, B. G., 1949. "Root-knot" nematodes—Part I. A revision of the genus *Meloidogyne goeldi*, 1887. *Proc. Helm. Soc. Wash.* 16:90–104.

Clark, E. W., and F. Morishita, 1950. C-M Medium: a mounting medium for small insects, mites, and other whole mounts. *Science* 112:789–790.

Cole, W. V., 1948. The use of phase contrast in the analysis of the osteopathic lesion. *J. Osteop.* 55(10):14–17.

— 1949. The demonstration of cellular elements by the use of filters in photomicroscopy. *J. Biol. Photogr. Assoc.* 17:115–120.

Conrady, A. E., 1905. An experimental proof of phase reversal in diffraction spectra. *J. Roy. Micr. Soc.* 1905:150–152.

Corti, A., 1948. Il lacunoma osservato col microscopio a contrasto di fase. *Atti accad. Lincei* (Roma) *Rend. Cl. Sci. Ser. 8A.* 4:132–135.

Coulston, F., 1941. The use of diaphane for mounting Giemsa type preparations. *J. Lab. and Clin. Med.* 26:869–873.

Cox, A., 1945. Phase retarding areas. *Nature* 155:425–426.

Crawford, G. N. C., and R. Barer, 1949. The actions of fixatives on living cells as studied by phase-contrast microscopy. *J. Anat.* (London) 83:73.

Crossmon, G. C., 1948. Microscopical distinction of carborundum among its natural and artificial associates. *Anal. Chem.* 20:976–977.

— 1949a. Dispersion staining with phase contrast microscope accessories. The microscopic identification of quartz. *Science* 110:237–238.

— 1949b. Mounting media for phase microscope specimens. *Stain Technol.* 24:241–247.

— 1950. The counting of blood cells by phase microscopy. *Am. J. Clin. Path.* 20:1041–1043.

Cuckow, F. W., 1947. Phase-contrast in the photomicrography of metals. *Nature* 159:639–640.

— 1949. The phase-contrast incident-light microscope. *J. Iron & Steel Inst.* 161:1–10.

Culiner, A., and J. Gluckman, 1948. The use of the "phase-contrast" microscope in clinical gynaecology; a preliminary report. *J. Obst. Brit. Emp.* 55:261–267.

Dalton, A. J., H. B. Kahler, B. J. Lloyd, and M. J. Striebich, 1949. A smear technique for preparing cells for study under the electron microscope. *Anat. Rec.* 103:437.

Dan, J. C., 1950a. Sperm entrance in echinoderms observed with the phase contrast microscope. *Biol. Bull.* 99:399–411.

— 1950b. Fertilization in the medusan, *Spirocodon saltatrix.* *Biol. Bull.* 99:412–415.

Danes, B., 1949. Ciliated pulmonary epithelium of *Triturus viridescens* in tissue culture. *Anat. Rec.* 103:590–591.

DeLamater, E. D., V. D. Newcomer, M. Haanes, and R. H. Wiggall, 1950. Studies on the life cycles of spirochetes. I. The use of phase contrast microscopy. *Am. J. Syph. Gon. Ven. Dis.* 34:122–125.

Dickie, A., and L. H. Hempelmann, 1947. Morphologic changes in the lymphocytes of persons exposed to ionizing radiation. *J. Lab. and Clin. Med.* 32:1045–1059.

Downs, W. G., 1943. Polyvinyl alcohol: a medium for mounting and clearing biological specimens. *Science* 97:539–540.

Dragesco, J., 1948. La technique microcinématographique sur films étroits. *Microscopie* (Paris) 1: M10–M40.

Duijn, C. van, Jr , 1948. Substitutes for cedarwood oil for use with immersion lenses. *Micr. & Ent. Mon.* 7:91–93.

Duryee, W. R., 1948. A film on the mechanism of cell division. *J. Washington Acad. Sci.* 38:31.

Dustin, P., Jr., 1949. Le microscope à contraste de phase et son utilization en cytologie pathologique. *Acta Clin. Belg.* 4:70–86.

Dyar, M. T., 1947. Isolation and cytological study of a free-living spirochete. *J. Bact.* 54:483–493.

Dyson, J., 1949. A transmission-type interferometer microscope. *Nature* 164:229.

Eisenstark, A., and K. T. McMahon, 1949. Some phase-microscope observations on *Azotobacter agile. Soil Sci.* 68:329–331.

Epstein, L. I., 1949, 1950. An extension of Toraldo's theory of phase contrast. I. *J. Opt. Soc. Am.* 39:1053; 40:291–294.

Epstein, L. I., 1950. The edge-effect in phase contrast. *J. Opt. Soc. Am.* 40:803.

Epstein, L. I., and D. R. Herriott, 1950. An extension of Toraldo's theory of phase contrast. II. *J. Opt. Soc. Am.* 40:576–578.

Evans, R. M., 1948. *An introduction to color.* John Wiley and Sons, N. Y. x+340 pp.

Farr, W. K., 1946. Calcium pectate in the cotton fiber. *Am. J. Bot.* 33:229.
    1949. The tertiary membrane of the plant cell wall. *J. Phys. and Coll. Chem.* 53:260–274.

Farris, E. J., 1947. A new method of semen analysis. *Anat. Rec.* 97:429.
    1948a. A technic for counting motile spermatozoa. *Anat. Rec.* 101:699.
    1948b. Motile spermatozoa as an index of fertility in man. *Anat. Rec.* 100:780–781; 101:700–701.
    1949. Spermatozoa of vertebrates. (Motion picture) Biol. Photogr. Assoc. 19th Convention, Cleveland, Ohio.
    1950. *Human fertility and problems of the male.* Author's Press, White Plains, N. Y. xvi+212 pp.

Fawcett, D. W., B. L. Vallee, and M. H. Soule, 1950. A method for concentration and segregation of malignant cells from bloody, pleural, and peritoneal fluids. *Science* 111:34–36.

Feissly, R., 1948. Personal communication. Paper on platelet counting with phase microscope, Séance du 4 Sept. *Acta Helvétique Sci.*

Feissly, R., and H. Lüdin, 1949. Microscopie par contrastes de phases. III. Applications à l'hématologie. *Rev. hématol.* 4:481–501.

Feissly, R., and R. Québatte, 1947. L'examen microscopique par les "contrastes de phases" (ses applications à l'histologie pathologique et à la cytologie sanguine). *Rev. hématol.* 2:411–424.

Fell, H. B., and A. F. Hughes, 1949. Mitosis in the mouse: a study of living and fixed cells in tissue cultures. *Quart. J. Micr. Sci.* 90:355–380.

Firor, W. M., and G. O. Gey, 1947. The study of malignant cells with phase difference microscopy. *Ann. Surg.* 125:604.

Fischbein, I. W., 1950. Electron microscopy of wet biological tissues by replica techniques. *J. Appl. Phys.* 21:1199–1204.

Fleming, W. D., 1943. Synthetic mounting medium of high refractive index. *J. Roy. Micr. Soc.* 63:34–37.

Fleury, P., A. Maréchal, and M. Anglade, 1949. *La théorie des images optiques.* (See Chapter VI, Contraste de phase.) Rev. d'optique, Paris. 322 pp.

Foster, L. V., 1950. Microscope optics. *J. Opt. Soc. Am.* 40:275–282.

Françon, M., 1946. Image d'un petit object rectangulaire parfaitement transparent par la méthode du contraste de phase. *Rev. d'optique* 25:257–266.

    1949. Le contraste de phase. *Microscopie* (Paris) 1:M117–M131.

    1949. Limite de séparation du microscope à contraste de phase. *Compt. rend. acad. sci.* 288:1413–1414.

    1950. Dispositif à contraste de phase pour microscope. *Rev. d'optique* 29:129–134.

Françon, M., 1950a. *Le contraste de phase en optique et en microscopie.* Rev. d'optique, Paris. 109 pp.

    1950b. Extra-objective device for phase-contrast. *Micr. & Ent. Mon.* 8:43–50.

Françon, M., and G. Nomarski, 1950a. Dispositif à contraste de phase indépendant du microscope et utilisant une lame de phase à absorption variable. *Compt. rend. acad. sci.* 230:1050–1051.

    1950b. Lame de phase à contraste variable par réflexion. *Compt. rend. acad. sci.* 230:1392–1394.

Frauchiger, E., 1946. Phasenmikroskopische Untersuchungen am Plexus chorioideus. *Schweiz. Arch. Neur. Psychiat.* 58:182–185.

Frederikse, A. M., 1933a. Der Brechungsindex des Protoplasmas. *Protoplasma* 19:473–484.

    1933b. Mikroskopische Beobachtung lebendiger Zellen. *Acta Brev. Neerl.* 3:121–122.

Ganz, E., 1944. Das Phasenkontrast-Verfahren nach Zernike zur Untersuchung ungefärbter mikroskopischer Präparate. *Vierteljahrs. Naturforsch. Ges. Zürich.* 89:268–280.

Garnett, W. J., 1945. Euparal. *Micr. & Ent. Mon.* 5:265–266.

Gatenby, J. B., and T. A. A. Moussa, 1949. The dorsal root ganglion cell of the kitten with Sudan dyes and the Zernike microscope. *J. Roy. Micr. Soc.* 69:185–199.

Gradwohl, R. B. H., 1948. *Clinical laboratory methods and diagnosis.* 4th ed. C. V. Mosby, St. Louis. (See Vol. I, p. 14.)

Gramont, A. de, 1948. Comment réaliser un contraste de phase. *Microscopie* (Paris) 1:M62–M64.

Gray, P., and G. Wess, 1950. The use of polyvinyl alcohol and its derivatives as microscopical mounting media. *J. Roy. Micr. Soc.* 70:287–291.

Greco, J. P., 1950. Refractive indices of currently used mounting media. *Stain Technol.* 25:11–12.

Grégoire, C., and M. Florkin, 1950. Étude au microscope à contraste de phase du coagulocyte, du nuage granulaire et de la coagulation plasmatique dans le sang des insectes. *Experientia* 6:297–298.

Grigg, F. C., 1950. Colour-contrast phase microscopy. *Nature* 165:368–369.

Groat, R. A., 1941. Clearing tissue with mixtures of tributyl and tri-*o*-cresyl phosphates. *Stain Technol.* 16:111–117.

    1950. Preparation of copolymers of isobutyl methacrylate and styrene for mounting media. *Stain Technol.* 25:87–94.

Haberman, J., 1948. Clearing brain tissue with anethole. *Stain Technol.* 23:143–144.

Hardy, J. I., and T. M. Plitt, 1940. An improved method for revealing the surface structure of fur fibers. *Wild Life Circular* No. 7. U.S. Government Printing Office, Washington, D. C. 10 pp.

Harrison, J. A., and E. H. Fowler, 1946. A serologic study of conjugation in *Paramecium bursaria.* *J. Exptl. Zool.* 101:425–444.

Harrison, J. A., O. W. Richards, J. A. Maurer, and E. H. Fowler, 1946. Serologic

reactions with two strains of *Paramecium bursaria*. *Anat. Rec.* 94:381. (Film shown also at Soc. Am. Bact. 46th meeting, Detroit. Program, p. 5.)

Hartley, W. G., 1947. A variable phase-contrast system for microscopy. *Nature* 159:880–881.

Hartroft, W. S., 1950. The islets of Langerhans in man visualized by phase contrast microscopy. *J. Clin. Endocr.* 10:828.

Haselmann, H., 1948a. Mikroskopie histologischer Objekte und das Phasenkontrastverfahren. *Klin. Wochenschr.* 26:124.

1948b. Protoplasmastrukturen und die Phasenkontrastmikroskopie. *Klin. Wochenschr.* 26:701; *Med. Klin. Münch.* 43:496.

1950a. Strukturprobleme der Phasenkontrastmikroskopie. *Anat. Nachr.* 1:86.

1950b. Beiträge zur Phasenkontrast-Mikroskopie. *Mikroskopie* (Wien) 5:214–224.

Haselmann, H., and W. Kappel, 1949. Ueber die Untersuchung lebendiger Gonokokken im Phasenkontrastverfahren. *Arch. Derm. u. Syph.* 187:501–505.

Heard, O. O., 1932. Some practical considerations on time lapse motion photomicrographic devices. *J. Biol. Photogr. Assoc.* 1:4–19.

Heilbrunn, L. V., 1937. *An outline of general physiology.* W. B. Saunders Co., Philadelphia. 603 pp.

Herschman, H. K., 1945. Evaluation of the finish of a metal surface by a replica method. *J. Res., Nat. Bur. Stds.* 34:25–31.

Herz, R. H., 1950. Autoradiography. *Med. Radiog. and Photogr.* 26:46–51.

Hoessley, G. F., 1947. Untersuchungen am Zentralnervensystem mit dem Phasenkontrast-Mikroskopierverfahren. *Acta Anat.* 3:271–294.

Hofer, A. W., 1947. Bacteriophage under the ordinary microscope. *J. Bact.* 53:781–792.

Hofer, A. W., and O. W. Richards, 1945. Observation of bacteriophage through a light microscope. *Science* 101:466–468.

Hoffman, G. T., and A. Rottino, 1950. Phase microscopy in studies of Hodgkin's disease lymph nodes in relation to histogenesis of the Sternberg-Reed cell. *Blood* 5:74–78.

Hogg, J., 1886. *The microscope: its history, construction and application.* 11th ed. Routledge & Sons, London. xx +764 pp.

Hughes, A. F. W., 1949. The technique of ciné-photomicrography of living cells. *J. Roy. Micr. Soc.* 69:53–64.

Hughes, A. F. W., and M. M'E. Preston, 1949. Mitosis in living cell of amphibian tissue cultures. *J. Roy. Micr. Soc.* 69:121–131.

Hughes, A. F. W., and M. M. Swann, 1948. Anaphase movements in the living cell. A study with phase contrast and polarized light on chick tissue cultures. *J. Exptl. Biol.* 25:45–70.

Hughes, A. F. W., and H. B. Fell, 1949. Studies on abnormal mitosis induced in chick tissue cultures by mustard gas (β,β'-dichlordiethyl sulphide). *Quart. J. Micr. Sci.* 90:37–55.

Jackson, A., 1948. *Amateur photomicrography.* Focal Press, New York. 180 pp.

Jelley, E. E., 1949. Microscopy. In A. Weissberger's *Physical methods of organic chemistry.* 2nd ed. Vol. 1, pp. 847–981. Interscience, New York. 1072 pp.

Jones, O. P., 1947a. The Golgi element in primitive erythroblasts of the 11-day rat embryo. *Anat. Rec.* 97:393.

1947b. A study of mitochondria in dry smears of embryonic blood. *Anat. Rec.* 97:347.

1947c. Mitochondria and their relation to the so-called hyaloplasm. *J. Lab. and Clin. Med.* 32:700–719.

1948a.   Mitochondrial influence on nuclear pattern of lymphoid cells. *Anat. Rec.* 100:681.

1948b.   Nuclear structure versus nuclear pattern. *Blood* 3:967–986.

Jones, O. P., and O. W. Richards, 1947.   A method of studying dry smears of blood with phase microscopy followed by staining techniques. *Anat. Rec.* 97:417–418.

Jupnik, H., 1944.   Preliminary experiments in phase difference microscopy. *J. Opt. Soc. Am.* 34:773.

Jupnik, H., H. Osterberg, and G. E. Pride, 1946.   Phase microscopy with vertical illumination. *J. Opt. Soc. Am.* 36:710.

1948.   Phase microscopy with vertical illumination. *J. Opt. Soc. Am.* 38:338–342.

Kastler, A., and R. Montarnal, 1948.   Phase-contrast in polarized light. *Nature* 161:357.

Kaufmann, B. P., and R. C. MacDuffee, 1949.   Chromosome structure as revealed by tryptic digestion. *Anat. Rec.* 105:495–496.

Keck, P. H., and A. T. Brice, 1949.   Image contrast in phase-contrast microscopy. *J. Opt. Soc. Am.* 39:507–514.

Kempson, D. A., O. L. Thomas, and J. R. Baker, 1948.   A simple method for phase-contrast microscopy. *Quart. J. Micr. Sci.* 89:351–358.

Kernohan, J. W., 1928.   A note on the use of "cellophane" as a cover glass and a camphor-sandarac mounting medium. *Trans. Am. Micr. Soc.* 47:272–273.

Keuning, F. J., 1950.   Das Phasenkontrastverfahren in der Mikroskopie. *Mikroskopie* (Wien) 5:49–61.

Kimball, R. F., 1949.   The effect of ultraviolet light upon the structure of the macronucleus of *Paramecium aurelia*. *Anat. Rec.* 105:543.

Kirk, P. L., and C. S. Gibson, 1939.   Refractive index measurements in qualitative organic microanalysis. *Ind. Eng. Chem., Anal. Ed.* 11:403.

Knöll, H., 1944.   Zur Anwendung der Phasenkontrastmikroskopie in der Bacteriologie. *Zeiss Nachr.* 5(2):38–53.

Köhler, A., and W. Loos, 1941.   Das Phasenkontrastverfahren und seine Anwendungen in der Mikroskopie. *Naturwiss.* 29:49–61.   For a translation see *Textile Res. J.* 17:82–95.

Koonz, C. H., and E. J. Strandine, 1945.   A rapid and simplified method for revealing the surface pattern of hair. *Trans. Am. Micr. Soc.* 44:63–64.

Kunz, A. H., and J. Spulnik, 1936.   Standard liquids for the microscopic determination of refractive index. *Ind. Eng. Chem., Anal. Ed.* 8:485.

Lachenaud, M., 1947.   Le procédé à contraste de phase de F. Zernike appliqué à la microscopie. *Rev. d'optique* 26:205–228.

Laporte, M., 1950.   The application of whitelight flash tubes to instantaneous photomicrography in ordinary or phase-contrast microscopy. *Compt. rend. acad. sci.* (Paris) 230:1592–1593.   (From *Phys. Abs.* 53:735.)

Lewis, S. R., C. M. Pomerat, and D. Ezell, 1949.   Human epidermal cells observed in tissue culture with phase-contrast microscopy. *Anat. Rec.* 104:487–503.

Lillie, R. D., 1948.   Histopathologic technic. Blakiston, Philadelphia. xi+300 pp.

Lillie, R. D., W. F. Windle, and C. Zirkle, 1950.   Interim report of the Committee on Histologic Mounting Media: Resinous media. *Stain Technol.* 25:1–9.

Lind, H E., and O. Ashley, 1950.   Limitations of the blood smear technique for the detection of malignancy. *Lab. Dig.* 13:6–9.

Lindegren, C. C., and G. Lindegren, 1947.   The cytosome theory. *Cold Spring Harbor Symp. Quant. Biol.* 11:115–129.

Linfoot, E. H., 1945.   Phase difference microscopy. *Nature* 155:76.

Locquin, M., 1948a.   Plaque de phase à absorption réglable en lumière polarisée. *Microscopie* (Paris) 1:M47–M48.

1948b. À propos de l'objectif dit "à réflecteur interne" de Spierer. *Microscopie* (Paris) 1 : M49–M50.

Locquin, M., and C. A. Baud, 1947.   Contraste d'amplitude et contraste de phase. *Bull. Histol. Appl. et Tech. Microscopie*, Lyon, 24 : 41–47.

Locquin, M., and M. Bessis, 1948.   Amélioration des images observées avec la technique de l'ombrage par l'examen au contraste de phase.   *Compt. rend. soc. biol.*, 142 : 1497–1498.

Loos, W., 1941a.   Das Phasenkontrastverfahren nach Zernike als biologisches Forschungsmittel.   *Klin. Wochenschr.* 20 : 849–853.

1941b.   Das Phasenkontrastverfahren und seine Anwendung in der Mikroskopie. *Zeiss Nachr.* 4 : 58–63.

Loos, W., W. Klemm, and A. Smekal, 1941.   Anwendung der Phasenkontrast-Mikroskopie auf Modellversuche zum Poliervorgang an Gläsern.   *Naturwiss.* 29 : 769–770.

Ludford, R. J., and J. Smiles, 1950.   Cytological characteristics of fibroblasts and sarcoma cells demonstrated by phase-contrast microscopy.   *J. Roy. Micr. Soc.* 70 : 186–193.

Ludford, R. J., J. Smiles, and F. V. Welch, 1948.   The study of living malignant cells by phase-contrast and ultra-violet microscopy.   *J. Roy. Micr. Soc.* 68 : 1–9.

Lüdin, H., 1947.   Ueber die Bedeutung der Lymphknotenpunction für die Diagnose der Lymphogranulomatose.   *Radiol. Clin.* 16 : 212–220.

1948.   Tumorzellnachweis in Organpunktaten mit dem Phasenkontrastverfahren. *Schweiz. med. Wochenschr.* 78 : 710–713.

Luneberg, R. K., 1944.   *Mathematical theory of optics.*   Brown University, Providence, R. I.   401 pp.

Lyot, B., and M. Françon, 1948.   Observation des défauts de poli et d'homogénéité au stéréoscope par la méthode du contraste de phase.   *Rev. d'optique* 27 : 397–398.

Magliozzi, J., 1947.   Contrast effects of phase changing elements in microscopy. *J. Opt. Soc. Am.* 37 : 982.

1948.   Phase contrast microscopy.   *Educ. Focus* 19 : 6–12.

Malies, H. M., 1948.   A lamp for phase-contrast and other purposes.   *Micr. & Ent. Mon.* 7 : 13–18.

Maresh, C., and G. L. Royer, 1949.   Shrinkage control of wool by melamine resins. I. Microscopical observations.   *Textile Res. J.* 19 : 449–457.

Martin, L. C., 1947.   Phase-contrast methods in microscopy.   *Nature* 159 : 827–830.

Marx, T., and F. Diehl, 1948.   Die Anwendung des Phasenkontrastverfahrens in der Oberflächenmikroskopie.   *Naturwiss.* 35 : 91–92.

Maurer, J. A., 1944.   Exposure control in photomicrography.   *J. Biol. Photogr. Assoc.* 12 : 173–185.

McCartney, J. E., 1944.   A new immersion oil ("Polyric").   *J. Path. and Bact.* 56 : 265–266.

Meyer, K. F., G. F. Hoessley, and A. Larson, 1948.   Mechanism of immunity in plague infections.   *Science* 108 : 681.

Michel, K., 1941.   Die Darstellung von Chromosomen mittels des Phasenkontrastverfahrens.   *Naturwiss.* 29 : 61–62.

1943.   Mikrophotographie.   Das Phasenkontrastverfahren.   *Hdb. wiss. angew. Photographie.*   (Hay's) Wien. Suppl. Vol. I, pp. 546–555.

1950.   Das Phasenkontrastverfahren und seine Eignung für zytologische Untersuchungen.   *Naturwiss.* 37 : 52–57.

Moeschlin, S., 1949a.   Phasenkontrastuntersuchungen in der Hämatologie. *Schweiz. med. Wochenschr.* 79 : 842–843.

1949b.   Same title.   *Acta Haematol.* 2 : 399–426.

Moment, G. B., 1944. A simple method for quieting paramecium and other small organisms during prolonged observation. *Science* 99:544.

Monk, C. R., 1938. An aqueous medium for mounting small objects. *Science* 88:174.

Morehead, F. F., 1950. Modern microscopy of films and fibers. *ASTM Bull.*, No. 163, pp. 54-57.

Murray, R. G. E., and H. C. Douglas, 1950. The reproductive mechanism of *Rhodomicrobium vannielii* and the accompanying nuclear changes. *J. Bact.* 59:157-167.

Narath, A., 1948. Zur Erklärung des Phasenkontrastverfahrens. *Optik* 4:9-10.

Noüy, P. L. du, 1929. Sur l'indice de réfraction, le coefficient de température et la dispersion du sérum sanguine. *Compt. rend. soc. biol.* 100:490. (From *Méthodes physiques en biologie et en médicine*, 1933. Baillière et Fils, Paris, 194 pp.)

O'Brien, H. C., and R. T. Hance, 1940. A plastic cover glass, isobutyl methacrylate. *Science* 91:412.

Odor, D. L., and R. J. Blandau, 1949. Observations of fertilization phenomena in rat ova. *Anat. Rec.* 103:580.

Oettlé, A. G., 1948. Golgi apparatus of living human testicular cells seen with phase-contrast microscopy. *Nature* 162:76-77.

Oettlé, A. G., 1950a. "Optical membranes": a common artifact. *J. Roy. Micr. Soc.* 70:255-265.

　　 1950b. Experiments with a variable amplitude and phase microscope. *J. Roy. Micr. Soc.* 70:232-254.

Oliver, J., 1948. The structure of the metabolic process in the nephron. *J. Mt. Sinai Hosp.* 15:175-222.

Oliver, J., F. Bloom, and C. Mangieri, 1947. On the origin of heparin. *J. Exptl. Med.* 86:107-116.

Oosterhuis, J. A. H., 1950. Phase-contrast microscopie. *de Analyst* 5:151-155; 167-171.

Osterberg, H., 1944. Phase difference microscopy as a problem in diffraction. *J. Opt. Soc. Am.* 34:773-774.

　　 1946a. A method of analysis of light polarizing systems. *J. Opt. Soc. Am.* 36:364.

　　 1946b. Inhomogeneous light polarizing systems. *J. Opt. Soc. Am.* 36:469-477.

　　 1946c. "Polanret" microscopy. *J. Opt. Soc. Am.* 36:710.

　　 1947a. The polanret microscope. *J. Opt. Soc. Am.* 37:726-730.

　　 1947b. The theory of measuring unresolvable particles with the phase microscope. *J. Opt. Soc. Am.* 37:523-524.

　　 1948a. The multipupil in phase microscopy. *J. Opt. Soc. Am.* 38:668; 685-688.

　　 1948b. Phase microscopy with critical illumination. *J. Opt. Soc. Am.* 38:1099.

Osterberg, H., and G. E. Pride, 1950. The measurement of unresolved, single particles of uniform thickness by means of variable phase microscopy. *J. Opt. Soc. Am.* 40:64-73.

Osterberg, H., and H. S. Schrader, 1947. Microscope with special light modifiers. U. S. Pat. 2427689.

Osterberg, H., and J. E. Wilkins, Jr., 1949. The resolving power of a coated objective. *J. Opt. Soc. Am.* 39:553-557.

Paff, G. H., F. Bloom, and C. Reilly, 1947. The morphology and behavior of neoplastic mast cells cultivated *in vitro*. *J. Exptl. Med.* 86:117-124.

Pantin, C. F. A., 1946. *Notes on microscopical techniques for zoologists.* Cambridge University Press. viii+73 pp.

Payne, B. O., 1947. Image formation in phase-contrast microscopy. *J.Sci.Instrum.* 24:163–165.

— 1950. A phase-contrast microscope with variable amplitude and phase. *J. Roy. Micr. Soc.* 70:225–231.

Perry, W. L. M., 1948. Cultivation of *Treponema pallidum* in tissue culture. *J. Path. and Bact.* 60:339–342.

Peters, V. B., and L. B. Flexner, 1950. Biochemical and physiological differentiation during morphogenesis. *Am. J. Anat.* 86:133–161.

Peters, V. B., J. P. Flynn, and L. Warner, 1950. The use of phase microscopy for the study of fixed material. *Anat. Rec.* 106:311.

Petrunkevitch, A., 1937. On differential staining. *Anat. Rec.* 68:267–280.

Picht, J., 1936. Bemerkungen über den Phasenunterschied im Bilde der Fraunhoferschen Beugungserscheinungen. *Z. Instrumentenkunde* 56:363–368; 481–489.

— 1938. Zum Phasenkontrastverfahren von Zernike. *Z. Instrumentenkunde* 58:1–12.

Pijper, A., 1949. The flagella of *Spirillum volutans*. *J. Bact.* 57:111–118.

Pollister, A. W., and C. Leuchtenberger, 1949. The nature of the specificity of methyl green for chromatin. *Proc. Nat. Acad. Sci.* 35:111–116.

Porter, J. R., 1947. *Bacterial chemistry and physiology*. John Wiley and Sons, New York, 1073 pp.

Powell, R. H., 1949. The Galileo phase-contrast microscope. *J. Roy. Micr. Soc.* 69:237–238.

Quekett, J., 1852. *Practical treatise on the use of the microscope*. 2nd ed. Baillière, London. xxii+515 pp.

Ralph, P. H., 1947. Observations on the surface of epithelial cells. *Anat. Rec.* 98:219–221.

— 1949. Phase microscopy photographs of cells of blood and blood-forming organs. *Anat. Rec.* 103:583.

— 1950. The human platelet. *Anat. Rec.* 106:234.

Ralph, P. H., and C. A. Doan, 1948. Observations on normal adult human leucocytes. *Anat. Rec.* 100:705.

Reid, W. M., 1948. Penetration glands in cyclophyllidean onchospheres. *Trans. Am. Micr. Soc.* 67:177–182.

Remuth, H., 1947. Applications of phase microscopy to textile fiber research. *Textile Res. J.* 17:69–81.

Rheinberg, J., 1904. On the influence on images of gratings of phase difference amongst their spectra. *J. Roy. Micr. Soc.* 1904:388–390.

— 1905. The influence on images of gratings of phase-differences amongst their spectra. *J. Roy. Micr. Soc.* 1905:152–155.

Richards, O. W., 1934. A simple and flexible apparatus for tachygraphic cinéphotomicrography. *J. Biol. Photogr. Assoc.* 3:64–71. (Brief description in *Science* 1934. 80:361.)

— 1944a. Phase-difference microscopy for living unstained protoplasm. *Anat. Rec.* 89:548.

— 1944b. Phase difference microscopy. *Nature* 154:672.

— 1946a. Phase microscopy. *J. Bact.* 51:563–564.

— 1946b. The size of living bacteria measured with the phase microscope. *J. Bact.* 51:585.

— 1947a. Growth of bacterial and fungal colonies as seen with the phase microscope. *J. Bact.* 54:4.

— 1947b. Phase photomicrography. *J. Biol. Photogr. Assoc.* 16:29–38.

1947c. Biological phase microscopy. *Cold Spring Harbor Symp. Quant. Biol.* 11:208–214.

1947d. Applications of phase microscopy in electron microscopy. *J. Appl. Phys.* 18:271.

1948a. Applications of the phase contrast microscope. *J. Washington Acad. Sci.* 38:30–31.

1948b. Phase microscopy in bacteriology. *Stain Technol.* 23:55–64.

1948c. Image contrast control with phase microscopy. *J. Opt. Soc. Am.* 38:668.

1949a. *The effective use and proper care of the microscope.* American Optical Co., Buffalo 15, N. Y. 63 pp.

1949b. *The effective use and proper care of the microtome.* American Optical Co., Buffalo 15, N. Y. 84 pp.

1949c. Contrast control in phase microscopy from appropriate choice of mounting medium. *Anat. Rec.* 105:546.

1949d. Tridimensional cellular structure. *Anat. Rec.* 105:546–547.

1950. When to use special microscopes. In *Biophysical Research Methods.* Edited by F. M. Uber. Interscience Publishers, N. Y. 678 pp.

Richards, O. W., and H. W. Wade, 1948. Applications of phase microscopy to the examination of the leprosy bacillus. *Int. J. Leprosy* 16:297–298.

1949. Same title. Vth Cong. Int. Lepra, Havana. pp. 517–525.

Richmond, J. C., and A. C. Francisco. 1949. Use of plastic replicas in evaluating surface texture of enamels. *J. Res., Nat. Bur. Stds.* 42:449–460.

Richter, R., 1947. Eine einfache Erklärung des Phasenkontrastmikroskops. *Optik* 2:342–345.

Riva, I., 1949. Présentation du microscope à contraste de phase "Koristka." *Microscopie* (Paris) 1:B40–B42.

Rossi, F., and G. Pescetto, 1950. Studi ultramicroscopici ed in contrasto di fase degli spodogrammi placentari. *Accad. med., Torino* 65:110–112.

Royer, G. L., and C. Maresh, 1947. Application of microscopy to the textile industry. *Soc. Dyers and Colourists* 63:287–293. *Textile Res. J.* 17:477–487. *Calco Tech. Bull.* No. 796, 13 pp.

Runge, H., A. Vöge, and H. Haselmann, 1949. Untersuchungen des Vaginal-Smears mittels Phasenkontrastmikroskopie. *Geburtsh. u. Frauenheilk.* 9:627–639.

Rytov, S., and M. Jabotinsky, 1947. Observation of refractional structures. *J. Phys. USSR* 11:92. (From *Phys. Abst.* 1947, 50:203.)

Salmon, M. V., 1947. Practical phase-contrast microscopy. *Micr. & Ent. Mon.* 6:177–188.

Saylor, C. P., A. T. Brice, and F. Zernike, 1949. Color phase contrast: requirements and applications. *J. Opt. Soc. Am.* 39:1053.

1950. Color phase-contrast microscopy: requirements and applications. *J. Opt. Soc. Am.* 40:329–334.

Scandone, F., 1948a. Phase contrast microscopy. *Galileo News* (1):3–13.

1948b. Report on recent advances on optics. *Galileo News* (2):3–23.

Schmitt, F. O., 1944. From O. Glasser's *Medical Physics*, Year Book Publishers, Chicago. p. 1589.

Schultz, J., 1947. The nature of heterochromatin. *Cold Spring Harbor Symp. Quant. Biol.* 12:179–191.

Scott, D. B., and R. W. G. Wyckoff, 1949. Metal shadowing for the optical microscopy of certain tissues. *Am. J. Clin. Path.* 19:63–66.

Shillaber, C. P., 1944. *Photomicrography in theory and practice.* John Wiley and Sons, New York. viii+773 pp.

Smith, A., 1946. *Medical research—a symposium.* J. B. Lippincott Company, Philadelphia. xx + 169 pp.

Smithson, F., 1946. Phase-contrast microscopy for mineralogy. *Nature* 158:621.

——— 1948. The application of phase-contrast microscopy to mineralogy and petrology. *Mineralog. Mag.* 28:384–391.

Spence, D. S., 1941. Notes on mounting. *Micr. & Ent. Mon.* 4:266–272.

Stoffel, J. A., 1947. Recent local developments in scientific research. *Pittsburgh Med. Bull.* 36:263–265.

Stowell, R. E., and V. M. Albers, 1943. A spectrophotometric analysis of tissue staining. *Stain Technol.* 18:56–71.

Sylvén, B., 1950. The cytoplasm of living tissue mast cells in visual phase-contrast. *Exptl. Cell Res.* 1:492–493.

Tahmisian, T. N., and D. M. Adamson, 1950. A phase contrast microscopy study of x-ray-induced pycnosis in the living cell. *Anat. Rec.* 108:84.

Taylor, E. W., 1946. The practical application of phase-contrast to the biologist's microscope. *J. Roy. Mier. Soc.* 66:1–8.

——— 1947. The control of amplitude in phase-contrast microscopy. *Proc. Roy. Soc.* A190:422–426.

——— 1949. The phase-contrast microscope with particular reference to vertical incident illumination. *J. Roy. Micr. Soc.* 69:49–52.

Taylor, E. W., and B. O. Payne, 1947. A variable phase-contrast system for microscopy. *Nature* 160:338.

Teucher, R., 1949. Phasenkontrastmikroskopie. *Orion* 4:229–231.

Thomas, O. L., 1947. Some observations with the phase-contrast microscope on the neurones of *Helix aspersa*. *Quart. J. Micr. Sci.* 88:269–273.

Thorell, B., 1947. *Studies on the formation of cellular substances during blood cell production.* Stockholm. 120 pp.

Tinsley, W., 1938. A perfusion stage for observation on daphnia. *J. Lab. and Clin. Med.* 23:1076–1078.

Toraldo di Francia, G., 1949. Il fenomeno di Gibbs nella microscopia in contrasto di fase. *Nuovo Cimento* 6:30–38.

Trager, W., 1949. Observations with the phase microscope on the malaria parasite *Plasmodium lophurae* and on its extracellular development. *J. Parasit.* 35:23.

Tulasne, R., 1949. Données nouvelles sur la cytologie des bacteries apportées par la microscopie de contraste. *Compt. rend. soc. biol.* 143:1392–1394.

Watts, W. E., and D. R. Mathieson, 1950. Studies on lymphocytes from persons treated with radioactive iodine. *J. Lab. and Clin. Med.* 35:885–889.

Waugh, D. F., and F. O. Schmitt, 1940. Investigations of the thickness and ultrastructure of cellular membranes by the analytical leptoscope. *Cold Spring Harbor Symp. Quant. Biol.* 8:233–241.

Weber, A. P., 1948. Das Phasenkontrast nach Zernicke als Hilfsmittel für mikroskopische Untersuchungen durchsichtiger Stoffe. *Optik* 4:213–215.

Wichterman, R., 1940. Cytogamy. *J. Morph.* 66:423–451.

Williams, R. C., and R. W. G. Wyckoff, 1946. Applications of metallic shadowcasting to microscopy. *J. Appl. Phys.* 17:23–33.

Williams, S. C., 1949a. The development of cultured cells from the hind-brain of 5-day chick embryo. *Anat. Rec.* 103:520.

——— 1949b. Developing cells from the hind-brain of 5-day chick embryo. *Anat. Rec.* 103:588.

Wilson, M. W., 1942. A quick, easy method for preparing tissues for microscopic examination by combining the techniques of Nelson and Terry. *J. Lab. and Clin. Med.* 27:537–542.

Wolf, J., 1944. Verbesserungen und neue Modifikationen der Adhäsions (Mikrorelief)-Methode. *Z. wiss. Mikr.* 59:240–245. (Lists earlier papers.)

1948. Il metodo del microrilievo e l'istologia plastica. *Minerva Med. Scientifica* 39(2):19–25.

Wolter, H., 1950a. Zur Deutung von Beobachtungen mit dem Phasenkontrastverfahren. *Naturwiss.* 37:272–276.

1950b. Farbige Phasenkontrastverfahren. *Naturwiss.* 37:491.

1950c. Zur Abbildung zylindrischer Phasenobjekte elliptischen Querschnitts. *Ann. Physik.* 7:147–156.

Wotton, R. M., and R. L. Zwemer, 1935. A note on "glychrogel" mounting solutions. *Stain Technol.* 10:21–22.

Wyckoff, R. W. G., 1947. Shadow casting for microscopy. *Photogr. Soc. Am. J.* 13:816–820.

Zahn, H., and H. Haselmann, 1950. Über die Zwischenmembran in tierischen Haaren. *Mell. Textb. Heidelberg* 31:225–230.

Zeiss, Firma Carl, 1936. Deutsche Reich Pat. 636168.

1941. *Phasenkontrast-Einrichtung.* Jena. 30 pp.

Zernike, F., 1934. Diffraction theory of the knife edge test and its improved form the phase contrast method. *Physica* 1:689–704. *Roy. Astron. Soc. M. N.* 94:377–384.

1935. Das Phasenkontrastverfahren bei der mikroskopischen Beobachtung. *Z. tech. Phys.* 16:454–457. *Phys. Z.* 36:848–851.

1942. Phase contrast, a new method for microscopic observation of transparent objects. *Physica* 9:686–698; 974–986.

1946. Same title. In Bouwers, A. *Achievements in optics.* Elsevier Pub. Co., New York, pp. 116–135.

1948. Observing the phase of light waves. *Science* 107:463.

1949. A new method for the accurate measurement of phase differences. *J. Opt. Soc. Am.* 39:1059.

1950. A precision method for measuring small phase differences. *J. Opt. Soc. Am.* 40:326–328.

Zinser, H.-K., 1947. Einer neuer Hinweis zur Diagnosestellung der Trichomonas vaginalis. *Zntrlbl. Gynäk.* 69:148–151.

Zirkle, C., 1940. Combined fixing, staining and mounting media. *Stain Technol.* 15:139–153.

Zollinger, H. U., 1948a. Phasenmikroskopische Beobachtungen an Zellkulturen. *Mikroskopie* (Wien) 3:1–11.

1948b. Cytological studies with phase microscope. 1. The formation of "blisters" on cells on suspension (potocytolosis) with observations on the nature of the cell membrane. *Am. J. Path.* 24:545–567.

1948c. II. The mitochondria and other cytoplasmic constituents under various experimental conditions. *Am. J. Path.* 24:569–589.

1948d. III. Alternations in the nucleus of "resting" and dividing cells induced by means of fixatives, anisotonic solutions, acids and alkalis. *Am. J. Path.* 24:797–811.

1948e. IV. Morphologic changes associated with the death of cells in vitro and in vivo. *Am. J. Path.* 24:1039–1053.

1948f. Experimenteller Beitrag zur Frage der Mitochondrienfunktion. *Experientia* 4:312–314.

AUTHOR INDEX

311

SUBJECT INDEX